The development and optimisation of a novel microfluidic immunoassay platform for point of care diagnostics

by

Ana Isabel Ferreira Barbosa

A Doctoral Thesis submitted in partial fulfilment of the requirements for the award of the degree of Doctor of Philosophy of Loughborough University

September 2015

Abstract

Protein biomarkers are important diagnostic tools for detection of non-communicable diseases, such as cancer and cardiovascular conditions. In order to be used as diagnostic tools they need to be detected at very low concentrations in biological samples (e.g. whole blood, serum or urine). This has been currently performed in central laboratories using expensive, bulky equipment and time consuming assays.

Microfluidic devices aim at translating commercial sensitive laboratory tests into Point-of-Care (POC) tests, which need to match the ASSURED policy (affordable, sensitive, specific, user-friendly, rapid & robust, equipment-free and delivered). Nevertheless, the microfluidic technology has not yet achieved the expected performance for POC diagnostic tests commercialisation purposes. The two main reasons appointed are the lack of high sensitivity assays using power-free and portable detection systems, and the high manufacturing costs of the microfluidic devices.

This PhD thesis presents the development and optimisation of a novel microfluidic platform, the Microcapillary Film (MCF), made from a melt extruded fluoropolymer (FEP), which is cost effective and easily mass produced. The MCF is a transparent flat film with embedded capillaries, which provides high surface area-to-volume ratio and excellent optical properties for sensitive low cost optical interrogation. Overall, the results achieved show that MCF platform allows rapid quantitation of protein biomarkers in biological samples, using PSA (prostate specific antigen) and IL-1β cytokine as proof-of-concept. The method uses low cost, portable and power-free equipment, such as flatbed scanner or smartphone camera for optical interrogation. In order to understand the higher sensitivity using low cost detection methods several studies were performed. From these studies, it was found that antibodies irreversibly adsorb to FEP-Teflon achieving a full monolayer at 400 ng/cm^2, suggesting vertical antibody orientation. Also, microcapilary environment favours enzyme kinetics allowing higher end products concentration easily detected with a flatbed scanner or a smartphone. In addition, it was found that stop flow sample incubations favours assays sensitivity and speed. Ultimately, it was shown that negative effects of biological sample matrix can be overcome in MCF through antibody surface coverage and sample incubation time manipulation, eliminating the need for sample preparation.

Key words: Immunoassay, diagnostics, point of care, microfluidics, microcapillary film, miniaturisation.

Acknowledgments

Firstly I would like to gratefully thank my supervisor Dr Nuno Reis for the support and guidance given through all the phases of the work presented, from experimental work planning and analysis to production of manuscripts and written thesis. He was always very present and supportive. I am also thankful for his enthusiasm that kept me going in the moments mine was running of.

Secondly I am thankful to Capillary Film Technology Ltd and Lamina Dielectrics Ltd for providing the Microcapillary Film (MCF) platform and for giving me a great inside of industry perspective in point-of-care diagnostics.

And then I am gratefull to Loughborough University, Chemical Engineering technical staff for always making sure I had all the equipament and training I needed to proceed with my work. Special thanks to David Smith, for his kindness and availability in the Bio Lab, and Paul Izzard for solving my IT related problems.

After these, there is a list of people that made my PhD process easier to handle. I am therefore grateful to: my parents, Jose Barbosa and Emilia Barbosa, for always making me feel I belonged somewhere; Ana Castanheira for being an excellent lab colleague and supporting me in my down days; Tina Sutar for her insights in biological assays; Augusto Barreto, Poonam Gehlot and Kalpita Sidapra for their work and motivation in the lab; Dr Alexander Edwards for his insights in clinical diagnostics and feedback in manuscripts and thesis production; Filipa Pereira, Patrick Isherwood and Alex Eeles for their help proof reading this thesis; Biancamaria Maniscalco for being my friend; Celia Dias e Maria de Fatima Gomes for their unconditional support; Panagiota Moutsatsou and Eleni Nyktari for their support as friends and housemates; Alex Eeles for the everyday motivation and suport during the last phase of this project; And to my office colleagues Raffaella Casasola, Serena Morena Morelli, Ekanem Ekanem, Umarat Santisukkasaem, Elena Simone for their support and PhD problems sharing.

Contribution of authors

This thesis is presented as a collection of manuscripts written by the candidate with the collaboration of the co-authors. The manuscripts are based on experimental data generated from experiments designed and executed by the candidate, who was also responsible for data collection and analysis. The supervisor appears as co-author in all manuscripts reflecting his supervisory role during the execution of the work and his involvement in the manuscript preparation.

On chapter 2 manuscript "*Antibody (IgG) Adsorption onto FEP-Teflon microcapillary surfaces for quantitative point-of-care diagnostics*" Augusto Barreto gave his contribution executing protein bioassays under the candidate supervision, during his undergraduate summer project exchange.

On chapter 3 manuscript "*Impact of HRP enzymatic optimization in sandwich ELISA microfluidic systems*" Ana Castanheira appears as co-author due to her equal contribution in the experiments and manuscript planning and execution.

On chapter 5 "*A Lab-in-a-briefcase for rapid PSA screening from whole blood*" Ana Castanheira and Alexander Edwards appear as co-authors due to their contribution in the manuscript preparation.

On chapter 6 "*Portable smartphone quantitation of prostate specific antigen (PSA) in a fluoropolymer microfluidic device*" Poonam Gehlot and Kalpita Sidapra appear as co-authors due to their contribution in the set up of MCF smartphone detection during their final undergraduate project. Alexander Edwards appears as a co-author due to his contribution in the manuscript revision.

Table of Contents

List of Figures

List of Tables

Thesis Outlines

Chapter 1 presents a theoretical introduction to the work described in the thesis and is divided in 5 sections:

- Section1.1 introduces the motivations behind the development of microfluidic diagnostics platforms for sensitive quantitation of protein biomarkers at point-of-care (POC) settings and refers the main objectives of this PhD thesis.
- Section 1.2 provides the basic background knowledge about immunoassays and their miniaturisation, which is important for the reader to understand the work carried out in this PhD project.
- Section 1.3 presents an overview of microfluidic immunoassays for protein quantitation field in the past 10 years and discusses the state-of-the-art of several aspects within this field, such as antibody immobilisation, biological matrix interferences, fluid control and detection modes.
- Section 1.4 presents the state-of-the-art of plastic microcapillary films (MCFs) since their invention in 2005, describing previous applications, manufacture process, geometry and optical properties of FEP-Teflon MCF used in immunoassays. Also, a description of all previous work performed with MCF immunoassays can be found in this section.
- Section 1.5 describes some general methodology aspects used for MCF immunoassays and described in more detail in the experimental chapters.

Chapter 2 describes the physical adsorption of antibodies to FEP-Teflon microcapillaries and discusses surface coverage and kinetic aspects of this process as well as their implications in immunoassay performance. Comparison of antibody adsorption aspects onto Linear low-density polyethylene (LLDPE), glass and FEP-Teflon microcapillaries have been made.

Chapter 3 describes the optimisation of HRP enzyme and OPD enzymatic substrate system in solution, which can be applied to immobilised enzymes in miniaturised systems due to the smaller diffusion distance in these environments. The impact of this optimisation in microfluidic immunoassays sensitivity and speed with low cost detection modes is discussed in this chapter.

Chapter 4 presents the effect of antigen continuous flow incubations in capillaries immunoassays and its impact on immunoassay performance. The flow effect is explored for high and low antigen systems.

Chapter 5 presents quantitation of clinical range PSA (prostate specific antigen) in whole blood samples using the Lab in a Briefcase. The Lab in a Briefcase presents a group of small components, including the MCF platform, that allow portable, power free and sensitive PSA quantitation in whole blood in 15 minutes. These results and concept were published in Lab-on-a-Chip (Barbosa et. al., 2014, 14, 2918).

Chapter 6 focus on the development of power free and portable detection mode for MCF assays, using a smartphone camera. Sensitive PSA quantitation was achieved in whole blood samples using colorimetric and fluorescence detection with a smartphone camera. This work was published in Biosensors and Bioelectronics (Barbosa et.al, 2015, 50, 5-14).

Chapter 7 describes the biological matrix interference in MCF immunoassays and discusses strategies for overcoming this interference by manipulating the immobilised antibodies density and sample incubation time. Proof of concept for three antibody-antigen systems, mouse IgG and anti-IgG, PSA and IL-1β sandwich assays, is presented.

Chapter 8 explores particle detection in FEP-Teflon microcapillaries. Carbon nanoparticles and gold nanoparticles were used as labels in the MCF platform for protein quantitation. PSA quantitation from 10 to 100 ng/ml with silver enhanced gold nanoparticles is presented in this chapter.

Chapter 9, the conclusion and future perspectives, presents a summary of the work performed in this PhD thesis and discusses future developments that could be undertaken to further improve automation and sensitive quantitation of biomarkers in the MCF platform at Point-of-Care settings.

Chapter 10 provides a list of all references cited in this thesis.

Glossary of Terms

IA	Immunoassay
MCF	Microcapillary Film
POC	Point-of-Care
PSA	Prostate specific antigen
LF	Lateral Flow
hCG	human chorionic gonadotropin
TnI	Troponin I
FEP	Fluorinated ethylene propylene
ELISA	Enzyme-Linked Immunosorbent Assay
CapAb	Capture Antibody
DetAb	Detection Antibody
CDR's	Complementary-Determining Region
CV	Coefficient of variation
LLoD	Lowe limit of Detection
ULoD	Upper limit of detection
LLoQ	Lower limit of quantitation
MTP	Microtiter Plate
HRP	Horseradish peroxidase
AP	Alkaline Phosphatase
SAV	Surface-area-to-volume ratio
TnT	Troponin T
CRP	C-reactive protein
CEA	Carcinoma embryonic antigen
AFP	α-fetaprotein
PDMS	Polydimethylsiloxane
BSA	Bovine Serum Albumin
PMMA	Poly(methyl methacrylate)
Fc	Constant fragment (antibody)
Fab	Variable fragment (antibody)
TNF-α	Tumor necrosis factor alpha
GA	Glutaraldehyde
LLDPE	Linear low density polyethylene
MSA	Multiple syringe aspirator
PBS	Phosphate buffer saline
OPD	o-Phenylenediamine dihydrochloride
FDA	Food and Drug Administration
4PL	4 Parameter Logistic

1. Introduction

1.1. Research gap and thesis aim

Clinical diagnostics influences about 70% of health care decisions, which means they are the foundation of an effective health care system. Life expectancy has increased massively in recent years due to clinical diagnostics developments. They provide critical physiological or biochemical information that physicians or patients need to take for the best health care decisions, and therefore improve patients' life quality and expectancy. Thus, it is generally believed that diagnostics should be ubiquous, accurate, simple and accessible, allowing every person on the planet to make appropriate decisions about their own health status. However, health care expenses in diagnostics represent only 3 to 5% of total health care budget.[1] Moreover, current diagnostic tests remain complex and rely on expensive equipment, which limits their performance to centralised laboratories and big hospital facilities.

Decentralising diagnostics requires developing diagnostic technologies that are simple, low cost, portable or semi-portable and reliable tests for a wide set of health conditions. Several health conditions, such as cancer, cardiac diseases and infectious diseases (e.g. sepsis), rely on extremely sensitive quantitation of proteins in complex biological samples, such as whole blood. Such evaluation can only be reliably achieved in a controlled laboratory environment utilising sensitive and high precision equipment, which is usually bulky, expensive and demands specialised technical personnel to operate them. In order to achieve diagnostics decentralisation it is therefore necessary to translate laboratory techniques into Point-of-Care (POC) tests or create new technologies capable of detecting important diseases at POC settings.

Diagnostics performance at POC requires the diagnostic test to meet the patient's need and not the other way around. There are several levels of POC testing, from the ones performed by the patient at his home (often called over-the-counter tests) to the ones performed by physicians and nurses in local health care facilities. All levels contribute to diagnostic decentralisation and therefore to increased accessibility and patient informed decisions.

POC testing is a need in both developed and developing countries. In developing countries, the health care facilities accessible to the majority of the population have very basic

laboratory equipment and workers with little training. Moreover, those facilities generally present intermittent electricity with power fluctuations, ambient temperature ranging from 10 to more than 40ºC, dust, wind, pathogens and no acess to pipped water. Thus maintaining and calibrating even moderately complex instruments is challenging. Performing diagnostic tests requires, therefore, a different approach in developed and developing countries.[2]

The role and impact of POC diagnostics differs with the setting. In developed countries POC tests contribute for what is called "personalised medicine", reducing the frequency of hospital visits, travel expenses, loss of work time and above all making patients more responsible for managing their own health conditions. According to some studies,[3] this improves patient adoption to diagnostic and treatment regimes, while reducing the levels of stress, since the patient has more control on his own well being.[2] POC tests also contribute for the autonomy of patients towards the healthcare systems, which improves their overall efficiency, as the patient will only dislocate for a health centre if the diagnostic results are abnormal. Therefore, with less affluence, health care centres can provide a better service to their patients. In developing countries, POC tests dictates patient's treatment but also survival rate, because in many cases they are the only mean of diagnostics available. The majority of the population has to travel large distances to access healthcare facilities. Travel is limited due to poor transport facilities and lack of economical income. Overall, the availability of POC diagnosis for a broad range of diseases will not just complement or improve the efficiency of the current healthcare system, but they are also the only way of increasing life expectancy for living in remote areas.

The targeted diseases for POC tests also vary with regions. Infectious diseases, such as respiratory infections, AIDS and malaria are the main cause of death in developing countries, while in developed countries (e.g. US) the main cause of death is due to cancer and heart diseases.[1] Non-communicable diseases, also known as chronic diseases, are non-contagious diseases responsible for 68% of deaths in 2012 worldwide, according to the fact sheet of the World Health Organization (WHO),[4] and include cardiovascular diseases, cancer, chronic respiratory diseases and diabetes.[5]

According to WHO, all POC diagnostics devices should follow the ASSURED policy: affordable, sensitive (avoid false negative results), specific (avoid false positive results), user-friendly (easy to perform and use non invasive specimens), rapid & robust, equipment-free and delivered (accessible to end users).[6]

A number of POC tests have effectively made a difference on improving the health systems in both developed and developing countries, which are the case of glucose test for diabetes monitoring. In this case, the well-established leader of POC testing is based in a redox-couple-mediated enzymatic oxidation of glucose and aims to detect a concentration of analyte on mM range, which is a much higher concentration than diagnostic markers.[2,7] Another well established technology for POC testing is the Lateral Flow (LF) immunochromatographic assay, which is based in the specific reaction between antigen-antibody and signal detection of antigen-antibody complex. The most successful product based on LF is the pregnancy test which measures the level of hCG (human chorionic gonadotropin) levels, however other LF products that measure ovulation confirmation, HIV, influenza AB and group A of *Streptococcus* bacteria are also commercially available.[2] This diagnostic test also targets antigens present at high concentrations. Some lab-on-a-chip technologies have been approved by FDA (Food and Drug Administration) or/and CE marked, such as iSTAT device for blood chemistries, coagulation and cardiac markers, and the Triage meter for cardiovascular diseases, drugs abuse and water parasites. Nevertheless, these devices have not yet achieved the mass production and commercialisation level of either glucose tests or LF tests.[7]

POC tests remain a need for non-communicable diseases. These health conditions can be treated and the survival rate increases with early diagnostics. Since the 19th century a correlation between organic compounds and certain health conditions has been established, and nowadays a number of measurable analytes and their concentration are used to diagnose certain diseases, but also to determine predisposition or the outcome of the disease (monitoring and prognosis).[8] These analytes are intrinsically different, although they can be grouped into protein, cells, and nucleic acids biomarkers. The type of analyte will define the type of assay performed and therefore the type of POC diagnostic device. Non-communicable diseases are usually diagnosed through protein biomarkers, such as CK-MB, myoglobulin, troponin I and T for cardiovascular diseases (predicting a heart attack or monitoring after a myocardial infarction);[9,10] D-dimer absence in blood can exclude a possible pulmonary embolism;[11] PSA (prostate specific antigen) and CA-125 are used for evaluation and progression of prostate[12] and ovarian[13] cancer, respectively, as well as other type of cancer biomarkers that are currently being developed.[14,15] Infectious diseases like sepsis can also be diagnosed through quantitation of cytokine levels.[16]

Diagnosis through quantitation of protein biomarkers requires sensitivity in the range of concentration nM to fM that cannot be met with existing LF tests.[7,8] For example, the clinical

threshold for Troponin I (TnI) in acute coronary syndrome, established in 2007, is 40 pg/ml of TnI;[17] sepsis diagnosis demands detection levels of cytokines (e.g. IL-6, TNFα, IL-10) in the range of 17 to 70 pg/ml;[16] PSA (prostate specific antigen) established clinical threshold is 4 ng/ml, although cut-off values of 1 ng/ml have been proposed for screening purposes.[18] Consequently, biomarker quantitation is essential for diagnosing non-communicable diseases, which are responsible for the largest number of deaths worldwide.

The main objective of this thesis is to develop protocols for quantitative protein sandwich immunoassays (IA) in a novel microfluidic platform allowing non-comunicable diseases to be detected for POC testing, which presupposes the creation of an ASSURED POC diagnostic platform. This was achieved through miniaturisation of IA in a fluoropolymer Microcapillary Film (MCF). The MCF consists of a parallel array of 10 microcapillaries embedded in a plastic film made of FEP-Teflon, produced by a patented melt-extrusion process, an affordable manufacturing process that uses low cost raw materials, therefore suitable for large scale cost effective fabrication of POC microfluidic devices.

The main objectives of this thesis are:

- To study and characterise passive antibody adsorption onto FEP-Teflon micro-capillaries;
- To study enzyme kinetics in miniaturised capillaries and its effect on assay sensitivity and speed;
- To understand the effect of flow and biological matrix in antibody-antigen binding kinetics and on FEP-Teflon capillaries IA and their input on assay sensitivity;
- To develop an optimised PSA (prostate specific antigen) immunoassay microfluidic test based on fluoropolymer MCF;

To test different optical detection modes (e.g. colorimetric, fluorescent, carbon nanoparticles and gold nanoparticle) and low-cost optoelectronics read-out systems (e.g. Flatbed Scanner and Smartphone) for rapid and sensitive PSA quantitation.

1.2. Fundamentals

1.2.1. Immunoassays: an extremely sensitive bioanalytical tool

An immunoassay (IA) is a very powerful analytical chemical tool that uses antibodies properties to detect and accurately quantify a substance in a complex heterogeneous sample. IAs are one of the most common analytical techniques used in life sciences. Therefore, there is a large range of antibodies specific to a vast range of compounds commercially available. The high affinity between antibody and antigen enables such assays to achieve high sensitivity (in this thesis expressed as a direct correlation of Lower Detection Limit)[19,20], and consequently the detection of very low concentration of antigen or antibody in a sample.[21]

Antibodies (immunoglobulins) are glycoproteins with a unique characteristic, the ability to bind to a large range of molecules and cells, the antigens, with remarkable specificity and high binding strength between the molecule and the antibody. This binding strength is termed affinity.[22]

Antibody properties are intimately related to their structure. Although immunoglobulins can be grouped in five different classes (IgG, IgA, IgM, IgD, IgE) that manifest structure diversity, they all share a monomeric subunit responsible for antigen binding. This monomeric subunit is constituted by two light chains (approximately 220 amino acids) and two heavy chains (450-575 amino acids) linked by disulphide bonds, responsible for stabilizing the molecular structure.[23] The N-terminal domain of the polypeptide light and heavy chains is variable (varies in sequence and number of residues from antibody to antibody) and the C-terminal domain is constant in both chains (Figure 1:1A). The fragment containing the variable domains of light and heavy chains, plus the first constant domains is called the Fab. The constant fragments belonging to the two heavy chains, consisting of CH_2 and CH_3 domains, are called Fc. Carbohydrates have been found in Fc fragment, although their biological functions are not yet known. The segment peptide that joins the Fab and Fc is called hinge (Figure 1:1).[23] The hinge region contributes to antibody flexibility, important for the antigen binding capacity.

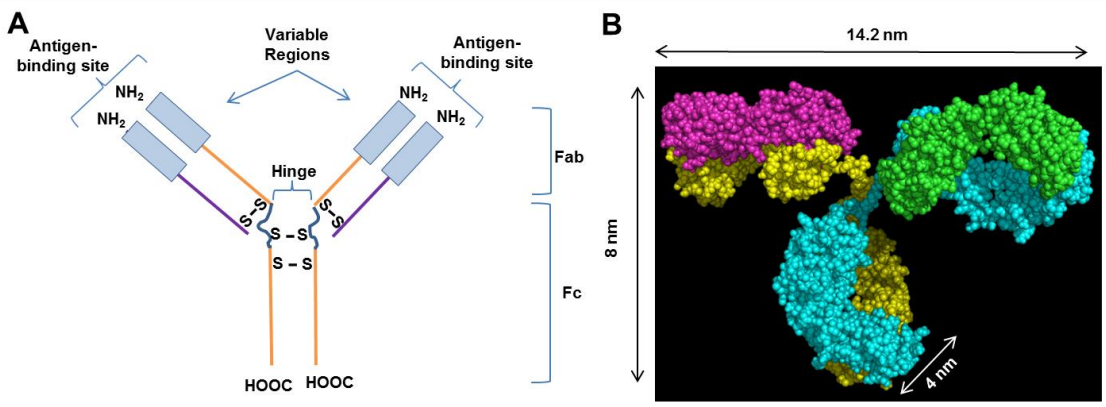

Figure 1:1 – Immunoglobulin G (IgG) structure used in IA.
A Schematic representation of IgG molecule, showing the Fab fragments, with the variable regions (blue rectangles) and constant regions (orange and purple lines), the Fc fragment, composed by constant domains, and the disulphide bonds (-SS-), responsible for the heavy and light chains bonding and the chemical stability of the molecule. **B** Tree dimensional structure of IgG molecule, with approximate dimensions of 14.2 x 8 x 4 nm and relative molecular weight of 150000 Da.[24]

The variable regions along the Fab fragment are involved in antigen binding. At the extremities of variable regions there are looped segments formed by hypervariable regions, which form a cleft in the three-dimensional structure. A specific part of the antigen (antigenic determinant or epitope) contacts with the antibody at this region, which is termed Complementary-Determining Region (CDR). Although the constant domains do not form bonds with the antigen, they are essential to produce the folding and maintaining the integrity of the binding site.[22] Depending on the cleft dimensions more than one epitope, specific part of antigen that binds to the antibody, can bind to a CDR. Antibody-antigen binding happens due to multiple non-covalent intermolecular forces, such as hydrogen bonds, electrostatic, van der Waals and hydrophobic, which although individually weaker than covalent bonds make the antibody-antigen complex stable due to the binding nature multiplicity. The balance or energy summation (strength) between attractive and repulsive forces of an epitope with a CDR or the summation of energy dictates the complex affinity.

The antigen binding specificity to an antibody is the key element for measuring analytes, the target molecule, in IAs. This specificity is given by the amino acids sequence and residues and by the folding of the polypeptide segments in the CDRs. A gene rearrangement process during B-cells differentiation makes possible the existence of a significant variety of antibodies creating specific CDRs to certain epitopes.

Antibodies are produced in mammals due to the presence of an immunogen, a molecule capable of inducing immune response when injected into an animal. An immunogen presents several epitopes, which allows the production of several antibodies specific to each epitope, generating a mixture of antibodies with different binding affinities and specificities. These antibodies are called polyclonal antibodies, since they are produced by more than one clone of B lymphocyte cells. Monoclonal antibodies, on the other hand, are the result of a selected clone of B lymphocyte, recognising only one epitope of the immunogen, therefore presenting similar affinity and specificity.[21,25]

1.2.2. Antibody-antigen equilibrium

IA are based in antibody-antigen interactions, whose understanding through the reaction kinetics is essential for assay development, since they will affect assay parameters, such as speed and sensitivity.

The law of mass action represents the reaction between antibody-antigen, and is defined according to equations (1:1) and (1:2), in the following way:

$$[Ag] + [Ab] \underset{K_{off}}{\overset{K_{on}}{\rightleftharpoons}} [Ag - Ab] \tag{1:1}$$

$$K_{eq} = \frac{K_{on}}{K_{off}} = \frac{[Ag - Ab]}{[Ag].[Ab]} \tag{1:2}$$

where [Ag] is the concentration of antigen, [Ab] is the concentration of antibody, $[\mathrm{Ag} - \mathrm{Ab}]$ is the concentration of antigen-antibody complex, K_{on} is the rate association constant, K_{off} is the rate dissociation constant, and K_{eq} is the equilibrium or affinity constant, which represents the ratio of bond and unbound analyte and antibody, a key feature to understand antibodies performance in IA.

Scatchard represented antibody-antigen equilibrium in equation (1:3), as follows:

$$\frac{B}{F} = K_a(N - B) \tag{1:3}$$

where B is the concentration of bond antibody; F is the concentration of free antibody; K_a is the affinity constant, and (N-B) is the concentration of unoccupied sites.

Antibody affinity is the strength to which a CDR of an antibody binds to a specific epitope on an antigen. This means that high affinity antibodies will move the equilibrium towards the formation of antibody-antigen complex and the quantity of antigen bond at equilibrium will be higher compared with low affinity antibodies. However, antibody affinity is difficult to obtain experimentally as it demands an antigen with only one epitope and one monovalent antibody. Such conditions are hard to get in real world situations, since most of antibodies have at least two CDRs. In addition, polyclonal antibodies bind to all the epitopes of an antigen with different affinities, which means that measuring the affinity constant of a reaction between polyclonal antibodies with an antigen, only gives an average affinity. The practical manifestation of antibody-antigen affinity or the functional antibody-antigen affinity is termed "avidity". Therefore, avidity is the overall strength of an antibody-antigen complex, which is dependent on the affinity of the antibody to the epitope, on the valency of antibody and antigen, and on the structural arrangement of the parts that interact. As the overall strength of antibody-antigen complex is influenced by conformational changes during immobilisation to solid surfaces or CDR distance, these aspects will also affect the avidity of an antibody-antigen complex. Avidity is a better measure of antibody binding in real world situations, because high avidity can compensate for low affinity.[21]

1.2.3. Immunoassays configuration

IAs have numerous applications, for example they can be used to detect pollutants in a water sample,[26] undesirable substances or microorganisms in food,[27] and metabolites, microorganisms and biomarkers in clinical diagnostics.[28] IAs can be homogeneous, if the signal occurs during the immunoreaction, avoiding separation between the bound and unbound immunoreagents, or heterogeneous, if they require separation between immunocomplex and free immunoreagents.[29] Due to the isolation of the antibody-antigen complex from unbound reagents, heterogeneous IA are the most sensitive and widely used for quantitative IA, presenting competitive and non competitive configurations (Figure 1:2).

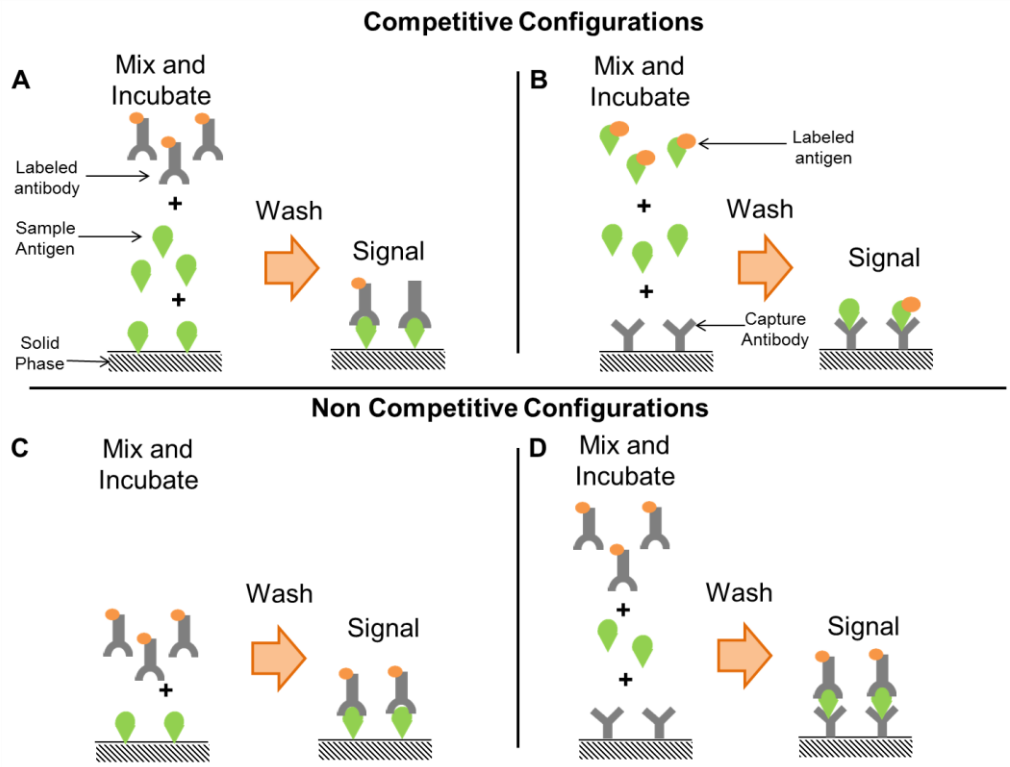

Figure 1:2 – Heterogeneous IA configurations.
A Immobilised antigen approach – immobilised antigen and free antigen compete for anti-antigen label antibody. **B** Immobilised antibody approach – label antigen competes with antigen from the sample for anti-antigen antibody bonding. **C** Immobilised antigen approach – label anti-antigen antibodies bind to immobilised antigen. **D** Sandwich approach – antigen binds to an anti-antigen antibody immobilised and a second label antibody, also specific to the antigen, binds to the complex.

In competitive IA the analyte is mixed with a limited quantity of tracer (label analyte or antigen). The mixed solution is incubated with a limited amount of antibody specific to the analyte. After incubation time, signal of bound or free tracer reagents is measured. In competitive IA the signal is inversely proportional to analyte/antigen concentration.[29]

In non competitive IA the detection antibodies or antigens are in excess, so that after incubation time all analyte/antigen is in an immunocomplex form, being this quantified and related to the analyte. In this case, the signal is directly proportional to the analyte/antigen concentration.[29]

Signal detection is extremely important in all IA configurations. The detection mode can be direct, when the signal-carrying or signal-generating molecule (e.g. radioisotope, enzyme, fluorescent or chemiluminescent label) is attached directly to one of the immunoreactants, or indirect, when the signal-carrying or signal-generating molecule is linked non covalently and

specifically bound to the immunocomplex after the immunoreaction is completed. An example of this happens whenever an enzyme label is conjugated with an avidin molecule and the enzymatic complex binds to the biotinylated detection antibody (DetAb) bound to the analyte/antigen.[29]

1.2.4. Sandwich ELISA

A sandwich ELISA (Enzyme Linked Immunosorbent Assay) immunoassay is a heterogeneous non competitive assay, which uses the sandwich approach and an enzyme as a detection label (Figure 1:3).

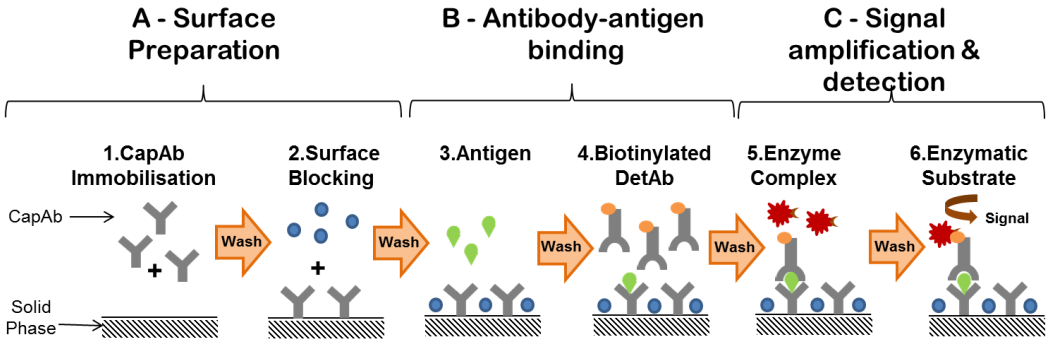

Figure 1:3 – General phases and steps of a sandwich ELISA heterogeneous immunoassay.

Immobilising an antibody on a surface is a feature of heterogeneous IA and is further discussed in this thesis, in chapter 2. The washing procedures are also essential to separate the bound from the unbound antigen and to ensure a better assay performance in terms of sensitivity. Therefore, one or more washing steps are generally performed after each step of an IA. In respect to sensitivity, the main washing steps are the ones related to the analyte, DetAb and enzyme removal, since these reagents are the ones responsible for non-specific binding which will decrease the signal to noise ratio. After immobilising the capture antibody (CapAb) on the surface, a solution containing a non-reactant protein is added in order to cover the remaining surface exposed and another washing step will remove unbound or loosely bound molecules from the surface.

The second stage of a sandwich assay is related to two antibody-antigen reactions, the binding of the antigen to the immobilised antibody and the binding of the DetAb to the bound antigen. These two reactions will be influenced by the antibody-antigen affinity, by the overall avidity of the immobilised antibody layer, which will depend on the concentration of

active CDR's on the antibodies, by diffusion distance from the bulk to the antibody immobilised layer, and by the biological matrix effect, which can frequently interfere in the antibody-antigen binding.

The last stage of a sandwich assay, highlighted in Figure 1:3, is the amplification and detection mode. The detection mode has to be coupled with a read out system (e.g. microtiter plate, microscope, fluorimeter, scanner, etc.) for signal detection and following quantitation, and will depend on it and on the solid support used for the assay. The selected detection system depends whether the assay is label free or uses labels for signal amplification. In ELISA, the label is an enzyme that produces a colorimetric, fluorescent or chemioluminescent signal related to the enzyme concentration, and proportional to the analyte concentration.

1.2.5. ELISA performance

Assays performance must be evaluated from the early stages of development. Certain parameters such as precision (or reproducibility), sensitivity, accuracy and specificity must be assessed during that process.

Precision is the measure of the variability of the signal in the same sample and is expressed in terms of coefficient of variation (CV), which is obtained by the ratio of the average and the standard deviation. Precision can be evaluated in the same assay run or in different runs, termed intra-assay and inter-assay variability, respectively. Intra-assay precision of IAs is generally $\leq 10\%$, while inter-assay precision can be up to 25% due to cumulative error effect during the different steps.[30]

Sensitivity expresses the analyte concentration, which produces a signal that is certain to be different from zero. This parameter is assessed through repeated performance of assay blanks, being the limit of sensitivity or the lower limit of detection (LLoD) given by the blank signal plus 2 or 3 times the blank standard deviation. Sensitivity requirement depends on the application of the assay.

The dynamic range of an assay is the analyte concentration interval within which is possible to quantify the analyte. It is limited by the lower limit of detection (LLoD) and the upper limit of detection (ULoD). The dynamic range requirement of an assay will also depend on the application of the assay. The limit of quantitation is provided by the lowest and highest

concentrations of analyte in a sample that can be determined with acceptable degree of accuracy and precision. Therefore, the lower limit of detection (LLoD) is usually determined by equation (1:4), while the lower limit of quantitation (LLoQ) is usually determined by equation (1:5):[31]

$$LLoD = Blank + (3 * \sigma) \quad (1:4)$$

$$LLoQ = Blank + (10 * \sigma) \quad (1:5)$$

where σ is the standard deviation of 10 measurements.

Accuracy in analytical chemistry defines how close an average of measurements is to the true value. The most common procedure to measure accuracy is the recovery test, which assesses the calibration of an assay and the influence of differences between samples and calibration matrix. It can be performed by testing 3 different analyte spiking concentrations in a biological sample and in buffer, and then dividing the assay value obtained in the biological sample by the actual value obtained in buffer.[31]

Another important aspect of IA analysis is the statistic model used for the assay calibration curve. In this thesis, all IA response curves were fit to the 4PL (4 parameter logistic) model, described in equation (1:6).

$$\text{Response} = \text{A} + \frac{(\text{B} - \text{A})}{1 + (\frac{\text{Conc.}}{\text{C}})^{\text{D}}} \quad (1:6)$$

The four parameters to be estimated are the constants A, B, C, and D, which represent: the top (A) and bottom (B) asymptotes of the model, the slope of the linear region (D), and the EC_{50} (C). This last constant refers to the concentration at which the response is halfway between the top and bottom asymptotes. The term "conc." refers to the analyte concentration.[32]

1.2.6. Considerations of solid-phase immunoassays

Solid phase methods provide simple means of separating bound and free reactants, however antibody-antigen reactions are different in solution and at solid-liquid interfaces, mainly due

to the reactivity of adsorbed antibodies and the kinetic constrains of antibody-antigen reactions at solid-liquid interfaces.[33]

Although many assays use antibody passive adsorption to a surface, the surface is not a passive component in the adsorption process. In fact, adsorbed antibodies usually undergo conformational changes that affect the number of active sites in the antibody monolayer and affect affinity of antibodies CDR's to the antigen. Monoclonal antibodies are more affected by conformational changes during adsorption than polyclonal antibodies, due to their higher specificity.

Antibody-antigen kinetics is also different in solid-phase IA compared to reactions in solution. At solid-liquid interfaces IA are generally diffusion limited and their association rate constants will depend on medium viscosity, reactor geometry and 3D structure of immobilised antibody. Therefore, Stenberg and Nygren (1988) proposed the introduction of the "sticking" coefficient into the equations, meaning that antibody-antigen can only bind when they position themselves in the correct alignment. This alignment is harder to happen when the antibody is immobilised, therefore the association rate constants are much lower in solid-phase IAs.[34]

Another example of kinetic constrain in a solid-phase immunoassay is the presence of a boundary layer, where the antigen is rapidly depleted by the immobilised antibody monolayer and its replenishment is limited by diffusion, creating a quasi-stationary state between bulk solution and solid-phase bound antigen. Since the antibody concentration is very high at the boundary layer the reaction between antibody-antigen is almost irreversible with very low dissociation rates.

Other aspect that makes antibody-antigen solid-phase kinetics different from solution kinetics is the possible presence of fractal clusters (agglomerates of highly organised antibody), which makes the association rate constant to become variable and the dissociation rate constant even lower.[33]

Standard ELISA platform

Microtiter plate (MTP) is the standard platform widely used in ELISA in laboratories around the world. It consists in a matrix of wells organized by columns and rows (Figure 1:4), where the reactions occur. The number and dimensions of wells are variable, but the most commonly found is the 96-wells plate. This consists of 96 wells, arranged in 8 rows by 12 columns. Each well has a maximum capacity of approximately 300 µl of which up to 200 to

250 µl is effectively usable (Figure 1:4). The most commonly used material for MTP manufacture is polystyrene.

IAs in MTP platform are very time consuming, need long incubation times, typically 4 to 10 hours due to mass-transport limitations,[35] and high reagents volumes. They also present a low multiplex potential and detection mode that, although accurate, relies in expensive and non portable equipment.[36]

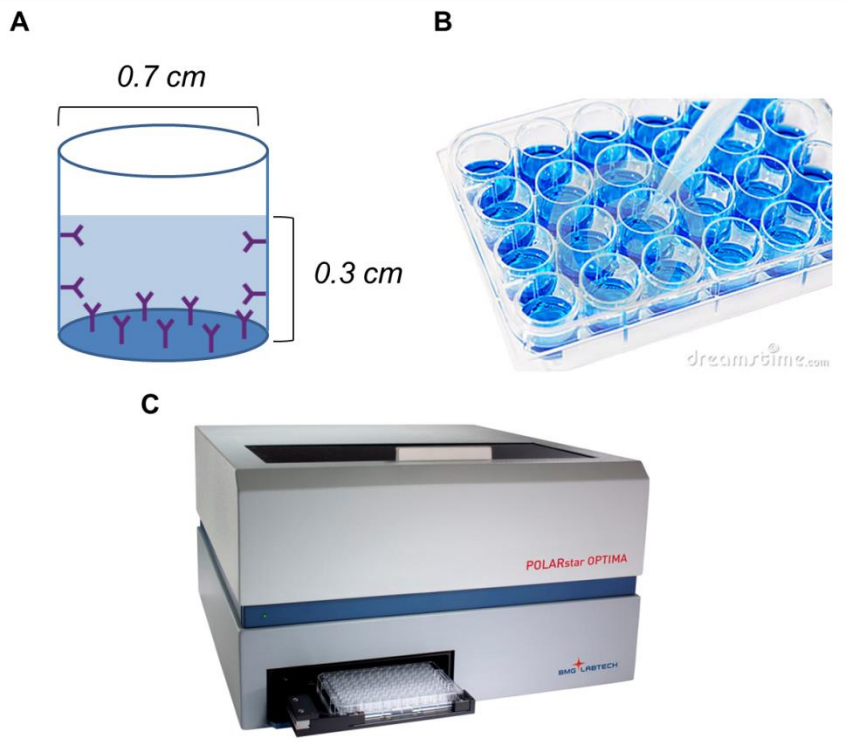

Figure 1:4 – The immunoassay standard Microtiter Platform (MTP).
A Diagram with dimensions of a single well, from the 96-well plate, filled with 100 µl of solution. **B** The 24-well MTP. **C** Microplate reader.

1.2.7. Enzymes: powerful tools for signal amplification in immunoassays

Enzymes have replaced the radioisotopes labels in heterogeneous IA, since they do not exhibit radioactive activity and present higher activity stability.[37,38] Enzymes are natural signal amplifiers, since a single enzyme molecule can convert up to 10^7 molecules of substrate (colorimetric, fluorimetric or chemiluminescent) per minute.[39,40] A drawback in the enzyme performance is related to its susceptibility to interferences (time, temperature, pH, inhibitory substances) during signal generation, while radioactive labels are more robust.

The two most common enzymes used as labels in IAs are horseradish peroxidase (HRP) and alkaline phosphatase (AP). HRP is a 44 KDa oxidoreductase that can be used with a variety of hydrogen donors to reduce hydrogen peroxide (H_2O_2) and this property has been utilised to generate coloured, fluorescent and luminescent products. AP is a 140 KDa enzyme that catalyses the hydrolysis of phosphate esters of primary alcohols, phenols and animes.[28]

Enzymes are biocatalysts that accelerate a substrate conversation, without altering the reaction equilibrium and suffering no transformation. Enzymatic reactions usually display saturation kinetics, since for a given enzyme concentration the reaction rate increases linearly with the substrate concentration up to a certain high concentration of substrate, in which the reaction rate reaches the maximum. In this situation, all enzyme active sites are occupied and the reaction rate is determined by the intrinsic turnover rate of the enzyme, which is the maximum number of enzymatic reactions catalysed per second. This kinetics is described by Michaelis-Menten model, described by equations (1:7) and (1:8) for single substrate reactions:

$$v_0 = \frac{v_{max.}[S]}{K_M + [S]} \qquad (1:7)$$

$$v_{max} = K_{cat}.[E]_{tot} \qquad (1:8)$$

where v_0 is the initial reaction rate, v_{max} is the maximum reaction velocity, $[S]$ is the substrate concentration, K_M is the substrate concentration responsible for ½ of v_{max}, K_{cat} is the enzyme turnover number, and $[E]_{tot}$ is the total enzyme concentration.

Although this model is applied only to single substrate enzymatic reactions, in multi-substrate reactions, by keeping the concentration of one substrate fixed, the enzyme behaves just like a single substrate, therefore Michaelis-Menten kinetic model can also be applied to IAs.

Enzymes are susceptible to inhibitors, substances that reduce or eliminate enzyme activity. Enzyme inhibition can be reversible, if the inhibitor substance is non covalently bound to the enzyme, to the enzyme-substrate complex or both, or irreversible, if the inhibitor changes the enzyme by covalent bound, for example. There are several types of reversible inhibition: competitive, uncompetitive, non-competitive, and mixed. These are fully reviewed elsewhere.[41,42]

In respect to IA it is important to understand how quickly an enzyme becomes saturated with a particular substrate, the maximum rate it can achieve and their optimal reaction conditions. This understanding will allow IA to be performed in less time, be more robust, and with higher sensitivity.

1.2.8. Immunoassay miniaturisation

Microscale IA differ from macroscale IA in several aspects, such as the importance of surface tension, the reduced volume on low concentration samples, and the antibody-antigen kinetics.

Surface tension effects are significant at small scales, and consequently it can affect the distribution of samples or reagents in the reactive surface. In biological fluids, such as blood, serum, and urine, additional intermolecular attractive forces create higher surface tension and increase viscosity.

Other significant difference in miniaturisation of IA relies on the sample volume. Although analyte concentration in the sample is the same, the number of analyte molecules is much lower in small volumes. For example, a sample with 1 nmol/L and a volume of 1 pL only contains 600 molecules, therefore quantitation becomes challenging. Other complication with low sample volumes is the fact that low concentration of analytes increases their dissociation rate from the immobilised antibody, which can affect quantitation.

Beyond the challenges, microscale IA present several advantages, especially concerning the reduced diffusion distance of a molecule, which is responsible decreasing equilibrium time. These aspects are responsible for the fast development of miniaturised IA systems. Quantitative heterogeneous IA miniaturisation has been accomplished particularly in microfluidic systems in the last decade, as the manipulation of liquids in microscale environments allows sequence of reagents to be loaded into a device. The higher surface-area-to-volume (SAV) of microfluidic systems increases the reactivity, making the IAs more sensitive and fast. This is further discussed in the following chapters.

Due to the small scale, the flow in microfluidic devices is generally laminar, and therefore characterised by low Reynolds number, described in equation (1:9), meaning the viscous forces are prevalent compared to inertial forces:

$$R_e = \frac{\rho . v . D_h}{\mu} \qquad (1:9)$$

where ρ (kg/m^3) is the fluid density, v (m/s) is the velocity of the fluid, μ (Ns/m^2) is the fluid viscosity, and D_h (m) is the hydraulic diameter of the channel. The flow in a pipe is laminar for Re $\leq$ 2100 and turbulent when Re $\geq$ 4000. The higher the hydraulic diameter, which in a circular capillary is equal to its diameter, the lower is the Reynolds number at the same flow rate.

The volumetric flow rate will also affect the flow regime in a pipe, as according to equation (1:10), affects superficial flow velocity:

$$Q = v . A \qquad (1:10)$$

where Q (m^3/s) is the volumetric flow rate, v (m/s) is the flow velocity, and A (m^2) is the cross sectional area. Laminar flow presents a typical velocity profile in tubes, showing maximum velocity in the centre and zero velocities at the walls of the tube (Figure 1:5).

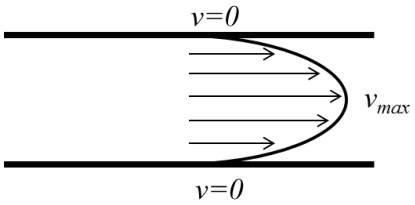

Figure 1:5 – Velocity profile of a fluid in laminar flow regime.

In laminar flow, molecules move parallel to each other and no mixing occurs.

1.3. Microfluidic immunoassays for quantitation of protein biomarkers: state-of-the-art

1.3.1. Summary

Non-communicable diseases, which include cardiovascular diseases, cancer, chronic respiratory diseases and diabetes, that are the mains causes of death worldwide. These chronic clinical conditions are diagnosed based on the quantitation of specific proteins released into the blood stream or other physiological fluids, including urine and saliva. The clinical thresholds for these diagnostics conditions are usual in the fM or pM range, which is challenging for current Point-of-Care (POC) tests. Microfluidic devices appeared around 15 years ago offering unparalleled sensitivity and automation for immunoassays (IA). The microfluidic research community expected them to become widely widespread and commercialised within few years, however this did not happen until now. The present review accounts the development and adoption of microfluidic devices in the last 10 years (from 2005 to 2015), which were able to quantify protein biomarkers in the fM or pM range. It also discusses the aspects of miniaturisation related to protein quantitation in parallel with their technological developments, in the perspective of potential POC diagnostic applications.

1.3.2. Introduction

Microfluidics is a technology characterised by the precise control and manipulation of fluids at the submillimetre scale. Therefore, it usually involves small sample volumes (μL, nL, pL, fL), small size (submilimeter channels or capillaries), reduced energy consumption and controlled microenvironment.

The current application of microfluidic devices covers several areas, including screening conditions for protein crystallization,[43] high throughput screening in drug development,[44] bioanalysis,[45] single cell analysis,[46] and chemical synthesis.[47,48]

Bioanalytical microfluidic systems, including the ones related to quantitation of biomarkers in diagnostics, have rapidly developed in the past ten years, and shown the possibility to quantify low analyte concentrations in complex samples using small, miniaturised devices. Microfluidic devices appear to fulfil the gap between the simple-to-use POC tests and high

precision laboratory bioanalytical techniques. Improving diagnostic has the impact of improving life quality and average life expectancy, since protein biomarkers quantitation are responsible for diagnosing the non-communicable diseases, which are the main cause of death worldwide. Nevertheless, microfluidic diagnostics are not widespread into clinicians' offices and patient's homes, as anticipated by the research community, mainly because microfluidic device fabrication is still not mass produced in a cost-effective way and micorfluidic devices are not capable of reliably detecting lower analytes concentrations. The current ASSURED POC microfluidic devices struggle to quantify low analyte concentrations (<nM) in biological samples,[7] mainly due to technological challenges related to sample preparation and the use of portable detection systems. Biological samples, such as blood or faeces, are complex and their matrix interferes with the bioanalytical procedure, therefore a better understanding is required. Another current bottleneck for the adoption of microfluidic diagnostics in POC is the signal detection, which is still commonly performed with a microscope located off the chip. The use of simpler and cheaper detection systems and readouts implies improving IAs signal amplification and using multiple steps assays, which complicates the IA procedure and makes difficult to implement in POC tests.[48] Therefore, finding new, cost effective, and simple approaches for signal detection or understanding on how simple established readout systems can provide sensitive interrogation is essential for broad POC diagnostics commercialisation. An additional challenge often ignored in microfluidic bioanalytical systems is the fluid actuation and on-chip reagents storage.[48]

Despite the limitations highlighted above, several microfluidic devices were developed with the capability of performing sensitive protein biomarker quantitation. Most of those devices developed to perform heterogeneous (solid phase) sandwich IA, whose fundamentals are discussed in section 1.2. Table 1:1 summarises some of the microfluidic devices reported in literature for biomarker quantitation, specifying some of their aspects related to performance and methodology.

The most commonly targeted biomarkers in POC diagnostics are the cardiac biomarkers: troponin I (TnI), troponin T (TnT), creatine kinase (CK-MB), C-reactive protein (CRP), and myoglobin (Mb). All these markers are used to evaluate the heart function and early detection of myocardial infarction and other cardiac conditions, including acute infarction or severe pulmonary embolism.[49] Other popular biomarkers include cancer biomarkers, like prostate specific antigen (PSA), carcinoma embryonic antigen (CEA), α-fetaprotein (AFP), and cancer

antigen 125. Cytokines (molecules involved in cell signalling) including TNF-α, IL-1, IL-4, IL-6, and IL-1 have been measured for sepsis and other inflammatory condition diagnosis.

Table 1:1 – Microfluidic heterogeneous IA for protein biomarkers quantitation reported between 2005 and 2015.

Microfluidic system and publishing year	Protein biomarker (analyte)	Manufacturing Process	Sample volume (µl)	LLoD[1] ng/ml (or pM)	Sample type	Immobilisation method/surface chemistry	Total assay time (min)	Fluid control	Detection mode	Readout system	Ref.
PDMS microfluidic immunoassay mosaic (2005)	TNF-α[2]	Reactive ion etching	0.6	~0.02 (0.38 pM)	1% BSA in buffer	Adsorption to PDMS	~12	Capillary pump; Continuous flow 30 nL/min)	Fluorescence; Fluorophore conjugation	Fluorescence scanner	[50]
Bio-barcode assay (2006)	PSA[3]	Multilayer Soft lithography	1	1.5 $x10^{-5}$ ($5x10^{-4}$pM)	Goat serum	Covalent binding (gluteraldehyde-amine coupling on magnetic particle surface	<60	Pump; Continuous flow (0.1 µl/min)	Light Scattered; Silver enhanced gold nanoparticles amplification	Verigene ID Scanning system	[51]
Plasma panel capillary immunoassay (2007)	Myoglobin; CK-MB; TnI[4]; FABP[5]	Glass capillaries manufacture	-	1.2 (71pM) 0.6 (7.14pM) 5.6 (233pM) 4 (267 pM)	Diluted plasma (12.5%)	Covalent binding (glass pre-treated with (APDMES)(3-aminopropyltriethoxysilane and glutaraldehyde)	<25 min	-	Chemiluminescence Enzymatic amplification	Photodiode detector	[52]
Dual network microfluidic chip (2008)	TNF-α	Photolitography	5-15	0.045 (0.9 pM)	Human Serum	Covalent binding (Tosylactivated paramagnetic microbeads)	< 60	Pump; Stop flow	Fluorescence; Enzymatic amplification	Inverted fluorescence microscope	[53]
Digital Microfluidic Platform (2008)	Human Insulin; IL-6[6]	Photolitography	<5	-	Buffer	Adsorption to hydrophobised glass surfaces with Teflon AF	7	Magnetic bead manipulation; Batch incubation	Chemiluminescence; Enzymatic amplification	Photomultiplier tube	[54]
Optomagnetic Immunoassay Technology (2009)	TnI	Injection moulding	1	0.16 (3 pM)	Non diluted plasma	Adsorption to plastic surfaces	5	Magnetic particle control; Stop flow	Label free; No amplification system;	Total internal reflexion biosensor and a CCD camera	[55]
PDMS microfluidic assay capillary driven (2009)	CRP[7]	Photo-lithography and photoplotted polymer masks	5	1 (9 pM)	Human Serum	Adsorption to Si wafers	14	Capillary Pump; Continuous flow (82 nL/min)	Fluorescence; Fluorophore conjugation	Fluorescence Microscope	[56]
BioCD protein array (2009)	PSA	-	-	4 (133 pM)	Diluted human serum (1:4)	Covalent binding (triethoxysilylbutyraldehyde (TESBA) cross-linking agent)	<120	Pipetting; Stop flow	Optical Interferometry (label free)	BioCD scanning system	[57]
Immuno-pillar microfluidic assay (2010)	CRP AFP[8] PSA	Injection moulding	0.25	0.1 (0.9, 1.5, 3.3 pM)	Human Serum	Adsorption to polystyrene beads	12	Pipetting Batch incubation	Fluorescence Fluorophore conjugation	Inverted Fluorescence Microscope	[58]
Microbead assay in a plastic chip (2010)	IL-8[9] Insulin	Hot embossing	3.3	-	-	Adsorption to magnetic particles	>65	Pump; Continuous flow (0.11 µL/min)	Fluorescence detection; Fluorophore conjugation	Epi-fluorescence upright microscope	[59]
Three dimensional helical glass tube with magnetic particles (2011)	CEA[10]	-	30	$4x10^{-3}$ (0.02 pM)	Buffer	Covalent binding (paramagnetic spheres coated with epoxy group)	8	Pump; Stop flow	Chemiluminescence; Gold nanoparticles functionalised with DNAzyme	Spectofluoro-meter	[60]
Flow through detection cell with magnetic graphene nanosheets (2011)	CEA AFP	-	200	$1x10^{-3}$ (0.005 and 14.7 pM)	Buffer	Covalent binding (GOPS onto magnetic graphene nanosheets)	<30	Pump; Stop flow	Eletrochemical	Electro-chemical analyser	[61]

Table 1:1 – Microfluidic heterogeneous IA for protein biomarkers quantitation reported between 2005 and 2015 (continuation).

Microfluidic system and publishing year	Protein biomarker (analyte)	Manufacturing Process	Sample volume (µl)	LLoD[1] ng/ml (or pM)	Sample type	Immobilisation method/surface chemistry	Total assay time (min)	Fluid control	Detection mode	Readout system	Ref.
Spiral flow based separation microfluidic assay (2011)	TnT[11]	Rapid prototyping techniques	1.5	10-100 (278-2780 pM)	Whole blood (microfluidc device include flow based separation channel)	Adsorption to cyclic olefin copolymer	5	Syringe with a pressure gauge Stop flow	Chemiluminsecence; Enzymatic amplification	Photomultiplier tube and oscilloscope	[62]
Silicon photonic microring resonator (2011)	CEA	Silicon-on-insulator	-	25 (125 pM)	100% FBS (fetal bovine serum)	Covalent (hydrazone-bond-formation chemistry)	30	Pump; Continuous flow (10 to 30 µL/min)	Label free (measure shifts in microring resonance)	Instrument that measures microring resonance	[62]
Silicon photonic microring resonator (2011)	CRP	Silicon-on-insulator	<10	0.02 (200 fM)	Diluted serum and plasma	Covalent (hydrazone-bond-formation chemistry)	~60	Pump; Continuous flow (10-30 µL/min)	Resonance amplification through streptavidin coated beads (~10µm diameter)	Instrument that measures microring resonance	[63]
Microfluidic Nanoelectrode array (2011)	PSA	UV lithography, electron-beam evaporation, and lift-off	0.18	0.01 (0.33 pM)	Buffer	Covalent binding (self assembled thiols monolayer to Au surface bound to a linker complex of metalized peptide nucleic acid conjugated with antibody)	~5	Pump; Stop flow	Electrochemical; Enzymatic amplification: glucose oxidase PSA conjugated)	Custom built potentiostat, remote source meter, shielded probe station	[64]
Lab-on-paper (2011)	AFP; Cancer antigen 125; CEA	Paper manufacturing	4	0.06 (0.9 pM) $6.6x10^{7}$ ($3.3x10^{8}$ pM) 0.05 (0.25 pM)	Buffer	Covalent binding (chitosan coating and glutaraldehyde cross-linking)	~6	Passive flow; Stop flow	Chemiluminescence; Enzymatic amplification	Luminescence analyser	[65]
Microfluidic Microtiter Plate (2012)	PSA IL-4[12]	Injecting moulding	5	0.016 (0.5 pM) $2x10^{-4}$ (0.02pM)	Buffer	Adsorption to polystyrene	120	Gravity; Stop flow	Chemifluorescence; Enzymatic amplification	Fluorescence plate reader	[66]
Multiplexed magnetic bead assay (2012)	IL-6 TNF-α	Soft lithography of PDMS	5	0.01 (0.47 pM) to 1 (47.6 pM)	Buffer	Covalent binding (carboxyl terminated beads with Sulfo-NHS and EDC chemistry)	~12	Pump; Continuous flow rate (1 µL/min)	Fluorescence; Fluorophore conjugation	Flow cytometer	[67]
Superparamagnetic beads (SPMBs) pattern-based immunoassay (2013)	CEA AFP	Soft lithography, electroplated nickel	~50	3.5 (17.5 pM) 3.9 (57.4 pM)	Serum	Covalent binding (iron oxide nanoparticles as the core with carboxyl groups on the surface)	40	Magnetic field manipulation; Stop flow	Fluorescence; Quantum dots	ICCD camera	[68]
Immunoassay glass capillaries with ZnO nanorodes (2013)	PSA AFP CEA	Glass capillaries manufacture	-	1 (33.3 pM) 5 (73.5 pM) 5 (25 pM)	Diluted human serum (10%)	Covalent binding (adding GPTS to ZnO nanorodes)	30	Pump; Continuous flow (50 µl/min)	Fluorescence; Fluorophore conjugation	Home made fluorescence read out	[69]
Power-free chip enzyme immunoassay (2013)	PSA	Laser cutting	115	3.2 (107 pM)	Non diluted human serum	Covalent binding (APTMS functionalisation of magnetic particles)	30	Magnetic field manipulation; Stop flow	Colorimetric Enzymatic amplification;	Cellphone camera	[70]

Table 1:1 – Microfluidic heterogeneous IA for protein biomarkers quantitation reported between 2005 and 2015 (continuation).

Microfluidic system and publishing year	Protein biomarker (analyte)	Manufacturing Process	Sample volume (µl)	LLoD[1] ng/ml (or pM)	Sample type	Immobilisation method/surface chemistry	Total assay time (min)	Fluid control	Detection mode	Readout system	Ref.
Silicon porous microarray (2013)	PSA	Double sided photolithography and chemical anisotropic wet-etching using KOH	-	1.7 (56.7 pM)	Whole blood (integrated acousto-phoresis-based separation of plasma)	Adsorption to porous silicon chips	15	Pump; Continuous flow (50 µl/min)	Fluorescence; Fluorophore conjugation	Confocal Microscope	[71]
Gold/Graphene origami immunosensor (2013)	CEA	Paper manufacturing	2	$8x10^{-4}$ (0.004 pM)	Human serum	Adsorption to gold/graphene	~60	Passive flow; Stop flow	Electrochemical	Photomultiplier tube	[72]
Autonomus capillary system (2014)	TnI	Laser etching	15	0.024 (1 pM)	Buffer	Covalent binding (PMMA with APTES and cross linked glutaraldehyde)	7 to 9	Capillary pump; Continuous flow assay (0.32 nL/min)	Fluorescence labelling	House built fluorescence reader	[73]
Microfluidic multilayer array (2014)	PSA TNF-α IL-1β IL-6	Soft litography	5 nL	0.03 0.052 0.017 0.021 (1pM)	Serum	Covalent to coated glass slides with epoxysilane	14	Pipetting; Stop flow	Fluorescence; Fluorophore conjugation	Fluorescence Microarray scanner	[74]
3-dimensional paper immunoassay (2014)	hCG[13]	-	20	$2.4\ x10^{5}$ ($6.7x10^{6}$ pM)[14]	Urine	Adsorption (hydrophilic nylon membrane)	10	Passive flow; Stop flow	Colloidal Gold-nanoparticles	Flatbed Scanner	[75]
Microfluidic microarray immunoassays (2014)	IL-6 IL-1β TNF-α PSA	Multilayer-soft-lithography	5	0.084 (4 pM) 0.07 (4 pM) 1.6 (30 pM) 0.45 (15 pM) 4 pM	Buffer	Covalent (glass slides with epoxy silane)	< 3 h	Pipetting; Stop flow	Fluorescence; Fluorophore conjugation	Fluorescence Microarray Scanner	[76]
Microtiter Graphene based immunoassay (2014)	CRP	Injection moulding	-	0.07 (0.6 pM)	Diluted whole blood and plasma	Covalent binding (graphene nanoplatelets and APTES to polystyrene surface)	< 30	Pipetting; Batch incubation	Colorimetric; Enzymatic amplification	Smartphone	[77]
Lab-on-a-disc with TiO_2 fibrous mat (2015)	CRP TnI	CNC Micromachining	10	$8x10^{-4}$ (~6 fM) 0.037 (1.5pM)	Whole blood (blood cell separation on the disc)	Covalent binding (PDMS coated with silicon and nanofibers of TiO_2 treated with GPDES	30	Rotation actuation; Stop flow	Chemiluminescence; Enzymatic amplification	Home built detection system with cooled PMT module and CCD camera	[78]
Surface plasmon resonance-based immunoassay (2015)	CRP	-	50	1.2 (11 pM)	Diluted (1:1000) whole blood, serum and plasma	Affinity binding (protein A/G covalently bound to the surface)	3	Pump; Continuous flow (10 µL/min)	Label free (Surface plasmon resonance)	BIAcore surface plasmon resonance	[79]

Notes: [1] LLoD – Lower limit of quantitation; [2] TNF-α – Tumor necrosis factor alpha; [3] PSA – Prostate Specific Antigen; [4] TnI – Troponin I; [5] FABP - Fatty-acid-binding proteins; [6] IL-6 – Interleukin 6; [7] CRP – C-reactive protein; [8] AFP - α-fetoprotein; [9] IL-8 - Interleukin-8; [10] CEA - Carcinoma embryonic antigen; [11] TnT – Troponin T; [12] IL-4 - Interleukin 4; [13] hCG - Human chorionic gonadotropin; [14] This value corresponds to 6.7 mIU/ml, based on 1U equilvalent to 1 µmol/min, and the mass and molar concentrations mentioned in the Table 3:1 corresponding to 1 minute activity.

This review focuses in four key areas essential to achieve ASSURED POC microfluidic devices capable of sensitive protein quantitation: 1) antibody immobilisation, 2) biological matrix interference, 3) fluid control, and 4) detection modes. A brief consideration about the manufacturing process of microfluidic devices and its relevance towards POC applications is also discussed. Additionally, it includes an analysis of microfluidic devices developed since 2005 for protein biomarker quantitation.

1.3.3. Antibody immobilisation

A universal important feature in heterogeneous IA is the presence of a solid phase which enables separation between bound and free reagents. Therefore, the first stage in a sandwich IA is surface preparation, including the capture antibody (CapAb) or antigen immobilisation and the blocking of the remaining binding sites. Immobilised antibodies must have the CDRs (complementary-determining region) available for the targeted analyte/antigen to bind, which means the immobilisation technique has to provide proper antibody orientation. The strength of the binding between antibody-antigen, also called the affinity, will differ depending on the antibody immobilisation process and the surface to which it was immobilised, since denaturation and conformational changes in antibodies can alter the structure of their CDRs.[80] Therefore, in solid phase IAs it is important to consider antibody-antigen avidity,[81] which is the sum of multiple antibody-antigen non covalent interactions.

There are several procedures for immobilising antibodies. The selected protocol usually depends on the microfluidic surface characteristics and on the long-term interactions between the antibodies and the surface. These ultimately impact also on the manufacturing of microfluidic tests and its successful commercialisation.

1.3.3.1. Passive adsorption to surfaces

Passive adsorption to surfaces is the simplest method for immobilising proteins, including antibodies. This requires placing the antibodies in direct contact with the surface, being a surface specific process, where the surface works as a “reactant”, also determining the amount of antibody adsorbed (surface capacity) and the orientation of antibody. The drawbacks of the adsorption mechanism are random orientation and weak

attachment to certain surfaces, since proteins may be removed by some buffers or detergents when performing the assays.[82]

An ideal antibody adsorption surface would have high affinity to the antibody constant fragment (Fc), so that the variable region (Fab), where the antigen binds, remains available for binding. The bond between antibody and surface has to be strong enough, so that the immobilised antibodies and the antibody-antigen complex are not removed during subsequent washings, which would decrease the sensitivity of the assay. However, the binding cannot be strong enough to denature completely the antibody or changing Fab's conformation and antibodies affinity to the antigen. Other important aspect about antibody surface adsorption is the specificity. It is important that the antibody affinity to the surface is higher than the antigen and other matrix proteins affinity to the surface to avoid competition for the binding sites on the surface. Also, higher antibody-antigen affinity compared to the surface-antibody or surface-antigen affinity is required in order to maximise the signal-to-noise ratio, which is directly linked to the sensitivity of the assay.

Plastics are usually preferred as surfaces for passive antibody adsorption. The most common example is the immobilisation of antibodies onto polystyrene Microtiter Plates (MTP), the gold laboratory standard for quantitative IA. Other plastics, such as, polypropylene and polyvinyl chloride (PVC) are also common in the diagnostics industry.[21] Plastics are hydrophobic surfaces, therefore the antibodies adsorb to plastic mainly by hydrophobic interactions, attaching their non-polar domains (CH_3 and CH_2) to the surface and establishing intermolecular bounds.

Some microfluidic devices relying on antibody adsorption onto plastic surfaces were able to successfully quantify protein biomarkers in low concentrations, such as: IL-4 and PSA, with antibody adsorbed onto polystyrene channels;[66] CRP, AFP, and PSA, with polystyrene beads;[58] human insulin and IL-6 with glass surfaces hydrophobised with Teflon AF;[54] and troponin-T by adsorption onto cyclic olefin copolymer.[62]

The use of thermoplastics in microfluidic devices fabrication is not as frequent as the use of silicon, glass and PDMS (polydimethylsiloxane) in academic environments. Thermoplastics are a class of synthetic polymers that exhibit softening behaviour above typical glass transition temperature, resulting from long-range motion of the polymer backbone, while returning to their original chemical state upon cooling. Compared to

more traditional microfluidic materials such as silicon and glass, thermoplastics offer considerable lower raw material and mass manufacturing costs and are, therefore, being used for manufacturing of microfluidic devices.[83]

Although antibody adsorption is a reliable approach for antibody immobilisation, the amount and activity of antibody adsorbed is extremely dependent on the surface used. Therefore, microfluidic devices usually use covalent attachment of antibodies onto surfaces. In contrast, plastics seem to be the surface most common for passive antibody adsorption in microfluidic devices used in protein biomarker quantitation.

Antibodies adsorption to glass appears to occur mainly due to electrostatic interactions. Nevertheless, these interactions do not appear to favour quantitative IA, as they are less strong and might allow multilayer formation, in which adsorbed antibodies become more polar binding to other antibodies, making it undesirable for IA quantitation. Consequently, microfluidic devices fabricated from glass usually use covalent immobilisation procedures.

Silicon is another popular material used for antibody adsorption on microfluidic devices, however, antibodies adsorb less to silicon surfaces due to reversible bonding,[84] being covalent immobilisation also preferred. CRP protein has been quantified with LLoD of 1 ng/ml (9 pM) in an assay using antibody immobilisation onto silicon wafers,[56] and PSA with LLoD of 1.7 ng/ml (56.7 pM), in an integrated acoustic immune affinity using antibody adsorption onto porous silicon chips.[71]

PDMS is a hydrophobic material preferred by microfluidic researchers yet presenting problems related to non-specific adsorption, therefore undesirable for POC microfluidic tests.[85] PDMS immunoassay antibody adsorption was used for sensitive quantitation of TNF-α with a LLoD of 0.02 ng/ml (0.38 pM).[50]Covalent attachment with previous surface modification appears to be the most common approach used for PDMS IAs surfaces.

Detection of hCG (pregnancy hormone) was reported using a hydrophilic nylon membrane based on antibody adsorption with a detection limit of $6.7x10^6$ pM (6.7 mIU/ml). The detection limit of a pregnancy biomarker, even at early pregnancy detection is several orders of magnitude larger than the LLoD required for cancer and cardiac biomarkers.[75]

Antibodies were also passively adsorbed onto gold surfaces, although these are not very common in microfluidic devices for protein quantitation. Nevertheless, the combination of gold and graphene is becoming popular due to potentiometric detection, as it was reported on the gold and graphene origami immunosensor study quantifying CEA with LLoD of $8x10^{-4}$ ng/ml (0.004 pM).[86]

Different surface chemistries promote different types of intermolecular bonds, which interfere with the signal-to-noise ratio. Surfaces properties and chemistries are therefore a paramount to high sensitivity required in biomarkers detection by IAs.

1.3.3.2. Covalent binding

Procedures for covalent immobilisation of antibodies onto surfaces will also depend on the type of surface, since it is necessary to find an intermediate linker to bind the antibody to the surface. Consequently, a wide variety of methods were developed and extensively reviewed by Kim *et al.* [87] Covalent immobilisation is usually regarded as more stable and offering higher surface coverage, important for assay sensitivity, being in theory preferable over passive adsorption. Nevertheless, covalent antibody immobilisation involves complex chemistries that do not guarantee proper antibody orientation and may reduce protein activity by linkage on antibodies active sites. This drawback has to be considered on the early stages of development of POC microfluidic devices.

The majority of recently reported microfluidic devices used for sensitive biomarker quantitation use surface silanization for antibody immobilisation. Silanization is the covering of a surface through self-assembly with organo functional alkoxysilane molecules.[88] Mineral components like mica, glass, and metal oxide surfaces can all be silanized, because they contain hydroxyl groups (-OH), which attack and displace the alkoxy groups on the silane. Typical organo functional alkoxysilanes are APTES ((3-aminopropyl)-triethoxysilane), APDMES ((3-aminopropyl)-dimethyl-ethoxysilane), APTMS ((3-aminopropyl)-trimethoxysilane), GPMES ((3-glycidoxypropyl)-dimethyl-ethoxysilane) and MPTMS ((3-mercaptopropyl)-trimethoxysilane).[88]

Proteins usually have a number of potential immobilising sites. The functional groups of the proteins suitable for covalent binding include: (i) the α-amino groups of the chain and the ε-amino groups of lysine and arginine; (ii) the α-carboxyl groups of the chain end and the β- and γ-carboxyl groups of aspartic and glutamic acids; (iii) the phenol ring

of tyrosine; (iv) the thiol group of cysteine; (v) the hydroxyl groups of serine and threonine; (vi) the imidazole group of histidine; and (vii) the indole group of tryptophan. Details about all this groups are summarised in Table 1:2.[89]

Table 1:2 - Available functional groups in proteins (including antibodies) and functional groups required on the surface for protein immobilisation.[82]

Side groups	Amino acids	Surfaces
$-NH_2$	Lys, hydroxyl-Lys	Carboxylic acid active ester (NHS), Epoxy, Aldehyde
-SH	Cys	Maleimide, Pyridyil disulphide, Vinyl sulfone
-COOH	Asp, Glu	Amine
-OH	Ser, Thr	Epoxy

Antibodies can be directly bound to a salinized surface, which has organo functional alkoxy silanes with amine groups and epoxy groups. This immobilisation technique has been utilised in many devices for protein biomarker quantitation. For example, TiO_2 nanofibers have been treated with GPDES (3-glycidoxypropyl) methyldiethoxysilane, reporting LLoD in serum of $8x10^{-4}$ ng/ml (0.007 pM) for CRP and 0.037 ng/ml(1.5 pM) for TnI (Figure 1:6A).[78] An IA performed in glass capillaries was able to quantify PSA with LLoD of 1 ng/ml (33.3 pM), α-Fetoprotein (AFP) with LLoD of 5 ng/ml (74 pM), and carcinoembryonic antigen (CEA) with LLoD of 5 ng/ml (25 pM), based on antibody covalent binding promoted by adding (3-glycidoxypropyl) trimethoxy silane (GPTS) to ZnO nanorodes.[69] A microfluidic device using magnetic graphene nanosheets was able to quantify CEA and AFP with a LLoD of $1x10^{-3}$ ng/ml (0.005 pM for CEA and 14.7 pM for AFP) using antibody covalent binding to 3-glycidyloxypropyl trimethoxysilane (GOPS) onto graphene nanosheets.[61] A multilayer array using glass slides, silanized with epoxysilane surface coating to promote covalent binding of antibodies, achieved a LLoD of 1 pM for PSA (0.03 ng/ml), TNF-α (0.05 ng/ml), IL-1β (0.017 ng/ml), and IL-6 (0.021 ng/ml) biomarkers.[74] Other microfluidic microarray with the same antibody immobilisation chemistry onto glass slides achieved LLoD of 0.45 ng/ml (15 pM) for PSA, 1.6 ng/ml (30 pM) for TNF-α, 0.07 ng/ml (4 pM) for IL-1β and 0.084 ng/ml (4 PM) for IL-6 biomarkers.[76] PSA was quantified with a

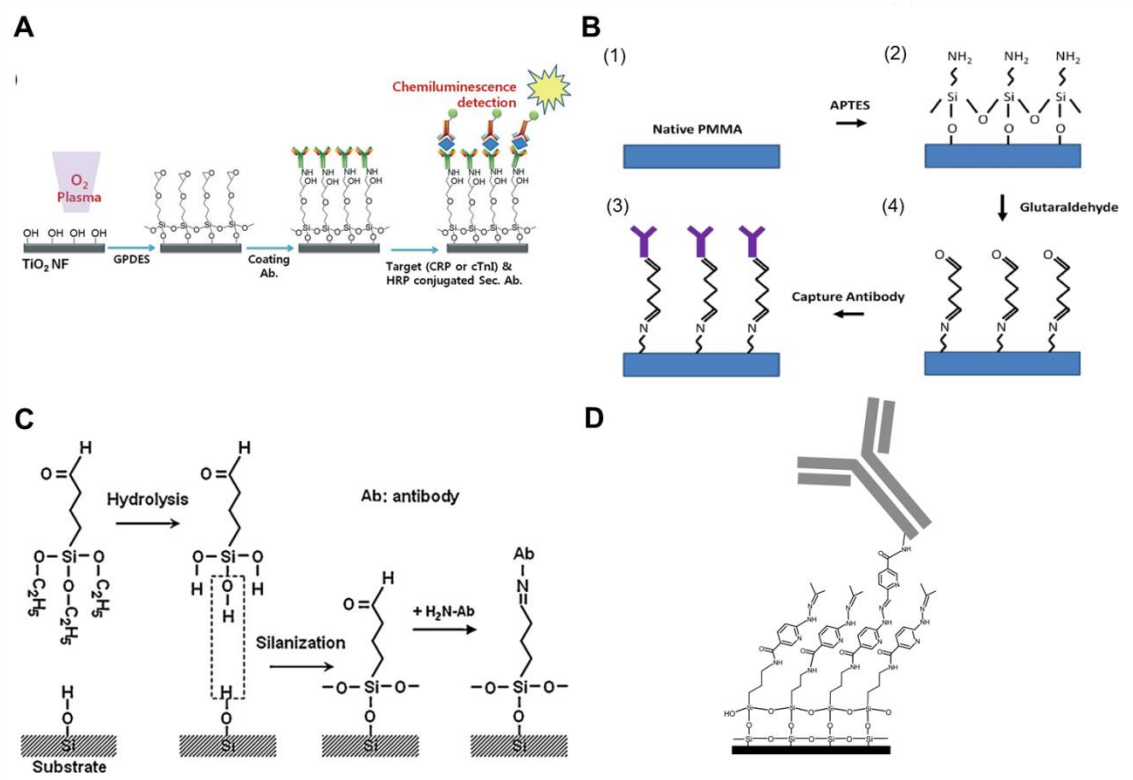

Figure 1:6 – Examples of antibody covalent binding to surface chemistries and strategies for microfluidic devices used in biomarkers quantitation.
A Schematic representation of antibody immobilisation and the immunoassay on the TiO2 NFs, starting with plasma activation of the surface and silanization process using GPDES ((3-glycidoxypropyl) methyldiethoxysilane).[78] **B** Silanization on PMMA (Poly(methyl methacrylate)) using APTES ((3-aminopropyl)-triethoxysilane) followed by glutaraldehyde.[73] **C** Aldehyde modification of SiO_2 surface and antibody immobilisation, using Triethoxysilylbutyraldehyde (TESBA).[57] **D** Silicon surface of microrings treated with APTES ((3-aminopropyl)-triethoxysilane) and S-HyNic (Succinimidyl 6-hydrazinonicotinamide acetone hydrazine) and antibodies modified with succinimidyl 4-formylbenzoate (S-4FB).[90]

LLoD of 3.2 ng/ml (107 pM), using APTMS (3-aminopropyl)-trimethoxysilane coated magnetic nanoparticles. A microtiter platform using graphene nanoplatelets and functionalised with APTES (3-aminopropyl)-triethoxysilane measured CRP with a LLoD of 0.07 ng/ml (0.6 pM).[77]

Silanisation and other surface modification chemistries also use aldehydes as cross linkers for protein immobilisation. Some studies showed that amine derivitization followed by glutaraldehyde (GA) linking yielded supports with greater amounts of immobilised enzyme and activity.[91] Aldehyde is a reactive compound that forms the labile Schiff base with the amine and can be further reduced to form a stable secondary amine bond using $NaCNBH_3$ or $NaBH_4$. GA is a bis-aldehyde compound that has two

reactive ends, and therefore can cross link two amine functional groups, which can be two proteins or a protein and a surface polymer with amine groups, such as the organo functional alkoxy silanes.[87] Consequently, GA has been used as cross linker for antibody immobilisation in microfluidic IA. GA antibody cross linking agent has been used with APTES ((3-Aminopropyl) triethoxysilane) for antibody covalent immobilisation to PMMA (Poly(methylmethacrylate)), yielding a LLoD of 0.024 ng/ml (1 pM) for TnI (Figure 1:6B).[73] The same compounds were used for immobilisation onto glass surfaces obtaining 5.6 ng/ml (233 pM) of LLoD for TnI.[52] The Bio-Barcode assay was able to quantify PSA, utilising glutaraldehyde amino coating to magnetic particles with LLoD =$1.5x10^{-5}$ ng/ml ($5x10^{-4}$ pM)[51] and the bioCD protein array, quantified PSA with LLoD of 4ng/ml (133 pM), utilising aldehyde surface modification of silica (Figure 1:6C).[57] GA cross linking was also used in chitosan surfaces on a lab-on-a-paper device capable of quantifying AFP, cancer antigen 125, and CEA with LLoD of 0.06 ng/ml (0.9pM), $6.7x10^{7}$ ng/ml (0.33 U/ml), and |0.05 ng/ml (0.25 pM), respectively.

1.3.3.3. Combined immobilisation techniques

The combination of covalent binding with passive adsorption or affinity binding is also commonly used in antibody immobilisation. Theoretically this is an approach that allows the highest control of antibody orientation and activity, since a specific and known affinity binding is being promoted. The two most common techniques for antibody immobilisation by affinity binding are the avidin-streptavidin and protein A/G. The first uses the strongest non covalent bond in nature (Kd = 10^{15} M^{-1}), allowing the use of harsh conditions during biochemical assays, while the protein A/G immobilisation, relies on the specific interaction with the Fc constant region of IgG molecules.[82] Recently, conjugating antibodies with DNA,[92] synthetic peptides,[93] or oligonucleotides[94] has also been applied to antibody immobilisation. All these techniques apparently lead to higher immobilised antibody affinity, due to proper orientation and good antibody density control. Nevertheless, only a few examples are found of microfluidic assays using this immobilisation approach. This might be due to complex immobilisation chemistry, since a combination of immobilising techniques must be considered. For example, achieving proper orientation and activity of immobilised protein A is challenging by itself and affects the antibody immobilisation step.[95] A surface plasmon resonance immunoassay detected PSA with a LLoD of

1.2 ng/ml (40 pM) by covalently immobilising protein A/G to a glass surface, and then promoting affinity binding of antibodies. A microfluidic nanoelectrode array was able to quantify PSA with a LLoD of 0.01ng/ml (0.3 pM) using antibodies conjugated with a linker complex of metalized peptide nucleic acid that covalently attached to a self assembled thiols monolayer.[64]

1.3.3.4. The relevance of surface area and surface-area-to-volume ratio

Antibody-antigen equilibrium (discussed in section 1.2) shows that a higher concentration of immobilised CapAb in a reaction medium will push the equilibrium towards the formation of antibody-antigen complex. In order to create a high sensitivity system with the concentration of antigen available very low, around pM or fM, the total amount, the density and the activity of immobilised antibodies are, therefore, extremely important for analyte quantitation. Due to antibody immobilisation, the total amount of antibody is limited, since the antibodies have to be organised on a monolayer and steric hindrance must be avoided. However, surface chemistry is not the only variable to be considered. In addition, the total surface area with immobilised antibody has also to be accounted for. Since antibody immobilisation is a reaction between an empty surface and an antibody solution, the surface-area-to-volume ratio of the microchannel or microcapillary is also important. This depends on the antibody affinity to the surface, which in turn depends on the antibody immobilisation technique. There are several examples of microfluidic platforms that achieved high sensitivity by enhancing the surface area available. For example, a lab-on-a-disc device used antibody immobilised on coated polystyrene beads to yield a LLoD of 0.27 ng/ml (11.3 pM) for TnI, 0.27 ng/ml (1.45 pM) for CRP, and 0.32 ng/ml (37.7 pM) for NTproBNP in whole blood samples.[96] Using a similar device but with electrospun TiO_2 nanofibers printed onto the surface of the chambers, the LLoD achieved for TnI was 0.037 ng/ml (1.5 pM) and for CRP was $8x10^{-4}$ ng/ml (0.007 pM), in whole blood and serum, respectively (Figure 1:7A).[78] This represented a 7-fold increment in LLoD for TnI and about a 300-fold increment on LLoD for CRP, by increasing the overall immobilisation area for CapAb.

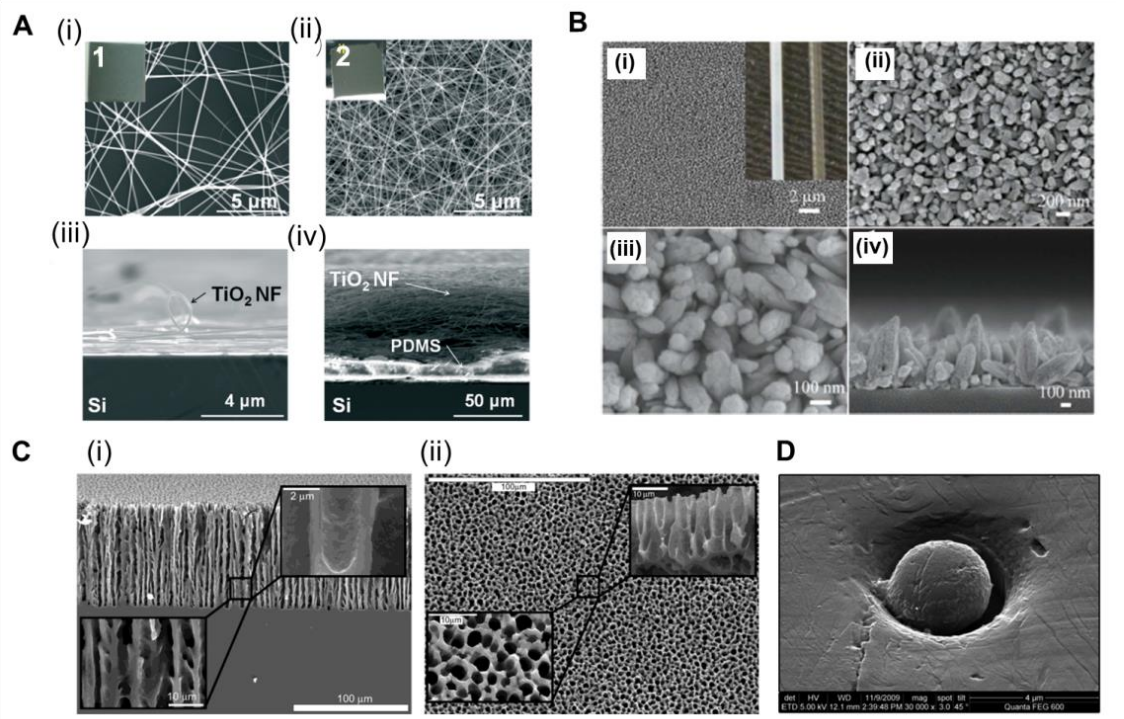

Figure 1:7 – Strategies used for enhancing surface area in microfluidic devices for antibody immobilisation.
A TiO_2 nanofibers used in a Lab-on-a-Disc for CRP and TnI detection. SEM images of the TiO_2 nanofibers (NFs): (i) top and (iii) side views of low-density TiO_2 NFs remaining on the donor Si substrate and (ii) top and (iv) side views of a high-density TiO_2 NF mat transferred to the target Si substrate; insets 1 and 2 are the photographs of the TiO_2 NFs (2 cm × 2 cm).[78] **B** SEM images of ZnO nanorods grown on the inner surface of a glass capillary. (i) to (iii) Top-view; (iv) cross-sectional view; the inset of (i) shows the optical images of a capillary after (left) and before (right) the nanorod growth. **C** SEM images of the porous silicon network. (i) Cross sections and (ii) top views of the rigid sponge like porous silicon network structure.[97] **D** Electron micrograph of a hot embossed microwell containing a microbead. The scale bar of the image is 4 μm, and the magnification is 30 000×.[59]

A glass capillary microfluidic device was able to quantify PSA, AFP, and CEA in serum with a LLoD between 1-5 ng/ml (33.3 pM for PSA, 74 pM for AFP, and 25 pM for CEA) based on ZnO nanorods deposited within the glass capillaries (Figure 1:7B).[69] A porous silicon array was able to increase PSA LLoD from 1.7 ng/ml (56.6 pM)[71] to 800 fg/ml (0.027 pM) just by increasing the CapAb concentration for passive adsorption.[98] This increment of more than 2000 times in PSA sensitivity was only possible due to large surface area of the porous substrate produced by electrochemical dissolution of monocrystalline silicon (Figure 1:7C).[97] A popular approach used for enhancing surface area is to immobilise the antibodies onto small beads (Figure 1:7D).

The antigen/analyte is immobilised onto the beads and detected with a second label antibody that binds to the complex antibody-antigen on the beads,[51,53,58–60,67,70,99] or the secondary antibody immobilised onto the inner surface of channels, which captures the complex bead-antibody-antigen.[55] The beads can be magnetic which facilitates the fluid actuation, the mixing, and the separation of bond from unbound antigen (washing). The use of magnetic beads in microfluidics has been fully reviewed by Tekin *et al*..[100] Other authors have generally reviewed the use of beads in microfluidic IAs.[100]

1.3.4. Sample preparation

Most of the protein biomarkers produced in the human body are released into the blood stream. Sensitive quantitation of these molecules involves therefore sample preparation of a complex biological matrix, such as human whole blood, since the matrix components of biological samples usually interfere with the assay performance.

The use of biological samples is fundamental for validation of assays performance, however most of developed microfluidic IAs still use buffers spiked with protein biomarker.[50,54,60,61,65–67,73,76] Some studies used other types of biological matrices as analyte diluents, as an attempt to mimic human biological matrices, such as non diluted goat serum,[51] or fetal bovine serum,[62] while other studies relied on diluted human whole blood,[79] plasma[52,79] or serum.[57,63,69,79] There are a few microfluidic devices that were able to quantify protein biomarkers in non diluted human plasma[55] or human serum.[53,56,58,70,72,74,99] However, so far there is no reported use of non diluted whole blood samples systematically in biomarkers quantitation in heterogeneous sandwich assays. Microfluidic devices capable of quantifying biomarkers from whole blood samples involved a level of sample preparation embedded in the chip structure. For example, a Lab-on-a-disc was capable of quantifying CRP and TnI from whole blood samples, by separating the red blood cells through centrifugation.[78] A silicon porous microarray integrated an acoustophoresis system for plasma separation from whole blood samples (Figure 1:8A).[71] Other microfluidic devices incorporated a flow based blood separation channel for whole blood protein quantitation (Figure 1:8B).[62]

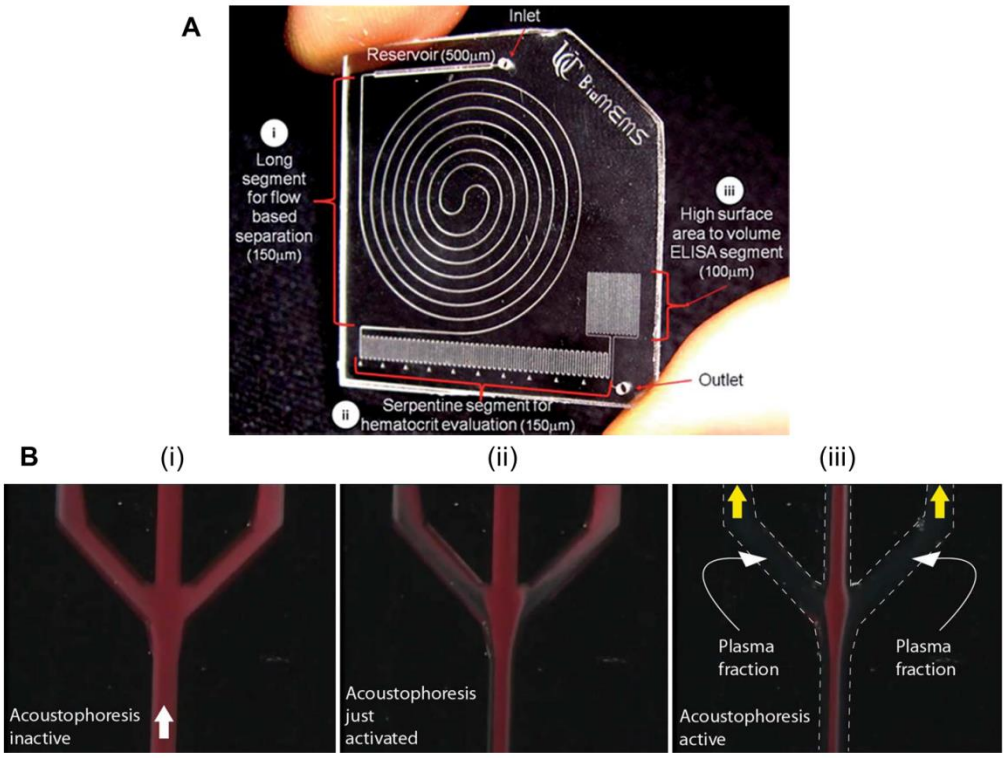

Figure 1:8 – Examples of microfluidic approaches for whole blood sample treatment. **A** Integrated blood analysis chip design fabricated in COC (cyclic olefin copolymer): (i) a blood sample is injected into a long spiral flow-based separation channel; (ii) haematocrit is evaluated based on the number of serpentine switchbacks that are filled with packed erythrocytes; (iii) the blood sample is then flowed into a high surface area to volume ratio ELISA protein quantitation segment where a biomarker of interest is evaluated.[62] **B** Sequence showing the starting phase of plasma production (i) with inactive ultrasound, (ii) starting acoustophoresis, and (iii) continuous phase of plasma production, with the final fractions of red blood cells removed via the central outlet.[71]

1.3.5. Fluid handling control

The usual procedure of sandwich heterogeneous IAs includes multiple sequential reagents addition, with multiple washing steps between reagent incubations. This procedure allows a higher amount of antigen to be bond to the immobilised antibodies due to the extended sample incubation time. This way the equilibrium towards the formation of antibody-antigen complex is favoured, whilst reducing interference of substances like the detection antibodies. When the DetAb binds to the analyte before it binds to the immobilised CapAb the sensitivity of the assay is usually reduced, as the detection-antigen complex takes longer and steric hindrance difficult binding to the immobilised layer.

The washing procedures are important to reduce the non-specific signal from the antigen, DetAb, or enzyme molecules that bond non-specifically to the solid surface. Consequently, sandwich assay requires a multistep procedure to achieve high sensitivity,[7] although attempts were made in a microfluidic device for one step sensitive protein biomarker quantitation. For example, Gervais *et al.* was able to quantify CRP protein with a LLoD of 10 ng/ml (90 pM) in 3 minutes, and < 1 ng/ml (9 pM) in 14 minutes, in PDMS chip involving integrated reagents with flow controlled by a capillary pump.[56] This was possible due to the reduced low flow rates (30 nL/min) promoted by the capillary pump. Consequently, fluid handling and actuation are paramount factors for achieving sensitive protein quantitation in microfluidic IAs.

1.3.5.1. Pressure driven systems

Pressure driven flow systems presuppose the use of an external fluid control actuation. The most common external fluid control in microfluidic systems are flow pumps, such as syringe pumps.

Pumps can deliver a wide range of flow rates from pL/min to ml/min, as well as allowing alternating between stop and continuous flow procedures, which are important for reagents loading and incubation in sandwich assays. They are easily connected to microfluidic channels or capillaries, generating laminar flow systems due to the small dimensions of the system. However, pumps are usually expensive, requiring power supply and compromising the portability of the system. Most of the developed microfluidic devices rely on external pumps for fluid control in order to achieve sensitive protein biomarkers quantitation in sandwich IAs. Few microfluidic devices use procedures with continuous flow of reagents for variable flow rates (Table 1:1),[51,59,62,67,69,79] while others opt to stop the flow for reagents incubation.[53,60,61,64,71] The geometries of these microfluidic devices are variable, however they all comprise microchannels or microcapillaries as reaction chambers.

1.3.5.2. Centrifugal forces

Another type of microfluidic devices uses centrifugal forces for fluid movement in IAs. For example, a Lab-on-a-disc capable of measuring CRP and TnI with a LLoD of 0.27 ng/ml (11.3 pM) and BNP with 0.32 ng/ml (37.6 pM), moves reagents from one chamber to the other, based on a rotation disc and a specific valve actuation.[78,96] Honda

et al. also described a disc based microfluidic platform capable of quantifying AFP, IL-6, and CEA with detection limits of 0.01, 0.026, and 0.26 ng/ml (0.14, 1.24, 1.3 pM), respectively, using centrifugal forces. Other IA have used centrifugal force for reagents actuation and are described in detail by Gorkin *et al.* in their critical review.[101]

1.3.5.3. Magnetic forces

The use of magnetic field is another form of fluid actuation implemented in microfluidic devices, which also allows performing heterogeneous IAs with multiple steps, and has been used in quantitation of protein biomarkers.[102] In these systems the CapAb is usually immobilised onto the magnetic beads surface and then moved through a sequence of chambers containing a series of reagents (Figure 1:9D).[54,99,103] It can also have the magnetic beads containing the antigen already captured binding to another coated onto the inner surface of the channel for further detection.[55]

1.3.5.4. Passive flow systems

In passive flow systems the fluid actuation is not promoted by an external mechanical or magnetic force, but by intrinsic device characteristic, such as surface properties. For example, LF technology relies on hydrophilic strip properties and geometry of nitrocellulose. Fluids move through the nitrocellulose membrane due to capillary forces.

Some microfluidic systems also rely on passive flow, with flow rates determined by the design of the device. Typical driving forces for propelling liquids in passive microfluidics are, for example, chemical gradients on surfaces, osmotic pressure, degassed PDMS,[104] permeation in PDMS,[105] gravity, and capillary forces.[106] However, generally the flow rates, sample volumes, and incubation times are more difficult to control using these systems. Compared to pressure driven systems, the possibility of using wax patterning hydrophobic barriers onto hydrophilic paper allowed patterning microchannels and reaction chambers onto paper creating paper microfluidic devices where fluids move through capillarity. Therefore, a lab-on-a-paper device was able to quantify α-AFP, cancer antigen 125, and CEA with LLoD of 0.06 ng/ml (0.9 pM), $6.6x10^{7}$ ng/ml (0.33 U/ml), and 0.05 ng/ml (0.25 pM), respectively.[65] Also, an origami gold/graphene paper immunosensor was able to quantify CEA with LLoD of $8x10^{-4}$ ng/ml (0.004 pM).[72] The pregnancy hormone, hCG was also quantitated, with an LLoD of $6.7x10^{6}$ pM (6.7 mIU/mL) in a paper microfluidic device (Figure 1:9C).[75]

Paper microfluidic devices achieved good sensitivities for protein quantitation by using printing channels and architecting 3D paper structures to control antibody immobilisation and reagents incubation times. These features are not found in LF devices though, which probably explains their lack on sensitive quantitation. Paper microfluidic diagnostics have been fully reviewed by Yetisen *et al.*.[107]

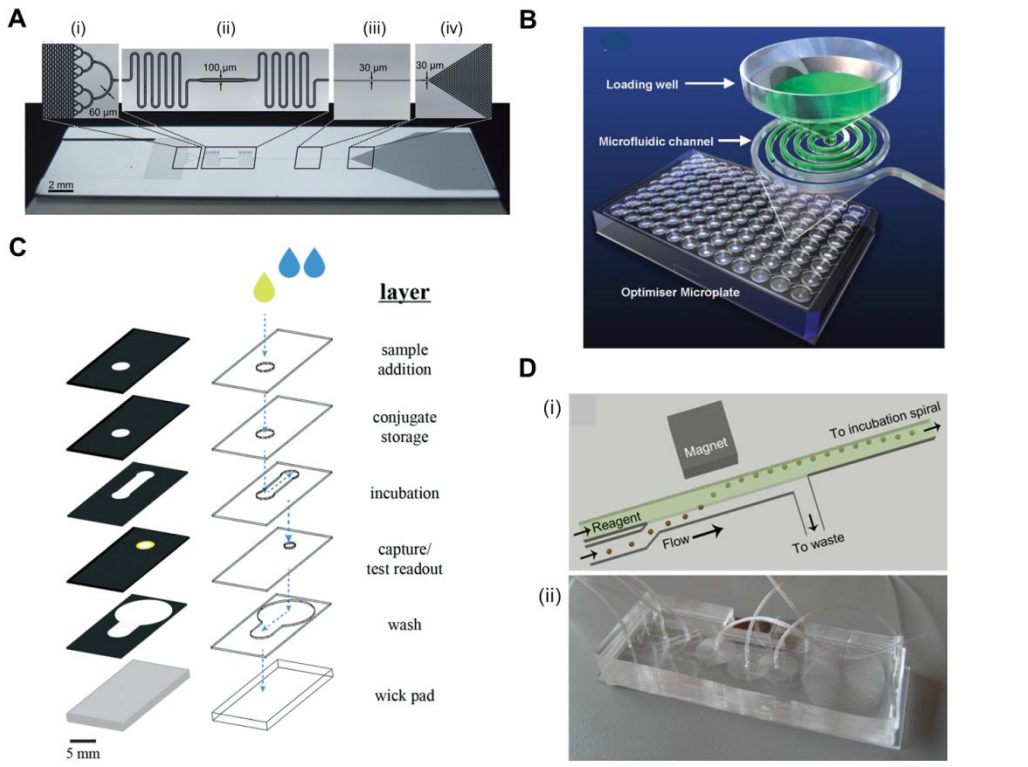

Figure 1:9 – Fluid control approaches implemented in microfluidic devices for protein biomarker quantitation.
A Fluidic control in a microchannel using capillary pumps with average flow rate of 82 nL/min: (i) sample collector ending with hierarchical delay valves; (ii) flow resistors and central deposition zone for detection antibodies; (iii) reaction chamber; and (iv) capillary pump.[56] **B** Microfluidic microtiter plate (optimiser microplate) with gravity controlling the fluid flow.[66] **C** Fluid handling through a 3D microfluidic paper device with hydrophobic patterned barriers (black areas).[75] **D** Magnetic automated bead transfer device: (i) the magnet pulls the beads from the carrier stream to the reagent stream and the current stream is diverted to waste; (ii) assembled three layers PDMS microdevice.[67]

In addition to capillary forces, gravity can allow a fluid to move along a microfluidic surface. A novel microfluidic microtiter plate was able to quantity PSA and IL-4 with LLoD 0.016 ng/ml (0.53 pM) and $2x10^{-4}$ ng/ml (13.3pM), respectively, using gravity as a force for fluid actuation (Figure 1:9B).[66]

A more complex and challenging approach, in terms of microfabrication was proposed by Zimmernann *et al.* and involves a series of autonomous capillary systems with liquids displaced by capillarity with accurate volumes of liquids and precise flow rates. The capillary pumps comprise microstructures of various shapes with dimensions in the range of 15–250 mm, positioned in the capillary pumps to encode a desired capillary pressure and provide a flow rate between 12 and 222 nL/min.[106] Capillary pumps integrated in microfluidic devices have been used to quantify TnI with LLoD of 0.024 ng/ml (1 pM),[73] TNF-α with LLoD of 0.02 ng/ml(0.38 pM),[50]and CRP with an LLoD of 1 ng/ml (9 pM).[56] The last was performed in one step using reagents integrated in the device and the assay triggered only by addition of sample (Figure 1:9A).

1.3.6. Detection modes, signal amplification and readout systems

An essential feature in IAs quantitation is the detection of the antibody-antigen complex. Miniaturised systems, due to the small volumes (pL to μL) used, are able to detect a few molecules up to a thousand molecules. Most heterogeneous IAs use optical detection based on labels, which are molecules that can produce a detectable signal. Depending on the nature of the signal, IAs can be characterised as colorimetric, fluorescent and chemiluminescent. Other IA detection modes are based on electrochemical signal changes or refractive index changes, whose techniques are called label free techniques, since they do not rely on labels.

Colorimetric assays measure antibody-antigen complex through colour intensity of a solution or particles. Colorimetric detection is inherently less sensitive than fluorescence and chemiluminescence, since in order to measure low concentrations of a chromogen, small differences in intensity must be measured at high light intensity, which limits the LLoD. Also, relationship between optical absorbance and intensity of transmitted light is logarithmic. Therefore, at high chromogen concentrations relatively large differences in optical absorbance correspond to small differences in the intensity of transmitted light, which usually corresponds to narrow dynamic range for IAs.[108] Nevertheless, chromogenic substrates offer speed, simplicity, well-established assay chemistry, high quality reagents, and widespread cost-effective readers. For this reason many researchers have been working on finding new ways to increase the performance of colorimetric detection; for example, through enzymatic amplification systems[109,110]

with a detectable chromogen in solution, or through the use other amplification systems, such as gold nanoparticles silver enhancement,[111–113] with the colour intensity given by small particles.

Enzyme amplification depends on biocatalytic capability of these molecules, as a single enzyme molecule can produce up to 10^7 molecules of substrate per minute, increasing the strength of the signal and therefore the sensitivity by a million fold, when compared to a label that produces just a signal event.[39]Colorimetric enzymatic amplification is discussed in more detail in chapter 3.

Silver enhancement is an amplification technique that makes use of larger gold nanoparticles, becoming easier to detect at low concentrations. This technique depends on silver ions adhering to gold nanoparticles surface. The gold has the capacity to catalyse the silver ions reducing to silver atoms promoted by electrons released from the reducing molecules in solution around the gold nanoparticles. Silver atoms have the same catalytic capability of gold nanoparticles, therefore successive layers of silver atoms are deposited increasing the particle size.[112]

To the best of our knowledge, there are no reports of colorimetric microfluidic IA applied to sensitive protein biomarkers quantitation without amplification. A microfluidic paper device was able to quantify hCG, the pregnancy hormone, using only colloidal gold nanoparticles and a flatbed scanner as a readout system, however pregnancy tests LLoD are much higher than cancer and cardiovascular diseases LLoD tests.[75] For example, PSA was quantified in a microfluidic platform using colorimetric enzymatic amplification and a cell phone with LLoD of 3.2 ng/ml (107 pM).[70] CRP was quantified with a LLoD of 0.07 ng/ml (0.6 pM) also based on colorimetric enzymatic amplification and a smartphone camera.[77] The bio-Barcode was able to quantify PSA using silver enhanced gold nanoparticles with a LLoD of $1.5x10^{-5}$ ng/ml ($5x10^{-4}$ pM).[51]

Fluorescence is mostly applied in microfluidic IA for sensitive protein quantitation. This is probably due to the fact that fluorescence detection systems are characteristically more sensitive, as they are measured relatively to the absence of light.[108] Fluorescence occurs due to certain molecules, fluorophores that emit light at a certain wavelength. For the emission to occur fluorophores need to absorb light at a different wavelength that will excite electrons forcing them to move to a higher energetic level. The

excitation and emission wavelength depends on the fluorescent molecule. Several microfluidic devices were able to detect protein biomarkers without the need of amplification systems, using fluorophores as assay labels. However, these IAs used expensive and bulky readout equipment. For example, an immuno-pillar platform was able to quantify CRP, α-AFP, and PSA with a LLoD of 0.1 ng/ml (0.9, 1.5, and 3.3 pM, respectively), using fluorophores (FITC, Alexa Fluor 555, and Dylight 649) directly conjugated to the DetAb and an inverted fluorescence microscope.[58] Some other fluorescent IAs used a combination of different readout systems and fluorophores, all directly conjugated to the DetAb, as described in the following examples. The CRP detection with LLoD of 1 ng/ml (9 pM) was performed by a microfluidic assay using Alexa Fluor 647 and detected with a fluorescence microscope.[56] Interleukin-8 and insulin were quantified in a microfluidic immunoassay using Alexa fluor 488 and an epifluorescence upright microscope.[59] IL-6 and TNF-α were quantitated with a LLoD between 0.01 ng/ml (0.48 pM) and 1 ng/ml (19.2 pM) using phycoerythrin and a Bio-Plex 200 flow cytometer as a readout system.[67] PSA was quantified with 1.7 ng/ml (56.7 pM) LLoD, in a porous silicon substrate, using FITC and a confocal microscope as a readout system.[71]

Fluorescente scanners were also successfully used in protein biomarker quantitation with fluorescent signal detection without signal amplification. For example, TNF-α was detected with a LLoD of 0.02 ng/ml (0.38 pM) in a mosaic microfluidic platform using detection antibodies directly conjugated to fluorophores Cy5 and Alexafluor 647[50]. PSA, TNF-α, IL-1β, and IL-6 were quantitated with LLoD of 1 pM (0.03, 0.05, 0.017, 0.021 pM, respectively) using neutravidin conjugated fluorophores Dylight 488, 550, and 650.[74] Also, IL-6, IL-1β, TNF-α, and PSA were quantified with LLoD between 4 and 30 pM with fluorophores Alexa fluor 647, phycoerythrin, and Alexa fluor 546, directly conjugated to DetAb.[76]

Several attempts to create a portable, low-cost and sensitive fluorescent readout system, capable of reading non-amplified fluorescent signals, have been reported. For example, TnI was quantified with a LLoD of 0.024 ng/ml (1pM) using detection antibodies conjugated with FITC (Fluorescein isothiocyanate) with a house built readout system, with dimensions of 10x7x7 cm^3, an LED (Nichia ultra bright blue LED) for fluorescence excitation, an excitation and emission filter, 10x objectives and a detector (H9858 photosensor module) (Figure 1:10A).[73] PSA, α-AFP, and CEA were quantified

using antibodies directly label with fluorophore Cy3, presenting a LLoD of 1 to 5 ng/ml (14.7 to 25 pM), respectively, with a home made fluorescence readout, consisting of white light emitting diode (LED) light, source, optical filters, an aperture, optical lens, and a photodetector (Figure 1:10B).[69]

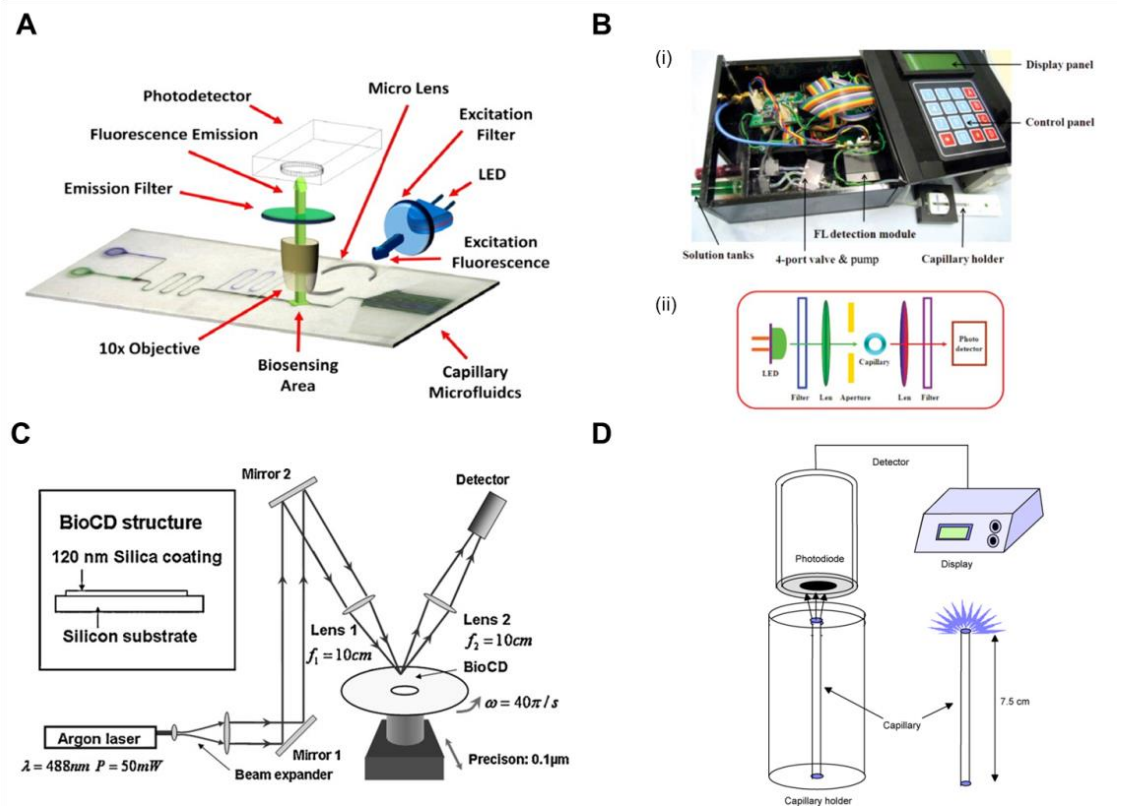

Figure 1:10 – Detection modes and readout systems used in microfluidic devices for protein biomarker quantitation.
A Configuration of fluoroimmunosensing device for autonomous capillary microfluidic signal detection system.[73] **B** Fluorescence detection system in glass microcapillaries: (ii) photograph of the homemade handheld analyzer (ii) and schematic layout of the fluorescence readout module.[69]**C** Changes in reflectance obtained during antibody binding in an immunoassay using system that obtains 2D reflectance map with 20 m transverse resolution on oxide silicon wafers.[57] **D** The set-up for the measurement of chemiluminescence using a photodiodetector and the special stand for the vertical positioning of the capillaries.[52]

Signal amplification in fluorescence systems can be achieved through enzymatic amplification. However this is far less common than the use of directly conjugated fluorophores, probably because the sensitivity is achieved without the need for extra steps in an immunoassay. TNF-α was quantified with LLoD of 0.045 ng/ml (0.86 pM) using streptavidin AP-conjugated and biotinylated antibodies, and an inverted fluorescent microscope.[53]

Fluorescence can be also detected by quantum dots nanocrystals, with quantum mechanical properties and excitation confined to the nanocrystal. For example, CEA and α-AFP were quantified with a LLoD of 3.5 (17.5 pM) and 3.9 (57.3 pM) ng/ml, using streptavidin conjugated to quantum dots and an ICCD camera.[99]

Chemiluminescence is caused by a molecular reaction of two (or more) ground state molecules producing a final molecule in an excited state. The energy in the reactants is transferred to the products and, while being formed they are also excited. In chemiluminescence the signal is usually amplified using enzyme labels (more commonly, HRP) and chemiluminescent substrate (most common is luminol). Many microfluidic devices use chemiluminescence for sensitive protein quantitation. Some examples of chemiluminescence assays are following described, most of them using the DetAb directly conjugated to HRP. For example, CRP and TnI were quantified using HRP with LLoD of $8x10^{-4}$ and 0.037 ng/ml (7 and 1.5 pM), respectively, measuring chemiluminescent signal with a home built system, constituted by cooled PMT module and CCD camera.[78] IL-4 and PSA (LLoD of $2x10^{-4}$ ng/ml, 0.5 pM, and 0.016 ng/ml, 0.02 pM, respectively) were also quantitated based on chemiluminescence, HRP and a microplate fluorescent reader.[66] Insulin and IL-6 have also been quantified by chemiluminescence, using biotinylated AP bond to streptavidin magnetic beads and a photomultiplier tube.[54] CEA has been quantified with a LLoD of 0.041 ng/ml (0.02 pM) with gold nanoparticles functionalised with DNAzyme.[60] Troponin T was quantified with LLoD in the range of 10 to 100 ng/ml (278 to 2780 pM) with HRP, using a photomultiplier and an oscilloscope.[62] Myoglobin, CKmb, TnI and FABP were quantified with LLoD of 1.2, 0.6, 5.6, and 4 ng/ml (71, 7.14, 233, and 267 pM), respectively, based on chemiluminescence, with HRP and a photodiode detector (Figure 1:10D).[52] AFP, Cancer antigen 125, and CEA were quantified with 0.06 ng/ml (0.9 pM), $6.6x10^{7}$ng/ml (0.33 U/ml), and 0.05 ng/ml (0.25 pM) of LLoD, respectively, by chemiluminescence with HRP and a luminescence analyser.[65]

Other detection modes used for microfluidic protein quantitation involved non optical detection modes, such as electrochemical detection, important for opaque substrates and dense optical matrices.[114] These have reported PSA quantitation with 0.01 ng/ml (0.33 pM) using glucose oxidase PSA conjugated in a competitive assay and a custom built potentiostat as readout system.[64] CEA and AFP were quantitated with $1x10^{-3}$ ng/ml

(0.005 and 0.014 pM) of LLoD using electrochemical detection and an electrochemical analyser.[61]

Label free techniques, based on refractive index changes of magnetic beads attachment to a surface were able to quantify TnI with a LLoD of 0.024 ng/ml (1pM), using a total internal reflexion biosensor and a CCD camera.[55] CRP was quantified with a LLoD of 1.2 ng/ml (11 pM), using BIAcore surface plasmon resonance.[79] Label free techniques can be performed with less steps, being usually faster, however not always as sensitive as the label techniques, and most of the times using expensive equipment. For example, a label free technique based on measuring shifts in microring resonance was able to increase sensitivity from µg/ml to pg/ml by amplifying the signal with streptavidin coated microbeads (Figure 1:11).[63]

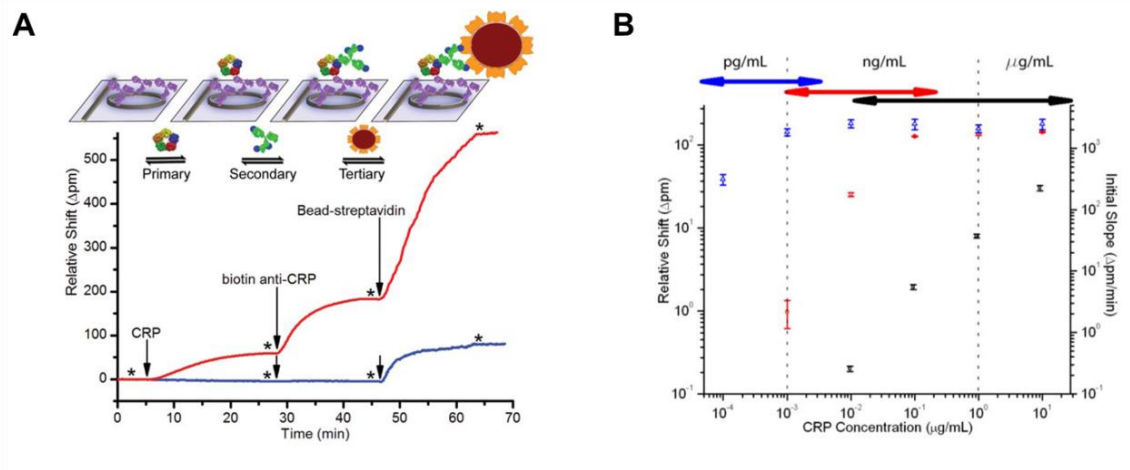

Figure 1:11 – The impact on CRP assay sensitivity and dynamic range of signal amplification on a microring resonator.
A Schematic and real-time data plot showing sequential addition of CRP, biotinylated secondary antibody, and streptavidin-functionalized beads on the microrings resonators. The red trace is 1 µg/ml of CRP and the blue trace is 0.01 µg/ml of CRP. **B** A log–log calibration plot showing the response of the microring resonators to varying concentrations of CRP using the three-step assay. Black squares indicate the initial slope of the primary binding (right axis), red circles indicate secondary antibody shift, and blue triangles indicate bead shift (left axis).[63]

Readout systems are important for sensitive protein quantitation in microfluidic devices, they are mainly responsible for the cost, but also for the higher sensitivity of the assays. Therefore, more than 90% of microfluidic IA use complex, non-portable and expensive readout systems to quantify protein biomarkers. Only a few microfluidic devices have

reported the use of readout systems with low cost optoelectronics compatible with the ASSURED policy, such as a flatbed scanner[75] or a smartphone.[70,77]

1.3.7. Manufacturing of microfluidic devices

Sensitive biomarker quantitation in microfluidic systems is achieved through a complex interaction of effects related to miniaturised sandwich IA and technological instrumentation currently available, which is mainly related to manufacturing processes and detection readout systems. In order to develop ASSURED POC microfluidic devices capable of sensitive protein quantitation all the effects related to IA miniaturisation must be combined in such a way that a low cost detection readout system can be used. The optimisation of an immunoassay in a microfluidic POC platform is very linked to the manufactoring tecnologies available, which set the geometry and materials used, and ultimately the economic cost that ditactes the adoption of the microfluidic POC test. According to Becker[115] the reduced level of microfluidic devices commercialised is related to underestimation of microfluidics manufacturing processes, which are usually overlooked by the designers and the people working the application area. Becker claims that there are no technical barriers to build microfluidic devices, however to be able to compete with convential solutions a thoughtful study of design and manufacturing planning must be performed. For example, the number of produced units will influence the cost of the microfluidic device, therefore for low to medium volumes of manufacturing processes lower initial investments are prefered, such as elastomer casting of soft polymers, including PDMS, and hot embossing. These are the most popular manufacturing techniques in academic environment. If a large volume of products is desired, for example in the field of POC diagnostics, injection molding is more suited, although requiring a high initial investment, it compensates at high product volumes with the low cost of raw materials.[115] Manufacturing techniques and materials used for fabrication of microfluidic devices was criticaly reviewed by Waldbaur *et al*.[116]

An analysis of the manufacturing processes used in microfluidics shows that most protein quantitation devices are fabricated for small scale production. Therefore, soft litography and fast prototyping techniques are most popular manufacturing processes.[50,51,54,56,62,64,67–71,73,74,76,78] This is certainly one of the reasons why

microfluidics are still not widely commercialised, as those tecnhiques lack scalability, and alternative technologies become expensive with a complex manufacturing process involving many steps. Nevertheless, some microfluidic devices already use scalable manufacturing process adequated to mass production of POC diagnostic devices, such as injection molding.[55,58,66,77] Several researchers have developed sensitive quantitation of protein biomarkers in paper due to the low cost of paper manufacturing.[65,72,77]

1.3.8. Current challenges and perspectives

Microfluidic protein quantitation is a promising area for POC diagnostics. The most sensitive analytical tool used for protein quantitation is sandwich IA, which are a type of heterogeneous solid phase IA, relying on antibody-antigen binding. According to fundamental kinetics of antibody-antigen binding, four main areas are responsible for formation of antibody-antigen complex: antibody immobilisation, biological matrix interference, fluid control, and signal detection modes. These are key aspects of microfluidic IA that should be deeply explored to achieve sensitive quantitation. Microfluidic devices have used several methods for antibody immobilisation, including passive adsorption, common in plastic surfaces, covalent binding, where silanization seems to be the base of most of covalent binding techniques and a combination of the two techniques involving with antibody orientated techniques, which is still not widely used. Antibody covalent binding is the most used method for antibody binding to surfaces, resulting in better stability and antibody density. Most microfluidic devices developed for sensitive protein quantitation use buffers or non biological matrices to mimic biological samples in IA, however some present integrated structures for plasma separation for whole blood samples. Fluid control is still mostly done by pumps, which are external instruments to the chip, therefore the reagents are loaded through pressure driven systems capable of stop flow incubation times and multiple steps assays. The most common detection mode is optical fluorescence that uses complex and expensive readout systems such as microscopes, flow cytometers or fluorescent scanners. Signal amplification is often used for microfluidic protein biomarker quantitation and usually related to detection mode and readout system. All of these aspects should be combined integrated in a microfluidic device aiming POC diagnostic applications.

At first sight, it appears that sensitive protein biomarker quantitation is easy and possible in microfluidic systems; however, microfluidic diagnostics are still not much widespread or commercialised. This might be due to the fact that microfluidic researchers are still at the stage of showing that is possible to quantify proteins on chip in academic environments and not concerned about industrial implications. This has been demonstrated by the large amount of microfluidic devices that rely on expensive and bulky external pumps and expensive and non-portable readout systems for IA biomarkers quantitation. In addition, most microfluidic devices are manufactured by prototyping techniques, instead of easily scalable manufacturing processes.

The future of microfluidic protein biomarker quantitation should involve simplifying the manufacture techniques by using low cost raw materials, so that they become scalable and simplifying the immunoassay procedure without compromising the sensitivity, eliminating external powered instruments, such as pumps and microscopes. This might be achieved through the immunoassay procedure and without the need of expensive powered instruments. For example, adding a signal amplification step to the immunoassay might eliminate the need to use an expensive readout system. The same way, using high surface area for antibody immobilisation might eliminate the need for signal amplification. Eliminating the need for sample preparation with better understanding of matrix effect in miniaturised IA performance will equally contribute to reducing the cost of microfluidic devices manufacturing.

Overall, a better understanding of miniaturised IA is essential for designing and planning the future manufacturing of microfluidic devices for affordable POC applications.

1.4. State-of-the-art of Plastic Microcapillary Films (MCFs)

In section 1.3 several microfluidic devices and IA used for protein biomarker quantitation were reviewed. One of the main conclusions is reflected on the urgent need for affordable microfluidic devices capable of sensitive protein quantitation, which can be achieved by mass production manufacturing processes and low cost raw materials.

In this section, the development of novel low cost microfluidic platform called the Microcapillary Film (MCF) is reviewed. MCF consist of a parallel capillary array film continuously manufactured from thermoplastics using a novel melt-extrusion process.[117] The number of capillaries in the film and internal diameter can vary according to the application. Invented at the University of Cambridge, in 2005, the MCF has been developed and demonstrated on a variety of applications (Table 1:3), including heat transfer,[118,119] organic synthesis,[120] measurement and characterisation of residence time distributions,[121] capture of superparamagnetic nanoparticles in a magnetic field,[122,123] and its use in therapeutics,[124] continuous flow transfer hydrogenation,[125] solar heat collector,[126] IA,[127] two-phase flow separation,[128] fast cation-exchange separation of proteins,[129] generation of singlet oxygen in continuous flows,[129] and high-throughput process analytics and photochemical synthesis.[130] Fluoropolymer MCFs are now produced by Lamina Dielectrics Ltd (Billingshurst, West Sussex, UK).

Table 1:3 – Innovations in Microcapillary Films (MCFs) outside this PhD thesis.

Innovations	Characteristics of the MCF	Reference
Extrusion of processable materials with a plurality of capillary channels (2005, 2008)	Variable number (1, 10 and 17 capillary array), variable diameter (from 200 to 750 μm), linear low-density polyethylene (LLDPE), polyvinyl alcohol (PVA) and Polyolefin elastomer	117,131,132
Fluid flow and heat transfer performance (2006)	17 bore MCF with mean diameter 200 μm produced from linear low-density polyethylene (LLDPE)	118
Measurement and characterisation of residence time distributions (2008)	19 capillary array, mean diameter 230 μm, (LLDPE)	121
Fast transient micro-heat exchange (2008)	19 capillary array, hydraulic diameter 200 μm, (LLDPE)	119
Development of voidage and capillary size (2008)	19 capillary array, mean hydraulic diameter 200 μm, (LLDPE)	133
Observation and modelling of capillary flow occlusion resulting from the capture of superparamagnetic nanoparticles in a magnetic field (2008)	19 capillary array, mean hydraulic diameter 200 μm, linear low-density polyethylene (LLDPE)	122
The in-flow capture of superparamagnetic nanoparticles for targeting therapeutics (2008)	19 capillary array, mean hydraulic diameter 410 μm, LLDPE	124
Solar heat colector (2009)	2 strips with 19 capillary array, 200 and 350 μm diameter, (LLDPE)	126
Microdroplet formation within a plastic microcapillary array (2009)	Single capillary used 740 μm internal diameter, LLDPE	134
Fabrication of voided polyethylene microstructures by heat melding of plastic microcapillary films (MCFs) to form microcapillary monoliths (MCMs) (2009)	19 capillary array, mean diameter 230 μm, linear low-density polyethylene (LLDPE)	135
Magnetic capture of superparamagnetic nanoparticles (2009)	19 capillaries mean hydraulic diameter of 210 μm, polyolefin plastomer resin	123
Continuous flow transfer hydrogenation (2010)	19 capillary array, 146 μm mean internal diameter EVOH	125
Organic synthesis (2010)	10 capillary array, mean hydraulic diameters between 150 and 400 μm, LLDPE	120
MCF immunoassays (2010, 2011)	10 capillary array, 200 μm diameter, FEP-Teflon	127,136
Separating aqueous phase slugs from the surrounding organic matrix phase in segmented two phase flow (2011)	1 capillary, 630 μm internal diameter polyolefin eleastomer	128
Fast cation-exchange separation of proteins (2011)	19 capillary array, diameter of 142 μm, EVOH	129
Through-wall mass transport as a modality for safe generation of singlet oxygen in continuous flows (2013)	10 capillaries array, mean internal diameter 104.2 μm ± 10.6 μm, FEP-Teflon	137
Rapid photochemical transformations, high-throughput process analytics and photochemical synthesis (2015)	10 capillaries, 103 to 494 μm, FEP-Teflon	130

1.4.1. The novel melt-extrusion process

Melt-extrusion is a manufacturing process where a raw thermoplastic in the form of nurdles or small beads are melted and shaped continuously.

The concept of extruding MCF was invented in 2004 and first published by Hallmark *et al.* Figure 1:12 shows a heated extrusion line, composed by a single-screw extruder and a gear pump, used in the production of MCFs.

Upon exiting the extrusion die, with a convergent mid-section, the extrudate is taken through a quench bath. Since the extrudate is quenched, it is transported outside the extrusion line. A sensor assembly is placed over the extrudate for monitoring process regime.[117]

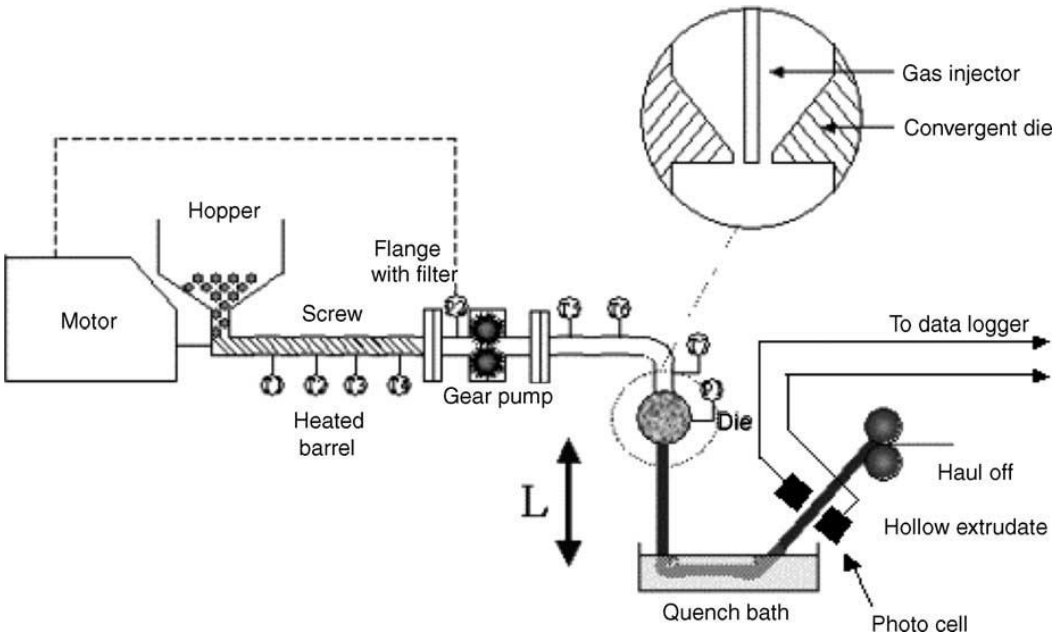

Figure 1:12 – The heated extrusion line used in the manufacturing of MCFs. L is the melt drawing length.[117]

The MCF presents multiple parallel capillaries, therefore multiple injectors have to be assembled within the single die, as shown in Figure 1:12. Assemblies were designed in such a way that the tips of each injector would be flushed with the exit of the die.[117]

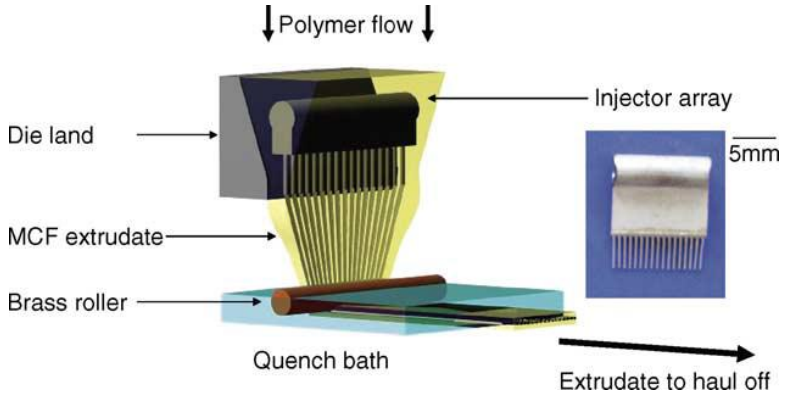

Figure 1:13 - Diagram of the extrusion die used in the manufacturing of MCFs. Above die shown in the inset photograph at the right hand side.[117]

1.4.2. Geometrical and polymer related aspects of the Microcappilary Film (MCF)

Several MCFs materials containing different bore number and diameters were manufactured from a range of thermoplastic materials, including: fluorinated ethylene propylene copolymer (FEP), ethylene vinyl acetate (EVA), ethylene vinyl alcohol (EVOH), linear low-density polyethylene (LLDPE), and cyclic olefin copolymer (COC). Those polymers differ on the refractive index, as shown in Table 1:4.

Table 1:4 – Refractive index of thermoplastics resins used in the manufacturing of MCFs.[136]

Thermoplastic polymer	Polymer Refractive Index
Fluorinated ethylene propylene (FEP)	1.338
Ethylene vinyl acetate (EVA)	1.48
Ethylene vinyl alcohol (EVOH)	1.51-1.52
Linear low-density polyethylene (LLDPE)	1.51
Cyclic olefin copolymer (COC)	1.53

Edwards *et al.* discovered the flat film geometry of MCF contributed to low refractive index of fluoropolymers which favour optical interrogation, with MCFs showing superior transparency compared to individual cylindrical capillaries (Figure 1:14).[127]

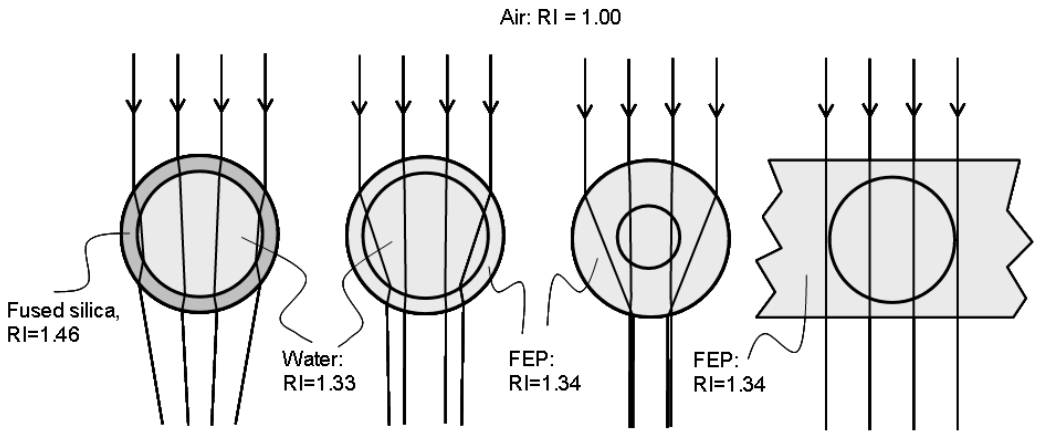

Figure 1:14 – Comparison of optical properties of a fused silica capillary and FEP capillaries with different geometries.[127]

The curvature of individual capillaries results in poor signal-to-noise ratios, with the light being focused at the centre of the capillary with the wall working as a lens. This is fairly independent of the refractive index of the wall material.

Fluoroploymer MCFs are fully transparent to light, and such transparency is paramount to achieve high assay sensitivity with optical detection, since all the light transmitted through the capillaries can be detected with minimal background from the polymer (Figure 1:15A).

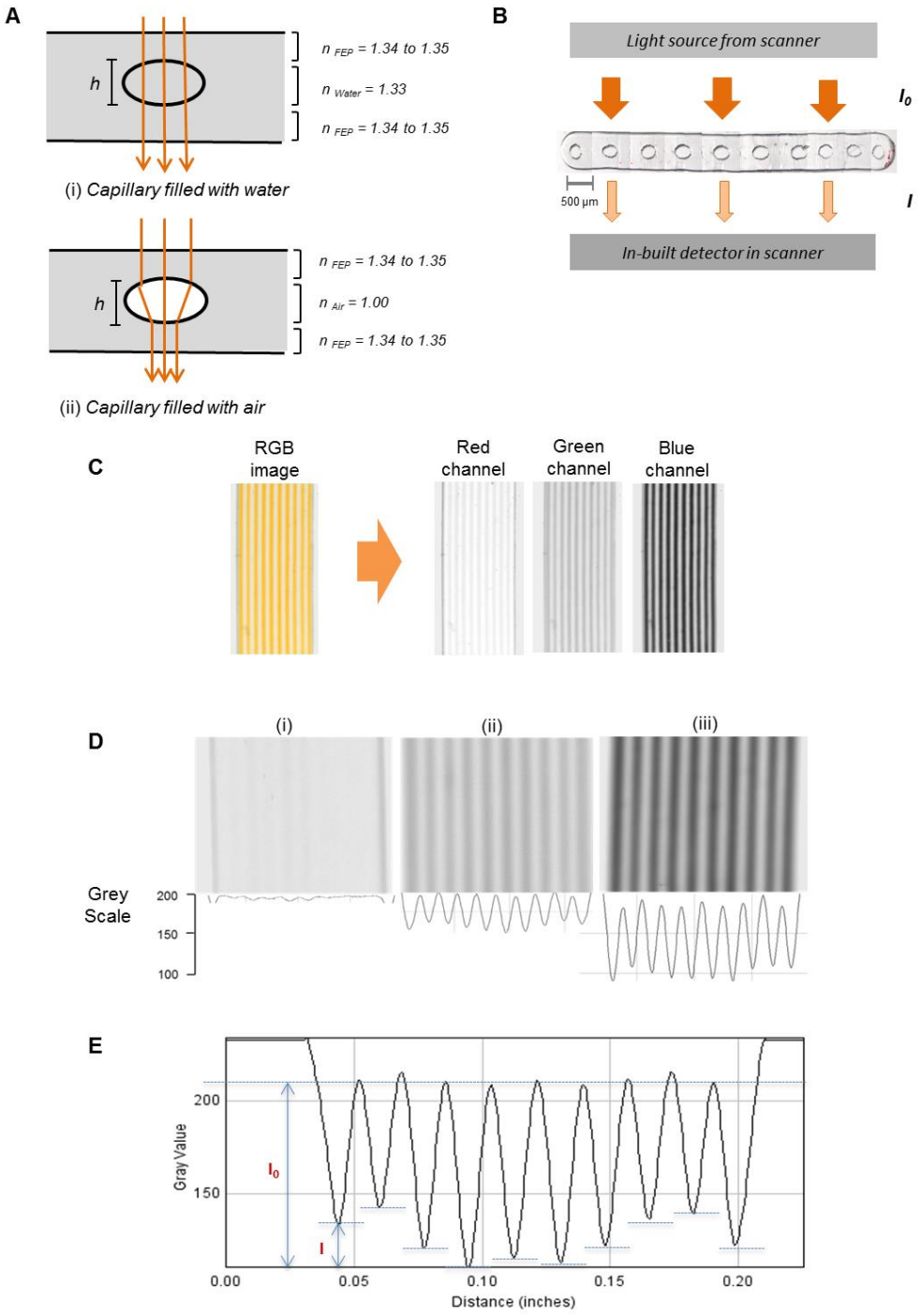

Figure 1:15 – Colorimetric signal quantitation in MCF ELISA using a flatbed scanner. **A** Relevance of geometry and refractive index matching on signal-to-noise ratio. **B** Colorimetric signal quantitation in the fluoropolymer MCF using an off-the-shelf flatbed scanner in transmittance mode. **C** Example of RGB channels separation obtained from ImageJ software, using chromogenic ELISA substrate. **D** Examples of blue channel image from scanned fluoropolymer MCF test strips following completion of a PSA sandwich assay using (i) 0 ng/ml, (ii) 15 ng/ml, and (iii) 60 ng/ml of recombinant protein (data collected in this PhD project and further explained in chapter 5). **E** Absorbance calculated from the grey scale based on Lambert-Beer law, $Abs = -Log_{10}(I/I_0)$.

The unique MCF transparency allows an immunoassay signal to be detected with a simple flatbed scanner (Figure 1:15B). The light emitted by the flatbed scanner lamp (I_0) crosses the MFC and is captured by the detector embedded by the flatbed scanner. When the capillaries are filled with a coloured solution, part of the light is absorbed reducing the transmitted light. The RGB (red, green and blue) image can be split into separate channels using simple image software, such as ImageJ (Figure 1:15C) to fit the absorption peak of the substance. Using the same software it is possible to plot the grey scale across the strip (Figure 1:15D). The grey scale varies from 0 (black) to 255 (white), meaning that every valley shape represents the absorbance in a single capillary. Higher concentrations of coloured solutions result in higher absorbance, therefore deeper valleys. The baseline depends on exposure settings of the detection but ideally kept to grey scale of 255. The ratio between incident light, I_0, and transmitted light, I, yields absorbance values as according to equation (1:11). Based on Lambert-Beer law, the absorbance is proportional to the concentration of the coloured product, as described by equation (1:12):

$$Abs = -log\, I/I_0 \tag{1:11}$$

$$Abs = \varepsilon.c.l \tag{1:12}$$

where I_0 is the incident light intensity, I is the transmitted light intensity, ε is the extinction coefficient of the substance, c is the concentration of the coloured solution and l is the light path distance, which corresponds to the height of a capillary at the centre of the peak signal.

In addition to the unique optical properties, the raw material used for the production of MCFs (thermoplastic resin) is cheap, typically £20/Kg, with a meter of MCF typically weighting 5-10 g. It is possible therefore to manufacture a meter of MCF for a cost around £0.10-0.20 which is sufficient to manufacture hundreds of microfluidic devices.

The capillaries in the film present very similar geometrical shape, creating the possibility for parallel independent micro reactors. However, due to the intrinsic characteristics of the melt-extrusion process, the geometry of the 10 capillaries can present slight differences since the polymer in the middle moves faster than the polymer at the edges of the film, making internal capillaries more elliptical than capillaries on the edges Figure 1:16.

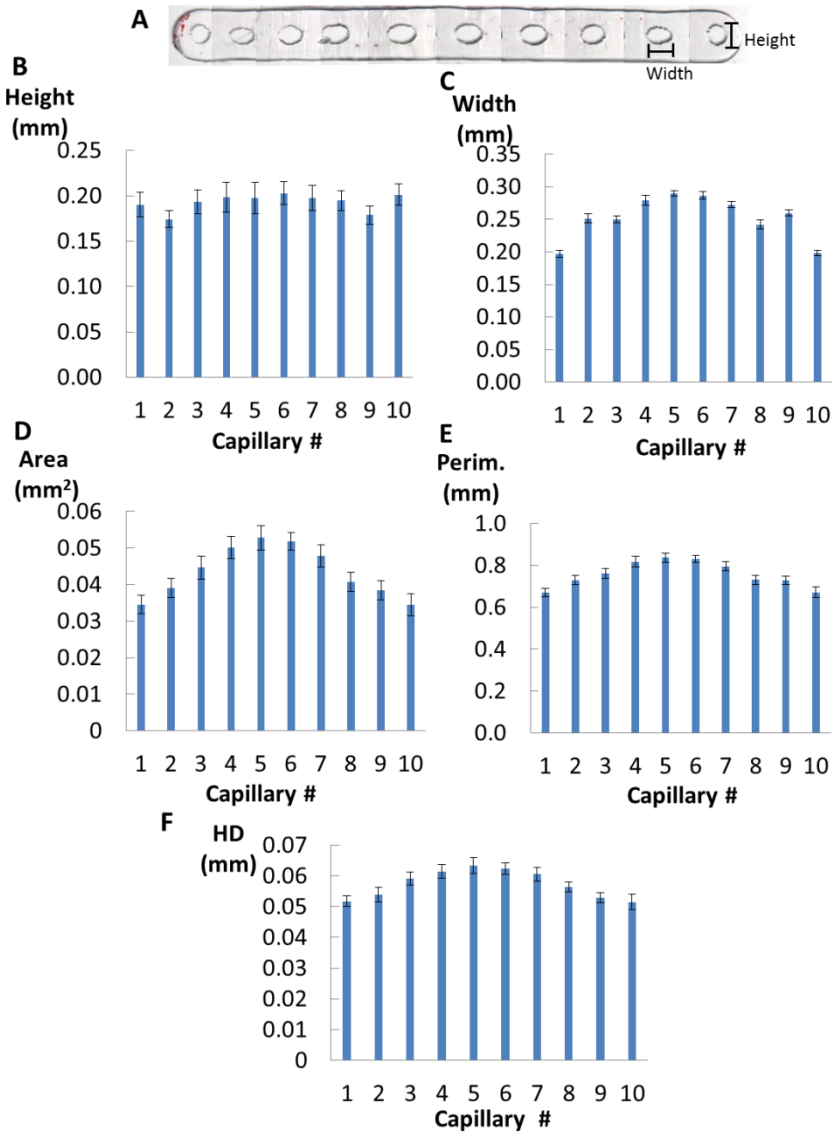

Figure 1:16 - Geometrical characterisation of the MCF batch used for the experimental work presented in this thesis.
A Cross sectional view of the 10 micro capillaries. **B** Capillary height according to MCF capillary number. **C** Capillary width according to MCF capillary number. **D** Capillary area according to MCF capillary number. **E** Capillary perimeter according to MCF capillary number. **F** Capillary hydraulic diameter (HD) according to MCF capillary number.

1.4.3. Preliminary data available for immunoassays in MCFs

The possibility of performing an immunoassay in the MCF was first reported by Edwards *et al.*.[127] The authors used a 10 capillary MCF with inner diameter 211 ± 10 µm, 4.5 ± 0.1 mm wide, and 0.6 ± 0.05 mm thickness (Figure 1:17), which is the same used on this thesis.

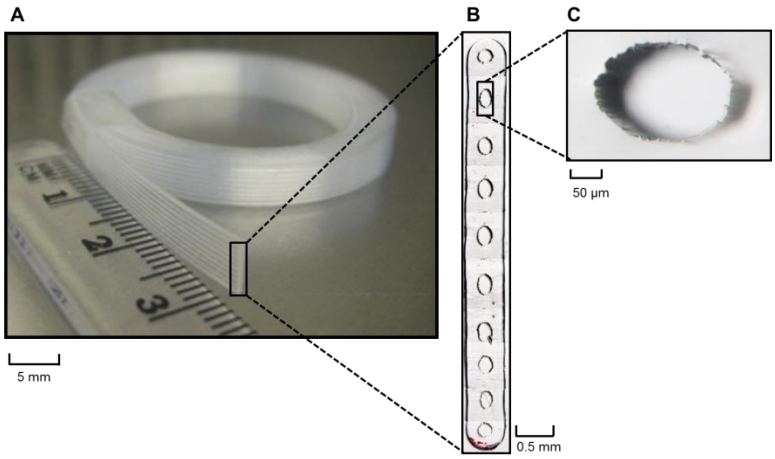

Figure 1:17 – Overview of the FEP-Teflon Microcapillary Film (MCF).
A 3 meters MCF reel. **B** MCF cross section showing the 10 capillaries. **C** Single capillary image.

The authors reported a multiplex device capable of quantifying biomolecules through a colorimetric ELISA, using the quantitation of Hepatitis B antibody, from 1 to 40 ng/ml in a non-competitive immunoassay, as a proof of concept. In this assay the antigen was immobilised by adsorption on the inner wall of the fluoropolymer MCF and a HRP label antibody used for detection. Simultaneous detection of Hepatitis B and FLAG peptide was also performed as a proof of concept for multiplex detection, using a fluorescence substrate and a confocal microscope. That preliminary work showed that proteins effectively adsorb to FEP-Teflon standing the washing steps. The Hepatitis B detection used a flatbed scanner for protein quantitation.

Chahín performed the first sandwich ELISA assay in the MCF platform for quantitation of PSA.[138] Using a chromogenic substrate, a flatbed scanner, and a syringe attached to a silicone tubing, the PSA ELISA was successfully translated from MTP to the fluoropolymer MCF. A set of variables were individually optimised which involved testing the effect of PSA CapAb concentration in the range from 1 to 20 µg/ml, concluding that the optimal concentration of CapAb was 10 µg/ml. Also, the optimal concentration of DetAb reported was 2 µg/ml, although its influence did not appear to significantly affect the overall assay performance. Chaín also optimised sandwich ELISA steps incubation times, concluding that 2 hours of incubation time was sufficient for the CapAb, followed by 10 minutes for the DetAb, and 30 minutes for the enzymatic

substrate. Enzymatic substrate (OPD) concentration was also optimised, being 1 mg/ml the optimal found.[138]

Table 1:5 – Optimised assay conditions found by Chaín for PSA MCF sandwich assay.[138]

Assay Step	Concentration (µg/ml)	Incubation time (min)
CapAb	10	120
Blocking	Reagent diluent	120
PSA	0.0025-0.08	10
DetAb	2	10
Enzyme	2	10
Substrate	1	30

These experiments used only one-concentration reagents per incubation time and these two variables (concentration and incubation time) are extremely related and have a high impact in signal-to-noise of the assay and on assay time. Further in this thesis is demonstrated the importance of DetAb concentration and incubation times for increment of assay signal-to-noise ratio, which is extremely important for sensitivity. Also, for IA optimisation in a platform is important to understand the limits of that platform. For example, it would be important to understand how much antibody active can be adsorbed in the MCF and then work from those ranges. Understanding the enzyme kinetics in miniaturised systems will be extremely important for reducing assay time and increase its sensitivity, as it can be seen further on this thesis.

1.5. General methodological considerations, unique to the work reported in this thesis

The fluid handling in Chaìn's study consisted of a pressured driven system driven by an individual and disposable syringe.[138] This thesis expanded the work conducted by Chaìn, by using different pressure driven fluid handling systems, such as the multiple syringe aspirator (MSA) device and peristaltic pumps (Figure 1:18). More details about the use of these fluid handling mechanisms are given in chapters 2 to 9.

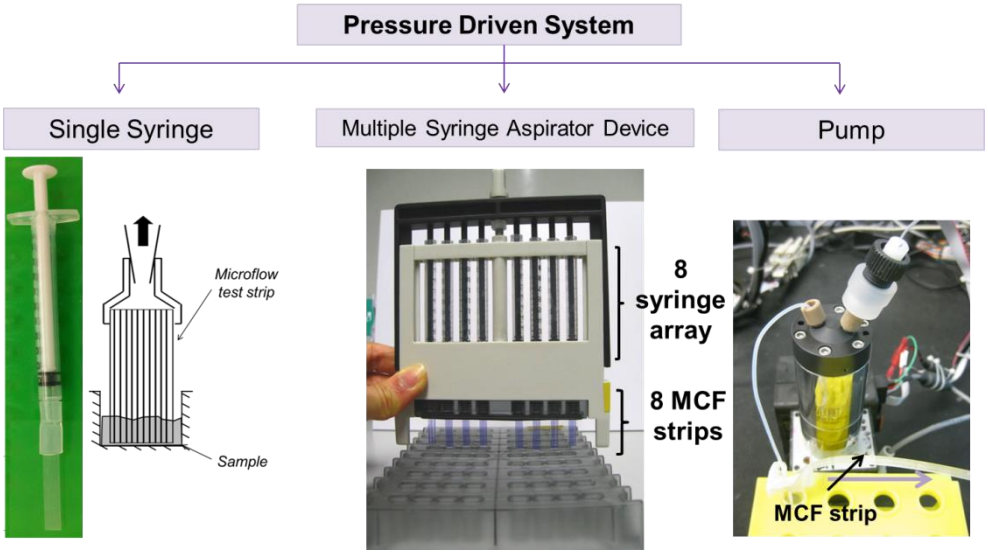

Figure 1:18 - Strategies used for fluid handling in MCF assays: single syringe, MSA (Multiple syringe aspirator) and peristaltic pumps.

The Multiple Syringe Aspirator (MSA) consists of 8 parallel syringes attached to a 3 cm length MCF strip at one end, via a rubber seal. The other end of the syringes is connected to a centrally controlled single knob, which pulls all syringe plungers simultaneously allowing aspirating a precise small volume (<100 µl) of reagents from the wells. The whole device fits into a SLA printed polyurethane microwell plate (Figure 1:19A). The MSA was tested by NG with the aim of reducing assay variability, which involved extended incubation times of 30 minutes for enzymatic substrate conversion, using OPD as chromogenic enzymatic substrate with flatbed scanner detection, and introducing the absorbance normalisation value by capillary height as data processing.[139]

The MSA device operates 8 MCF strips simultaneously, which simplifies the ELISA procedures previously discussed in section 1.2. A schematic of an optimised PSA sandwich ELISA using the MSA is presented in Figure 1:19B. Every turn of the knob pulls 13 µl.[139] In the PSA assay 78 µl were used in each ELISA steps, which corresponds to 6 full rotations of the central knob in the MSA. The PSA standard/sample is first aspirated, and the MSA left to incubate on the well allowing the PSA to bind the CapAb immobilised in the pre-coated strips (Figure 1:19B(ii)(1)). The MSA is then moved to next row of wells containing pre-loaded DetAb (Figure 1:19B(ii)(2)), and the procedure repeated for enzyme conjugate, washing step and enzymatic substrate (Figure 1:19B(ii)(3)-(5)). After the full optimisation of PSA assay

presented in this thesis, no additional intermediate washing steps were required to achieve the desirable assay performance.

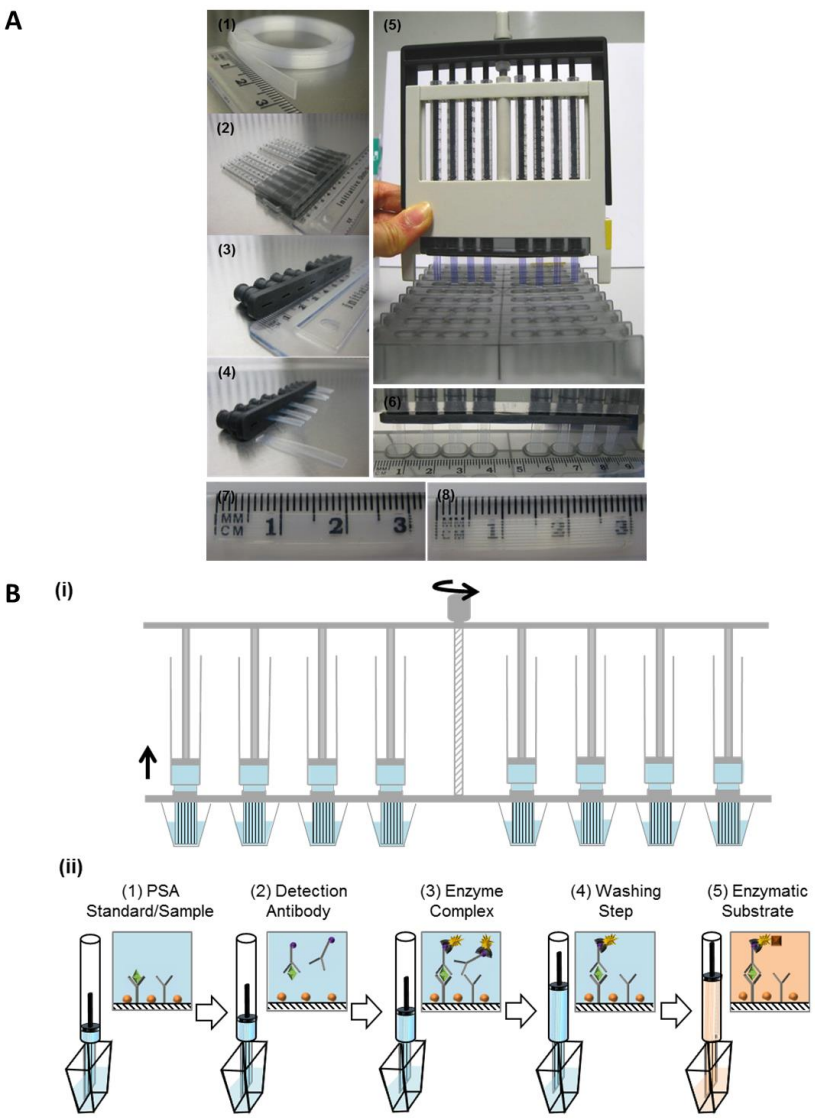

Figure 1:19 – Multiple syringe aspirator (MSA) device used for PSA ELISA in the fluoropolymer MCF.
A MSA components: (1) close photograph of a meltextruded MCF reel with 10*211 µm i.d. embedded microcapillaries; (2) cartridge incorporating an array of eight parallel 1 ml syringes used for fluid aspiration; (3) close up at the rubber push-fit seal; (4) push-fit of 30 mm long pre-coated MCF strips in the rubber seal; (5) fully assembled device, with a plastic frame used to hold syringes, a syringe plugholder with a central knob allowing fluid aspiration by rotation, a rubber seal with MCF test strips incorporated which interfaces with a sample tray with preloaded reagents; (6) close up at the polyurethane microwell plate with 72 wells, organized in 8-wells arrows allowing all sandwich assays reagents to be pre-loaded; (7) MCF filled with PBS buffer, revealing excellent transparency; and (8) MCF filled with air, revealing opaque film. **B** Sequential, semi-automatic fluid aspiration in the MSA: (i) with every full rotation of the central knob the syringes aspirate simultaneously 13 µl of reagents/samples from the wells through the MCF strip; and (ii) solution are sequentially aspirated, with no need for intermediate washing steps.

The work presented in this thesis was focused on the technological developments of MCF IA technology in light of preliminary work discussed in section 1.4.3, of section 1.4. The work aimed at establishing principles for immunoassay miniaturisation. Therefore, the novel aspects of this work can be summarised as follows:

- Studying antibody adsorption onto FEP-Teflon micro capillary surfaces;
- Optimising kinetics of HRP substrate conversion in miniaturised systems, with particular focus on sandwich assays in the MCF;
- Studying the effect of flow in antibody binding in FEP-Teflon micro capillaries;
- Fully optimisation of sandwich PSA immunoassay for operation with whole blood samples, without sample preparation;
- Developing new protocols for colorimetric, fluorescence and particle detection of PSA in MCF strip;
- Studying biological matrix components interference in antibody-antigen binding equilibrium and kinetics.

2. Antibody (IgG) Adsorption onto FEP-Teflon microcapillary surfaces for quantitative point-of-care diagnostics

2.1. Abstract

The adsorption characteristics of antibodies onto FEP-Teflon surfaces were studied in a Microcapillary Film (MCF) produced from FEP-Teflon, being relevant to the development of a new generation of microfluidic sandwich immunoassay (IA) devices.

Antibodies were adsorbed onto FEP-Teflon as a monolayer with maximum coverage of 400 ng/cm^2, which coincides with the theoretical monolayer coverage of vertically oriented antibodies. When different antibody surface coverages were applied to IL-1β cytokine detection, the antibody binding capacity increased up to 220 ng/cm^2 and decreased for surface coverages above 275 ng/cm^2.The maximum binding capacity of an adsorbed antibody layer on FEP-Teflon therefore happens slightly above half monolayer coverage, which agrees with previous studies performed on other surfaces.

The microcapillary film (MCF) geometry, 10 bore with 200 μm diameter embedded in a FEP-Teflon flat film, allows the necessary surface area to obtain a monolayer dense enough to perform sensitive IA. The geometry is combined with a surface chemistry (FEP-Teflon) that favours irreversible antibody binding of a monolayer to the surface, maintaining their antigen binding capacity.

The integration of FEP-Teflon antibody adsorption capacity with its excellent transparency allows femtomolar detection of cytokines (IL-1β, IL-6, IL-12 and TNF-α) and rapid and sensitive detection of prostate cancer antigen (PSA) using colorimetric signal detection with a flatbed scanner as a readout system. This transforms the microcapillary film (MCF) into a quantitative platform for point-of-care diagnostics.

Keywords: Biosensor, point-of-care, microfluidic, capillary geometry, antibody adsorption, ELISA, FEP-Teflon.

2.2. Introduction

Immunoassays (IA) are powerful laboratory assays that use antibodies specificity for bioanalytical purposes, with applications in the environment,[140] food,[141] disease diagnostic and other pharmaceutical industries.[142] Point-of-care diagnostics devices are proficient at detecting a wide range of health conditions from cancer to infectious diseases, and are necessary for personalized medicine in developed countries[2] and early diagnostics in remote areas of developing countries.[6] Consequently, adapting IA for miniaturized devices capable of portable, power-free, disposable and low cost disease detection with minimal sample preparation is an urgent demand for global health. [143]

Immunoglobulin G is the main type of antibody used in IAs. These biomolecules with 150 KDa present an Y shape, with two variable regions (Fab fragments), capable of binding specifically to other molecules, and one constant region (Fc fragment).[144] The most sensitive format of immunoassays, the heterogeneous sandwich IAs, presupposes an antibody immobilisation onto a solid surface (capture antibody), followed by several reaction steps which rely on the maintenance and stability of the immobilised antibody layer. The density, uniformity, stability and orientation of the antibody immobilised layer is fundamental for development of sensitive and robust assays. [21]

Sandwich immunoassays rely on a solid support and detection modes, which have to be capable of detecting a signal that correlates with the immobilised antibody-antigen complex. [33]

In laboratories the gold standard for IAs support is the microtiter plate (MTP) and the microplate reader, however this technology is not suitable for point-of-care detection. In recent years, several microfluidic technologies have emerged with new materials for IAs solid support. Miniaturized microfluidic systems are portable, disposable and automated, thus suitable for analytical procedures outside the laboratory, including point-of-care disease diagnostics.[7] However, a miniaturized support creates a miniaturized signal, which needs to be precisely detected and quantified. This is a major challenge for point-of-care microfluidic devices to overcome as they often need a sophisticated equipment for signal measurement such as microscopes, which contradicts the ideal of simple, portable, power-free and cost effective microfluidic IAs for point-of-care testing. [56,58]

Subsequently, microfluidics solid supports must compensate the detection mode with their high analytical eficiency, which is intrinsically related to their size. The Scatchard model[145] shows that higher concentrations of antibody favor the formation of antibody-antigen complex in an antibody-antigen binding reaction. Accordingly higher numbers of immobilised antibodies will capture more analytes (antigens) in the microfluidic system.[145]

Individual capillaries have been widely used as a solid support phase for bionalytical purposes, as small diameter capillaries allow reduced reagent consumption, fast reaction times and easy incorporation of flow systems.[146]

In order to attach a higher number of immobilised antibodies onto a surface it is necessary to have a large surface available in the immobilisation zone (the solid phase area where analytes bind and signal detection can be performed). In microfluidics IAs, where antibodies are immobilised in the inner walls of a channel, the immobilisation area is mainly reserved to a particular part of the channel, known as the reaction chamber. Microfluidic channels are usually very small (typically in the order of 100-500 μm), therefore yielding large surface-area-to-volume ratios. Consequently the immobilisation zone surface area is typically very small, which limits the number of immobilised antibodies. Hence, complex antibody immobilisation methods are needed in order to obtain a dense antibody monolayer and expensive laboratory signal detection systems are required for performance of sensitive and robust IAs. [50,56,147] Although surface area-to-volume ratio is important for point of care (POC) diagnostics, the total antibody immobilisation surface area is relevant for sensitive POC assay cost and portability. *Kai et al* (2012) understood this balance between total surface area and surface-area-to-volume ratio, reporting a novel microfluidic microplate with microchannels providing similar surface area to conventional microplates, but with a 50 times increment in surface-area-to-volume ratio. A fluorescent plate reader was still needed for signal detection however.[66]

Geometry limits the number of antibodies in the surface and the rate they adsorb to the surface. Nevertheless surface chemistry and antibody immobilisation methods determine the density, uniformity and effectiveness of bond antibodies and their orientation.

Passive adsorption on bare substrates is the most simple and one of the most common antibody immobilisation methods.[87]Antibody adsorption happens mainly due to electrostactic, van der Waals, hydrogen bonding and hydrophobic interactions. It therefore depends on the surface chemistry, pH, temperature and ionic strength of the buffer during antibody adsorption. Hydrophobic substrates, such as plastics and PDMS[87,148,149] are usually chosen for antibody adsorption, since hydrophobic interactions are strong enough to effectively bind an antibody to a surface.[87,150,151] Beyond allowing simple antibody immobilisation, thermoplastic resins are cheap and enable mass fabrication.[21,87] These are important features for manufacturing point-of-care diagnostic devices.

The microcapillary film (MCF) is a melt extruded thermoplastic film that contains embedded hollow capillaries.[117] Several plastic polymers were used to produce the MCF by melt-extrusion, such as fluorinated ethylene propylene copolymer (FEP), ethylene vinyl alcohol (EVOH) and linear lower density polyethylene (LLDPE). The cost for pelleted FEP material is in the range of £20/kg, which means a 10-plex, 50mm long MCF FEP test strip can be produced for less than £0.10 using the melt extrusion procedure.[127]

Previous studies reported the use of 10*200 μm fluorinated ethylene propylene copolymer (FEP-Teflon)[1] for immunoassays. This polymer was chosen for its excellent transparency, allowing sensitive signal detection with low cost readout systems.[127,152] According to *Barbosa et al.* (2014) PSAcould be quantified on this platform with a lower limit of detection (LLoD) of 0.9 ng/ml of PSA in 13 minutes total assay time, using a flatbed scanner as a readout system and passive adsorption as the antibody immobilisation technique.[152] The LLoD was improved to 0.08 ng/ml using fluorescence detection with a smartphone.[153] Also, *Castanheira et al.* (2015) reported (IL-1β, IL-6, IL-12 and TNF-α) using the same method.[154]

Fluoropolymers have excellent chemical and thermal resistance and form non-reactive surfaces with a variety of chemicals and solvents which make them ideal for many applications, including medical diagnostics.

[1] Fluorinated ethylene propylene (FEP) is a plastic copolymer of hexafluoropropylene and tetrafluoroethylene, invented by DuPont under the brandname Teflon FEP.

In this study we aim to characterize antibody adsorption onto FEP-Teflon microcapillary films (MCFs) (Figure 2:1), demonstrating that antibody adsorption is reliable for MCF sandwich assays in point-of-care diagnostics.

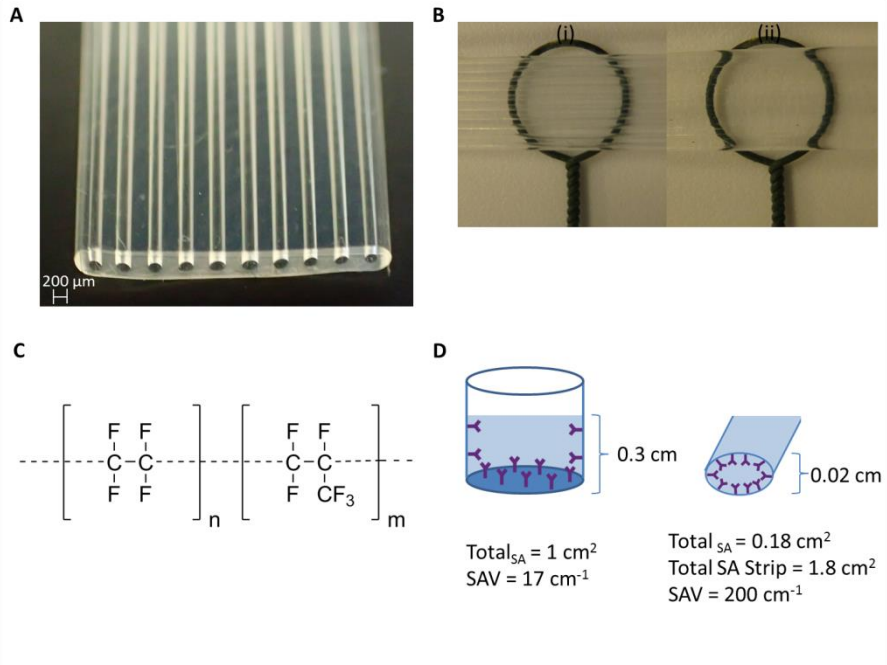

Figure 2:1 – MCF produced from fluorinated ethylene propylene copolymer (FEP-Teflon).
A Photograph of a 10 bore 200 µm bore FEP-Teflon microcapillary film. **B** Transparency of FEP-Teflon MCF (i) capillaries filled with air (ii) capillaries filled with PBS buffer. **C** Chemical composition and structure of FEP-Teflon polymer. **D** Geometry comparison between the gold IA standard, the microtiter plate, and the MCF. Note that a typical MCF test strip has 10 capillaries and 3 cm in length.

2.3. Materials an Methods

2.3.1. Materials & Reagents

Mouse IgG (whole antibody) was purchased from Life Technologies (Paisley UK), rabbit Anti-IgG (whole molecule) conjugated with peroxidase and SIGMAFAST^{TM} OPD (o-Phenylenediamine dihydrochloride) tablets were supplied by Sigma-Aldrich (Dorset, UK). The BCA Protein Assay Reagent (bicinchoninic acid) was sourced from Thermo Scientific (Lutterworth, UK). The IL-1β recombinant protein, Anti-Human IL-1β biotin and Anti-Human IL-1β purified were supplied from

eBiosciences (Hatfield, UK). High sensitivity streptavidin-HRP was supplied by Thermo Scientific (Lutterworth, UK).

Phosphate buffered solution (PBS) and Bovine Serum Albumin (BSA) were sourced from Sigma Aldrich, Dorset, UK. PBS pH 7.4, 10mM was used as the main experimental buffer. Anhydrous Sodium Carbonate was supplied from Fisher Scientific and HEPES from Sigma-Aldrich, Dorset, UK. The blocking solution consisted of 3% w/v protease-free BSA diluted in PBS buffer, except for IL-1β assays, which used a superblocking solution supplied by ThermoScientific (Lutterworth, UK). For washings, PBS with 0.05% v/v of Tween-20 (Sigma-Aldrich, Dorset, UK) was used.

The MCF was fabricated from FEP-Teflon using a melt-extrusion process by Lamina Dielectrics Ltd. (Billinghurst, West Sussex, UK). The MCF presented 10 bore parallel capillaries with the mean 0.2 mm internal diameter. An MCF produced from LLDPE was also produced at Cambridge University[117] and presented 19 parallel capillaries with 0.2 mm internal diameter. Glass capillaries, 152 mm in length and 0.58 mm internal diameter, were purchased from World Precision Instruments, Inc. (Hitchin, Hertfordshire, UK).

2.3.2. Determination of adsorbed mass antibody

The MCF was trimmed into 20 cm strips, and each strip filled with a solution with concentrations of 0, 6.25, 12.5, 25, 50, 100, 200 and 400 μg/ml of mouse IgG, prepared from a serial dilution of 400 μg/ml Mouse IgG in PBS and incubated for 2 hours at room temperature (20 ºC). The solution inside MCF strips was collected using a syringe attached to a silicone tube and transferred into microplate wells. BCA protein assay was used for quantifying the antibody concentration in the aliquots based on solution depletion technique.

In order to understand the effect of temperature on antibody adsorption, the temperature was kept constant during IgG incubations at 37 ºC and at 4ºC.

The pH effect on IgG adsorption to FEP-Teflon was studied by preparing IgG serial dilution solutions in Sodium Carbonate buffer 10 mM at pH 10.7, in Phosphate buffer (PBS) 10 mM at pH 7.4 and HEPES 10 mM at pH 4.8. The IgG solutions were incubated inside the FEP-Teflon capillaries for 2 hours at room temperature.

The effect of surface chemistry on IgG adsorption was studied by comparing antibody adsorption in FEP-Teflon with LLDPE (CH3 plastic polymer, with 102º water contact angle) and glass capillaries (silica with 15º water contact angle), pH 7.4, for 2 hours at room temperature.

For IgG quantification in aliquots 25 µl of solution was placed in a microwell and 200 µl of BCA working reagent (1 reagent B: 50 reagent A) was added to each well and mixed for 5 seconds with a multiple channel micropipette. The microwell plate was covered with parafilm to avoid liquid evaporation and incubated at 37 ºC for 3 hours. Every sample was tested in triplicate. A set of IgG standard solutions was placed in the same microwell plate to obtain a calibration curve. For this purpose 25 µl of IgG solution from each concentration previously prepared were mixed with 200 µl of BCA working reagent (1:50).

Following incubation of IgG standards and samples with the BCA working reagent, the microtriter plate was left to cool down for a few minutes at room temperature. The end point absorbance was measured at 562 nm using a microplate reader (Epoch, BIOTEK).

The absorbance values of IgG standard solutions were used to build a calibration curve. The equation obtained from this calibration curve was used to estimate the initial concentration of IgG in solution and the remaining IgG concentration in the microcapillaries. The concentration of IgG adsorbed (µg/ml) was obtained from a mass balance to the IgG in the microcapillaries (2:1) and converted to adsorbed density (ng/cm^2) through equation (2:2).

$$[\text{Ads IgG}] = [\text{Initial IgG solution}] - [\text{Remaining IgG solution}] \quad (2:1)$$

$$\frac{\text{SA}}{\text{V}} = \frac{4}{\text{D}} \quad (2:2)$$

where *SA* is the surface area, *V* the volume and *D* the mean hydraulic diameter of the capillary.

The percentage surface coverage was calculated by considering a theoretical antibody monolayer with the antibody orientation being vertical. The percentage surface coverage was normalised by the total surface area for comparison of different capillary materials.

2.3.3. Kinetics of adsorption to capillary surfaces

A solution containing 20 μg/ml of mouse IgG in PBS was prepared and aspirated into 8 FEP-Teflon MCF strips each of 20 cm in length. The IgG incubation time on each strip varied from 0 to 120 minutes. After IgG incubation the solution inside the capillaries was placed in a microwell and 25 μl of this solution were used for protein quantitation with BCA assay. The procedure was repeated with 40 and 200 μg/ml IgG solutions in FEP-Teflon MCF and with 20,40 and 200 μg/ml IgG in MCF fabricated with LLDPE and glass capillaries.

2.3.4. Quantitation of antibody adsorbed onto FEP-Teflon by ELISA technique

To study the effect of immobilised antibody density in overall antibody binding in an IA (i.e. capacity of a coated solid phase to specifically capture molecules) 8 FEP-Teflon MCF strips were incubated for 2 hours at room temperature with 0, 6.25, 12.5, 25, 50, 100, 200 and 400 μg/ml of mouse IgG in PBS. The strips were then washed with 1 ml of PBS-Tween and then incubated for 10 minutes at room temperature with 0.06 μg/ml of anti-IgG conjugated to peroxidase. The strips were washed with 1 ml PBS-Tween after which 1mg/ml of OPD enzymatic substrate was aspirated. The MCF strips were scannned in transmittance mode using a Flatbed Scanner (HP ScanJet G4050 Scanner) after 5 minutes of OPD incubation and a digital image with a resolution of 2400 dpi was processed using Image J (NIH, Maryland, USA) sofware for absorbance calculation. The experiments were repeated with 0.6 and 6 μg/ml of Anti-IgG, peroxidase conjugated.

The effect of immobilised IgG incubation time in antibody binding was studied by incubating 40 μg/ml of IgG in PBS in FEP-Teflon MCF strips from 0 to 120 minutes, before washing the strips with 1 ml PBS-Tween. A solution of 0.6 μg/ml of Anti-IgG, peroxidase conjugated was then added and incubated for 10 minutes. After another washing step, OPD enzymatic substrate was added at the concentration of 1 mg/ml. The MCF strips were then imaged after 5 minutes incubation of OPD in transmittance mode.

2.3.5. MCF ELISA Digital Image Analysis

RGB digital images were split into 3 separated channels in Image J. The blue channel images were used to calculate absorbance values, based on the grey scale peak height of each individual capillary of FEP-Teflon MCF as described elsewhere.[127,152] Absorbance (Abs) was calculated for each individual capillary based on equation (2:3):

$$\text{Abs} = -\log_{10}\left(\frac{I}{I_0}\right) \quad (2:3)$$

Where I is the transmitted light and corresponds to I_0 minus peak height and I_0 is the maximum grey scale value. The absorbance values were averaged across 10 capillaries for the MCF strip.

2.3.6. IL-1β sandwich ELISA

6 cm long FEP-Teflon MCF strips were filled with IL-1β monoclonal antibody solutions of 20, 40, 100 and 140 μg/ml and incubated for 2 hours. The remaining binding sites were blocked with super blocking solution by incubating the MCF for 2 hours. The strips were then washed with 1ml of PBS-Tween. Each coated MCF strip was trimmed into two 3 cm long strips, which were used as a positive and a negative IL-1β test. These strips were inserted into the multiple syringe aspirator device, which allows simultaneous fluid aspiration in all eight MCF strips, through manual rotation of a knob. A dilution with 0.5 ng/ml of recombinant IL-1β was incubated for 2 minutes in four of the MCF strips and the remaining strips incubated with PBS solution. After a washing step a solution of 10 μg/ml of IL-1β biotinyated detection antibody was aspirated and incubate for 10 minutes. A 4 μg/ml solution of High Sensitivity Streptavidin-HRP was aspirated following another washing step with PBS-Tween and incubated for 10 minutes, followed by a washing step. A solution with 4 mg/ml os OPD enzymatic substrate was then aspirated into the capillaries and incubated for 5 minutes, and the strips imaged with the Flatbed Scanner at 2400 dpi.

For the IL-1β response curves, two 30 cm long FEP-Teflon MCF strips were filled with 40 μg/ml of IL-1β capture antibody (CapAb). One of the strips was incubated for 30 minutes and the other for 2 hours. The strips were then blocked with superblocking

solution by incubating for 2 hours, followed by a washing step. The MCF strips were then trimmed into smaller 3 cm long pieces and inserted into the multiple syringe aspirator device (MSA). Eight solutions of IL-1β from 0 to 1 ng/ml were aspirated into the MCF strips and incubated for 5 minutes, followed by a washing step. Then a 10 μg/ml solution of IL-1β biotinylated antibody was aspirated into the MCF strips and incubated for 10 minutes, followed by a washing step and 4 μg/ml high sensitivity streptavidin-HRP incubation for 10 minutes. A solution of 4 mg/ml of OPD was aspirated into the eight MCF strips following a washing step, and the strips were imaged after 5 minutes incubation.

2.4. Results and Discussion

2.4.1. Surface capacity of FEP-Teflon MCF for antibody adsorption

A key challenge to commercialisation of microfluidic POC diagnostic devices is the possibility of mass production methods for microfluidic platforms, which are currently lacking, as most lab-on-a-chip devices are made through micromachining methods. For mass produced diagnostic devices the antibody or protein needs to be immobilised in bulk quantities, therefore the immobilisation method has to be simple, easy, reproducible and cost effective, which is often achieved with antibody adsorption to polymeric materials.[87]

Adsorption is the most common method for antibody immobilisation, however it is very specific to surface chemistry, total surface area available for binding, surface geometry, pH, temperature and buffer ionic strength.[151] The antibody adsorption onto FEP-Teflon MCF is shown in Figure 2:2.

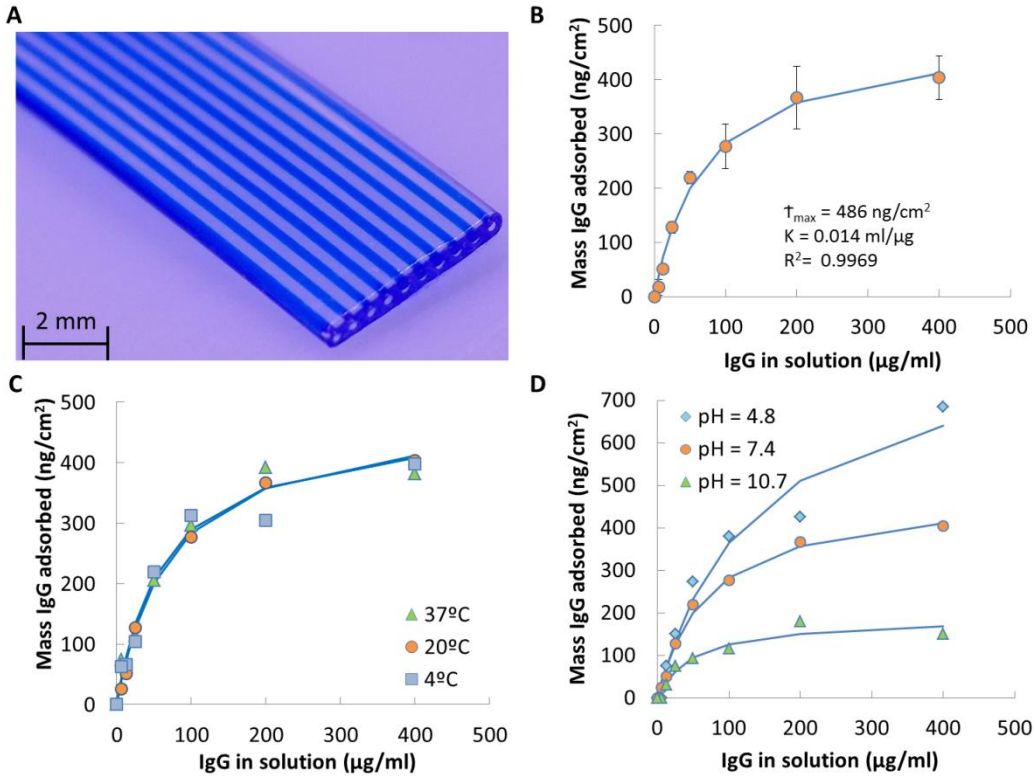

Figure 2:2 - IgG adsorption onto FEP-Teflon MCF 200 µm i.d.
A FEP-Teflon MCF used. **B** IgG Langmuir in standard MCF IAs conditions pH 7.4 and 20ºC. **C** IgG langmuir adsorption at 4, 20 and 37 °C, pH 7.4. **D** IgG langmuir adsorption at pH 4.8, 7.4 and 10.7, at 20 ºC. The IgG incubation time was 2 hours in all experiments described in the figure. The continuous lines in the figure represent the values predicted with the Langmuir adsorption model using the least squares solver equation.

Antibody adsorption to FEP-Teflon experimental data presented in Figure 2:2 was fitted to the Langmuir adsorption model, using the equation (2:4) and the least squares solver equation. The parameters τ_{max} .and K obtained from the model are presented in Table 2:1.

$$\tau = \tau_{max} \frac{Kc}{1 + Kc} \qquad (2:4)$$

Where τ is the surface coverage in equilibrium, τ_{max} is the number of adsorption sites available given by a maximum adsorbed concentration, K is the adsorption constant and c the antibody concentration in solution.

Temperature is one of the factors that most influences protein adsorption, as higher temperatures generally increase the adsorbed quantity of protein. [151] Surprisingly the

amount of antibody adsorbed to FEP-Teflon capillaries did not appear to be affected by the temperature in the range of 4 to 37 ºC (Figure 2:2 and Table 2:1). This is an advantage for mass production of coated MCF strips as the manufacture set up does not require temperature control, lowering the cost of manufacturing and enabling a higher degree of freedom for operators.

In conventional ELISA surfaces antibody adsorption is known to be higher around the isoelectric point of IgG (pH 6.8 – 9.0), as electrostatic interactions are minimised allowing higher packing densities on the surface.[151] Nevertheless, Figure 2:2D and Table 2:1 shows that adsorption at a pH lower than the antibody isoelectric point (pH=4.8) increased the amount of IgG adsorbed onto FEP-Teflon microcapillaries (853 ng/cm^2), whereas at a pH higher than the isoelectric point (pH 10.7) the amount adsorbed decreases (190 ng/cm^2) compared to the isoelectric point condition with a Γ_{max} of 486 ng/cm^2 (Figure 2:2). This might be explained by protein denaturation at lower pH values, which promotes unfolding and aggregation of antibody molecules. *Wright et. al* (1945) reported that at pH 4.95 approximately 50% of the antibody present in solution was denatured.[155]

The antibody adsorption conditions chosen for FEP-Teflon MCF sandwich assays in our previous studies[152–154] were 20 ºC and pH 7.4, and at those conditions the adsorption isotherm in Figure 2:2B shows a maximum surface coverage of 404 ng/cm^2 (approximately 80 µg/ml of adsorbed IgG) for a 200 µm i.d. microcapillaries, which is obtained with 400 µg/ml of IgG in solution. This demonstrates a low affinity of IgG for the FEP-Teflon surface with an adsorption constant of 0.014 ml/µg (Table 2:1).

Table 2:1- FEP-Teflon IgG adsorption parameters variation with pH and temperature.

	Temperature			**pH**		
	4°C	20°C	37 °C	4.8	7.4	10.7
K (ml/µg)	0.015	0.014	0.016	0.007	0.014	0.019
Γ_{max} (ng/cm^2)	472	486	472	853	486	190
R^2	0.9856	0.9963	0.9891	0.9801	0.9963	0.9412

Based on the dimensions of antibody molecules, *Buijs et al.(1995)* suggested a relationship between the adsorbed amount and the molecular orientation on the surface, thus 200 ng/cm^2 would represent a monolayer with antibodies in a "flat-on" orientation, 260 ng/cm^2 in an "end on" orientation with Fab fragments in line, and 550 ng/cm^2 also in an "end-on" orientation with Fab fragments close together and parallel.[156] This

suggests antibody adsorption to FEP-Teflon at the conditions studied happens by a monolayer formation with the maximum adsorbed amount of 404 ng/cm^2, which suggests a packed antibody monolayer with antibodies oriented "end-on".

Antibody adsorption to FEP-Teflon was found to be similar to protein adsorption onto hydrophobic surfaces and other fluorinated surfaces. A study of protein IgG adsorption onto Teflon AF (amorphous fluoropolymers) using optical waveguide light mode spectroscopy[157] showed a maximum surface density of approximately 200 ng/cm^2 at 40 μg/ml of IgG solution, where in the FEP-Teflon micocapillaries the adsorbed mass, using 40 μg/ml IgG solution, is 220 ng/cm. Another study used a Quartz Crystal Microbalance with Dissipation in a Ch_3-terminated surface and shows a maximum coverage of 468 ng/cm^2 with 100 μg/ml of IgG in solution. This is 40% higher than the surface coverage obtained in the FEP-Teflon MCF (275 ng/cm^2) using the same IgG concentration in solution.[158] This might be due either to the difference in geometry or the surface chemistry, with FEP-Teflon presenting a lower affinity for antibody adsorption.

The reduced affinity to antibodies for hydrophobic surfaces favours the formation of a less dense monolayer, which is preferred for sensitive ELISA in miniaturised devices. Antibody density on hydrophilic surfaces yields higher mass adsorbed with the possible formation of antibody multilayers.[159]Higher adsorption affinity is promoted by electrostatic interactions between antibodies and hydrophilic surfaces. [159] Hydrophobic surfaces are usually chosen for antibody adsorption onto biosensors as immobilised antibodies are more resistant to surfactants and show low desorption due to irreversible binding between antibody and surface, which is essential for heterogeneous IAs.[158,160,161] The irreversibility is related to the conformational changes that part of the antibody suffer when adsorbed to a hydrophobic surface. These conformational changes are reduced in hydrophilic surfaces, therefore antibodies are easier to remove from those surfaces. Other studies mentioned antibody denaturation of the Fab region with loss of antibody binding capacity to Teflon surfaces.[80,162]

In order to understand the effect of density immobilised antibodies in antibody-antigen binding in the MCF platform, a mouse anti-IgG conjugated with peroxidase was used to detect the mouse IgG immobilised at different antibody densities on FEP-Teflon MCF capillaries (Figure 2:3). This system intended to mimic antibody-antigen binding. Note

that information about antibody orientation cannot be obtained from these results, as mouse anti-IgG is able to bind to the whole IgG mouse molecule.

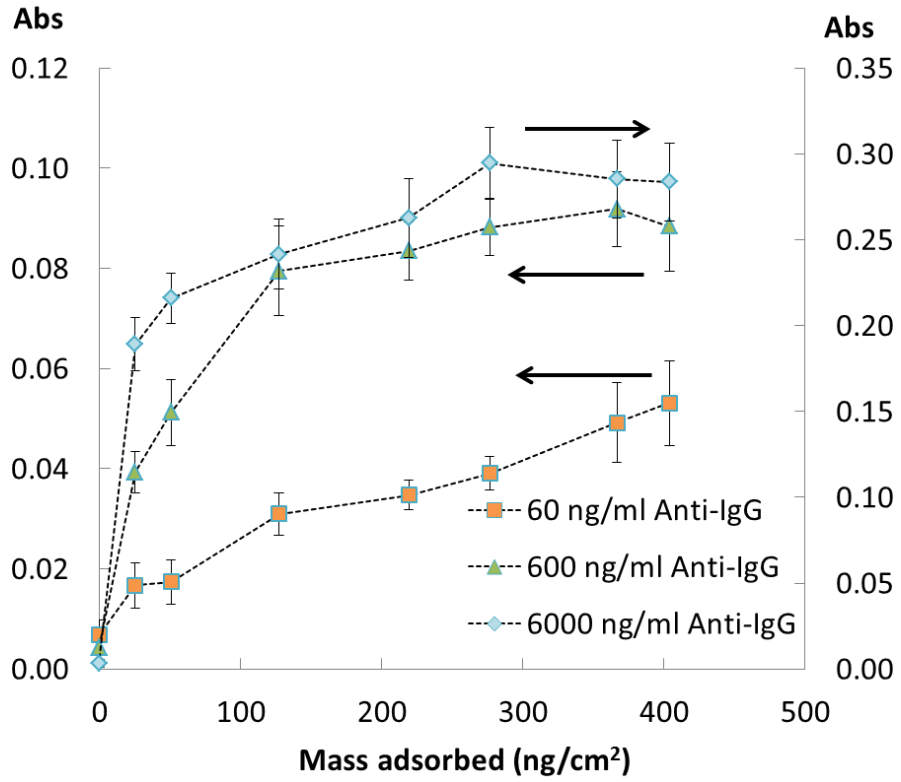

Figure 2:3 - Effect of antibody density on detection zone in antigen-antibody binding on FEP-Teflon capillaries.

Three different concentrations of anti-mouse IgG were used and results summarised in Figure 2:3. At higher anti-mouse IgG concentrations the signal saturated at around 200 ng/cm^2 of adsorbed antibody, while for lower anti-mouse IgG concentration the signal increased proportionally to the antibody density. This shows higher antigen concentrations are more easily detected in the MCF with a flatbed scanner and a chromogenic substrate. A more sensitive detection is achieved by incrementing the density of immobilised antibody; however it is important to note that the affinity constant between mouse IgG and mouse anti-IgG is very low, therefore higher sensitivity requires a higher density of immobilised antibody, once the high avidity must compensate the individual low affinity of antibodies. Steric hindrance between antibodies is not a problem in this system since anti-mouse IgG can bind to all immunoglobulin parts. Although the FEP-Teflon MCF strips were washed with 0.05% PBS-Tween before adding the mouse Anti-IgG, based on several repetitions no

detectable loss of antibody was detected with the washing. FEP-Teflon microcapillaries present a highly hydrophobic surface (123º contact angle), which favours the irreversible nature of antibodies on the surface. [163,164]

2.4.2. Kinetics of adsorption antibody (IgG) onto FEP-Teflon MCF

The kinetics of IgG adsorption has not been previously studied, and it influences the time required for the coating of FEP-Teflon capillary surfaces. Adsorption time is also important for establishing a strong bond with the substrate or influencing the binding capacity of the adsorbed antibody.

The experimental data for antibody adsorption kinetics were fitted to equation(2:5). This is the solution of a differential equation given by the difference between the adsorption process, the reactant, free binding sites and the desorption process. The experimental results and estimated parameters are presented in Figure 2:4 and Table 2:2, respectively.

$$\tau = \frac{K_{on}\, c}{k_{on}\, c + K_{off}} [1 - \exp[-(K_{on} c + K_{off}) t]] \qquad (2:5)$$

Where τ is the surface coverage at time t, c is the antibody bulk concentration, k_{on} is the adsorption rate and K_{off} is the desorption rate.

Figure 2:4A shows IgG adsorption to FEP-Teflon is surprisingly fast, with K_{on} in order of 10^5 $M^{-1}.min^{-1}$ (Table 2:2). Equilibrium is reached after 5 to 10 minutes incubation and independently of the concentration of IgG loading into the microcapillaries. The percentage of surface coverage (Φ) is related to a theoretical monolayer with all antibodies in the "end on" position, considering the size of the IgG molecule is 14 x 8.5 x 4 nm with 8.5 nm being the longitudinal axis.[165]

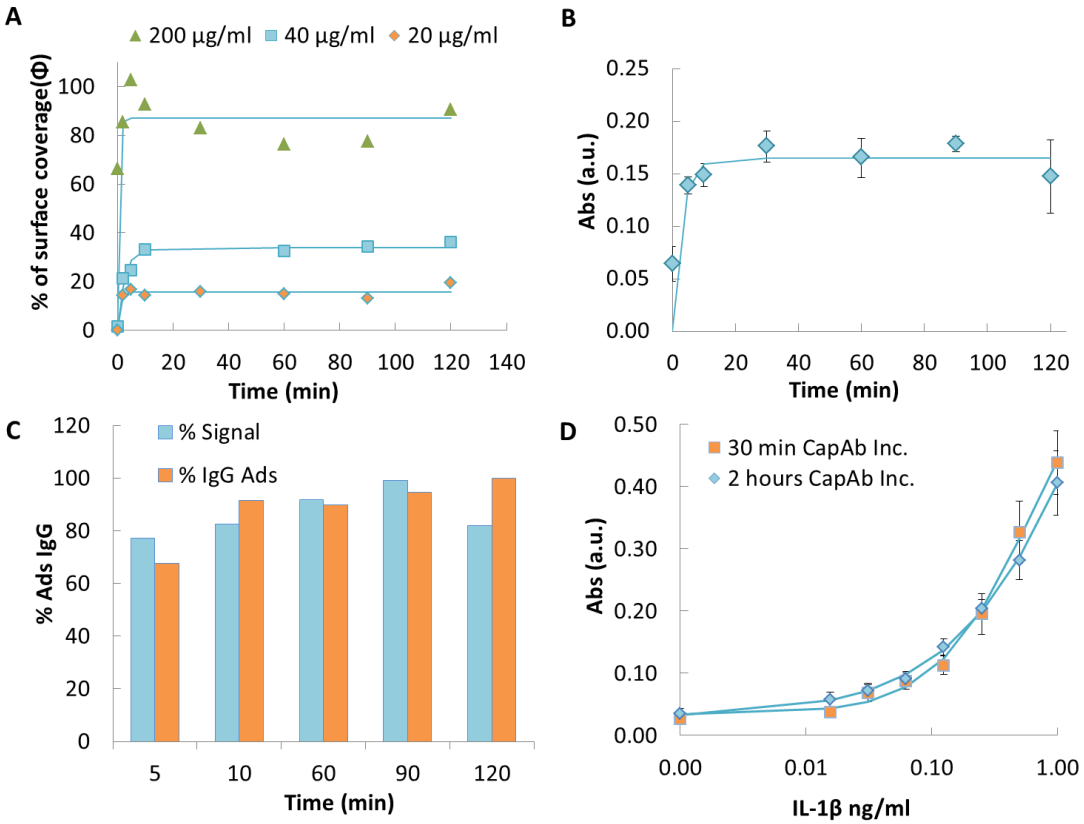

Figure 2:4 - Antibody adsorption kinetics onto FEP-Teflon microcapillaries.
A Antibody adsorption kinetics with mouse IgG concentrations of 20, 40 and 200 µg/ml, determined by solution depletion technique. The continuous line represents the values obtained by the model described in equation (2:5). **B** Antibody adsorption kinetics with 40 µg/ml of mouse IgG, determined by ELISA, using 0.6 µg/ml of Anti-IgG peroxidase conjugated as detection antibody. **C** Kinetics of IgG adsorbed obtained by BCA assay (orange bars) and by ELISA (blue bars). The continuous line represents the values obtained by the model described in equation (2:5). **D** IL-1β full response curves using 40 µg/ml of capture antibody incubated for 30 and 2 hours (120 minutes). The continuous line represents the values obtained by the 4 parameter logistic model, commonly used for full response in IAs.

A second method used for determination of the kinetics of antibody adsorption onto FEP-Teflon consisted of using anti-IgG conjugated with peroxidase to detect the mouse IgG molecules on the surface of the microcapillaries (Figure 2:4B). The MCF strips were washed with 1 ml of PBS-Tween before adding the conjugated anti-IgG peroxidase. The results are comparable with the ones obtained by the solution depletion technique in Figure 2:4A.

Table 2:2 - FEP-Teflon IgG adsorption kinetic parameters variation.

	K_{on} ($M^{-1}.min^{-1}$)	K_{off} (min^{-1})	R^2
20 µg/ml IgG	$9.01x10^5$	1.0666	0.9453
40 µg/ml IgG	$3.09x10^5$	0.2968	0.9811
200 µg/ml IgG	$8.45x10^5$	0.9083	0.6444

Both methods showed that maximum antibody adsorption happens within 10 minutes of incubation (Figure 2:4C). These findings are applicable to sandwich assays, since IL-1β full response curves are similar, with a coating procedure of 30 minutes or two hours' antibody incubation (Figure 2:4D).

Monoclonal antibodies, commonly used in sensitive IAs, present higher affinity compared to polyclonal antibodies used in Figure 2:4B. In order to demonstrate the impact of monoclonal antibody adsorption onto FEP-Teflon microcapilaries, a sandwich assay was performed using a monoclonal pair of antibodies for IL-1β cytokine (Figure 2:5).

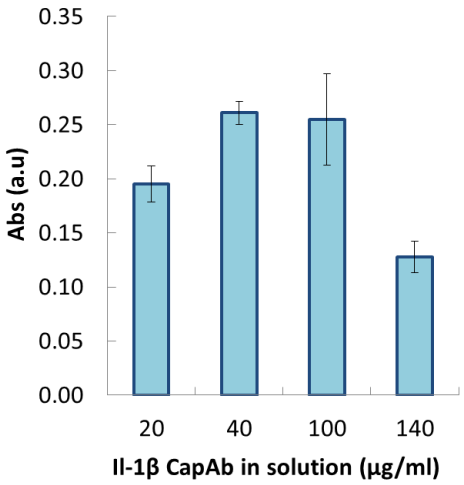

Figure 2:5 - IL-1β sandwich ELISA in FEP-Teflon capillaries.
Relation between IL-1β capture antibody (CapAb) concentration and Abs signal (IL-1β concentration used was 0.5 ng/ml).

IL-1β sandwich assay signal increased up to 100 µg/ml of CapAb and decreased at higher concentrations (Figure 2:5) which could not be seen with the mouse IgG-anti-IgG system. This difference is related to the fact that IL-1β CapAb is a monoclonal

antibody that binds a single epitope in the antigen molecule, therefore a very dense layer of immobilised antibody can prevent the binding by steric hindrance. According to *Xu et al.* (2006) the binding capacity of an immobilised antibody is greater below 50% of full monolayer coverage, and above this the antigen binding sites of the immobilised antibody can become inaccessible to the antigen. In addition, higher bulk concentrations decrease the degree of irreversibility of antibodies bond to the surface, with the irreversibly adsorbed amount being a maximum 250 ng/cm^2 on a hydrophilic silicon oxide surface.[161]

Meridith et al. (2012) used a quartz crystal microbalance with dissipation monitoring to detect a shift in dissipation value of the crystal almost to zero for antibody mass adsorbed below 200 ng/cm^2, meaning that this initial mass is very attached to the surface, which suggests antibody "flat-on" orientation. Neutron reflexion studies revealed a layer thickness of 4 nm, which is close to the short axial length of an antibody for a mass adsorbed of 220 ng/cm^2, also suggesting a "flat-on" orientation.[161]

Above 200 ng/cm^2 these authors showed that the dissipation slope increases, meaning new antibodies are adsorbed onto the surface in a less rigid mechanical coupling, suggesting "end-on" orientation of molecules. Surprisingly, in this study no decrease in antibody binding capacity is found with increasing surface density, suggesting a monolayer is achieved at approximately 468 ng/cm^2, and increases in bulk IgG concentration lead to higher dissipation values, suggesting a multilayer formation. [158]

The 40 to 100 μg/ml concentrations of antibody in Figure 2:5A correspond to 220 ng/cm^2 and 275 ng/cm^2 respectively, which is slightly above half a full monolayer. The conjugation of these studies with these new results from IgG adsorption onto FEP-Teflon in Figure 2:1B and Figure 2:5A and the performance of sandwich assays in the MCF platform suggests the optimum value for sandwich IAs in FEP-Teflon surface coverage is a half monolayer (200 to 275 ng/cm^2). At around this value antibodies start adopting vertical orientations and further from this value the packing density starts to compromise access to the antigen epitope in the antibody Fab region.

A further set of experiments aimed to directly compare IgG adsorption onto FEP-Teflon microcapillaries with an MCF product from LLDPE and individual glass capillaries.

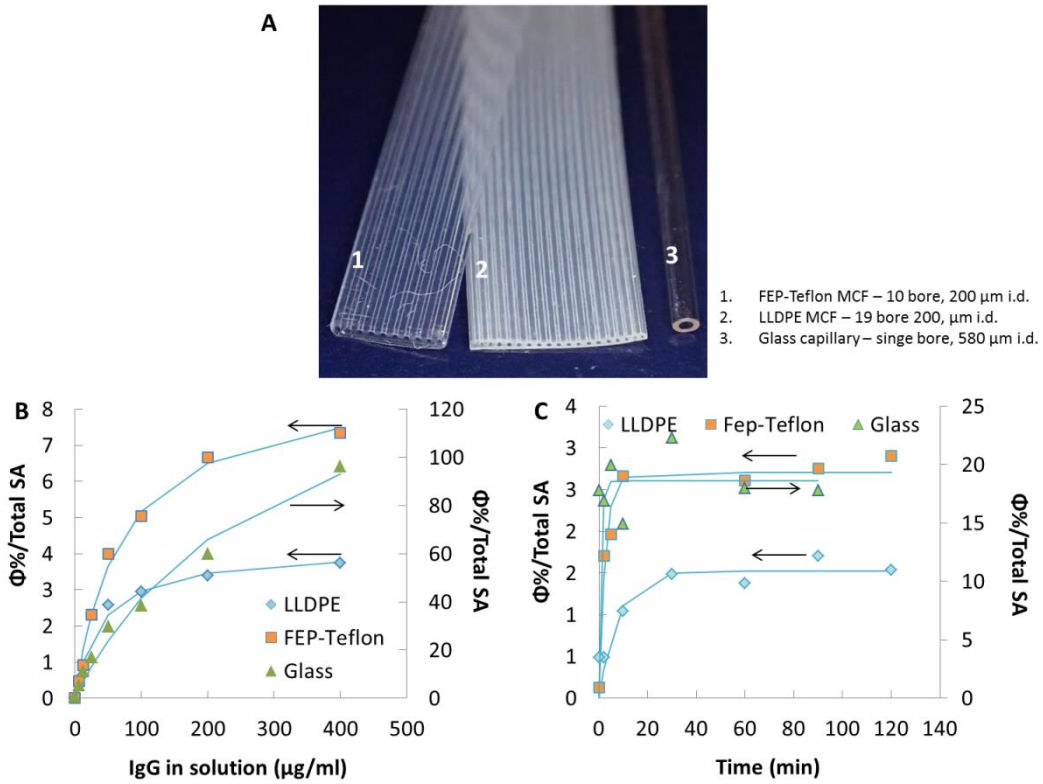

Figure 2:6 - Langmuir and kinetics of IgG adsorption to different capillary surfaces. **A** Microcapillary surfaces used in this study. **B** IgG adsorption langmuir onto LDPE (19 bore, ~200 µm i.d.), FEP-Teflon (10 bore, ~200 µm i.d.) and glass (single bore, 580 µm i.d.). **C** IgG adsorption kinetics onto LDPE, FEP-Teflon and glass (40 µg/ml of IgG). The % of surface coverage adsorbed was normalised by the theoretical surface area available in the different capillary surfaces.

The Langmuir isotherms in FEP-Teflon, LLDPE and glass capillaries showed significant differences in respect to the mass of antibody adsorbed when the amount adsorbed is normalised by the total surface area of the capillaries (Figure 2:6B and Table 2:3). This might be due to different levels in surface hydrophobicity, as FEP-Teflon presents a higher contact angle (123º) when compared with LLPED (102º) and glass (15º).

Table 2:3 - IgG Adsorption parameters to different capillary surfaces.

	FEP-Teflon	**LDPE**	**Glass**
K (ml/µg)	0.014	0.025	0.003
Γ_{max} (%Φ/Total surface area)	8.80	4.15	158.66
R^2	0.9963	0.9921	0.9925

Some studies reported a higher mass of protein adsorbed onto hydrophilic surfaces, such as bare glass, compared to hydrophobic surfaces such as plastic.[163,166]This is in agreement with the results in Figure 2:6B. Although glass is capable of adsorbing a higher mass of antibodies, these studies[163,166] also mention the possibility of multilayer formation and easy desorption from the glass surfaces. The adsorption isotherm model adjusted for glass adsorption presented a more linear shape than those presented for the plastic polymers, which suggests continuous antibody adsorption in a multilayer.

Some hydrophobic surfaces are known to adsorb a lower amount of antibody,[157] promoting the formation of a monolayer, with the immobilised antibody strongly attached to the surface,[164] which is essential for performance in heterogeneous IAs. There was a major difference in the amount of antibody adsorbed to FEP-Teflon, being double the amount adsorbed onto LLDPE. This confirms that the higher hydrophobicity of FEP-Teflon favours antibody adsorption. This uniquely combines with the excellent optical properties of FEP-Teflon MCF previously reported.[127]

Adsorption kinetics on FEP-Teflon were also found to be faster than that in LLDPE microcapillaries, with equilibirum reached within 10 minutes for FEP-Teflon and glass surfaces and 30 minutes for LLDPE (Figure 2:6 and Table 2:4).

Table 2:4 - IgG Adsorption kinetic parameters to different capillary surfaces (IgG concentration = 40 µg/ml).

	K_{on} (M^{-1}.min-1)	K_{off} (Min^{-1})	R^2
FEP-Teflon	$3.09x10^5$	0.2968	0.9811
LDPE	$1.14x10^5$	0.1003	0.9610
Glass	$2.38x10^5$	1.1672	0.1083

2.5. Conclusion

This study showed that antibody adsorption onto FEP-Teflon microcapillaries results in a monolayer with maximum coverage of approximately 400 ng/cm^2. This can be related to a theoretical monolayer with antibodies in a vertical orientation. This surface coverage was obtained within 10 minutes as a result of the small diffusion distance in the microcapillaries. A full sandwich assay with IL-1β human cytokine showed that the signal drops off above ~50% of surface coverage. FEP-Teflon microcapillaries are

capable of adsorbing 50% more antibody than LLPED microcapillaries. Glass capillaries are capable of adsorbing 90% more than FEP-Teflon and LLPED microcapillaries, which suggests that multilayer formation is not desirable for IAs

This adsorption behaviour of antibodies onto FEP-Teflon along with its excellent transparency allows for the performance of sensitive IAs with femtomolar detection of analytes (e.g. cytokines) using a simple flatbed scanner as a readout system.

3. Impact of HRP enzymatic optimization in sandwich ELISA microfluidic systems

3.1. Abstract

We developed a simple yet effective method for rapid and very sensitive ELISA detection in microfluidic devices using a low-performance optoelectronic detector based on maximized HRP enzymatic amplification and a conventional chromogenic substrate OPD. Experiments with PSA and IL-1β in a fluoropolymer microcapillary film revealed over one order of magnitude increase in sensitivity and 10-fold decrease in incubation time required for the enzymatic substrate by increasing the molar ratio of OPD/H_2O_2 from 1:3 to 1:1 and OPD concentration from 1 to 4 mg/ml. This is expected to lead to the development of affordable microfluidic point of care (POC) tests that are optically interrogated using low-cost optoelectronic components by exploring the unique amplification capabilities of enzymes and microfluidics devices.

3.2. Introduction

Assay miniaturisation is one of the main trends in clinical diagnostics, and several studies have succeed in applying microfluidic devices in a range of shapes and detection methods [148,149,167,168] for rapid and sensitive detection of different analytes for different clinical situations. This includes infectious diseases,[169,170] biomarkers[171] and food allergens[172] to name a few, and typically requires the ability of detecting molecules in the nanomolar to picolomar concentration range. This is achieved with the use of expensive detection equipment that is often incompatible with the user requirements for POC tests. An alternative approach that surprisingly remains underexplored is to further potential the natural "amplification" capability of well-established enzymes[173] to yield rapid and sensitive detection, using inexpensive and widespread chromogenic colorimetric substrates and low-cost optoelectronic components,[174] such as flatbed scanners,[175] smartphones[176,153] and other cost effective readout systems.[177]

It appears established within the scientific community that high-sensitivity detection can only be achieved with direct fluorescence labelling of molecules, since fluorophores

provide high amplification power required for detecting very low concentrations of molecules in biological sample. However fluorescence has main drawbacks in respect to microfluidic POC testing, such as scattering noise, crosstalks, misalignment, autofluorescence of substrate, and low collection efficiency.[178]

Our research group is pioneering the application of a low-cost microfluidic material to immunoassays (IAs), based on a fluoropolymer Microcapillary Film (MCF).[127] The hydrophobic surface of Teflon-FEP is ideal for immobilising IA reagents in the inner surface of the microcapillaries, whereas the refractive index of material similar to that of water allows unique signal-to-noise ratios which favours optical simple detection. We have recently reported a 13 min colourimetric prostate cancer antigen (PSA) sandwich assay from whole blood with limit of detection below 1 ng/ml using both a flatbed scanner and a smartphone.[152, 153] Sensitivity was further improved to <0.08 ng/ml with the use of a fluorescence enzymatic substrate which to our knowledge was unique in the field of microfluidics research. We believe enzymatic amplification combined with unique characteristics of microfluidic devices is the key to high-sensitivity POC test with low-cost, modest-performance optoelectronic components.[8]

In this study we present a new method for optimised Horseradish peroxidase (HRP) conversion of a very popular chromogenic substrate, *o*-phenylenediamine dihydrochloride (OPD), adapted to microscale enzymatic conversion and enzyme-linked immunosorbant assay (ELISA) detection. HRP is one of the most popular enzymes in ELISA technique for presenting a very high turnover number. We noticed the composition of commercial OPD/H_2O_2 substrate is adapted to standard laboratory systems controlled by diffusion, such as microwell plates,[85,179,180] where HRP performance is sub-optimum. Miniaturisation of ELISA allowed overcoming diffusion limitations. Consequently HRP enzyme can be used to produce much higher conversion rates of OPD and consequently achieve strong colourimetric signal with reduced incubation times. This resulted in a massive improvement in both assay speed and assay sensitivity, as supported by our experience with PSA and human IL-1β assay development. PSA is the mostly widely used prostate cancer biomarker with a cut off value of 4 ng/ml, and its monitorization is a vital tool for disease control.[181,182] The cytokines cut of values are in the order of pg/ml concentrations[183] and are important biomarkers for early detection of sepsis[184,185] and infectious disease.[186,187]

3.3. Materials and Methods

3.3.1. Materials

2,3-diaminophenazine (DAP) and SIGMAFAST™ OPD (o-phenylenediamine) tablets were supplied from Sigma Aldrich Ltd (Dorset, UK).

A Human kallikrein 3/ Prostate Specific Antigen (PSA) ELISA kit was purchased from R&D Systems (Minneapolis, USA; cat nº DY1344). The kit contained a monoclonal mouse Human Kallikrein 3/PSA antibody (capture antibody or CapAb), a Human Kallikrein 3/PSA polyclonal biotynilated antibody (detection antibody or DetAb) and recombinant Human Kallikrein 3/PSA (standard).

Human cytokines reagents were purchased from eBiosciences (Hatfield, UK): IL-1β (cat no: human recombinant protein #14-8018; Anti-Human IL-1β biotin #13-7016;Anti-Human IL-1β purified #14-7018); IL-12p70 (cat no: human recombinant protein #14-8129; Anti-Human IL-12p70 biotin #13-7129; Anti-Human IL-12p70 purified #14-7128); IL-6 (cat no: human recombinant protein #14-8069; Anti-Human IL-6 biotin #13-7068; Anti-Human IL-6 purified #14-7069); and Tumor Necrosis Factor-α (TNFα) (cat no: human recombinant protein #14-8329; Anti-Human TNFα biotin #13-7349; AntiHuman TNFα purified #14-7348).

ExtrAvidin-Peroxidase (cat. no E2886) was sourced from Sigma Aldrich Ltd (Dorset, UK) and High Sensitivity Streptavidin-HRP was supplied by Thermo Scientific (Lutterworth, UK; cat no 21130) and used for enzyme detection for IL-1β assay.

Phosphate buffered solution (PBS, Sigma Aldrich, Dorset, UK; cat. no P5368-10PAK), pH 7.4, 10mM was used as IA buffer. The diluent and blocking solution consisted either of SuperBlock (Thermo Fisher Scientific, Loughborough, UK; cat. no 37515) or 1 to 3% w/v protease-free albumin from bovine serum (BSA, Sigma Aldrich, Dorset, UK; cat no A3858) diluted in PBS buffer. For washings, PBS with 0.05% v/v of Tween-20 (Sigma-Aldrich, Dorset, UK; cat no P9416-50ML) was used.

Nunc maxisorp ELISA 96-well MTPs were sourced from Sigma Aldrich (Dorset, UK). The Microcapillary Film (MCF) was supplied by Lamina Dielectrics Ltd (Billingshurts, West Sussex, UK).

3.3.2. Methodology

The miniaturised platform consisted of a 10 bore, ~200 µm internal diameter fluoropolymer microcapillary film (MCF)[127] produced by continuous melt-extrusion process, which due to its geometrical shape and transparent properties can be easily integrated with low cost and easy access readout system, such as a flatbed scanner.

Comparison of MCF and MTP lower detection limit

Different concentrations of DAP were detected in the MCF using a flatbed scanner (HP ScanJet G4050) and in the 96 well plate using a Microplate Reader (Epoch, Biotek). A stock solution of 1 mg/ml of DAP (Sigma-Aldrich, Dorset, UK; cat. no. E2886) was prepared in dimethyl sulfoxide (DMSO) (Sigma-Aldrich, Dorset, UK; cat. no.D8418) and a 1:2 dilution series in PBS was made to complete the calibration curves. Absorbance values were calculated by determining the grey scale peak height for each individual microcapillary in the MCF using ImageJ software (NIH, Maryland, USA), or using the embedded Gen5 data analysis software for microtiter plate (Epoch, Biotek).

Optimisation of Substrate concentration

In order to find the best combination of OPD/H2O2 concentration, stock solutions of 4 mg/ml of both OPD and H2O2 concentrations were prepared in deionized water and a 1:2 dilution series prepared. The solutions were placed in a Nunc MaxiSorp ELISA 96-well microwell plate using a matrix arrangement (OPD and H2O2 concentrations varied along the rows and columns, respectively). EA-HRP was used in solution in a concentration of 0.0156 µg/ml.

Determination of kinetics of enzymatic OPD substrate conversion

The initial enzymatic rates of HRP conversion of OPD to DAP were determined by testing different concentrations of OPD and HRP using both immobilised and solubilized enzyme. A start solution with 1 µg/ml of EA-HRP was immobilised by overnight incubation in the first well of the first column of the microtiter plate, followed by 1:2 dilution solutions in each column. Then, 1:2 dilutions of 1 mg/ml of each substrate (OPD and H_2O_2) were prepared and placed along the rows in the microtiter plate, reading immediately the absorbance values with a microtiter plate reader. To

understand the role of diffusion, the procedure was repeated with the enzyme in solution, by spiking each well with the same quantity of EA-HRP.

Aquisition of full response curves for Sandwich ELISA in MCF

Full response curves for PSA and IL-1β were performed in the MCF using different concentrations and molar ratios of OPD/H_2O_2. To obtain the calibration curves, two 30 cm length MCF strips (strips #1 and #2) were coated with 10 µg/ml of human kallikrein 3/PSA capture antibody (CapAb) diluted in phosphate-buffered saline or 20 µg/ml of Anti-Human IL-1β purified (strips #3 and #4). The MCF strips were incubated for 2 hours at room temperature (20°C) to allow the CapAb to adsorb on the microcapillary surface, and subsequently blocked with 1% BSA (strips #1, #2 and #3) or superblock blocking buffer (strip #4), for 2 hours at room temperature. The strips were washed using PBS with 0.05% (v/v) of Tween-20. Each MCF coated strip was trimmed into 30 mm long test strips, and each strip incubated with a serial dilution 0-60 ng/ml of PSA (recombinant human kallikrein 3/PSA) for 20 min (strip #1 and #2) or a serial dilution 0-1 ng/ml of IL-1β for 30 min (strip #3) and 0-5 ng/ml in strip #4. Then, 2 µg/ml of human kallikrein 3/PSA polyclonal biotinylated antibody or 10 µg/ml of Anti-Human IL-1β biotinylated were used as detection antibodies and incubated for 15 min and 10 min, respectively. EA-HRP in a concentration of 4 µg/ml was incubated for further 15 min in coated MCF strips #1 and #2 and for 10 min in strip #3. The enzyme used in strip #4 (IL-1β assay) was High Sensitivity Streptavidin–HRP with 4 µg/ml, incubated for 10 min. Three washing steps were performed afterwards. Subsequently, 1 mg/ml of OPD and 1 mg/ml H_2O_2 (equivalent to molar ratio 1:3) solution was added to strip #1 (PSA assay) and #3 (IL-1β assay) and 4 mg/ml of OPD and 1 mg/ml H_2O_2 (molar ratio 1:1) were added to strips #2 (PSA assay) and #4 (IL-1β assay). The MCF strips were scanned as RGB images with a HP ScanJet G4050 (Hewlett-Packard, CA, USA) flatbed scanner at 2,400 dpi resolution in transmittance mode in intervals of 2–3 min over 30 min of incubation.

Analysis of MCF strips digital images

RGB digital images were split into 3 separated channels in Image J. The blue channel images were used to calculate absorbance values, based on the grey scale peak height of each individual capillary of FEP-Teflon MCF as described elsewhere.[127] Absorbance (Abs) was calculated for each individual capillary based on equation (3:1):

$$\text{Abs} = -\log_{10}\left(\frac{I}{I_0}\right) \quad (3:1)$$

Where I is the grey scale peak height (transmitted light intensity) and I0 is the maximum grey scale value. The absorbance values were averaged across 10 capillaries for MCF strip.

3.4. Results and discussion

A key aspect that remains clearly underexplored in miniaturization of ELISA tests is the incubation of enzymatic substrates, which perhaps is the most crucial, yet powerful, step in a colorimetric or fluorescence ELISA. OPD (MW=108.1 g/mol) is widely used as a HRP chromogenic substrate by the biggest worldwide manufacturers and suppliers of bioanalytical reagents to life sciences laboratories, and typically recommend 0.4 mg/ml of OPD and 0.4 mg/ml of H_2O_2 (MW=34.0 g/mol) or 0.5-1 mg/ml of OPD and 0.3 mg/ml of H_2O_2. Nevertheless, datasheets are usually not detailed enough regarding the OPD/H_2O_2 molar ratio, which is of paramount importance for ELISA detection in miniaturized tests that are optically interrogated with less sophisticated readout systems. We believe enzymatic conversion using off-the-shelf chromogenic substrates is a solution for the well desirable portability, sensitivity and low-cost of POC tests for detection of molecules in the nanomolar to femtomolar range, which represents the core of clinical diagnostics market.

In order to optimize OPD enzymatic conversion in our novel IA microfluidic platform,[152] which uses a flatbed scanner as a readout system, we studied the stoichiometry of HRP conversion of OPD to 2,3-diaminophenazine (DAP) (Figure 3:1A), realising that two molecules of OPD and one of hydrogen peroxidase (H_2O_2) are necessary for the enzyme to be able to convert OPD (colorless) into DAP (brownish color), which yields a theoretical optimal molar ratio of 2:1.

In more detail, HRP catalyzes the transfer of two electrons from a substrate to hydrogen peroxide to produce an oxidized substrate and water. OPD (MW=108.1 g/mol) is one of the most popular and sensitive chromogenic substrate for HRP detection. Two molecules of this substrate react with one molecule of hydrogen peroxide (H_2O_2;

MW=34.0 g/mol) peroxide and form one molecule of DAP (the oxidized colored product) (MW=210.2 g/mol) and water, as shown in

Figure 3:1A. OPD suppliers usually recommend the concentration of 0.4 mg/ml to be used in ELISA and the same concentration of hydrogen peroxide, i.e. a 1:3 molar ratio. OPD is ideal for use with low-cost, portable optoelectronic components as the product of DAP presents a peak of absorbance at 450 nm, which is ideally aligned with blue colour/channel in the illumination source.

The concentrations of 0.4 mg/ml for both OPD and H_2O_2 as recommended by the suppliers yield a 1:3 OPD/H_2O_2 molar ratio in sandwich ELISA assays which, according to Nicell *et. al* has an inhibitory effect in HRP catalytic activity by H_2O_2.[188]

We compared initially the chromogenic sensitivity and dynamic range of a flatbed scanner in respect to DAP detection against a conventional bench-top microplate reader (Figure 3:1B). The microplate based detection of DAP was about 256 times more sensitive (0.244 pg/ml) than in a 10-bore MCF produced from Teflon-FEP with a flatbed scanner (65.2 pg/ml). This links to the much shorter light path distance of ~200 µm microcapillaries compared to ~3mm light path distance is a microwell. We noticed, however, the DAP scanning in the MCF presented a much broader dynamic range, equivalent to 5% to 100% of OPD conversion, whereas the dynamic range for microwell is limited to the range of 0.02%-15% conversion. Despite DAP being more sensitive in a microwell plate, it lacks quantitation capability for high rates of OPD conversion, whereas in the small microcapillaries the Lambert-Beer law is valid on a very broad range of equivalent OPD substrate concentrations. We hypothesized therefore that substrate concentration should be dramatically increased in order to achieve much faster and more sensitive IAs, should HRP be capable of handling such high concentrations of OPD and/or H_2O_2. Consequently, we tested the effect of both OPD and H_2O_2 concentration in the presence of a constant solubilised ExtraAvidin-HRP (EA-HRP) concentration and noticed HRP conversion of OPD in the commercial formulations is characterized by an inhibition by H_2O_2 (Figure 3:1C and D).

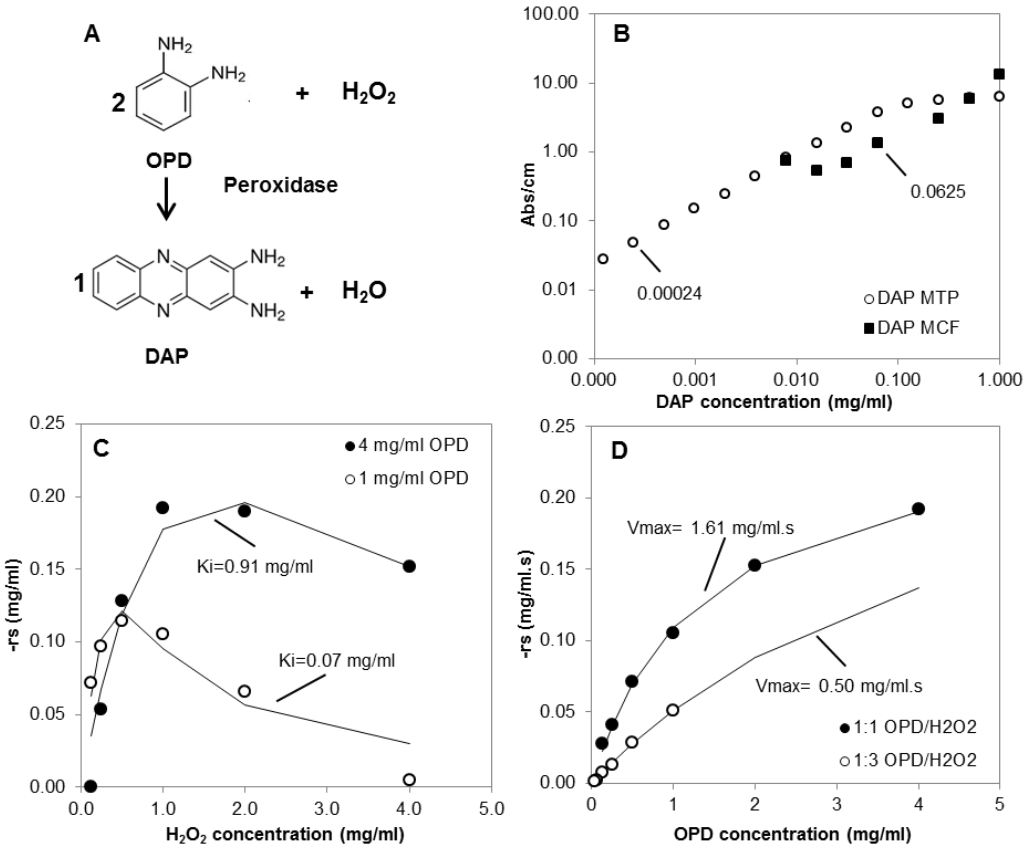

Figure 3:1- Aspects of colorimetric detection in MCF and peroxidase inhibition.
A HRP conversion of OPD chromogenic substrate. **B** Response curves for detection of DAP (coloured product) in a miniaturised Microcapillary Film (MCF) with a flatbed scanner and in a 96 microwell plate (MTP) using a microplate reader. **C** Initial enzymatic conversion rates for different molar ratios of OPD and H_2O_2. **D** Initial conversion rates of OPD as function of H_2O_2 and OPD concentration. The concentration of EA-HRP was kept constant at 15.6 ng/ml.

The initial rates of OPD conversion, $-r_s$ increased with increasing concentration of H_2O_2 (inhibitor, [I]) up to a value of 0.5-1.0 mg/ml (Figure 3:1C), beyond which the initial rate velocities start decreasing. This enzymatic behavior is coherent with inhibition by substrate, in this case H_2O_2, mathematically described by equation (3:2):[189]

$$-r_s = -r_{max}\frac{[I]}{K_s + [I] + \frac{[I]^2}{K_i}} \qquad (3:2)$$

This experiment also allowed determining the ideal concentration of both OPD and H_2O_2, which were 4 mg/ml and 1 mg/ml, respectively, i.e. equivalent to a molar ratio of 1:1 OPD/ H_2O_2. Fitting the substrate enzymatic inhibition model in equation (3:2) a value of 0.07 mg/ml and 0.91 mg/ml were obtained for inhibition constant, K_i with 1.0 mg/ml and 4.0 mg/ml of OPD respectively, indicating a higher degree of enzyme

inhibition with the use of lower OPD concentration. With a molar ratio of 1:3 OPD/H_2O_2 used in commercial OPD substrates, the value of $-r_s$ obtained was 0.11 mg/ml.s whereas with 1:1 molar ratio a maximum $-r_s$ value of 0.191 mg/ml.s was obtained which represents a 1.7 fold increase.

In Figure 3:1D the impact of OPD/H_2O_2 molar ratio is further elucidated. In this experimental set the concentrations were changed for both OPD and H_2O_2 in order to keep initial OPD/H_2O_2 molar ratio constant. This revealed OPD substrate is not responsible for the inhibition, with the values of $-r_s$ increasing as a first order kinetic model for low concentration of OPD and clearly trending to a zero order for higher concentrations of substrate, which is typical of a non-competitive or mixed inhibition kinetic model, mathematically described in equation (3:3):[190]

$$-r_s = -r_{S,max}\frac{[S]}{\alpha K_m + \alpha'[S]} \quad (3:3)$$

Where Ki and Ki' are the inhibitor constants representing the inhibition effects and are described below, in equations (3:4), (3:5), (3:6) and (3:7):

$$\alpha = 1 + \frac{[\mathrm{I}]}{\mathrm{K_i}} \quad (3:4)$$

$$\alpha' = 1 + \frac{[\mathrm{I}]}{\mathrm{K_i'}} \quad (3:5)$$

$$\mathrm{K_i} = \frac{[\mathrm{E}][\mathrm{I}]}{[\mathrm{EI}]} \quad (3:6)$$

$$\mathrm{K_i'} = \frac{[\mathrm{ES}][\mathrm{I}]}{[\mathrm{ESI}]} \quad (3:7)$$

This model considers the inhibitor can bind the enzyme or the enzyme-substrate complex reducing the overall enzyme activity. The kinetic model parameters were found by best-fitting the model in to the experimental data using *Solver* tool in Excel, and are summarized in Table 3:1. These revealed a significant difference in the maximum rate of substrate conversion, $-r_{s,max}$ shown in Figure 3:1D, representing a 3.2-fold increase in maximum rate of conversion of OPD.

Table 3:1 - Kinetic parameters (non-competitive/mixed inhibition) for the two different molar ratios of OPD/H_2O_2 studied.

	1:3 OPD/H_2O_2	**1:1 OPD/H_2O_2**
$-r_{s,max}$ (mg/ml.s)	0.50	1.61
K_m (mg/ml)	8.39	8.39
K_i (mg/ml)	5.53	1561.00
K'_i (mg/ml)	5.32	0.39

It is clear from Table 3:1 that the inhibition has higher impact on enzyme kinetics at a molar ratio of 1:3. As previously discussed, K_m remains approximately constant at both molar ratios tested, with the value of $-r_{s,max}$ being strongly affected by the molar ratio. This reinforces the non-competitive inhibition model typical of HRP.[190] Based on equation (3:6) and (3:7) the smaller the values of both K_i and K_i', the more efficient is the inhibitor binding either the enzyme itself or the enzyme-substrate-inhibitor complex. Comparing the two curves in Figure 3:1D, K_i at 1:1 molar ratio was about 280 times higher than the value of K_i at 1:3 molar ratio, suggesting the inhibitor, I (in this case H_2O_2) binds directly to the enzyme. For 1:3 molar ratio, the value of K_i obtained was very similar to that of K'_i, which again is typical of a non-competitive inhibition,[190] where the reaction is only inhibited by the formation of enzyme-inhibitor complex (Equation (3:5)).

Overall, it appears that when in excess H_2O_2 inhibits HRP enzymatic kinetics by reducing the enzyme activity, however it does not affect the affinity of HRP to the substrate. This inhibition effect is surpassed by changing the molar ratio initially recommended by the manufacturers from 1:3 to 1:1.

Although molar ratio of OPD/H_2O_2 revealed paramount to the rate of generation of colourimetric signal by affecting HRP kinetics, the diffusion and mass transfer limitations need to be taken into account in respect to the speed and magnitude of colourimetric signal produced, which ultimately controls both speed and sensitivity of the IA. In heterogeneous IA, the enzyme is eventually "immobilised" on the plastic surface and consequently the kinetics of substrate conversion is modified because of mass transfer limitations. Immobilised enzyme reactions present lower initial velocities, due to migration time of substrate molecules to the walls and to possible conformational

changes during adsorption process.[191] This is the typical situation in a microtiter plate, where the maximum distance of molecular diffusion is in the range of 3 mm, which can represent several minutes for a medium size molecule. Further experiments with solubilized enzyme in a microwell (Figure 3:2A) confirmed the increase in the rate of colorimetric signal generation with the increase of OPD concentration. Nevertheless, experiments with immobilised enzyme (Figure 3:2B) revealed not being advantageous to use higher rates of conversion of OPD as this leads to the rapid accumulation of product near the plastic wall and fluctuations in the rate of conversion of OPD which is not beneficial for IA, where typically the end-point or kinetics rate is expected to be linked to the concentration of analyte in the sample. The absorbance values obtained were lower than those for solubilized enzyme as, in one hand, the enzyme immobilisation process might interfere with enzyme catalytic activity[192] and, on the other hand, the total enzyme molecules available are dependent on the quantity of molecules bond to the wall. We calculated the turnover number of the enzyme in this specific system by analyzing the velocity rates with the changing of enzyme concentration and, assuming that ExtrAvidin contains two molecules of peroxidase, the turnover number was 1.95×10^6 s^{-1}.

In miniaturized ELISA platforms such as MCF, diffusion distances are very short and, consequently, an increase in conversion rates of substrate is extremely beneficial. With a maximum diffusion distance of ~100 µm, substrate conversion with HRP will approach the situation shown in Figure 3:2A for solubilized enzyme, which ultimately translate into stronger colorimetric signal generated with much shorter incubation times. This feature will enhanced signal-to-noise ratios and ultimately improved sensitivities, assuming the enzyme is working at maximum activity. Note that when using EA-HRP in a sandwich ELISA, it is known that extravidin binds to the biotinylated antibody, therefore eliminating the problem of catalytic enzymatic activity reduction due to its conformational change.

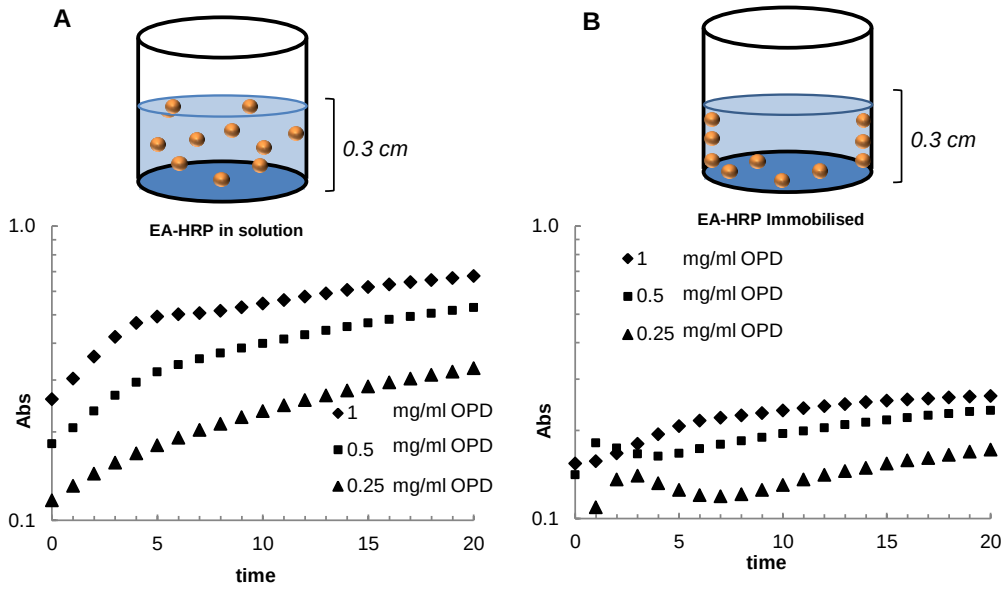

Figure 3:2 - Kinetics of HRP conversion of OPD for varying concentration of chromogenic substrate.
A EA-HRP in solution. **B** EA-HRP immobilised on plastic surface of a 96 microtiter plate well. Concentration of H_2O_2 was kept constant at 1 mg/ml H_2O_2, and final concentration of EA-HRP immobilised or in solution was kept at 15.6 ng/ml.

To illustrate the multiple benefits of the 1:1 molar OPD/H_2O_2 and higher OPD concentration we have performed multiple PSA and IL-1β sandwich assays optimized for the MCF. Figure 3:3 shows the effect of OPD incubation on the performance of these two assays. The incubation time required for PSA was reduced in 10-fold when compared to the conventional 1:3 molar ratio, and both the signal and sensitivity (or lower limit of detection defined as absorbance of blank plus three standard deviations) were improved from 11.5 to 0.7 ng/ml. In the case of human IL-1β quantitation the sensitivity was much further improved from 100 to 6 pg/ml. The reaction also revealed much faster as the signal obtained with just 3 minutes of OPD incubation was about 3-fold stronger than the signal obtained with 30 minutes OPD incubation with 1:3 molar ratio.

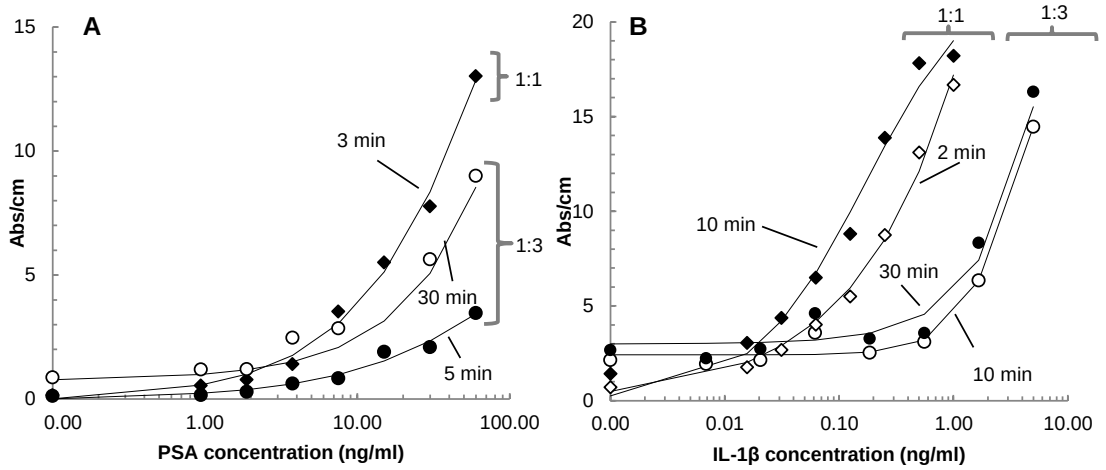

Figure 3:3 - Comparison between two different OPD and H2O2 molar ratio in MCF sandwich assays.
A 4 mg/ml of OPD and 1 mg/ml of H_2O_2 (1:3 molar ratio) makes the PSA MCF assay 10 times faster and with 16x higher sensitivity. **B** IL-1β assay improved sensitivity from 100 pg/ml to 6 pg/ml with 3 fold reduction in assay time. The times shown relate only to the time of incubation of OPD before optical interrogation of the microfluidic MCF strips.♦ 1:1 molar ratio OPD:H_2O_2 and ● 1:3 molar ratio OPD:H_2O_2.

3.5. Conclusions

HRP conversion of OPD is characterised by H_2O_2 inhibition of enzyme activity that leads to extended incubation times and weak signals difficult to detection with less sophisticated optoelectronic components. By increasing the OPD concentration from 1.0 to 4.0 mg/ml and OPD/H_2O_2 molar ratio from 1:3 to 1:1 the value rate of enzymatic conversion was increased by 4-fold, which is very beneficial for microfluidic devices that contain short diffusion distances. It also avoids the rapid depletion of substrate that characterises commercial OPD formulations. A number of sandwich assays with PSA and IL-1β detection in fluoropolymer microfluidic MCF strips and a flatbed scanner have shown systematically one or more orders of magnitude increase in sensitivity and/or speed of the assay. This allows mimicking the performance and reliability of sophisticated laboratory detection equipment using low-cost optoelectronic equipment, which is expected to trigger the development of affordable POC tests that fully exploit the low-cost and unique amplification capabilities of enzymatic ELISA detection.

4. The flow effect on assays speed and sensitivity in microcapillary immunoassays

4.1. Abstract

We present experimental results of effect of flow on antibody-antigen binding in a novel microfluidic IA (immunoassay) platform, based on fluoropolymer, the Microcapillary Film (MCF). Experimental results were fitted to a kinetic model and the association/dissociation rate constants and equilibrium constants estimated, confirming the impact of flow in the assays speed and sensitivity. The range of flow rate studied for antigen was 10 to 1000 μl/min. From the data presented in this study we conclude that assay sensitivity is affected by sample flow rates ≥10 μl/min, since increasing shear stress challenges antibody-antigen binding in the microcapillary system, decreasing the amount of antigen bond to the immobilised antibody. For high antigen concentration systems, flow rates of 10 μl/min will only affect assay speed, without compromising the sensitivity.

Understanding the flow effect is a fundamental step for automation of Microcapillary Film (MCF) assays, bringing the technology one step closer to Point-of-Care diagnostics.

Keywords: Flow rate, point-of-care, microfluidic, capillary geometry, antibody binding, ELISA, automation.

4.2. Introduction

Point-of-care (POC) tests require automation of reagent loading and often the replacement of solutions. To design the device and engineer the operating mode it is important to understand how fluid flow affects a diagnostic test, commonly performed with IAs, using the specificity of antibody-antigen bonding. Therefore, understanding the effect of flow on antibody-antigen binding, which will be translated in IA performance, such as sensitivity and speed, is fundamental for the development and automation of quantitative POC tests.

Flow rate is fundamental for IA technologies, including lateral flow (LF) and microfluidic IAs (IA).[193] In LF technology, a set of different pads, the detection pad with immobilised antibody, the sample pad for sample deposition and the conjugate release pad with dried label antibody, are integrated into a test strip to perform a rapid sandwich assay. The sample flows along the different pads, due to the hydrophilic properties of the porous substrate the nitrocellulose membrane, mixing the sample with the label antibody and transporting the bond and unbound antigen to the test and control lines into the waste reservoir.[193] Currently, competitive and sandwich LF formats are able to detect and quantify vitamin-D,[194] progesterone,[195] hCG,[196] prostate specific antigen,[197,198] and hepatitis C virus (HCV).[199]

Traditionally, LF and IA are performed in one single step. This feature is very useful for POC diagnostics, since the test is fast and easy to carry out. However, this feature is also one of the main reasons for poor sensitivity of LF technology, because the lack of washing steps increases the non-specific binding and does not allow a signal amplification step. In addition, LF rely on a wicking effect or with a capillary action, defined as the time required for water to travel up and completely fill a 4 cm length strip membrane,[193] which is essential for assay sensitivity. The porosity and the pore size of the membrane also determine the flow rate at which the analyte passes the test line; the higher the flow rate, the shorter the time for interaction between the immobilised antibody and sample analyte, causing the effective analyte concentration to decrease with the square of the increase of flow rate and decreasing the sensitivity of the test.[200]

Analyte residence time is a problem recognized in LF IA and in some paper based IA, since there is no flow control strategy, and several researchers have suggested strategies

to overcome this technical bottleneck. *Rivas et al.* (2012)[201] introduced wax-printed hydrophobic pillars onto the nitrocellulose membrane that delays the flow and increase vorticity, achieving a 3-fold improvement in sensitivity. *Parolo et al.* (2012)[202], increased the sensitivity of gold nanoparticles-based LF by changing the size of the pads, in order to find a balance between flow speed and sample volume. They understood that by changing both conjugation and sample pads sizes in a certain configuration, the speed flow in the conjugation pad would not change significantly, giving enough time for label antibodies to recognize the analyte. In addition, a larger sample pad, meant a larger sample volume and a bigger conjugated pad, meant a larger volume of label antibodies, therefore more analyte could be bond to label analyte, resulting in the formation of higher number of immune-complexes, which allowed for an 8-fold improvement in LF sensitivity.

The lack of flow control in one step assays, the small test zone area, and small sample volume, are some of the LF technological obstacles for sensitivity improvement.

Adding multiple steps to LF, such as washing and signal enhancement steps in a modified two-dimensional paper network format, can increase sensitivity by 8-fold when compared to unmodified LF IA technologies. Nevertheless, flow rate and therefore analyte residence time in the capture area is still not controllable.[196]

Microfluidic IA technologies refer to systems where the fluid is manipulated through channels with micrometer dimensions. Generally, the microchannel presents a capture zone with immobilised CapAb in a limited zone of the channel.[87] In microfluidic technologies flow is easily controlled manually or by pump systems and can be adjusted so that analytes have enough time to bind immobilised antibodies and higher analyte amount from the sample volume forms antibody-antigen complex, achieving higher sensitivities compared to LF. Therefore, flow control is not usually a problem for microfluidic IAs, it can avoid antigen depletion from the bulk solution. *Hu et al.* (2006) reported an antigen-antibody binding model in a 20 μm height microchannel, in which increment in flow rate decreased the equilibrium binding time, in other words the presence of flow would speed up the assay because it would increase the analyte mass transport. Slow velocity should just be considered to decrease total sample consumption, since sample consumption is proportional to the product of flow velocity and the equilibrium time. The flow rates explored in the study varied from 0 to 0.192 μl/min.[203]Another study reported similar conclusions, with flow rate range studied from

0 to 0.02 µl/min.[204] Besides avoiding solution depletion, microfluidic IA can use flow to deliver reagents present in a liquid phase, with the inlet often connected with tubes to external pumps and reservoirs. High sensitivity microfluidics is related to the possibility of performing multiple steps assays, including washing steps (reducing the non-specific signal) and signal amplification, which increases the overall signal-to-noise of the assay.[7]

However, sensitivity of microfluidic IAs is usually dependent on sample incubation time, with longer incubation times translating into larger amounts of bond analyte compared to bulk analyte. This feature is not desirable for point-of-care applications, where speed is one of the required conditions being affordable, sensitive, specific, user-friendly, rapid, robust, equipment-free, delivered (ASSURED).[6] Also, most of the microfluidic external control is not disposable, which does not suit the ASSURED point-of-care demands.[205] Although all microfluidic IA devices developed use liquid flow, the effect of flow in antibody binding in microfluidic systems is not well understood. In this chapter we aim to explain the effect of flow rate on antibody binding, and consequently the flow effect on assays speed and sensitivity, in novel microfluidic tests strips manufactured from a fluoropolymer, the Microcapillary Film (MCF). The MCF is a plastic flat film with 10 parallel embedded holes, with a diameter of approximately 200 µm, melt extruded from FEP-Teflon.

Understanding the antibody-antigen kinetics and equilibrium constants, as well as the factors that affect the reaction in the MCF IA platform is an important aspect in the development of POC tests, which aims at increasing assay speed and sensitivity. Assay speed is related to rapid antibody-antigen binding (high association constants, K_{on}) and assay sensitivity is related to analyte capture capacity of the system (high equilibrium constants, K_{eq}).

4.3. Materials an Methods

4.3.1. Materials & Reagents

Purified Mouse IgG, Anti-Mouse IgG (whole molecule) peroxidase conjugated, SIGMAFAST^{TM} OPD (o-Phenylenediamine dihydrochloride) tablets, Phosphate buffered solution (PBS), Tween-20 and Bovine Serum Albumin (BSA) were purchased from Sigma-Aldrich (Dorset, UK).

The IA buffer used was 10 mM PBS at pH 7.4. The blocking solution consisted of 3% w/v protease-free BSA diluted in PBS buffer and the washing solution was PBS with 0.05% v/v.

The MCF used was fabricated from fluorinated ethylene propylene co-polymer using a melt-extrusion process by Lamina Dielectrics Ltd. (Billinghurst, West Sussex, UK). FEP-Teflon MCF presents 10 parallel microcapillaries with mean 0.2 mm hydraulic diameter.

MCF strips were connected to Vici M6 pumps, supplied from Valco International (Parkstrasse 2, CH-6214 Schenkon). Sets of 30 cm length MCF strips were glued to a 5 mm i.d., ¼'' o.d. High-Density Polyethylene (HDPE) tubing with slow setting epoxy.

4.3.2. System overview and kinetic model

Capture antibodies were immobilised on the overall surface area of the 10 bore 200 μm diameter FEP-Teflon MCF shown in Figure 4:1B. The MCF presents a large surface for antibody immobilisation (each 4 cm strip presents 0.25 cm^2 of surface area available per capillary) when compared with capture areas of reported microfluidic channels, e.g. fused silica capillary micro-reactor with $3.1x10^{-2}$ cm^2, spotted antibodies onto an open PDMS with $3x10^{-2}$ cm^2 and a reaction chamber with $1x10^{-3}cm^2$. [56,147,206]

The flow within the MCF capillaries is laminar with a parabolic profile for flow profile for all the flow rates studied, 10 to 1000 μl/min, with Reynolds numbers of varying between 0.1 and 100, respectively.

The antibody-antigen kinetics were fitted to a theoretical IA mathematical model that aims to describe the role of transport of analyte in a microchannel (convection and diffusion), the kinetics of binding between the analyte and the capture antibodies, and the surface density of the capture antibody (CapAb) on the assay. Equation (4:1), was solved analytically for a constant analyte concentration and used for estimating the rates of association (K_{on}) and dissociation (K_{off}) of antibody binding in the MCF system.[204]

$$\Phi = \frac{k_{on}\ \Phi_{max}\ C}{k_{on}\ C + K_{off}}(1 - \ e^{-(K_{on}\ C + K_{off})t} \qquad (4:1)$$

Where Φ is the surface density at time *t*, *C* is the analyte concentration, K_{on} is the association rate, K_{off} is the dissociation rate, and Φ_{max} is the maximum surface coverage, which in our system was given by the highest absorbance obtained.

4.3.3. Flow effect determination on antibody binding in FEP-Teflon microcapillaries

For optimization of immobilised antibody in high analyte concentration systems, mouse IgG solutions with 0, 0.1, 1 and 10 μg/ml were aspirated into different 4 cm MCF strips and incubated for 2 hours at room temperature. The solution inside the strips was replaced by 3% BSA blocking solution, which was left to incubate for an additional 2 hours at room temperature. The strips were then washed again with 1 ml PBS-tween solution. A dilution of 1/1000, corresponding to 1 μg/ml of anti-IgG conjugated to peroxidase was added to each strip and incubated for 10 minutes. Each strip was washed again with 1 ml PBS-Tween and 1 mg/ml of OPD/H_2O_2 substrate aspirated and left to incubate for 10 minutes. The strips were imaged using a flatbed scanner (HP G4050) in transmittance mode, with a minimum resolution of 2,400 dpi.

After determining the optimum concentration of immobilised antibody, four 30 cm MCF strips were filled with 10 μg/ml of mouse IgG diluted in PBS solution, and left for 2 hours at room temperature for adsorption of antibody. The strips were then blocked with a solution for 2 hours at room temperature. The MCF strips were washed with PBS-Tween and emptied before being connected to the Vici pump, by injecting air with a syringe attached to a silicone tube. The MCF capillaries were filled with 1 μg/ml of Anti-IgG peroxidase conjugated at 10000 μl/min for 2 seconds, and then, each 30 cm MCF strip was continuously infused with anti-IgG at variable flow rate, 10, 100 and

1000 µl/min and 4 cm MCF strips were trimmed from the strip at regular time intervals of two minutes following the first minute: 1, 2, 4, 6, 8 and 10 minutes, and quickly washed with 1 ml of PBS-Tween solution (Figure 4:1C). One of the MCF strips was used as a control, where the incubation of anti-IgG was performed in the absence of flow, therefore incubation was done in the absence of flow. The MCF strips were then filled with 1 mg/ml of OPD substrate and left to incubate for 10 minutes. Digital images of the strips were taken by a flatbed scanner and analysed by ImageJ (NIH, Maryland, USA) software.

In order to test the flow effect in low analyte concentration systems a 1:2 serial dilution with an initial anti-IgG dilution 1µg/ml was prepared, and aspirated and incubated for 10 minutes in 4 cm long MCF strips coated 10 µg/ml of mouse IgG and blocked with 3% BSA for two hours at room temperature, as described previously. After 10 minutes incubation of Anti-IgG, the strips were washed and filled with 1 mg/ml of OPD substrate for 10 minutes, before being imaged with a flatbed scanner.

For immobilised antibody concentration optimization in low analyte systems, 8 MCF strips were filled with 0, 0.1, 1, 10, 20, 40, 80, 100 µg/ml of mouse IgG and left to incubated at room temperature for 2 hours. Blocking and washing procedures were the same as previously described. A 0.06 µg/ml solution of anti-IgG was aspirated and incubated for 10 minutes in the different MCF strips, followed by a washing with PBS-Tween and 10 minutes incubation with 1 mg/ml OPD substrate. The strips were then imaged with a flatbed scanner.

In order to test the flow effect on antibody binding, two 30 cm MCF strips were incubated with 100 µg/ml of mouse IgG for 2 hours at room temperature. Blocking and washing procedures were the same as previously described. A 0.06 µg/ml dilution of Anti-IgG was added to the 30 cm MCF strips. In one of the strips used as control, the incubation occurred in the absence of flow and in the other strip the incubation was with10 µl/min. The MCF strip was trimmed at varying time intervals as described above: 1, 2, 4 6, 8 and 10 minutes (Figure 4:1). Each trimmed strip was washed with 1 ml of PBS-Tween and 1 mg/ml of OPD substrate was added and incubated for 10 minutes. The strips were then imaged with a flatbed scanner.

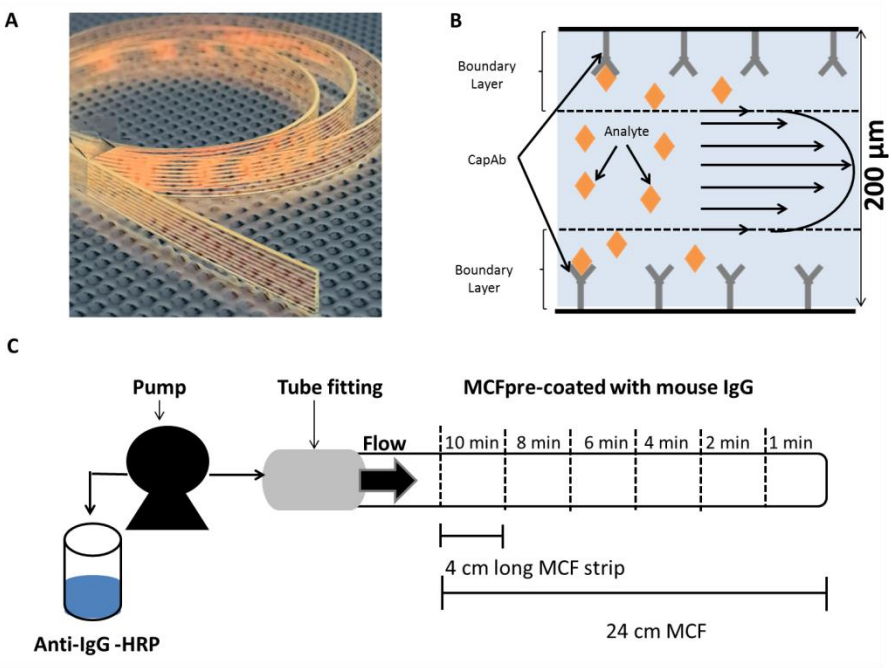

Figure 4:1 – In flow MCF flow IA.
A 100 cm long MCF strip. **B** Diagram of microcapillary IA configuration in laminar flow. **C** Experimental set up used for MCF flow experiments.

Table 4:1- Anti-IgG volume passed in 4 cm MCF strip/minute.

	Total volume of IgG passed through the 4 cm long strip per minute of experimental time
No Flow	13 µl
10 µl/min	13 µl + 10 µl
100 µl/min	13 µl + 100 µl
1000 µl/min	13 µl + 1000 µl

4.3.4. Image analysis of MCF strips

Digital RGB images were split into 3 separated channels images in *Image J* software. The blue channel images were used to calculate absorbance values, based on the peak grey scale height for each individual capillary as described elsewhere.[127,152] Absorbance was calculated according to (4:2)

$$\text{Abs} = -\text{Log}_{10}\left(\frac{I}{I_0}\right) \qquad (4:2)$$

I is the transmitted light and corresponds to I_0 minus peak height and I_0 is the baseline grey scale value (emitted light). The absorbance values presented here correspond to average of absorbance values from 10 capillaries on each MCF strip.

4.4. Results and Discussion

Understanding the effect of flow in microfluidic sandwich IAs is fundamental for developing rapid, sensitive and robust miniaturized diagnostic tools. Few diagnostic biomarkers have high clinical thresholds, such as hCG, used for pregnancy with a cut-off value of 0.5 mg/mL[207] and CRP protein, a cardiac biomarker, which 1 μg/ml indicates the low risk of future cardiovascular complications.[208] The majority of biomarkers requires quantitation at very low concentration, such as cytokines in sepsis diagnostic, where 17 to 70 pg/ml cytokines (e.g. IL-6, TNFα, IL-10) levels can predict a particular disease and thereby help to select the appropriate treatment.[184,209] Also, troponin used in cases of heart failure has for cardiovascular diseases prediction demands equivalent to a clinical threshold of ≤ 40 pg/mL.[17] Therefore, POC tests have to be able to measure analyte concentration in a broad range of concentrations, besides integrating all the ASSURED conditions.

There is limited understanding on the effect of flow on sensitivity. In the present chapter the effect of flow on antibody binding was studied for high and low analyte concentrations, using mouse, a mouse IgG and anti-IgG-HRP system to mimic antibody-antigen interaction. The use of this system is prevalent in direct IAs, since it shows diffusion and rate constants similar to many antibody-antigen interaction.[210] For high concentration of analyte (1 μg/ml of Anti-IgG) mouse IgG was immobilised in the FEP-Teflon MCF at a density of about 50 ng/cm^2, which represents around 12.5% of an "end-on" antibody monolayer.

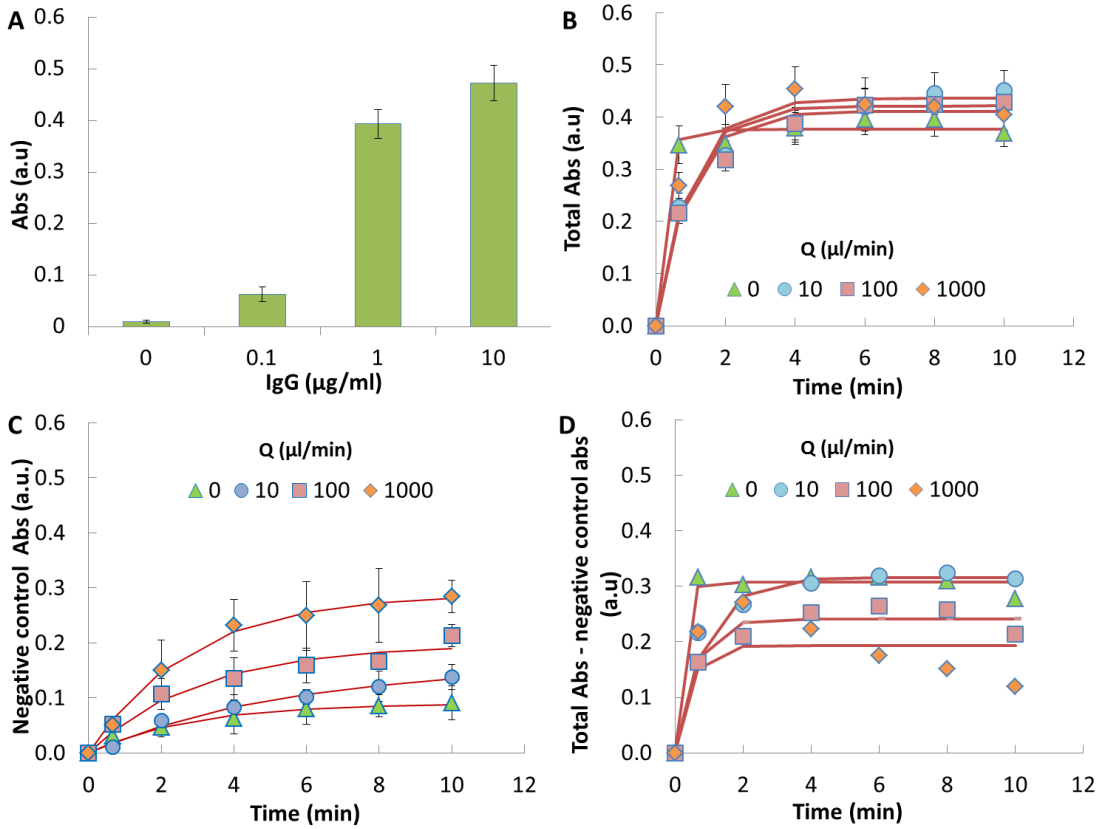

Figure 4:2 – Flow effect on antibody binding in the FEP-Teflon MCF at high antigen concentration regimes (1 µg/ml nti-IgG).
A MCF optimization of immobilised mouse IgG for 1 µg/ml of Anti-IgG. **B** Kinetics of IgG and Anti-IgG binding at continuous flow rates from 0 to 1000 µl/min, for 1 µg/ml analyte concentration, considering the total absolute absorbance signal. **C** Non-specific Anti-IgG binding kinetics (negative control) at different flow rates (from 0 to 1000 µl/min) for 1 µg/ml of Anti-IgG. **D** Kinetics of IgG and Anti-IgG binding at different flow rates (from 0 to 1000 µl/min), for 1 µg/ml analyte concentration, considering the absorbance signal related only to antibody-antigen specific binding (Specific signal = Total absorbance – Negative control absorbance).

The antibody-antigen equilibrium can be described by equation (4:3),

$$\text{CapAb} + \text{Ag} \rightleftharpoons \text{CapAb-Ag} \qquad (4:3)$$

where CapAb, is the concentration of immobilised antibody (mouse IgG); Ag is the concentration of antigen (Anti-IgG); and CapAb-Ag is the concentration of antibody-antigen complex.

It was found that flow slightly delays the time to reach equilibrium (Figure 4:2B), presenting a K_{on} of 6.97 x 10^6 $M^{-1}s^{-1}$ and a K_{off} 4.42 x10^{-2} s^{-1} in the absence of flow and K_{on} of 1.48 x 10^6, 1.83 x 10^6 and 1.8 x 10^6 $M^{-1}s^{-1}$, for anti-IgG incubation with 10, 100

and 100 µl/min flow rate, respectively (Table 4:2). These values are comparable to those found in literature for the same antibody pair. [211,212]

Table 4:2 – Kinetic parameters of antigen antibody binding with flow in antigen excess systems.

		Total Signal	Background Signal	Specific Signal
No flow	K_{on} ($M^{-1}s^{-1}$)	$6.97x10^{6}$	$4.88x10^{6}$	$6.97x10^{6}$
	K_{off} (s^{-1})	$2.77x10^{-2}$	0.3263	$4.42x10^{-2}$
	K_A (M^{-1})	$2.52x10^{8}$	$1.50x10^{7}$	$1.58x10^{8}$
	R^2	0.99315	0.99812	0.99184
10 µl/min	K_{on} ($M^{-1}s^{-1}$)	$1.90x10^{6}$	$4.40x10^{6}$	$1.48x10^{6}$
	K_{off} (s^{-1})	$5.38x10^{3}$	0.15404	$8.88x10^{-3}$
	K_A	$3.54x10^{8}$	$2.86x10^{7}$	$1.67x10^{8}$
	R^2	0.98559	0.99444	0.98495
100 µl/min	K_{on} ($M^{-1}s^{-1}$)	$1.83x10^{6}$	$9.79x10^{6}$	$1.83x10^{6}$
	K_{off} (s^{-1})	$5.61x10^{-3}$	0.26635	$1.81x10^{-2}$
	K_A	$3.26x10^{8}$	$3.67x10^{7}$	$1.01x10^{8}$
	R^2	0.99015	0.98011	0.97774
1000 µl/min	K_{on} ($M^{-1}s^{-1}$)	$1.83x10^{6}$	$1.57x10^{7}$	$1.83x10^{6}$
	K_{off} (s^{-1})	$4.59x10^{-3}$	0.25749	$2.56x10^{-2}$
	K_A	$3.98x10^{8}$	$6.09x10^{7}$	$7.13x10^{7}$
	R^2	0.981044	0.99812	0.77352

In the absence of flow the maximum absolute signal, therefore maximum sensitivity, is reached in less than 1 minute, while in the presence of flow the equilibrium is reached after 4 minutes. There were no differences observed between the different flow rates studied, (Figure 4:2B). It is important to mention that the absolute signal results from anti-IgG bond specifically to the immobilised antibody, but also to any anti-IgG capable of binding directly to the wall of the microcapillaries. In order to obtain only the specific signal the experiments were repeated without immobilised mouse IgG, and MCF strips only blocked with 3% BSA. Background signal increased with increase of incubation time of antigen of and with the increment in flow rate (Figure 4:2C), presenting K_{eq} of 1.50×10^{7} M^{-1} in the absence of flow and 2.86×10^{7}, 3.67×10^{7} and 6.09×10^{7} M^{-1} for 10, 100 and 1000 µl/min, respectively. The association rate constants were also higher in the presence of flow in stagnant conditions (Table 4:2).

This increase in the non-specific signal at the MCF assays results in a drop in the signal-to-noise ratio of the assay, therefore reduced sensitivity of the assays. In brief, for high analyte concentration system the presence of flow delays the antibody-antigen binding, but also promotes direct binding of label IA reagents to the capillary walls, reducing the specific binding for flow rates range at 100 and 1000 µl/min (Figure 4:2 and Table 4:2).

The increment in assay time and reduction sensitivity, in flow, can be explained by the effect of shear in the microcapillary walls, which increases with the flow rate. According to Figure 4:1C and Table 4:1, with 10 µl/min flow rate the 3 initial MCF strips, corresponding to times 1, 2, and 4 minutes, did not have Anti-IgG solution replacement, which means that the initial filling solution was just being dragged along the capillary, decreasing the mouse IgG-Anti-IgG complex formation. However, since the antigen concentration is high and the antigen solution is being replaced with fresh solution, the equilibrium is maintained with the absence of flow and 10 µl/min. Shear can affect assay signal and sensitivity in three-fold. Firstly, the increment of shear stress close to the capillary wall promotes the decrease of boundary layer thickeness decreasing consequently the residence time of analyte in the system; secondly by promoting removal of antigen from the antibody-antigen complex; thirdly, by incrementing the boundary layer instability, which difficults the bonding between antibody and antigen.

Based on the fact that anti-IgG incubation at 10 µl/min appeared to not change the equilibrium constant (Keq) (no flow conditions Keq =1.58E x108 M-1and 10 µl/min Keq =1.67 x 108 M-1,Table 4:2), this flow rate was used for analysing the kinetics of antibody-antigen binding for mouse IgG and Anti-IgG. The concentration of CapAb was optimized for low antigen concentration, 60 ng/ml (Figure 4:3A) and it was found that instead of 10 µg/ml, the optimum concentration was 100 µg/ml, which corresponds to approximately 70% of "end-on" antibody monolayer, as mentioned in chapter 2.

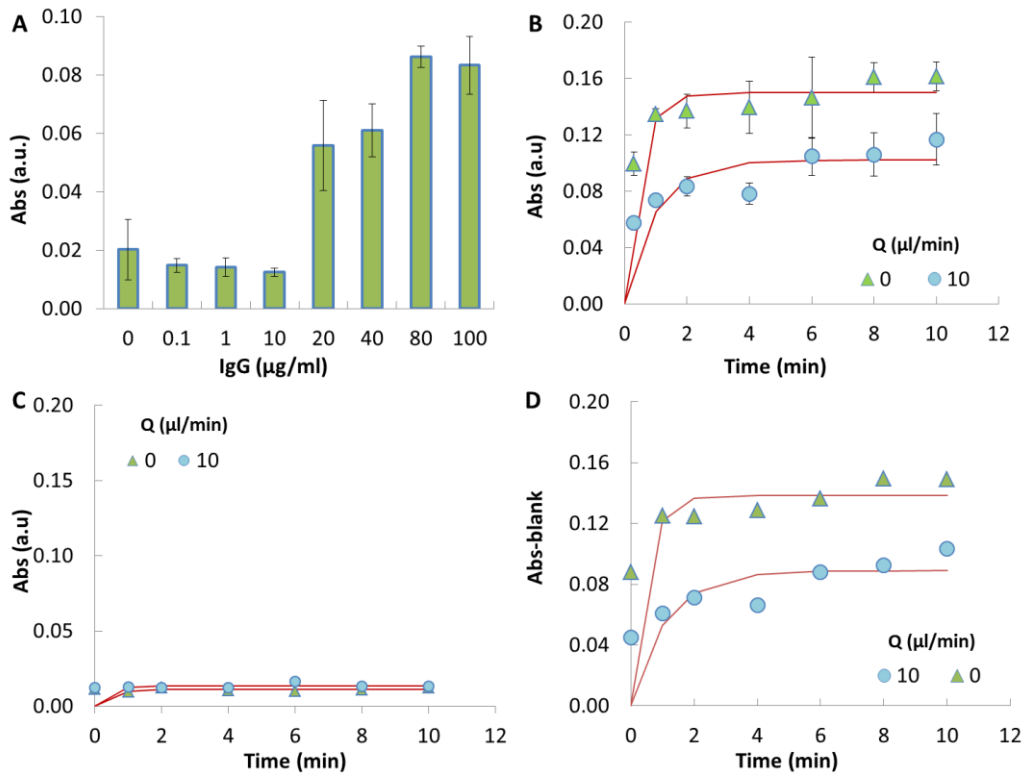

Figure 4:3 - Flow effect on kinetics of antibody binding in the MCF at low antigen concentration (60 ng/ml).
A Optimisation of immobilised concentration of mouse IgG **B** Kinetics of IgG and Anti-IgG binding in the absence and in the presence of flow (Q=10 µl/min), considering the total absolute absorbance signal,. **C** Non-specific Anti-IgG binding kinetics (background development) in the absence and presence of flow (10 µl/min) for 0.06 µg/ml of Anti-IgG. **D** Kinetics of IgG and Anti-IgG binding in the absence and presence of flow (10 µl/min), considering Specific signal = Total absorbance – Background signal.

With a small antigen concentration of 60 ng/ml of anti-IgG, the association rate constant (kon) dropped from 6.11 x 106 M-1s-1 in the absence of flow to 1.67 x 106 M-1s-1 at 10 µl/min and the equilibrium constant (Keq) dropped from 5.64 x 108 M-1 to 2.0 x 108 M-1 respectively (Figure 4:3B). These best fitted constants are summarised in Table 4:3.

Table 4:3 – Kinetic parameters of antigen antibody binding with flow in antigen limited systems.

		Total Signal	Specific Signal
No flow	K_{on} ($M^{-1}s^{-1}$)	$6.62x10^{6}$	$6.11x10^{6}$
	K_{off} (s^{-1})	$8.88x10^{-3}$	$1.08x10^{-2}$
	K_A (M^{-1})	$7.46x10^{8}$	$5.64x10^{8}$
	R^2	0.8812	0.8879
10 µl/min	K_{on} ($M^{-1}s^{-1}$)	$2.19x10^{6}$	$1.67x10^{6}$
	K_{off} (s^{-1})	$8.40x10^{-3}$	$8.35x10^{-3}$
	K_A (M^{-1})	$2.60x10^{8}$	$2.00x10^{8}$
	R^2	0.79490	0.81943

This shows that in high sensitivity systems, for flow rates as small as 10 µl/min assay time is increased, increasing up to 4 minutes the time to reach the equilibrium. Assay sensitivity also reduced in low analyte systems, since the maximum signal in continuous flow is lower than the one obtained with antigen incubation in the absence of flow. The background increment was not significant, due to the low concentration of the analyte (Figure 4:3C), therefore in low analyte concentration systems the decrease observed on assay sensitivity is directely related to the shear effect on antibody-antigen binding.

Parsa et al. (2008) reported an antibody-antigen binding numerical model in a PDMS microchannel with h=50 µm and w=500 µm and a binding surface of 100-1500 μm^2. In this model for unlimited sample and incubation time (approximately 10 hours) the analyte capture flow rate was not affected, however when time decreased to 5 or 10 minutes, the captured analyte decreased with the incubation time, but still increased within flow rates from 0.1 to 100 µl/min. The negative effect of flow was only evident in time and sample volume constraint, where the analyte capture decreased with the flow rate, being almost zero at 100 µl/min for the range of sample volume studies (1 to 15 µl). The captured area used in the numerical simulations was 0.0005 cm^2. This flow effect was validated with experimental data with mouse IgG and anti-IgG system, where the fluorescent signal was proportional to the bond complex, but decreased with the flow rate from 0.1 to 100 µl/min.[210] In the Fep-Teflon MCF, the initial sample volume inside the capillaries was13 µl for a capture area of 2.5 cm^2 (corresponding to 4 cm long MCF strip) and the maximum incubation time tested was 10 min. Therefore, the flow

effect observed in the MCF antigen incubation is coherent with the model described by *Parsa et al* (2008), whose reported flow rates ≥ 1 µl/min can decrease the capture analyte of a system. The experimental results presented in the same study show a decrease in analyte capture from flow rates to ≥ 0.1 µl/min. *Zimmermann et al.* (2005) reported a microfluidic antibody-antigen binding model in which the analyte capture would increment with flow rates of ≤ 0.02 µl/min. and *Hu et al.* (2006) reported the same finding for flow rates at ≤ 0.2 µl/min. These flow rates are 500 times and 50 times smaller than the ones used in the MCF flow antigen incubation studies, explaining the different conclusions about the flow effect for these models and the MCF flow experimental results.

In general, flow has a significant impact on assay sensitivity not only for LF technology but also in microfluidic devices. Consequently, several sensitive microfluidic IAs required stopped flow during antigen incubation. For example, IL-4 biomarker was measured with a Lower Limit of Detection (LLoD) of 0.2 pg/ml and PSA presented a LLoD 16 pg/ml in a microfluidic microplate, both requiring 20 minutes stagnant incubation of sample.[66] Other microfluidic devices used polyesterene beads with immobilised CapAb inside an immunopillar chip, reported LLoD around 100 pg/ml of CRP, AFP and PSA, with 5 min sample incubation.[58] Flatbed Scanner colorimetric MCF IAs have presented a LLoD's in femtomolar range with cytokines detection[154] and LLoD of < 1 ng/ml PSA in 2 min with stagnant sample incubation.[152] A glass capillary immunoasensor with portable fluorescence detection reported an LLoD of 1 ng/ml for PSA and 5 ng/ml for AFP, with 20 min continuous sample incubation at 50 µl/min.[69] Although antibodies immobilised layer and detection modes are important for assay sensitivity, flow rates during sample (analyte) incubation times also play an important role. When same biomarkers are incubated for longer time the LLoD systematically increases at Q=50 µl/min. This is coherent with the data presented in this study, which shows at flow rates larger than 10 µl/min the analyte capture decreases which involves a decrease in equilibrium constants (Figure 4:3D and Table 4:3). Flow rate impacts on sensitivity and according to this data it also impacts on the antibody-antigen binding kinetics. Sandwich assays performed in microfluidic IAs used capillary pumps to control the flow rate in the range of 0.028 to 0.2 µl/min.[213] *Cesaro-Tadic et al.* (2004) reported tumor necrosis factor α (TNF- α) microfluidic assay with a LLoD of 20 pg/ml with 12 minutes sample incubation time at 0.03 µl/min (30 nL/min) using capillary

pumps.[50] *Gervais et al.* (2009) reported a microfluidic fluorescent CRP one step sandwich assay with 1 ng/ml detection limit within 14 min at 0.082 µl/min (82 nL/min) also using a capillary pump. The main drawback of such microfluidic sandwich assays appeared to be the use of high resolution and expensive readout equipment, i.e. such as fluorescente microscopes. Recently, *Mohammed et al.* (2014) reported a LLoD of 24 pg/ml of Troponin I involving sample incubation time of 4 minutes with capillary flow where the reaction chamber geometry decreases the flow velocity, increasing the residence time of analyte in the system. The signal was obtained using a house build and fully enclosed fluorescent reader.[73]

In summary, microfluidic IA devices present, in general a higher sensitivity than LF assays due to good flow control with external devices, such as pumps or manual syringe. However, IA yet the flow has a substantial negative effect on sensitivity which requires detailed consideration when automating microfluidic IAs.

4.5. Conclusion

LF technology offers simplicity and speed in diagnostics; however this technology lacks the sensitivity essential for some important diagnostic diseases such as sepsis and cardiovascular diseases. This reduced sensitivity is mainly due to a lack of flow control in one step, LF IA. Microfluidic technology offers sensitive IAs with the possibility of flow control; however, understanding the effect of flow on antibody-antigen binding over a broad range of flow rates in microfluidic platforms is important for automation and design of POC tests.

In the present study it was concluded that sample incubation in FEP-Teflon MCF strips requires a flow rate below 10 µl/min, and preferably below 0.1 µl/min if the assay requires quantitation of low analyte concentrations. For high analyte systems a flow rate of 10 µl/min can be used yet extended incubation times are required to avoid any impact on assay sensitivity. Future work will consist in validation of these broad conclusions, with different sandwich assays, with different orders of magnitude of LLoD, e.g. the PSA, Cytokines and cardiac biomarkers assays in the MCF platform.

5. A Lab-in-a-briefcase for rapid PSA screening from whole blood

5.1. Abstract

We present a new concept for rapid and fully portable Prostate Specific Antigen (PSA) measurement, termed “Lab-in-a-Briefcase”, which integrates an affordable microfluidic ELISA platform utilising a melt-extruded fluoropolymer Micro Capillary Film (MCF) containing 10 bore, 200 μm internal diameter capillaries, a disposable multi-syringe aspirator (MSA) plus a sample tray pre-loaded with all required immunoassay (IA) reagents, and a portable film scanner for colorimetric signal digital quantitation. Each MSA can perform 10 replicate microfluidic IA on 8 samples, allowing 80 measurements to be made in less than 15 minutes based on semi-automated operation and no requirement of additional fluid handling equipment. An assay was optimised for measurement of a clinically relevant range of PSA from 0.9 to 60.0 ng/ml in 15 minutes with CVs in the order of 5% based on intra-assay variability when read using a consumer flatbed film scanner. The PSA assay performance in the MSA remained robust in the presence of 1:2 diluted and non-diluted human serum and whole blood, where matrix effect could be overcome by extending the incubation times of the samples beyond 2 min. The PSA "Lab-in-a-briefcase" is particularly suited to a low-resource health setting where diagnostic labs and automated IA systems are not accessible, by allowing PSA measurement outside the laboratory using affordable equipment.

5.2. Introduction

Prostate cancer is the second most common cause of cancer and the sixth leading cause of death by cancer among men population worldwide.[214] Currently Prostate Specific Antigen (PSA) is the most reliable tumor biomarker for prostate cancer diagnosis and for monitoring disease recurrence after treatment. The highest prostate cancer incidence rates have been estimated to occur in the highest resource areas of the world, however higher mortality rates are seen in low- to medium-resource areas of South America, the

Caribbean, and sub-Saharan Africa.[214] Two possible reasons for high mortality rates in low resource settings are lack of early detection and absence of appropriate diagnostic testing, alongside limited treatment options.

PSA serum concentration in healthy males is in the range of 0-4 ng/ml and increases in men with prostate cancer.[12] Several studies of screened populations showed individuals with PSA levels in the range of 4–10 ng/ml had a 22-27% likelihood of developing cancer, with those with PSA levels of ≥10 ng/ml having a risk increasing to 67%.[215,216] The Food and Drug Administration (FDA) approved the determination of PSA serum levels to test asymptomatic men for prostate cancer, in conjugation with digital rectal exam (DRE), in men aged 50 year-old or older with a cutoff blood PSA value of 4 ng/ml.[182,181] However, some organizations and studies advise undergoing periodic PSA screening from the age of 40 for African American men and men with prostate cancer family history.[217] After diagnosis and treatment of primary disease, regular PSA measurements are also routinely used to monitor disease progression and inform clinical decision making. Prostate cancer recurrence is investigated when the PSA blood levels reach 0.4 ng/ml in patients with radical prostatectomy treatment,[218,219] and 2 ng/mL above the post-treatment PSA nadir (absolute lowest level of PSA after treatment) for patients submitted to radiotherapy.[220,221]

Although the efficacy of cancer screening programs is generally complex recent studies have suggested that PSA screening may be able to decrease prostate cancer mortality.[222,223]

PSA levels are commonly quantified in blood samples in laboratories by sandwich enzyme-linked immunosorbent assay (ELISA). The microtiter plate (MTP) remains a common platform for ELISA in diagnostic laboratories offering several advantages including established methods and wide range of reagents and kits, alongside wide availability of plate readers, automated plate handling instruments and plate washers. MTP-based ELISA is highly quantitative and sensitive enough to reach a low Limit of Detection (LLoD) in the picomolar range.[224] However, MTP ELISA cannot be performed outside the laboratory, requires long incubation times and must be performed by trained personnel. These limit the suitability of MTP for the ever increasing demand for measurement of biomarkers such as PSA[225,226] and prevent PSA screening or monitoring in low resource areas where diagnostic laboratories have limited capacity.[227] A rapid, inexpensive, portable and quantitative ELISA platform is therefore urgently

required for both high and low resource health systems, in order to simplify PSA screening and monitoring. This should integrate simple manual fluid handling with a simple signal measurement system and avoid the need for expensive instrumentation.

One approach to point-of-care PSA quantification is to develop a fully quantitative lateral flow assays, for example by using fluorescence detection[228] or scanning band intensity of colorimetric lateral flow strips.[197]Although lateral flow assays have the assay speed, simplicity, low cost and portability appropriate for point-of-care diagnostics, the suitability for quantitative applications remains unclear, and so they remain most suited to qualitative diagnostic tests.[229] Lateral flow systems also lack the capacity to perform multiple replicate tests in a single assay, preventing the use of internal standard reference assays alongside the sample.

Recently microfluidic devices have overcome several limitations of MTP for performing ELISA by capturing the analyte on the surface of a microchannel or using particles entrapped inside the microchannels to increase the surface-to-volume ratio and reduce diffusion distances, resulting in greatly reduced assay times.[148] Many microfluidic IA systems have been reported for detection of a wide range of analytes, including measurement of cancer biomarkers such as PSA.[66,230] Major remaining challenges for microfluidic devices include controlling fluid flow and developing simple inexpensive detection systems. For example, power-free Lab-on-a-Chip PSA measurement in serum was achieved by manually moving magnetic particles through a device using a permanent magnet.[70] Mobile phone cameras were used for colorimetric signal quantitation.[70,194] However, the inability of using several replicates in the same run might compromise assay precision, and these devices do not have the capacity for running internal reference samples alongside sample. A major drawback for most microfluidic devices also remains the high fabrication cost preventing rapid product development from laboratory prototypes.

We propose here a new "Lab-in-a-briefcase" concept for rapid, manual, portable and cost-effective PSA screening, based on an affordable miniaturized ELISA platform that utilises a melt-extruded MicroCapillary Film (MCF).[117] We developed a manually operated device capable of performing 80 microfluidic quantitative ELISA tests in <15 minutes and read using a flatbed scanner. Standard reference curves and sample replicates are measured simultaneously, allowing internal assay calibration. The entire system can be carried in a small briefcase, a handbag or a laptop case and the assay can

be performed by a single operator with minimal training, and requires no additional equipment or instrumentation. We present here optimization and performance data for this new system that demonstrates its ability to measure clinically relevant PSA concentrations in human serum and whole blood over a range of operating temperatures. This portable microfluidic system has the potential to give large population access to affordable PSA screening and monitoring.

5.3. Materials and Methods

5.3.1. Reagents and Materials

A Human kallikrein 3/ Prostate Specific Antigen (PSA) ELISA kit was purchased from R&D Systems (Minneapolis, USA; cat nº DY1344). The kit contained a monoclonal mouse Human Kallikrein 3/PSA antibody (capture antibody), a Human Kallikrein 3/PSA polyclonal biotynilated antibody (detection antibody) and recombinant Human Kallikrein 3/PSA (standard). ExtrAvidin-Peroxidase (cat. nº E2886), SIGMAFASTTM OPD (o-Phenylenediamine dihydrochloride) tablets (cat. nº P9187), o-Phenylenediamine dihydrochloride (cat. nºP1526-25G), urea hydrogen peroxide (cat. nº 289132), phosphate-citrate buffer tablets, pH 5.0 (cat. no P4809) were sourced from Sigma Aldrich Ltd (Dorset, UK). 3, 3', 5,5' Tetramethylbenzidine (TMB) (cat. nº DY999) from R&D Systems (Minneapolis, USA) was also used as an alternative enzymatic substrate. High Sensitivity Streptavidin-HRP was supplied by Thermo Scientific (Lutterworth, UK; cat no 21130) and used for enzyme detection.

Phosphate buffered solution (PBS, Sigma Aldrich, Dorset, UK; cat. no P5368-10PAK), pH 7.4, 10mM was used as IA buffer. The diluent and blocking solution consisted either of SuperBlock (Thermo Fisher Scientific, Loughborough, UK; cat. no 37515) or 1 to 3% w/v protease-free albumin from bovine serum (BSA, Sigma Aldrich, Dorset, UK; cat nº A3858) diluted in PBS buffer. For washings, PBS with 0.05% v/v of Tween-20 (Sigma-Aldrich, Dorset, UK; cat no P9416-50ML) was used. Nunc maxisorp ELISA 96-well MTPs were sourced from Sigma Aldrich (Dorset, UK). Normal Human Serum Off the Clot, from a single female donor Post-Menopausal (product code S1221) was supplied by SunnyLab (Broad Oak Road, Sittingbourne, UK). The whole blood used

was obtained from umbilical cord through NHS England, collected into a bag with added citrate phosphate dextrose (CPD) as anticoagulant.

5.3.2. "Lab-in-a-briefcase" components

The "Lab-in-a-briefcase" (Figure 5:1) comprises four components: 1) a set of 15 x 12 x 1 cm^3 disposable Multiple Syringe Aspirator (MSA) devices, each of which can perform 10 replicate ELISA tests on each of 8 samples; 2) customised microwell plates pre-loaded with reagents that interfaces with the MSA; and 3) a portable USB powered film scanner for colorimetric signal quantitation; and 4) a portable computer for real-time data analysis. If required, diluent plus disposable pipettes can be included for diluting samples to increase assay dynamic range. The overall dimension of this portable lab can be 40 x 30 x 15 cm^3 and weighting up to 3 kg.

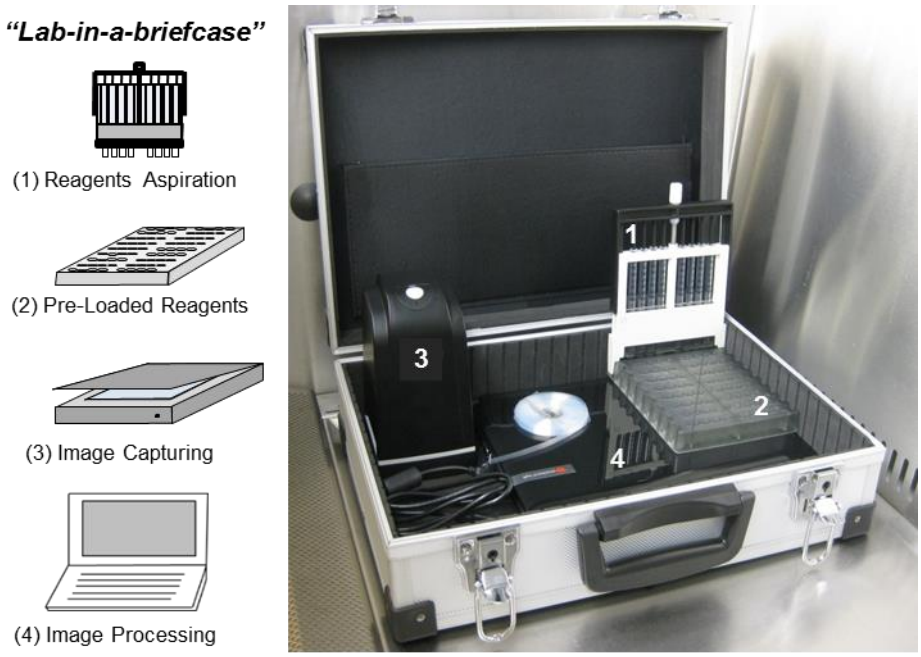

Figure 5:1 - Main components of "Lab-in-a-briefcase" for PSA screening.

Each MSA device includes unique design features that minimizes the possibility of operator error (e.g. asymmetric edges and a single thumb-wheel to control sample and reagent aspiration). The fluid aspiration within the MSA cartridge is driven by 8 plastic, 1ml syringes driven by a simple thumb-wheel and central threaded rod. Each syringe is connected to a single 30 mm long strip of fluoropolymer MCF containing 10 bore,

200µm internal diameter microcapillaries pre-coated internally with monoclonal CapAb (Figure 5:2). The MSA combines with a customized microwell plate, loaded with reference standard samples, assay reagents and wash buffer, plus empty sample wells for clinical samples. One MSA device plus microwell plate can analyse 8 independent samples, allowing the option of comparing a single sample with 7 reference samples, or as many as 4 samples with 4 reference samples.

MCF is a long, continuously manufactured plastic film containing a parallel array of microcapillaries with controlled size and shape, resulting from air aspiration/injection through a specially designed melt-extrusion die.[117] The surface characteristics (hydrophobic) and the geometry of the fluoropolymer MCF (flat film) make it a reliable platform for IA techniques, including ELISA.[127] The "Lab-in-a-briefcase" uses a MCF ribbon produced from fluorinated ethylene propylene (FEP-Teflon), containing 10 embedded capillaries with a mean hydraulic diameter of 206 ± 12.2 µm manufactured by Lamina Dielectrics Ltd (Billingshurts, West Sussex, UK). The external dimensions of the fluoropolymer MCF used in this study were 4.5 ± 0.10 mm wide by 0.6 ± 0.05 mm thick.

The hydrophobicity of MCF fluoropolymer allows the antigen and antibodies to be immobilised on the inner surface of the microcapillaries by passive adsorption.[127] MCF extruded from FEP has exceptional optical transparency because its refractive index of 1.34 to 1.35[231] matches the refractive index of water (1.33), allowing simple optical detection of colorimetric substrates[127]

5.3.3. PSA Sandwich ELISA in the fluoropolymer MCF

For each duplicate run using the MSA, the inner surface of the microcapillaries in a 50 cm long fluoropolymer MCF was coated with Human Kallikrein 3/PSA capture antibody (CapAb) within a concentration range of 10-40 µg/ml in phosphate saline buffer (PBS). This solution was incubated overnight at 4ºC or for a minimum of 2 hours at room temperature (20 ^{o}C). The MCF surface was then blocked using the IA diluents, 1 to 3% BSA/PBS or SuperBlock Solution, for at least 1 hour at room temperature, after which the MCF was washed and trimmed to produce eight 30 mm long fluoropolymer MCF test strips which were inserted into the push-fit seal and then fitted into the MSA.

Recombinant PSA protein standards loaded into the sample wells of the plate were aspirated into MCF strips in the MSA cartridge with 6 full revolutions of the central wheel (Figure 5.2), and cartridge left in the plate with MCF immersed in samples for incubation. Each wheel rotation draws up 13 µl through the MCF test strips, thus 6 turns correspond to 78 µl of reagent per 10 bore assay strip. This volume was in great excess compared to the small internal volume of each 30mm strip (approximately 10 µl) to ensure complete solution replacement, which allowed skipping washing steps in the sandwich IA.

The MSA cassette was then moved to the next row of wells in the MSA plate containing biotinylated detection antibody (DetAb) within the range 0.5-2 µg/ml in PBS. The solution was aspirated with 6 turns of the wheel and incubated for required time. Subsequently this procedure was repeated for the enzyme conjugate (ExtrAvidin Peroxidase and High Sensitivity Streptavidin-HRP). Finally, the MCF test strips were washed 3 to 4 times with PBS-T (washing buffer) using 6 turns of the thumb wheel per wash.

The enzymatic substrate (OPD or TMB) was then aspirated into the MCF strips and the MSA containing the MCF strips was laid flat on a HP ScanJet G4050 Film Scanner, and RGB images with 2,400 dpi resolution scanned in transmittance mode (Figure 4:4) were taken at a given time interval. The MSA provides good alignment of the test strips with the glass surface of the scanner, at a distance within the focal distance of the linear CMOS detector (about 6 mm). The volume of the 1 ml disposable syringes was sufficient to deliver homogeneous aspiration of each IA reagents and good washing before the addition of the colorimetric substrate. RGB images of the fluoropolymer test strips array were then taken every 2 to 5 min for up to 30 minutes, and analysed using ImageJ (NIH, Maryland, USA) to quantify absorbance on each individual capillary (Figure 4:4) from the grey scale pixel intensity. The RGB image was split into red, green and blue channels, and for OPD substrate the blue channel was used as it provided maximum light absorption, whereas with TMB the red channel showed the highest absorbance.

5.3.4. PSA Sandwich ELISA optimization the fluoropolymer MCF

Assay optimization studies were done according to an experimental matrix which consisted in analyzing the effect of 7 factors: CapAb concentration, DetAb concentration, DetAb incubation time, PSA incubation time, enzyme concentration, enzyme incubation time, and matrix effect. All factors were optimized according to the maximum signal-to-noise ratio and total assay time (Figure 5:2 and Figure 5:5A).

Kinetic studies, involving optimum incubation times, were performed using the optimized concentrations of 40 µg/ml CapAb, 1 µg/ml of DetAb; 1 µg/ml of high sensitivity streptavidin, and 4 mg/ml o-phenylenediamine dihydrochloride (OPD) with 1 mg/ml Hydrogen Peroxide.

The matrix effect was studied after the assay optimization process (Figure 5:5A). It was tested by performing in parallel three different PSA full response curves, one with buffer solution spiked with diluted concentrations of recombinant proteins (0% serum) and the others diluting the PSA standards in 100% and 50% (in PBS) female serum, respectively within a total assay time ≤15 minutes. To complement the study of sample matrix on PSA sandwich assay other set of experiments where PSA standards were spiked in non-diluted serum and whole blood matrices were performed. Resulting absorbance values were compared to absorbance values of PSA standards diluted in buffer. To finalize matrix effect studies sample incubation time was increased to ≥10 minutes and two PSA assays were performed in parallel, one in buffer (0% serum) and the other in non-diluted serum (100% serum) in a total assay time ~30 minutes. For the purpose of this comparison, the assay conditions were: 10 µg/ml CapAb incubated overnight at 4ºC, 2 µg/ml of DetAb incubated for 10 minutes, 4 µg/ml of Extravidn Peroxidase incubated for 10 minutes, 4 mg/ml of o-phenylenediamine dihydrochloride (OPD) and 1 mg/ml with Hydrogen Peroxide incubated for 3 minutes.

The 4 Parameter Logistic (4PL) mathematical model was fitted to experimental data by the minimum square difference for each full PSA response curve. The lower limit of detection (LLoD) was calculated by the mean absorbance of the blank plus three times the standard deviation of the blank samples.

5.3.5. PSA IA Optimization in the MCF

The effect of CapAb concentrations (10, 20 and 40 µg/ml) and DetAb concentrations (0, 0.5, 1 and 2 µg/ml) on colorimetric signal was tested by comparing absorbance values obtained in test strips incubated with 0 ng/ml (negative control), 1.5 ng/ml (lower end) and 30 ng/ml (upper end) recombinant protein diluted in the assay buffer. Since the optimum CapAb and DetAb concentrations were established, the effect of DetAb concentration and DetAb incubation times (0, 2.5, 5, 10 minutes) was fully tested using 4.0 ng/ml of recombinant protein. A third set of experiments was performed which aimed optimising the conditions for the enzyme complex, High Sensitivity Streptavidin-HRP (0, 1, 2 and 4 µg/ml). All core sandwich PSA IA steps were optimised in respect to maximum signal-to-noise ratio.

A chromogenic OPD enzymatic substrate was used, which consisted in 1 mg/ml OPD and 1 mg/ml H_2O_2 (enhanced recipe) or 4 mg/ml OPD and 1 mg/ml H_2O_2 (fully optimised recipe); note the manufacturer recommended 0.4 mg/ml OPD and 0.4 mg/ml of H_2O_2 for ELISA in MTPs. Horseradish peroxidase is an enzyme with a large turnover, therefore we have found that higher concentrations of OPD and/or H_2O_2 results in one order of magnitude increases in absorbance in the microcapillaries, where the diffusion of a small molecule such as OPD and DPA across the whole diameter of the capillary can happen in few seconds.

5.3.6. PSA IA in the Microtiter Plate (MTP)

The protocol recommended by ELISA kit manufacturer was followed for PSA assay detection in a 96-well MTP which is summarized in Table 5:1. The OPD was added to each well, slightly mixed and absorbance measured at 450 nm using the Epoch (BioTek) microplate reader. In this instance no stop solution was used, in order to compare directly the colorimetric data obtained in the MCF strips with the flatbed film scanner. Absorbance values were expressed as cm^{-1} based on a light path length of 0.30 cm for a 96 microtiter plate well.

Table 5:1 - Experimental conditions used for sandwich ELISA detection of PSA in a 96 well MTP.

Step	Concentration	Incubation Time	Volume (per well)	T (ºC)
CapAb	1 µg/ml	overnight	100 µl	4
Washing	-		4*100 µl	20
Blocking (BSA)	1% (w/v)	2 hours	300 µl	20
Washing	-		4*100 µl	20
PSA standards	0.9-60 ng/ml	120 minutes	100 µl	20
Washing	-		4*100 µl	20
DetAb	0.2 µg/ml	120 minutes	100 µl	20
Washing	-		4*100 µl	20
Enzyme (Extravidin)	1 µg/ml	20 minutes	100 µl	20
Washing	-		4*100 µl	20
Substrate (OPD)	0.4 mg/ml	30 minutes	100 µl	20

5.3.7. Measurement of Absorbance, Absorbance Ratio and Intra-assay variability in MCF strips

The absorbance (*Abs*) in the MCF strips was measured from the grey scale pixel intensity of scanned images using image analysis. This consisted in running a profile plot across the greyscale images of the MCF strips (blue channel) and measuring the baseline grey scale pixel intensity across each strip (I_0) and the peak height (I) at the center of each capillary, from where *Abs* could be directly determined by equation (5:1).

$$\text{Abs}=-log(I/I_0) \qquad (5:1)$$

This procedure was repeated for each individual capillary on each separate MCF strip. Response curves for PSA performed in the MCF strips were compared to those performed in the MTP by considering a mean light path distance of 200 µm for each capillary in the MCF strips.

In order to understand signal variability across the different microcapillaries within the same MCF strip (intra-assay variability), MCF strips were immersed in liquid nitrogen, sliced with a razor blade and observed using a long distance microscope (Nikon SMZ1500). The mean hydraulic diameter, and width (w) and height (h) for each capillary (Figure 5:3) was then measured using Image J software. For each strip at least

10 slices were analysed at 30 mm intervals which corresponds to the distance of the pre-coated MCF strips required to operate the MSA.

In parallel, MCF strips from the same batch were filled with a 1:2 dilution series of 2 mg/ml of 2,3-diaminophenazine (DAP), the colored product resulting from the enzymatic conversion of the chromonogenic OPD substrate. The MCF strips were then scanned using same film scanner and absorbance values determined by image analysis using Image J. This allowed normalizing Abs values in respect to DAP reference solution, which was expressed in this paper as Absorbance Ratio (Abs ratio) values:

$$\text{Abs ratio} = \frac{Abs_{PSA}}{Abs_{DAP}} \qquad (5:2)$$

5.3.8. Robustness studies for PSA sandwich ELISA in the MCF

The effect of temperature on the PSA assay performance was tested by running full response curves using the optimised PSA protocol and all reagents brought to the operating temperature of 4, 20 or 37 °C.

The intra-assay variability studies was accomplished by measuring the absorbance of lower, middle and upper range of PSA values (3.75, 7.5 and 30 ng/ml PSA) in the 10 capillaries of one MCF strip. These values were already normalized by DAP absorbance, which means that the variability obtained is only intrinsical to the assay and it does not depend of the platform geometry variation.

The inter-assay variability was determined by performing PSA assay in the MCF for three PSA concentrations: 3.75, 7.5 and 30 ng/ml (lower, middle and higher range) in three different days and using different MSA devices. The absorbance was measured for 20 samples (n=20) of each PSA concentration studied. For every PSA concentration the inter-assay variability was obtained by calculating the coefficient of variation (CV) between the absorbance of 3 independent PSA sandwich assay runs.

5.4. Results and discussion

5.4.1. Optimisation of manual and portable Lab-in-a-briefcase ELISA

The inexpensive microengineered MCF material was first presented as a miniaturised IA platform for low cost microfluidic direct ELISA[127], but the majority of IA require a sandwich format including an immobilised CapAb. To demonstrate the potential of the melt-extruded microfluidic material MCF for delivering affordable, sensitive, clinical testing using a sandwich protocol, we developed a complete ELISA system that shares many benefits with MTP assays but in a portable kit requiring no additional equipment or any complex fluid handling. The core of this system is a manually driven multi-syringe device, termed a MSA, combined with a customized microwell plate, that together aspirate samples and all required reagents sequentially through MCF strips to perform a full sandwich ELISA (Figure 5:2). The different geometry, size, and surface-to-area ratio of MCF leads to significant differences in optimal ELISA assay conditions when compared to MTP assays, specifically higher reagent concentrations combined with shorter incubation times. Initial studies therefore focused on identifying the optimal assay conditions for the required sensitivity and for fast total assay times (Figure 5:2) and were based on the optimal signal-to-noise ratio of the assay.

A concentration of 20 µg/ml of CapAb and 2 µg/ml of DetAb (detection antibody) resulted in the highest absorbance signal for the assay as shown in Figure 5:2 however it also resulted in higher background signals (strip with 0 ng/ml of recombinant protein) with incremental CapAb concentrations for all range of DetAb concentrations tested. With 40 µg/ml of CapAb the concentration of DetAb significantly affected the background signal. This happened because the detection antibody is polyclonal, so it can bind directly to the CapAb or to other proteins on the fluoropolymer surface significantly increasing the background signal. The best signal-to-noise ratio was therefore obtained with 40 µg/ml of CapAb and 0.5 µg/ml of DetAb. This was also valid for 1.5 ng/ml and 30 ng/ml PSA (lower and upper limits, respectively, of PSA studied range), based on 5 minutes substrate incubation time. The large surface-area-to-volume ratio in the 200 µm MCF allows coating the plastic fluoropolymer surface with a concentration of CapAb more than 10x higher than on a 96-well plate. This can potentially improve the sensitivity of the assay in the MCF, as the kinetics of antigen-

antibody binding is favored by high surface density of CapAb molecules. This is only possible until a given surface coverage, above which the antibodies binding capacity decreases for reason well established in literature.[158]

In a further set of experiments a MCF reel was coated with 40 µg/ml of CapAb varying the DetAb concentration and DetAb incubation time. Then, the full sandwich assay was completed using 4 ng/ml of recombinant protein. Figure 5:2B shows that for all DetAb concentrations studied the absorbance values increased until 1 µg/ml of DetAb. The highest absorbance signals were obtained for 5 minutes incubation time of DetAb, followed by 10 minutes and 2.5 minutes. The background signal increased with the increase in the concentration and incubation time of the DetAb, being 10 minutes incubation and 2 µg ml of DetAb the conditions resulting in higher background signals. Figure 5:2B shows that 1 µg/ml of DetAb incubated for 5 minutes resulted in the highest signal-to-noise ratio with 40 µg/ml of CapAb. The use of a detection monoclonal antibody would increase the sensitivity of the assay, however this issue can be easily overcome by varying the concentration and incubation time for the DetAb.

In respect to the enzymatic complex, the highest signal was obtained with 4 µg/ml of High Sensitivity Streptavidin-HRP with 5 minutes incubation (Figure 5:2C), however it is important to take in consideration that these conditions also led to the highest background signal. The presence of colorimetric signal at 0 µg/ml of enzyme showed enzymatic conversion of OPD in the absence of enzyme which might have been induced by the transmitted light in the flatbed scanner.

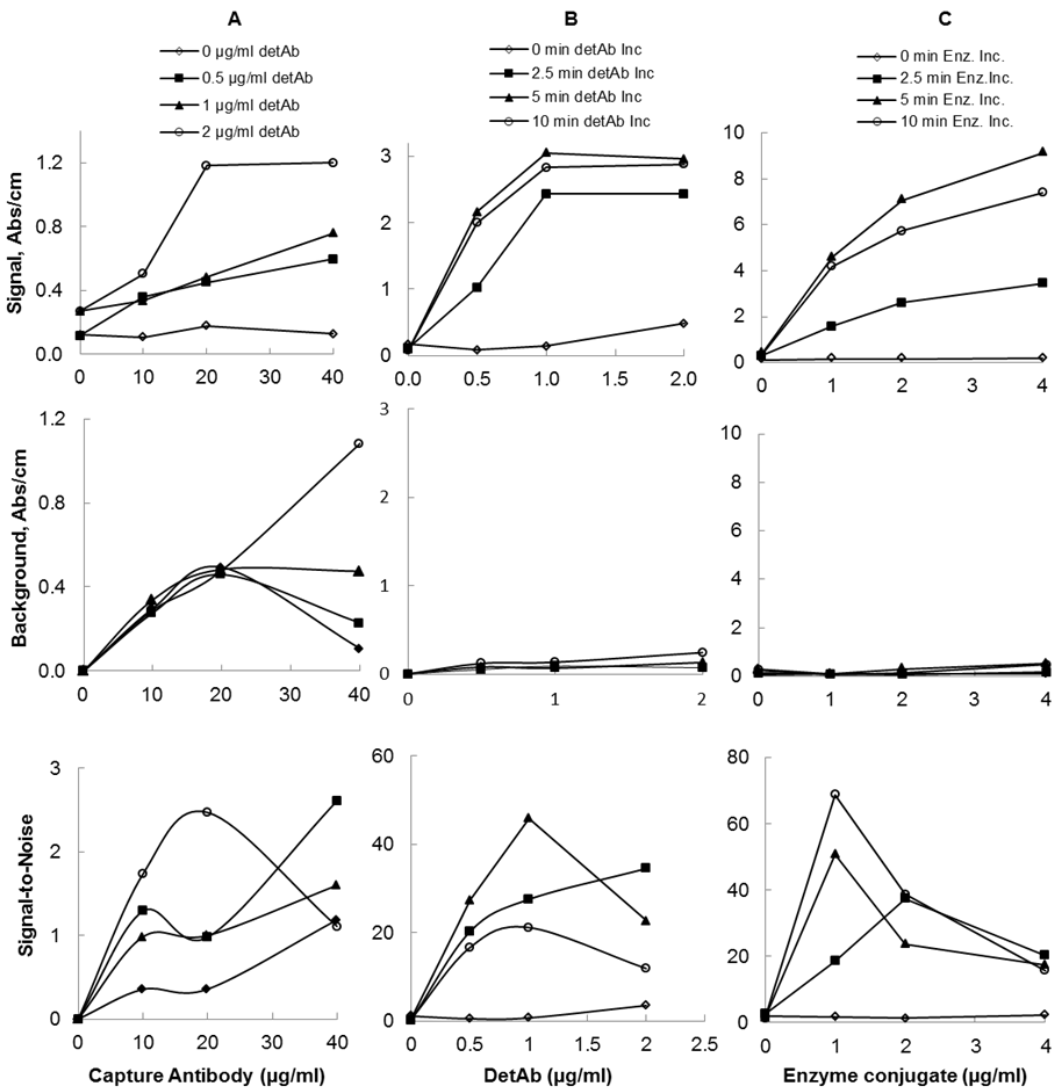

Figure 5:2 - Optimisation of PSA sandwich assay conditions in the fluoropolymer MCF platform using the MSA.

A Signal, background and signal-to-noise ratio of MCF PSA assay with varying concentartions of capAb and detAb concentration, using 1.5 ng/ml of recombinant protein and 4 µg/ml of Extravidin Peroxidase. **B** Signal, background and signal-to-noise ratio of MCF PSA assay for varying concentrations and inbuation times for detAb (capAb 40 µg/ml; 4 ng/ml recombinant protein; 4 µg/ml Extravidin Peroxidase. **C** Signal, background and signal-to-noise ratio of PSA assay with varying Enzyme concentration and Enzyme incubation times (40 µg/ml of capAb; 3.75 ng/ml of PSA concentration; 1 µg/ml of detAb concentration; High sensitivity streptavidin-HRP).

5.4.2. Effect of MCF dimensions on assay signal

Having established optimal assay conditions, the next focus was on understanding assay variability. One of the main challenges in microfluidic IA is to maintain the sensitivity

and precision of gold standard MTP methodology, whilst achieving a major reduction in total assay times. The cost-effective continuous melt extrusion process used to produce MCF offers the potential for low device cost, but has the potential for small variation in the shape and diameter of the microcapillaries along the plastic film and across each film strip. The extent of variation and effect of variations in geometry of microcapillaries on assay performance have not previously been reported, and were studied here by measuring MCF geometry both directly and also indirectly by imaging dye solutions within MCF strips.

According to the Lambert-Beer law, *Abs* is linked to the extinction coefficient of a substance, ϵ, concentration, *c* and light path distance, *l*. Small differences in the shape or size of microcapillaries will therefore affect absorbance independently of assay signal if path distance *l* changes (Figure 4.4), which could increase assay variability both from capillary to capillary across a single MCF strip, or between strips taken from film batches with variable dimensions. Initially, the mean hydraulic diameter and capillary height *h* for each capillary was measured using an optical microscope in 10 replicate thin samples cut from MCF strips (Figure 5:3A). Although informative, this was a difficult and laborious task because the fluoropolymer MCF material was soft and could be deformed during sample slicing, potentially increasing the variability of measured geometry. A second non-invasive method to measure variation in capillary geometry was therefore developed whereby MCF strips were filled with solutions of fixed concentrations of DAP, the coloured product resulting from HRP enzymatic conversion of the chromogenic OPD substrate, and scanned using same settings as PSA strips. From the known extinction coefficient of these solutions, variation in capillary height *h* could therefore be measured from *Abs* values calculated from the scanned images. As expected, when measured capillary height was compared to absorbance, a correlation between Abs values for DAP was seen with h (Figure 5:3B). When a single DAP reference strip was used to provide reference absorbances, and a normalized absorbance ratio calculated (using Equation 2), the effect of small differences in pathlength distance on PSA assay absorbance was eliminated resulting in a significant decrease on the intra-assay variability across the entire concentration range (Figure 5:3C).

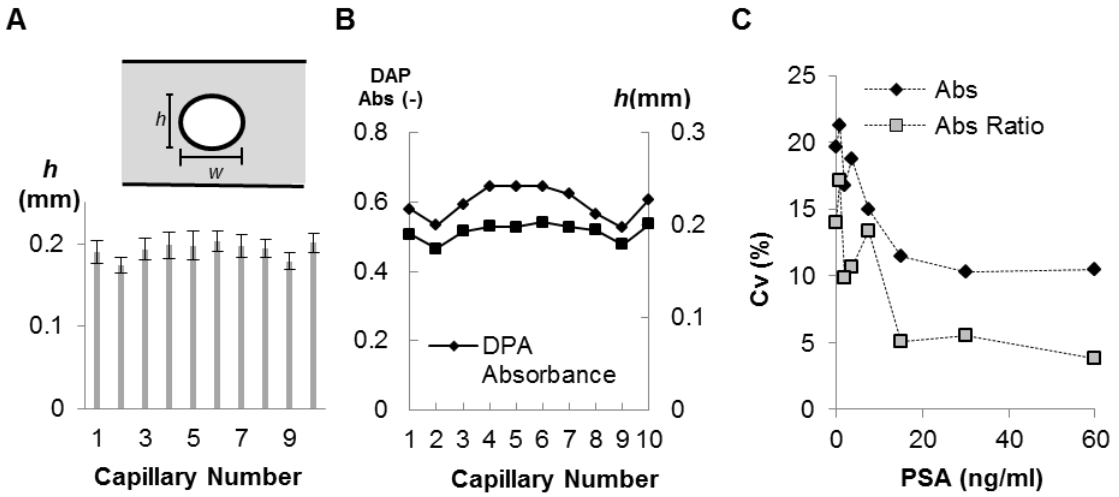

Figure 5:3 - Correlation between capillary height (h) and absorbance (Abs) variability across a 10 bore fluoropolymer MCF material.
A Variation in h across and along the MCF strip (error bars represent 2 standard deviations from multiple measurements along 1m long MCF strip). **B** Correlation between h and DAP absorbance. **C** Coefficient of Variation (CV) of absorbance values for different PSA concentration, before and after normalisation with DAP absorbance; CV is obtained from the ratio between the Relative Standard Deviation (STDEV) absorbance along 10 capillaries for a given PSA concentration and the mean value of absorbance in the same 10 capillaries.

5.4.3. Kinetics of ELISA in MCF capillaries

Quantitative heterogeneous IA usually require extended incubation times to attain the antibody-antigen binding equilibrium. These are dependent on the reagents mass transfer and kinetic limitations.[232] The long incubation times required for sandwich PSA IA in the MTP are linked to the long diffusion distances in the plastic wells that can be dramatically reduced in a miniaturized system. Kinetic studies for each core sandwich ELISA step in the fluoropolymer MCF after assay optimization confirmed the very short times required to achieve full signal response in a system with a diffusion distance 15 times smaller. An incubation time for recombinant protein of 2 min was found sufficient in the MCF, whereas for DetAb and enzyme conjugate no benefit was seen in extending incubation times beyond 5 min (Figure 5:4). In respect to the enzymatic chromogenic substrate (OPD) incubation times up to 10 min followed a zero order reaction (Figure 5:4(iii)) which is ideal for obtaining a broad dynamic range in IA, as an early reading can provide good assay performance for higher concentrations, and in contrast low concentrations with weak initial signal can be more clearly measured. As

expected for enzyme assays, measurement of reaction rate rather than endpoint absorbance can also provide good indication of sample concentration.

Many microfluidic platforms reported successful quantitation of biomarkers over a certain dynamic range with total assay time ranging from 2 minutes to several hours.[147] [101] The MCF ELISA can successfully quantify PSA in diluted human serum in 15 minutes, requiring <5 minutes sample incubation time (Table 5:2). This total assay time could also be achieved by the Immuno-pillar chip and a capillary driven device using PDMS substrate, which were able to run human serum sandwich assays, presenting similar MCF sensitivity, within 12 and 14 minutes total assay time respectively.[58,56] Although, time competitive these devices are tailored to single sample and single test, in contrast to the independent 8 samples measured 10 times each in the MSA. In addition these microfluidic devices use fluorescence microscopes for signal detection, which allows the high sensitivity of the assays, but also increases the cost and difficulties for platform operator, characteristics not suitable for POC applications. Colorimetric detection by a flatbed scanner or other portable device (e.g. smartphone camera) is ideal for POC settings. It is easy-to-use, portable, user-friendly, rapid and cost effective detection strategy.[234,148] So far no other microfluidic platform has reported a fully quantitative sandwich IA in ≤15 minutes using biological samples and colorimetric detection by a flatbed scanner.

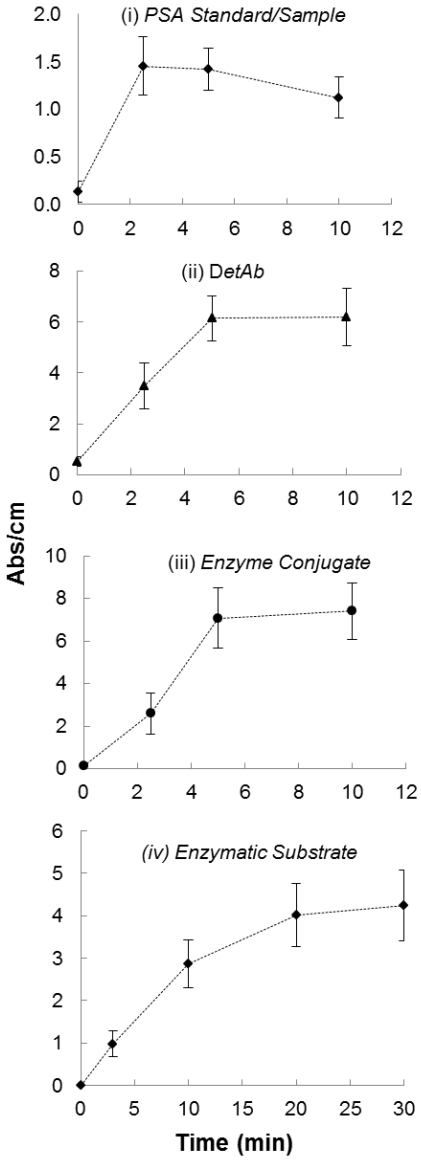

Figure 5:4 - Kinetic study of all assay steps illustrating minimum incubation times required for signal saturation with 3.75 ng/ml of PSA recombinant protein.

Table 5:2 - Incubation times of ELISA reagents in the standard Microtiter Plate (MTP) and in the novel Microcapillary Film (MCF).

	Time (min)	
Assay Step	**MTP**	**MCF**
PSA Incubation	120	2
DetAb Incubation	120	5
Enzyme Incubation	20	5
Enzymatic Substrate Incubation	20-30	1.5- 3
Total	280	13.5-15

5.4.4. Assay performance with biological samples

IA performance can often be affected when human samples are tested, with the high and variable concentration of unrelated proteins, lipids, and other biomolecules plus changes in viscosity often producing unwanted background or loss in signal.[235] [237] Identifying these interferences and managing them is fundamental for sensitive and reproducible IA.[237] Managing matrix effects becomes even more urgent in POC settings, where the sample processing needs to be minimized or eliminated to speed up the testing process.[234]

After PSA assay optimization (Figure 5:5A) the PSA assay was tested with 100% human serum. The full PSA response curve obtained presented a loss in absolute absorbance signal without a significant loss in sensitivity compared to buffer (Figure 5:5B and (Table 5:2). This observation showed however that the biological matrix was interfering with the assay. A further set of experiments compared performance in 100% human serum with 100% whole blood as sample matrices for the PSA standards. The results showed that the absorbance values are similar for serum and for the whole blood, but still lower that the ones performed in buffer for concentrations (Figure 5:5C). These observations confirm that the PSA MCF assay presents the same performance in serum and in blood simplifying sample preparation process, by eliminating the need of sample preparation. To our knowledge this finds no precedent in microfluidic devices. Therefore, an attempt to reduce matrices interferences was done by diluting the human serum 1:2 and using the diluted serum as the sample matrices for full response curves of PSA MCF sandwich assay as it has been reported in other microfluidic IA studies.[238] In that case, the absolute Abs values and sensitivity of PSA assay in buffer and diluted serum were similar for 15 minutes total assay time (Figure 5:5D). This means that sample dilution can be used to overcome the matrix effect.[239,238] Other attempt to overcome the matrix effect consisted in increasing sample incubation times, so the PSA (26 KDa protein[240]) protein could have time to diffuse through the matrix viscous liquid and bind to the immobilised antibody on the capillary walls. These experiments performed in 100% serum showed that with 15 minutes sample incubation no difference was noticed between the PSA absorbance values in buffer and in non-diluted serum (Figure 5:5E). These results suggest that matrix effect in PSA MCF system is due to a viscosity increment in the PSA diluent and not to the presence of specific proteins in the

matrix.[235] At 20 °C the viscosity of buffer is approximately 1 mPa.s whislt he viscosity of serum is known to be higher.[241] The diffusion coefficient of a spherical particle through liquid with low Reynolds number is directly proportional to diffusion time and inversely proportional to viscosity. This can justify the need for higher sample incubation times for assays performed in non-diluted biological samples and the same absorbance values for 1:2 diluted serum samples with 2 minutes sample incubation. Therefore to overcome viscosity effect of non-diluted serum an extended sample incubation time should be considered, otherwise the sample would need to be diluted 1:2 to match he viscosity to that of the buffer. The absorbance values of PSA assay in the whole blood were similar to the ones performed in non-diluted serum, despite blood viscosity was reported to be between 3.36 and 5.46 mPa.s.[241] The larger viscosity of blood compared to serum relates to the viscoelastic properties of red blood cells, which appears not to interfere to protein diffusion in the liquid matrix (i.e. blood serum).Consequently, whole blood samples can be used in the PSA sandwich ELISA in the MCF platform as long as the minimum of 10 minutes sample incubation is undertaken or blood sample is diluted in 1:2. Overall, the PSA assay in the MCF was fully quantitative in the current clinical range (>4 ng/ml),[242,243] and in lower proposed ranges (2.6 to 4 ng/ml) (Figure 5:5 and Table 5:3),[244,181] presenting LLoD below 0.9 ng/ml of recombinant protein (Table 5:3) with a precision varying from 3 to 9% based on the intra-assay variability in buffer and in biological samples. The LLoD was calculated by adding 3 times the blank standard deviation to the mean blank absorbance, the absorbance value obtained was transformed in a PSA concentration using the 4PL mathematical model. The cross-correlation coefficient, R^2 between the 4PL model and the experimental data is also shown inTable 5:3.

Given that variation in capillary geometry across the MCF strip had already been identified as a significant component of assay variance (Figure 5:3C), it was possible to reduce assay variability by normalizing absorbance values. This was done by dividing each capillary absorbance by the average of absorbance of a reference solution of DAP strip in the same capillary number, obtaining absorbance ratio (Figure 5:5).

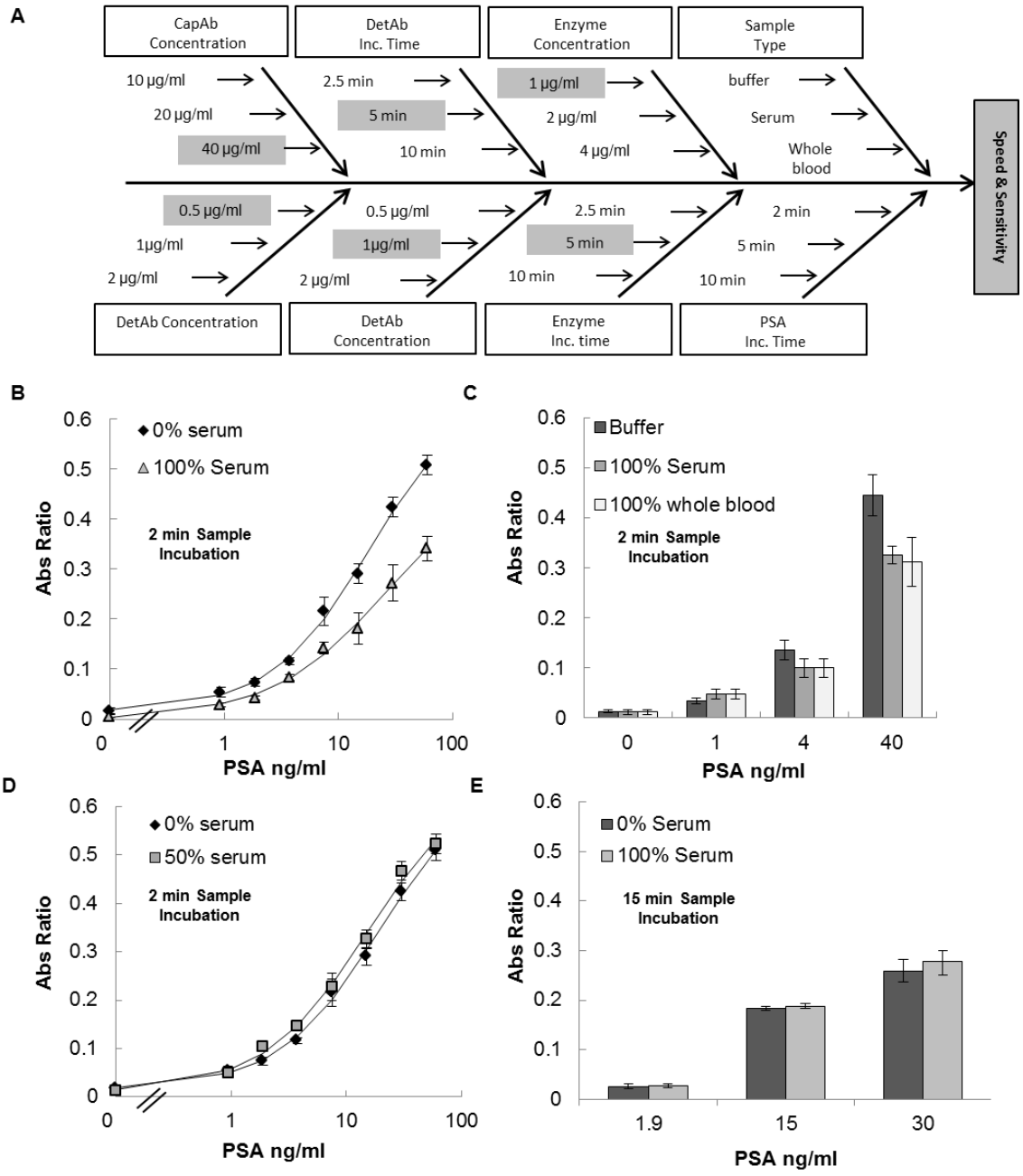

Figure 5:5 - PSA sandwich ELISA in MCF platform using the MSA device.
A Optimisation process and selected experimental conditions. **B** MCF PSA assay response curves in 0% and 100% human female serum, spiked with recombinant protein using total assay time of 15 minutes. **C** PSA sandwich assay in buffer, non-diluted serum and whole blood in 15 minutes total assay time (<5 minutes sample incubation time). **D** MCF PSA assay response curves in 0 and 50% Human Female Serum, spiked with recombinant protein in 15 minutes total assay time (<5 minutes sample incubation time). **E** PSA sandwich assay in 0 and 100% buffer in ~ 30 minutes total assay time (15 minutes sample incubation).

Table 5:3 - Parameters of fully-optimised response curves in the MCF using MSA device.

Assay Parameter	0% Serum	50% Serum	100% Serum
Dynamic Range	0.9–60.0 ng/ml (R^2 = 0.9988)	0.9 – 60.0 ng/ml (R^2 =0.9981)	0.9 – 60.0 ng/ml (R^2 = 0.9988)
Sensitivity (LLoD)	<0.9 ng/ml	<0.9 ng/ml	<0.9 ng/ml
Precision	5% at 3.8 ng/ml	9% at 3.8 ng/ml	7% at 3.8 ng/ml

Since optimized conditions were established for the MCF (Figure 5:5A), full PSA response curves were performed and compared to a 96-well microtitre plate. Performance of the two platforms was comparable (Figure 5:6), despite the >94% reduction in assay time in the MCF platform (Table 5:2). A major difference between assays in the MCF and the MTP is that the former only requires one washing step (before adding enzymatic substrate), while the MTP involved several washes after each incubation step. The assay sensitivity in the MCF was not affected by removal of washing steps, which reduced the total number of steps required, bringing sandwich IA closer to point-of-care (POC) devices. The normalized Abs/cm signal in the MTP (Figure 5:6) was almost 50-fold lower than in MCF platform using the optimised IA conditions, a reflection of the shorter pathlength of the microcapillary assay and optimized MCF assay conditions.

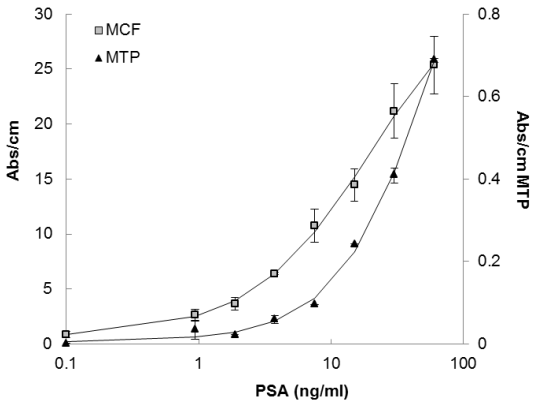

Figure 5:6 – Comparison of MCF vs MTP PSA colorimetric IA.

MTP PSA assay was performed using conditions suggested by manufacturer and summarised in Table 5:1; MCF PSA assay was performed in the optimised conditions (Figure 5:5A and Figure 5:2).

5.4.5. Robustness of PSA sandwich ELISA in the MCF using MSA devices

POC testing devices should ideally present robust performance on a range of temperatures, as temperature fluctuations are difficult to control outside laboratory setting. Temperature has been reported to affect IA performance in terms of linear range, precision and limit of detection.[245,246] A separate set of experiments explored the effect of temperature on PSA sandwich assay performance. Consequently, PSA full response curves were performed with reagents pre-stabilized at 4, 20 and 37 ºC in the MSA with a reduction in the absolute values of absorbance for 4 ºC (related to lower HRP enzymatic activity), but limited impact in respect to the LLoD or linearity of the PSA IA. In general, temperatures around 20 ºC favored the sensitivity and precision of the assay (Figure 5:7A). Similar results were found by *Imagama M. et al* (1982) where the lowest non-specific binding and the highest specific binding were obtained by incubation at 20°C when compared with incubation at 37°C.[246] Although temperature presents minimum impact on assay performance, the MSA allows performing a full response curve at the same conditions of a given biological sample, therefore providing an internal calibration ideal for POC settings.[234]

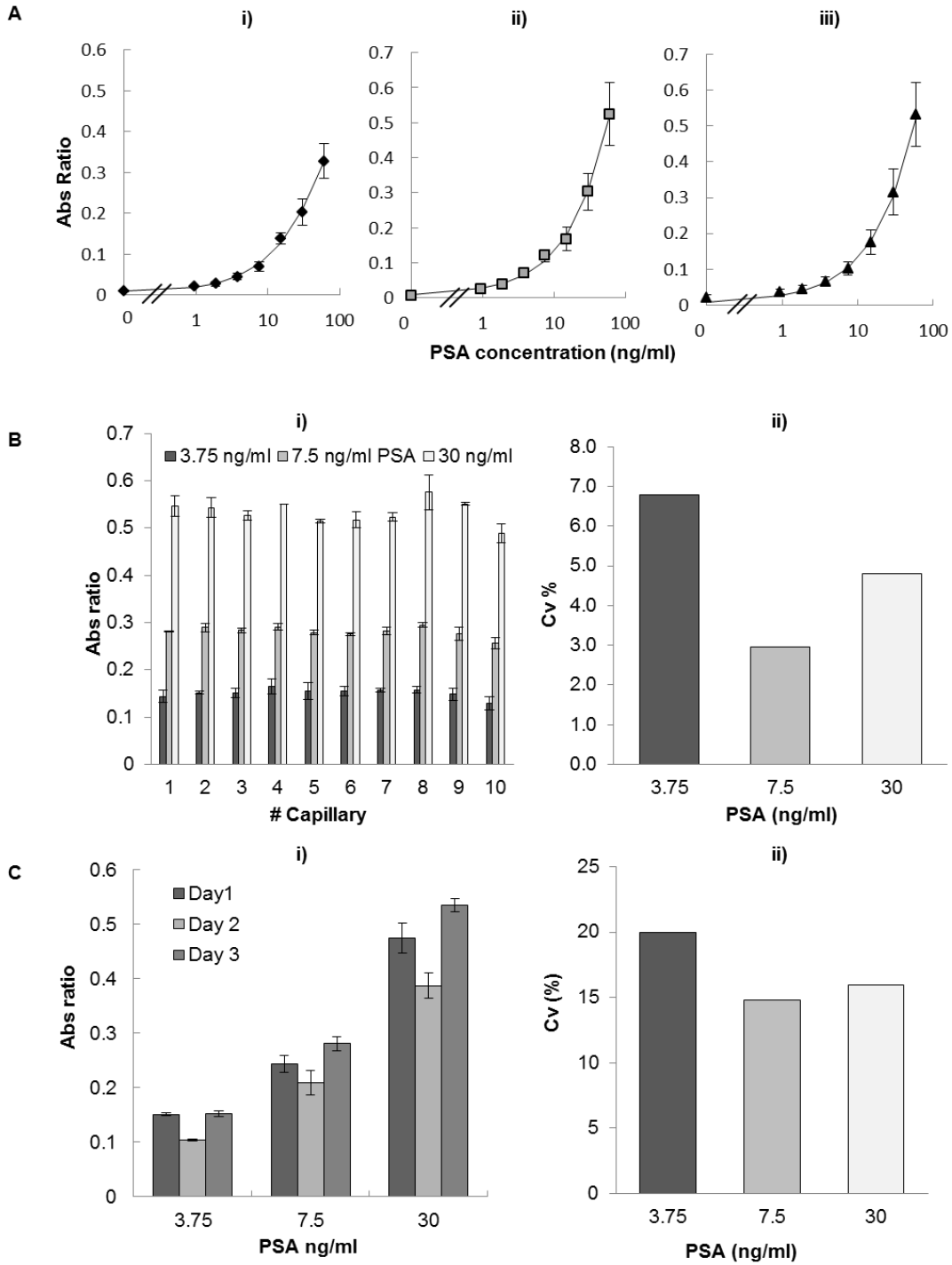

Figure 5:7 - Robustness of PSA sandwich assay in the MCF.
A Effect of temperature on the performance of PSA IA in the MCF **i)** 4ºC;**ii)** 20ºC;**iii)** 37ºC.**B** Intra-assay variability studies in lower, middle and upper range of PSA response curve **i)** Absorbance ratio per capillary **ii)** Coefficient of variation calculated by the ratio of standard deviation of 10 absorbance values by the average of those values. **C** Inter-assay variability studies for lower, middle and upper range of PSA assay using different MSA devices **i)** Inter-assay variability per day and **ii)** Coefficient of variation calculated by the ratio of standard deviation of 20 absorbance values by the average of those.

A further set of experiments aimed at specifically studying the precision of PSA assay in the MCF at 20°C. This experiments showed an intra-assay precision <7% in the lower, middle and upper range of the PSA response curve (Figure 5:7B). Note that 10 samples corresponding to 10 capillaries were analyzed in this process, being the CV calculated by the ratio between the standard deviation of Abs values with the absorbance average of the 10 samples. The inter-assay variability was determined by performing the assay in three different days and using three different MSA devices. A total of 20 samples was analysed in order to calculate CV values. The results showed <20% of inter-assay variability (Figure 5:7C) which is within the value accepted (25% of variation) for validation of heterogeneous IA according to a pharmaceutical industry perspective.[30] All absorbance values were previously normalized by DAP absorbance eliminating the effect of capillary geometry variation in the determination of intra and inter-assay variability.

5.5. Conclusions

We presented a new "Lab-in-a-briefcase" concept for sandwich IA employing inexpensive, compact components for POC and field diagnostics detection, and demonstrate system performance for the important cancer biomarker PSA (prostate specific antigen) from human serum and whole blood. This portable lab, with 40 x 30 x 15 cm^3, uses a miniaturised ELISA platform, fluoropolymer MCF which offers rapid, low volumes and cost-effective assays, comparable to MTP ELISA. The flat geometry of the plastic film combined with optical clarity of the fluoropolymer material provides the opportunity for a simple optical detection using USB powered film scanners. A simple and efficient MSA is used to simultaneously fill 8 pre-coated MCF test strips or 80 capillaries using an array of 1 ml disposable plastic syringes. The components of our portable lab allow the use of conventional ELISA and commercialized assay chemistry on the field, outside the laboratory setting. As a proof-of-concept the PSA ELISA detection using the lab components was performed in 15 minutes in biological samples with a LLoD of <0.9 ng/ml PSA and 3 to 10% intra-assay variability. This means PSA MCF ELISA was 20x faster than the standard MTP ELISA, whilst maintaining similar assay performance in respect to precision and LLoD. This has the potential of enabling PSA screening into patient home or into remote areas. Future improvement to the "Lab-

in-a-briefcase" for PSA screening can be achieved by further miniaturising all components or interfacing to wireless, smartphone technology for simple-optical signal quantitation.

6. Portable smartphone quantitation of prostate specific antigen (PSA) in a fluoropolymer microfluidic device

6.1. Abstract

We present a new, power-free and flexible detection system named MCFphone for portable colorimetric and fluorescence quantitative sandwich IA detection of prostate specific antigen (PSA). The MCFphone is composed by a smartphone integrated with a magnifying lens, a simple light source and a miniaturised IA platform, the Microcapillary Film (MCF). The excellent transparency and flat geometry of fluoropolymer MCF allowed quantitation of PSA in the range 0.9 to 60 ng/ml with < 7 % precision in 13 minutes using enzymatic amplification and a chromogenic substrate. The lower limit of detection was further improved from 0.4 to 0.08 ng/ml in whole blood samples with the use of a fluorescence substrate. The MCFphone has shown capable of performing rapid (13 to 22 minutes total assay time) colorimetric quantitative and highly sensitive fluorescence tests with good %Recovery, which represents a major step in the integration of a new generation of inexpensive and portable microfluidic devices with commercial IA reagents and off-the-shelf smartphone technology.

6.2. Introduction

Decentralization of diagnostic testing to near the patient sites is both a trend and a need in clinical diagnostics. IA platforms (the most common laboratory bioanalytical tool) and detection systems must therefore be adapted for point-of-care (POC) testing, which requires the ability to design affordable, portable, and user-friendly IA systems capable of rapid and sensitive detection using well established IA chemistries.

Diagnostic tests are routinely used to diagnose and select treatment options for many critical health conditions, including cardiovascular diseases, sepsis, ovarian and prostate cancer, demand quantitation of one or multiple analytes. [247–250] Agglutination and lateral flow assays are the most widely used POC IA tests, however these formats are usually qualitative or semi-quantitative, lacking both the sensitivity for many important

biomarkers and the ability to perform multiplex analysis.[234] This has driven the development of microfluidic IA platforms,[8] combining minimal diffusion distances and high surface-area-to-volume ratios for improved performance, with the use microchannels or beads for rapid and sensitive detection of analytes from small sample volumes.

Optical detection is often preferred in POC testing, as it can rapidly and simply provide high-resolution microscopic and macroscopic information.[251,252]The recent fall in cost of optoelectronic components now offers cost benefits for portable detection systems. Two most common optical detection techniques used in microfluidic IAs are fluorescence and chemiluminescence, due to their excellent sensitivity.[148] However, the readout equipment used to detect these signals is complex and expensive, typically requiring a fluorescence or confocal microscope or high-sensitivity optical sensors, and therefore not portable or cost-effective for POC use.[253] The opportunity for using simple portable optical detection in microfluidic diagnostics has recently arisen because of the rapid expansion in consumer electronics such as high-performance smartphones cameras that are now ubiquitous, and have driven down the price of high performance digital image sensors combined with portable computers.[251] Smartphones are portable, widely available, user-friendly and low cost, and are therefore suitable for integration into a microfluidic platform for POC diagnostics.

Examples of microfluidic diagnostic tests based on smartphone measurement include colorimetric detection of *Salmonella* from an immunoagglutination assay,[254] measurement of urine, saliva and sweat pH,[176,255] quantitation of vitamin D measured using a competitive lateral flow IA,[194] and prostate specific antigen (PSA) quantitation from a sandwich microfluidic IA with a lower limit of detection (LLoD) of 3.2 ng/ml PSA in serum samples.[103] Most smartphone detection systems reported so far are based on colorimetric detection. [256] Although colorimetric detection is usually more cost-effective, easy-to-use and rapid,[148] fluorescence detection should present higher sensitivity for quantitative POC diagnostics, allowing low analyte cut off values in small sample volumes which is vital for many clinical biomarkers. Smartphone fluorescence detection has been reported in some bioassays, such as quantification of albumin using a dye based assay,[257] in a lateral flow assay,[258] and finally to detect bacteria using a lateral flow assay with fluorescence nanoparticles.[259] However, smartphone fluorescence detection has not yet been reported in sandwich ELISA

systems for accurate quantitation of analytes, and this would bring POC microfluidic diagnostics to a new level of portability and sensitivity.

In this study we present a flexible smartphone based colorimetric and fluorescence detection system, termed the MCFphone, capable of detecting PSA from whole blood in the relevant clinical range in 13 minutes using colorimetric detection and 22 minutes using fluorescence detection. PSA is the mostly widely used prostate cancer biomarker, and continuous monitoring of PSA levels in patients with prostate cancer is a vital diagnostic tool. PSA blood levels determination in conjugation with digital rectal examination was approved by the Food and Drugs Administration to test asymptomatic men aged 50 year old with a cut off value of 4 ng/ml of PSA.[181,182]Many studies suggested that prostate cancer mortality can be decreased by early detection, and so screening programs have been proposed utilising PSA quantitation in blood. We propose that a quantitative whole blood PSA sandwich assay in a rapid, sensitive, and portable test device would allow POC prostate cancer monitoring and screening even in remote areas of developing countries where laboratory facilities are limited. The MCFphone detection system could easily be combined with the "Lab-in-a-briefcase" assay platform reported recently,[152] replacing the flatbed scanner readout system and increasing portability, flexibility and sensitivity.

6.3. Materials and Methods

6.3.1. Materials & Reagents

Enzymatic chromogenic and fluorescence products 2,3-diaminophenazine (DAP) and fluorescein isothiocyanate (FITC), dimethyl sulfoxide (DMSO), streptavidin alkaline phosphatase, SIGMAFASTTM OPD (o-Phenylenediamine dihydrochloride) tablets and FDP (fluorescein diphosphate) were sourced from Sigma-Aldrich (Dorset, UK). High sensitivity streptavidin-HRP was supplied by Thermo Scientific (Lutterworth, UK).

Human kallikrein 3/ Prostate Specific Antigen (PSA) ELISA kit was purchased from R&D Systems (Minneapolis, USA). The kit contained a monoclonal mouse Human Kallikrein 3/PSA antibody (capture antibody or CapAb), a Human Kallikrein 3/PSA polyclonal biotynilated antibody (detection antibody or DetAb) and recombinant

Human Kallikrein 3/PSA (standard). Phosphate buffered solution (PBS) and Bovine Serum Albumin (BSA) were sourced from Sigma Aldrich, Dorset, UK. PBS pH 7.4, 10mM was used as the main IA buffer. Carbonate buffer 50 mM pH 8 and Tris Buffer 50 mM pH 9.2 were used for fluorescence detection with alkaline phosphatase. The blocking solution consisted in 3% w/v protease-free BSA diluted in PBS buffer. For washings, PBS with 0.05% v/v of Tween-20 (Sigma-Aldrich, Dorset, UK) was used. The whole blood used was obtained from donation system at Loughborough University, Sports Department, and collected into 5 ml tubes with citrate phosphate as anticoagulant.

The MicroCapillary Film (MCF) platform is fabricated from fluorinated ethylene propylene co-polymer (FEP-Teflon®) by melt-extrusion process by Lamina Dielectrics Ltd. (Billinghurst, West Sussex, UK). The number and internal diameter of the microcapillaries is easily controlled by the design of the die and the operational conditions set during the continuous melt-extrusion process. The two primary light sources used include an Auraglow AG166 Blue LED bulb, from Argos UK and an Ultraviolet Mini Lantern UV Fluorescent purchased from Mapplin UK. A 60x magnification attachment for iPhone® 4/4S purchased from Amazon (Slough, Berkshire) and a 50mm square dichroic additive green filter sourced from Edmund Optics (York, UK).

6.3.2. MCFphone – System overview

The MCFphone detection system is composed by a 10 bore fluoropolymer MCF strips pre-coated with immobilised CapAb and blocked with BSA protein (1), smartphone (iPhone® 4S, 8 megapixels camera) (2) integrated magnifying lens (3), light source (blue LED, with peak wavelength of 450 nm for chromogenic detection) (4), or UV black light for fluorescence detection (5), and a dichroic additive green filter (6) for fluorescence detection (Figure 6.1A).

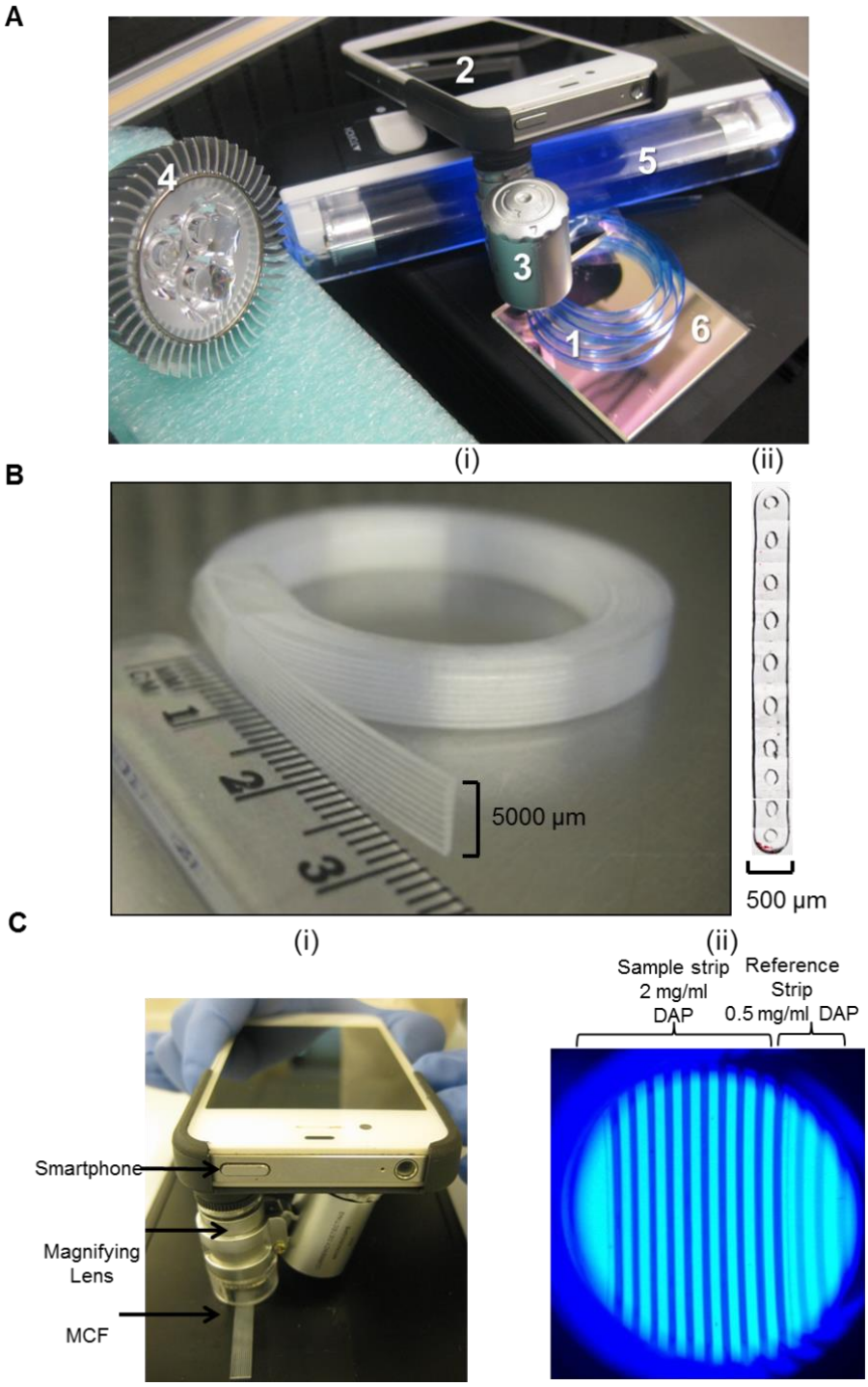

Figure 6.1 - MCFphone system overview.
A Main components of MCFphone (1) Microcapillary Film (MCF) (2) Smartphone (3) Magnifying lens (4) Blue LED (5) UV black light for fluorescence detection, light source for chromogenic detection (6) dichroic filter. **B** The Microcapillary Film (MCF), melt extruded from fluorinated-ethylene-propylene (FEP) copolymer (i) 5 meter MCF reel (ii) MCF cross section with 10*200 µm embedded in the FEP polymer. **C** MCFphone detection in operation (i) MCFphone components (ii) MCFphone colorimetric image of a sample and a reference strips filled up with 2,3-diaminophenazine (DAP), the product of HRP conversion of o-Phenylenediamine dihydrochloride.

The MCF used consisted of a fluoropolymer melt-extruded plastic film with 10 embedded parallel microcapillaries and a mean 200 µm internal diameter. Each strip has 4.5 ±0.1 mm in width and 0.6 ± 0.05 mm depth (Figure 6.1B). This platform was first presented as a cost-effective microfluidic IA platform by Edwards *et al.* (2011); the hydrophobicity of FEP material allows simple yet effective immobilisation of antibodies by passive adsorption on the plastic surface of the microcapillaries, and the transparency of the MCF material results in high signal-to-noise ratios (Edwards et al., 2011) which is fundamental for sensitive signal quantitation.

The MCFphone working principle consists in illuminating the MCF test strip sample with a light source (blue LED for chromogenic detection and UV black light for fluorescence detection) and capturing the signal (digital image) with a smartphone camera attached with a magnifying lens (Figure 6.1C). The digital images were then analysed with *Image J* software (NIH, Maryland, USA) for colourimetric or fluorescence signal quantitation.

6.3.3. PSA sandwich ELISA (Enzyme Linked ImmunoSorbent Assay)

6.3.3.1. Fabrication of MCF test strips

A solution of 40 µg/ml of Human Kallikrein 3/PSA CapAb in PBS buffer was aspirated into a 100 cm lengh MCF and incubated for two hours at room temperature in a petri dish covered with a wet tissue to avoid evaporation of solution in the microcapillaries. A 3% BSA solution in PBS buffer was then aspirated and incubated in the MCF for an additional two hours at room temperature to block any additional binding sites in the microcapillaries. The MCF strip was then washed with 0.05% Tween in PBS, and stored in the fridge at 4 ^{o}C or used immediatetly. The MFC was then trimmed into 3 cm long test strips and interfaced with a single 1ml syringe using a short 3 mm i.d. silicon tubing and a plastic clamp or integrated in a 8-channel multi-syringe aspirator; this semi-automatic device allows 8 test strips and a total of 80 capillaries to be filled simultaneously using a set of 1 ml plastic syringes with minimum training as described elsewhere.[152]

6.3.3.2. PSA sandwich assay

The PSA sandwich assay consisted in pre-loading 150 µl of sample and IA reagents into each well in microplate especially designed to interface the MCF strips. The test strips were then immersed in microplate wells and solutions aspirated sequentialy by manually moving the piston plunger of the disposable syringe as illustrated in Figure 6.2A. In all experiments shown in this paper 8 MCF strips were operated simultaneously based on the multi-syringe aspirator, which is capable of runing a 7 point full response curve plus a control or analysing multiple samples simultaneously. From the perspective of end use, it only requires rotating the knob that controls the position of the piston plungers in the array of 1ml disposable syringes and moving the device along a multiplexed microplate containing all pre-loaded reagents. On each incubation step, about 78 µl of solution are aspirated corresponding to 6 full rotations of the knob. With this design, the total number of steps required to complete the PSA sandwich IA was reduced to 5, and all waste solutions were kept inside the 1ml disposable syringes throughout the assay. The incubation times used for PSA IA were 2, 5, 5 and 1 minute for the sample, DetAb, enzyme and enzymatic substrate, respectively. The concentration of biotinylated DetAb was 1 µg/ml and PSA recombinant protein standards were diluted in PBS or whole blood where appropriate.

For colorimetric detection, 1 µg/ml solution of high sensitivity streptavidin-HRP was used for enzymatic amplification, and the chromogenic substrate consisted of 4 mg/ml OPD and 1 mg/ml H_2O_2. Smartphone microphotographies of the MCF strips were taken with a iPhone® 4S at 20 seconds interval for a total of 2 minute after addition of the enzymatic substrate. For fluorescence detection, 2 µg/ml of alkaline phosphatase was diluted in carbonate buffer 50 mM pH 8, and the fluorescence enzymatic substrate consisted in 0.25 mM solution of fluorescent substrate FDP; the MCF strips were photographed at 60 seconds interval for a total of 10 minutes. On both colourimetric and fluorescence assays, the MCF strips were extensively washed with PBS-Tween before aspirating the enzymatic substrate.

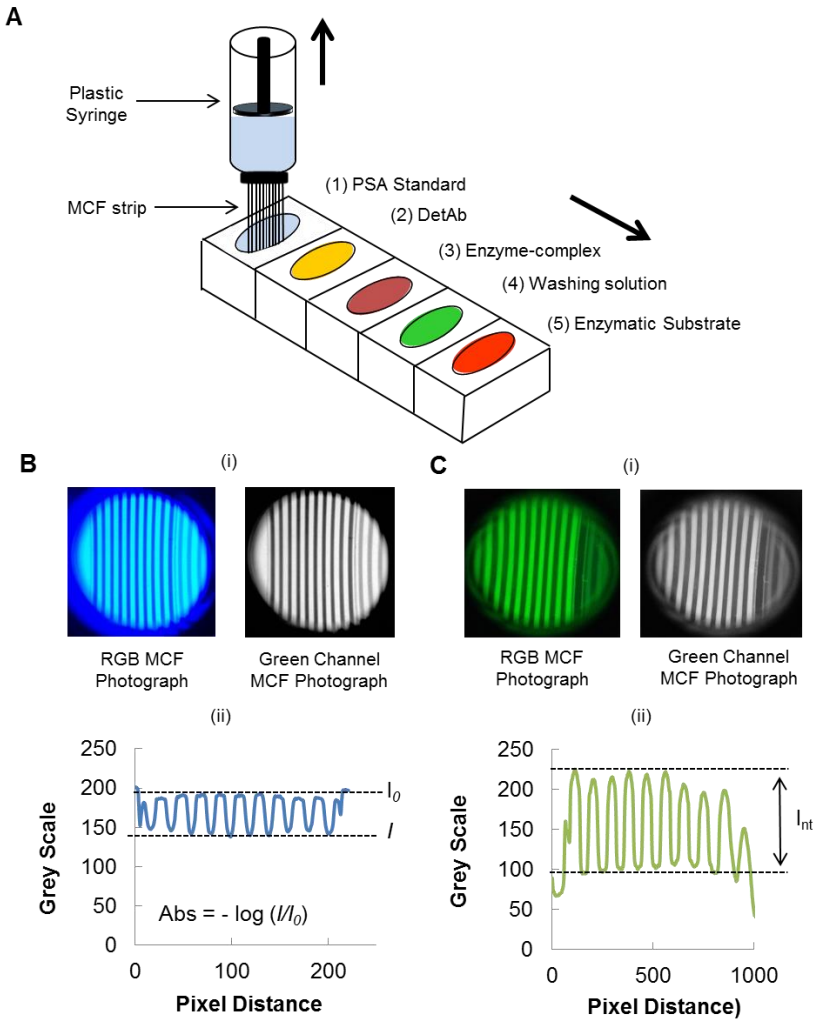

Figure 6.2 - PSA sandwich assay with MCFphone signal quantitation.
A PSA sandwich assay steps. **B** Colorimetric signal quantitation (i) RGB and green channel image (1 mg/ml) with reference strip (0.5 mg/ml) of 2,3-diaminophenazine (DAP) (ii) Correspondent grey scale analysis. **C** Fluorescence signal quantitation (i) RGB and green channel image (0.5 mM of fluorescein isothiocyanate, FITC, with reference strip of 0.125 mM) (ii) Correspondent grey scale analysis.

6.3.4. Colorimetric and Fluorescence detection

Accurate quantitation with smartphone cameras demands control of environment light,[256], since the exposure time of the camera is automatically adjusted in response to the amount of light passing through the detection region.[194] In order to control environmental light during colorimetric detection a small polyethylene box and a blue LED, with peak 450 nm emission (absorption peak for DAP) were set together. The blue LED was placed so that the light penetrated along the length of the channels rather than across them. However, even with the external environment light control, the light

passing through the detection region was not always consistent due to different absorbance of the samples. To eliminate the effect of different exposure times of the camera, all smartphone images were taken with a reference MCF strip (Figure 6.1B (i)) loaded with the final product of enzymatic conversion; the signal from this strip was then further used for data normalisation as detailed in section 6.3.5.

To test for sensitivity of smartphone detection, MCF strips were filled with the chromogenic substance 2, 3-diaminophenazine (DAP, resulting from OPD enzymatic substrate conversion) in 1:2 serial dilution in distilled water, from 0.074 to 9.5 mM and imaged with the MCFphone. Sensitivity of the detection system was calculated by analysing the grey scale in the microphotographs of the MCF strips and adding 3 times the blank standard deviation to the blank value. This gives the minimum absorbance value detectable with the colorimetric setup, therefore setting the sensitivity of the system.

Fluorescence quantitation was carried out in the dark using an Ultraviolet Mini Lantern UV to excite the fluorescence product in the microcapillaries. The UV light was placed under a mask with an aperture sufficient to place both the MCF strip sample and reference. The MCF strips were then overlap with a green dichroic additive filter allowing only the green colour (530 nm) to pass through and be capture by the smartphone placed on the top of the filter.

Sensitivity of fluorescence detection mode was tested by filling up 8 MCF strips with 1:2 serial dilution of Fluorescein Isothiocyanate (FITC) in distilled water in the 7.8 to 500 µM concentration range. The strips were placed in the dark metal support according to fluorescence MCFphone detection setup and smartphone photographs recorded. In the same way to colorimetric system sensitivity, fluorescence sensitivity was calculated by adding 3 times the blank standard deviation to the blank after image analysis.

6.3.5. Image Analysis

The iPhone® 4S images were analysed with *ImageJ* software, and consisted in splitting the acquired RGB images into Red, Green and Blue (RGB) channels for both colorimetric and fluorescence detection modes. For colorimetric quantitation, the absorbance (Abs) was calculated from the mean pixel intensity in grey scale in the green

channel as shown in Figure 6.2B (i) based in equation (6:1), where I0 is the mean grey scale intensity of the baseline and I is determined based on the difference between the baseline and the maximum grey scale peak height, h as seen in equation (6:2) (Figure 6.2C (ii)). The microcapillaries in the MCF have a circular to elliptical geometry, therefore the transmittance images have a minimum grey scale intensity at the centre of the capillaries where the light path distance is maximum. The Abs value presented for each MCF sample studied is a mean Abs value calculated by averaging the whole array of 10 individual microcapillaries in each MCF strip. The Abs value for each strip was further normalised based on the Abs value of the reference strip in order to compensate for the automatic settings of the smartphone camera, yielding the Absorbance ratio, Absratio shown in equation (6:3).

$$\mathrm{Abs} = -\log_{10}\left(\frac{\mathrm{I}}{\mathrm{I}_0}\right) \tag{6:1}$$

$$\mathrm{I} = \mathrm{I}_0 - \mathrm{h} \tag{6:2}$$

$$\text{Abs Ratio} = \frac{\mathrm{Abs}_{\mathrm{sample,i}}}{\mathrm{Abs}_{\mathrm{ref}}} \tag{6:3}$$

For fluorescence quantitation in the MCFphone, the split green channel image (Figure 6.2C (i)) was used to produce a grey scale plot from where the fluorescence intensity, I_{int} was measured for each individual microcapillary in the MCF strips (Figure 6.2C (ii)). The intensity of the peaks for each capillary was then normalised by the mean intensity peak of the reference strip, $I_{int,ref}$ thus eliminating variability of camera exposure settings. Consequently, fluorescence signal is presented as an average of fluorescence intensity ratio (fluorescence ratio) of the 10 capillaries in each MCF strip equation (6:4).

$$\text{Fluorescence ratio} = \frac{\mathrm{I}_{\mathrm{int,sample}}}{\mathrm{I}_{\mathrm{int,ref}}} \tag{6:4}$$

The LLoD was determined as the minimum concentration yielding a signal higher than the blank value plus 3 times the standard deviation of the blank. When appropriate this

value was calculate using a 4PL (4 parameter logistic model) best-fitted to the experimental response curve.

6.3.6. Recovery PSA experiments from whole blood samples

%Recovery was calculated for three different anticoagulated fresh whole blood samples (samples S1, S2 and S3) spiked with 0.74, 6.7 and 60 ng/ml of PSA recombinant protein. Fluorescence intensity was then determined in the MCFphone for the different blood samples using procedure described in section 6.3.5. The %Recovery was calculated based on the ratio of the Abs or fluorescence signal in assay buffer to the signal in the blood sample in percentage basis. A iPhone® 5s was used to microphotograph the MCF test strips.

6.4. Results and Discussion

6.4.1. Sensitivity of MCFphone for detection of chromogenic and chemifluorescence substrates

Optical detection based on simple and cost-effective technologies like a smartphone demands specific optical properties from the assay platform to be able to use small changes in transmitted light intensity for analyte quantitation. The MCF fluoropolymer has special optical properties, such as high degree of transparency obtained by a matched refractive index of FEP material with an aqueous sample, combined with the film flat geometry that minimises light diffraction, reflection or scattering.[127] This favours sensitive IAs that combined with short diffusion distances yields a powerful miniaturised and portable POC IA concept.

Colorimetric detection is inherently less sensitive than fluorescence, due to fundamental limitations of colorimetry itself. From one hand, in order to measure low concentrations of a chromogen, small differences in intensity must be measured at high light intensity, which limits the LLoD. On the other hand, relationship between optical Abs and intensity of transmitted light is logarithmic. Therefore, at high chromogen concentrations relatively large differences in optical absorbance correspond to small

differences in the intensity of unabsorbed light, which usually corresponds to narrow dynamic range for IAs.[108] However, colorimetric detection is still widely used in IAs, offering speed, simplicity, well established assay chemistry and high quality reagents, and widespread availability of cost-effective readers. For this reason researchers still focused in finding new ways to increase the performance of colorimetric detection, for example through enzymatic amplification systems.[109,110] Besides being inherently less sensitive, colorimetric detection sensitivity can also be limited by the working range of the instrument.

In our recent study, we have measured PSA in biological samples in less than 15 minutes using a flatbed scanner (Barbosa et al, 2014).[152] In this study we aimed turning the "Lab-in-a briefcase" power-free, by using a portable detection system. Understanding the sensitivity and dynamic range of colorimetric measurement using the MCFphone setup is therefore fundamentally important, since performance for absorbance measurement will limit the working range and sensitivity of MCF IAs. As a benchmark, a spectrophotometer was used to measure a range of concentrations of DAP, the chromogenic product of enzymatic conversion of the substrate OPD commonly used in enzyme-linked immunosorbent assays (ELISA). At the peak absorption of 425 nm (Figure 6.3A), the spectrophotometer has a LLoD of < 2.3 µM of DAP (Figure 6.3B). In contrast, the MCFphone sensitivity for DAP measurement was 148 µM (Figure 6.3C), i.e. 2 orders of magnitude less sensitive than a sophisticated spectrophotometer with a 1 cm thick cuvette. This drop in sensitivity can be accounted for by the broad wavelengths measured of RGB system, compared to the specific narrow wavelength selection in a spectrophotometer. Also, the MCFphone presents a 50-fold reduction in the light path when compared to the spectrophotometer cuvette, which reduces the absolute absorbance for any concentration of a chromogen.

Sophisticated benchtop instruments allow higher sensitivity measurement for colorimetric substrates, however they are not suitable for POC. Clinical relevant sensitivities from colorimetric portable detection system must therefore be achieved by assay optimisation, for example using enzymatic amplification, as previously observed in ELISA systems, and as demonstrated in the PSA assay results presented in this paper.

Fluorescence detection systems are characteristically more sensitive since they are measured relatively to an absence of light.[108] The MCF phone fluorescence calibration curve, presented a dynamic range of 7.8-500 µM for FITC and a LLoD below 7.8 µM

(Figure 6.3D). The fluorescence detection system selected for further study with PSA IAs uses UV light which emits radiation between 340 and 400 nm to excite fluorescein to emit green light at 530 nm. Although this reduces the absorbance efficiency compared to excitation at the peak absorbance of around 480 nm, this system exploits a large stokes shift resulting in a large increase from excitation to emission wavelength, thus eliminating the interference of the incident light with the image acquired by the smartphone which is very insensitive to UV light. This system does not require the use of an expensive bandpass filter, further increasing the simplicity of the optics. Combined with a good quantum efficiency fluorescein is an attractive substrate.[39]

The MCFphone achieved similar sensitivity with fluorescence detection to absorbance measurement in the bench-top spectrophotometer, allowing sensitive and portable measurement and justifying the use of fluorescence detection in microfluidic IAs.[148,260] The MCFphone is a flexible detection system, with a choice of rapid colour detection or sensitive fluorescence detection that can be selected to suit different applications.

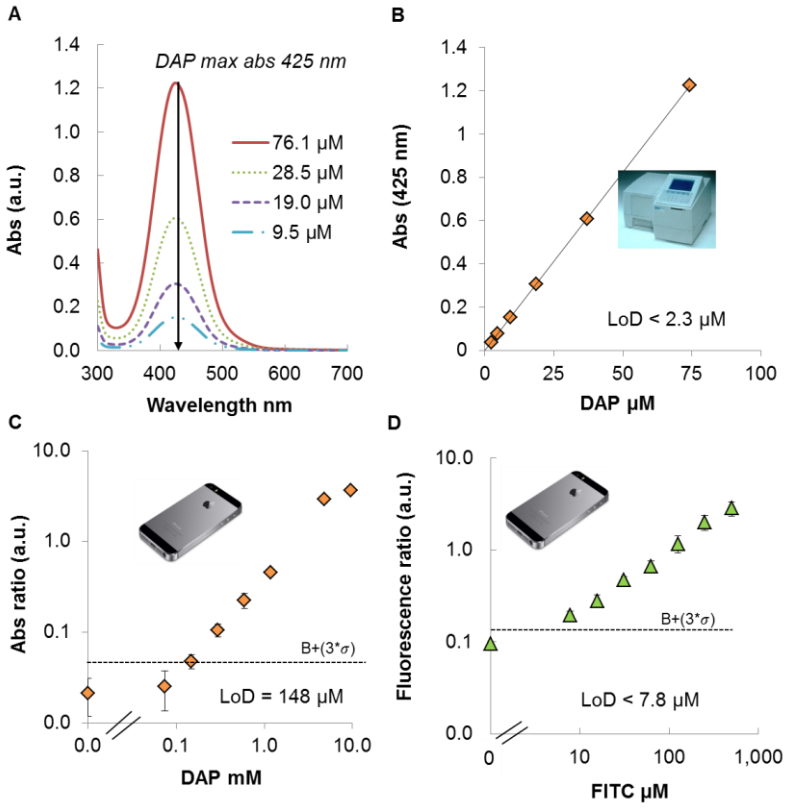

Figure 6.3 - Sensitivity of MCFphone for colorimetric and fluorescence detection. **A** Absorption spectrum of 2,3-diaminophenazine (DAP). **B** Sensitivity of spectrophotometer DAP relative. **C** MCFphone chromogenic sensitity determination (DAP serial dilution). **D** MCFphone fluorescence sensitivity determination (fluorescein isothiocyanate, FITC serial dilution).

Sophisticated benchtop instruments allow higher sensitivity measurement for colorimetric substrates, however they are not suitable for POC. Clinical relevant sensitivities from colorimetric portable detection system must therefore be achieved by assay optimisation, for example using enzymatic amplification, as previously observed in ELISA systems, and as demonstrated in the PSA assay results presented in this paper.

Fluorescence detection systems are characteristically more sensitive since they are measured relatively to an absence of light.[108] The MCF phone fluorescence calibration curve, presented a dynamic range of 7.8-500 μM for FITC and a LLoD below 7.8 μM (Figure 6.3D). The fluorescence detection system selected for further study with PSA IAs uses UV light which emits radiation between 340 and 400 nm to excite fluorescein to emit green light at 530 nm. Although this reduces the absorbance efficiency compared to excitation at the peak absorbance of around 480 nm, this system exploits a large stokes shift resulting in a large increase from excitation to emission wavelength, thus eliminating the interference of the incident light with the image acquired by the smartphone which is very insensitive to UV light. This system does not require the use of an expensive bandpass filter, further increasing the simplicity of the optics. Combined with a good quantum efficiency fluorescein is an attractive substrate.[39]

The MCFphone achieved similar sensitivity with fluorescence detection to absorbance measurement in the bench-top spectrophotometer, allowing sensitive and portable measurement and justifying the use of fluorescence detection in microfluidic IAs.[148,260] The MCFphone is a flexible detection system, with a choice of rapid colour detection or sensitive fluorescence detection that can be selected to suit different applications.

6.4.2. Effect of Enzyme on sensitivity of PSA sandwich ELISA in the MCFphone

Enzymes are the most versatile and common group of labelling substances used in IAs.[108] Macromolecules are measurable at very low concentrations typically in the picomolar to femtomolar range by utilizing its catalytic properties to generate coloured, fluorescent, or luminescent compounds from a neutral substrate. A single enzyme molecule may cause the conversion of 10^7 molecules of substrate per minute, increasing the strength of the signal and therefore the sensitivity by a million-fold when compared

to a label that produces just a signal event.[39] When enzymes are associated with antibodies in a sandwich IAs, the most specific and sensitive type of heterogeneous IAs,[29] a powerful analytical tool is produced.

Although the colorimetric substrate measurement in the MCFphone was about 2 orders of magnitude less sensitive than the benchtop spectrophotometer, this system was still able to quantify PSA in its clinical relevant range (i.e. a clinical threshold of >4 ng/ml requiring further examination) with LLoD of 0.9 ng/ml PSA (Figure 6.4A) in 13 minutes total assay time reaction time is important for POC applications, where quick tests are required.

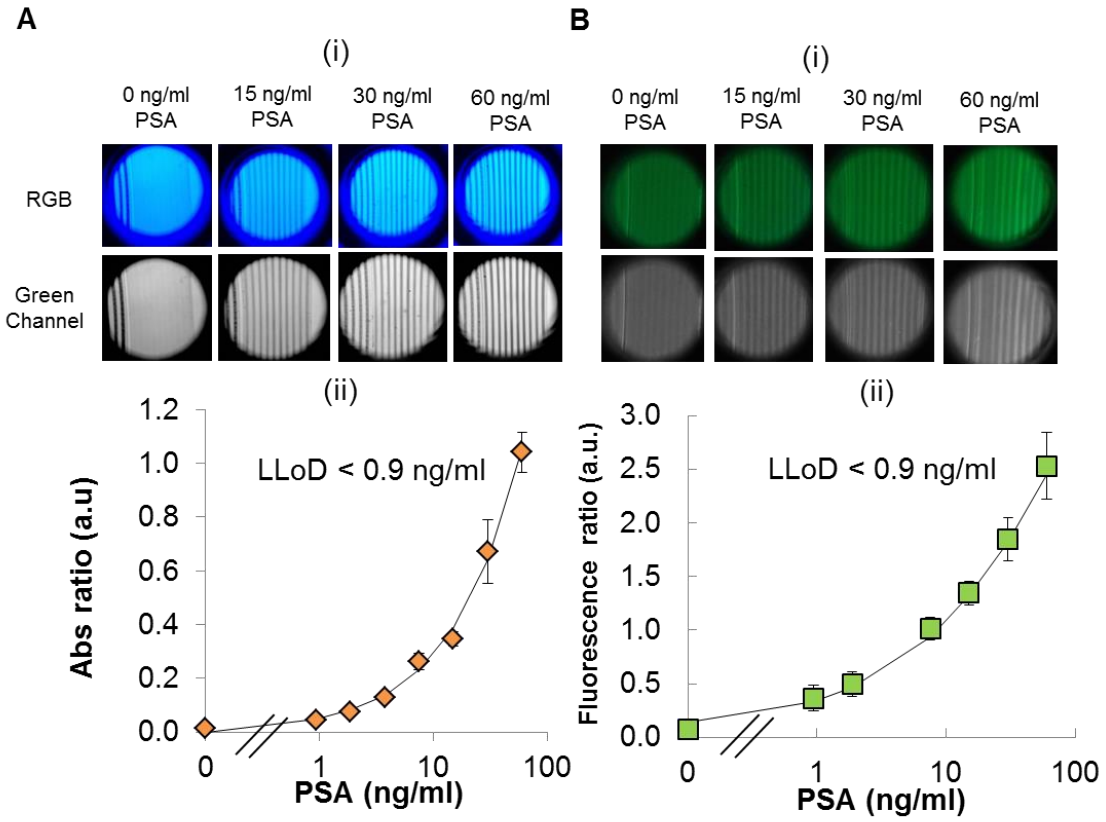

Figure 6.4 - PSA full response curves in buffer, with MCFphone colorimetric and fluorescence systems.
A PSA MCFphone colorimetric quantitation: (i) RGB and green channel digital images, and (ii) full response curve, showing a lower limit of detection, LLoD < 0.9 ng/ml PSA.
B PSA MCFphone fluorescence quantitation: (i) RGB and green channel digital images, and (ii) full response curve with LLoD clearly below 0.9 ng/ml of PSA.

In conventional microtiter plate based ELISA high sensitivity is achieved using long incubation times and long assay times, however kinetic studies in MCF platform

showed that is possible to achieve high sensitivity with short incubation times and that long incubation times will actually increase the background decreasing sensitivity. Therefore, short incubation times favoured higher signal-to-noise-ratios in the PSA IA.

Despite previous optimization of PSA assay, the best sensitivity was achieved by combining a sandwich heterogeneous assay format with a horseradish peroxidase (HRP) label. HRP has a high turnover number and due to short diffusion distance of capillaries it was possible to increase the OPD substrate concentration and optimize the molar ratio of OPD to H_2O_2 contributing to faster and higher signal amplification and compensating for the lower sensitivity of colorimetric MCFphone readout.

Fluorescence measurement using the MCFphone gave greater sensitivity than colorimetric, achieving similar LLoD to the benchtop spectophometer. This increased sensitivity resulted in even greater assay sensitivity when a full PSA response curve was tested (Figure 6.4B) and a LLoD of 0.08 ng/ml PSA was achieved. The increased sensitivity of the assay can be attributed to fluorescence detection combined with other factors including the alkaline phosphatase label that like HRP has high enzymatic turnover and the ability of the fluorogenic product (fluorescein) to absorb UV radiation around 380 nm and emit green radiation around 530 nm, which was enhanced with the use of the dichroic additive green filter.

Although fluorescence detection increased sensitivity, the fluorogenic substrate incubation time was longer than that for the chromogenic substrate (i.e. 10 versus 1 minute), due to differences in reaction rates of the two enzymes. Further optimisation may be required to reduce the overall assay time, and previous work with HRP has demonstrated the improvements to assay time and sensitivity that are possible with systematic assay optimisation in MCF IAs.[152]

Similar studies measured PSA with a microfluidic device incorporating colorimetric smartphone detection, and reported 3.2 ng/ml PSA as the LLoD in 30 minutes total assay time using magnetic microbeads,[103] thus a 3.5 lower sensitivity for double of the assay time compared to the MCFphone.

Fluorescent measurements performed with the immuno-pillar microfluidic platform reported a LLoD of 0.1 ng/ml in 12 minutes total assay time, which means similar sensitivity, but double of time for fluorescence detection on MCFphone. However, it is important to emphasise that the detection equipment used to quantify PSA in the

immuno-pillar platform was an inverted fluorescence microscope, which is not portable, cost-effective or power-free, therefore not suitable for POC applications.[58] An immunochromatographic test integrated with a Laser Fluorescence Scanner was able to detect PSA in biological samples with a lower limit of detection of 0.02 ng/ml PSA in 15 minutes total assay time.[228] This assay was able to obtain better sensitivity than the MCFphone in less time. Nevertheless, lateral flow tests have certain limitation compared with microfluidic devices, for example they lack the possibility to perform calibration curves in simultaneous with the samples,[229] which can be an important feature for biomarker quantitation at POC. Besides the drawbacks of lateral flow technology, the Laser Fluorescence Scanner is not as flexible as a smartphone, since it can be used for colorimetric detection, for data analysis and for results communication all in one single power-free and portable device, which is quickly becoming a cost-effective equipment. In addition, this is the first time to our knowledge that a smartphone is used to quantify fluorescence in a sandwich ELISA assay.

6.4.3. PSA measurement in whole blood samples

In POC testing, sample processing needs to be minimised or eliminated to speed up the diagnostic process,[234] so whole blood samples are preferred. However, whole blood has one of the most complex matrices, with interference possible due to serum proteins that can bind non-specifically to analytes, antibodies or surfaces.[237] This biological fluid also presents a high viscosity that can alter the binding efficiency [235] and the diffusion time of the analyte to the immobilised antibody. Significant work has been published describing methods to overcome the effect of biological matrices in order to achieve robust assay sensitivity and reproducibility in other laboratory and POC assay platforms.[237] Matrix effects are system specific, depending on matrix type, detection method, antibody system and platform. The matrix effect has already been reported by our research group for sandwich ELISA detection of PSA in whole blood in the MCF platform using a flatbed scanner readout system.[152] From these studies we concluded that PSA could be accurately quantified in whole blood samples in the MCF platform. However, non-diluted whole blood matrices did show lower signals for the same incubation times as buffer matrices. This signal reduction could be overcome either by dilution or by extended sample incubation times. As the aim of this work is to create a

rapid POC diagnostic system, sample dilution was chosen here instead of extended sample incubation times to maintain the sensitivity and reproducibility of PSA assay in biological samples and restrict total assay time. Sample dilution is often used in serology and does not represent an additional step in the assays, as the sample wells can be provided with diluent buffer.

In this study, the MCFphone fluorescence detection system was used to quantify PSA from diluted whole blood (Figure 6.5). The sensitivity calculated and assay signal were in the same order of magnitude (Figure 6.5A and Table 6:1) when compared to the assay performed in buffer across all the PSA assay range.

Table 6:1 - Sensitivity comparison between MCFphone colorimetric and fluorescence PSA assay.

	Lowest PSA conc. tested (ng/ml)	**Data correlation with 4PL model (R^2)**	**LLoD (ng/ml)**	**Precision**
PSA colour assay	0.9	0.9979	0.40	7% at 15ng/ml PSA
PSA fluorescent assay	0.9	0.9933	0.08	8% at 15 ng/ml PSA
PSA fluorescent assay in whole blood	0.08	0.9978	0.04	11% at 2.2 ng/ml PSA

Further experiment using whole blood from 3 additional patients showed a %Recovery very consistent when spiked with PSA concentration in the low linear range (0.74 ng/ml), middle range (6.7 ng/ml) and higher linear range (60.0 ng/ml). In all cases, %Recovery values calculated for the different whole blood samples remained within 80-120%, which is regarded as the desirable range, with the exception of S2 spiked with 60.0 ng/ml of PSA which returned 74.2%. This ultimately demonstrates the MCFphone as an efficient PSA measurement system from fresh anticoagulated whole blood samples, simplifying sample preparation required for clinical testing. Future studies will aim understanding blood matrix effect on variability between samples, and test the MCFphone with patients diagnosed with prostate cancer.

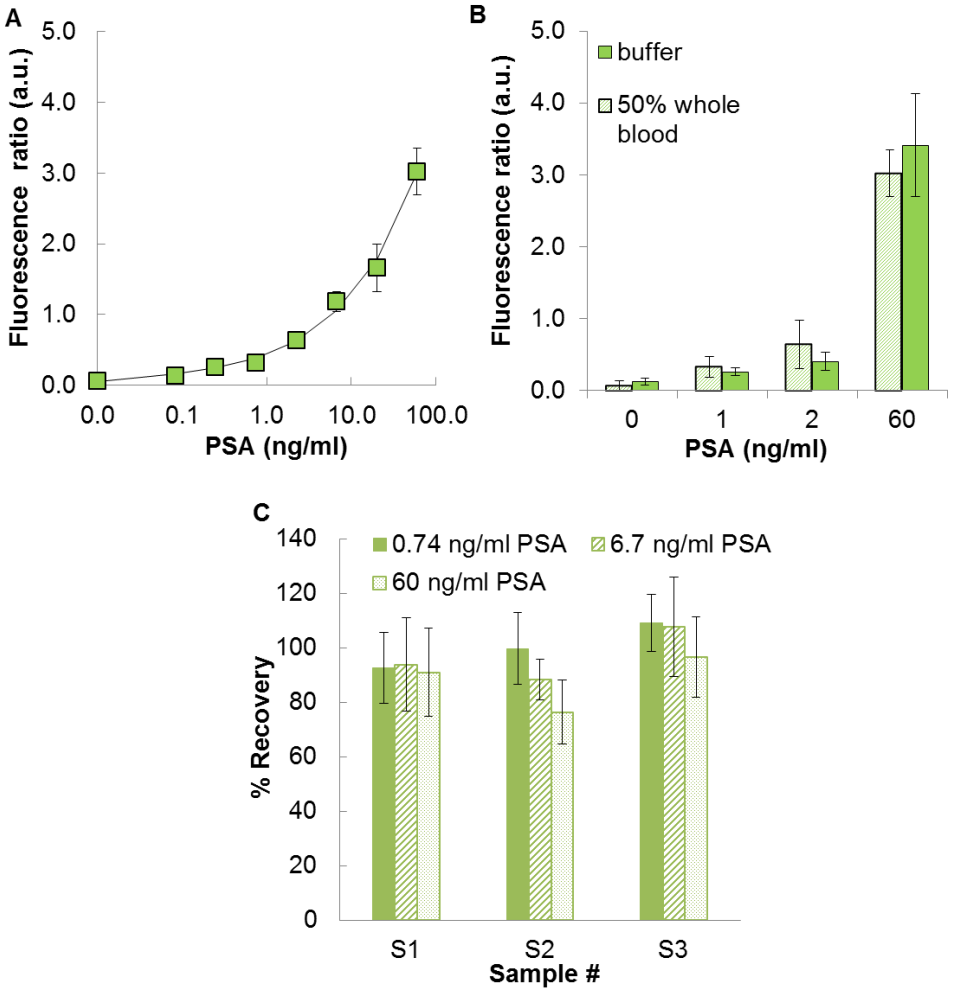

Figure 6.5 - Smartphone fluorescence detection of PSA in the MCF in whole blood. **A** Full response curve using 1:3 dilution series. **B** Comparison between PSA sandwich assay in buffer and 50% whole blood. **C** %Recovery for 3 different blood samples from female donors spiked with 3 different concentrations of recombinant protein (PSA), 0.74, 6.7 and 60 ng/ml. Average coefficient of variation different samples % of recovery is 12% for 0.74 ng/ml PSA, is 15% for 6.7 ng/ml PSA and 16% for 60 ng/ml PSA.

6.5. Conclusions

The MCFphone is a flexible, power-free and portable IA detection system capable of rapid colorimetric detection and sensitive fluorescence detection from whole blood samples. In this present study, the MCFphone was able to detect and quantify PSA within the dynamic range of 0.9 to 60 ng/ml PSA in 13 minutes, using colorimetric detection and within 0.08 ng/ml to 60 ng/ml of PSA, using fluorescence detection from whole blood samples. Considering the PSA clinical range of 4 ng/ml for prostate biopsy, this device can provide reliable measurements for prostate cancer screening and

detection in remote areas outside laboratory facilities. Further improvements in fluorescence sensitivity could be obtained with optimization of enzymatic reaction, a more robust and intense UV light source and filters, as well as higher resolution smartphone cameras. Automation of multistep ELISA and further integration and miniaturisation of all fluidic and optoelectronics components will addressed in future publications with the MCFphone concept.

7. Managing biological matrix interference in microfluidic microcapillaries

7.1. Abstract

In this study it was shown that was possible to eliminate the sample matrix effect in the Microcapillary Film (MCF), a novel FEP-Teflon platform for rapid immunoassays (IA). This was achieved without any sample preparation in three different sandwich assays systems: mouse IgG-anti-IgG, PSA (prostate specific antigen) and IL-1β cytokine. The choice of appropriated capture antibody (CapAb) coverage and sample incubation time enabled the biological matrix interference elimination in the MCF sandwich assays. Other variables were studied in order to understand biological sample interference in microcapillaries, such as viscosity and diffusion distance. It was found that viscosity interferes with antibody-antigen binding kinetics, but not with the reaction equilibrium. While diffusion distance, in this system, was intrinsically related with CapAb surface coverage, therefore reducing the diffusion distance altered the antibody-antigen equilibrium.

Comparison between IL-1β sandwich assay in whole blood and human serum shows similar absorbance values, which suggests blood cells do not interfere with IA in FEP-Teflon microcapillaries.

The possibility of performing quantitative sandwich assays without any type of sample preparation has not been previously reported in literature and it can bring microfluidic diagnostic research for Point-of-Care (POC) closer to commercialisation.

Immunoassays (IA) are analytical tools that use the unique capacity of antibodies to specifically recognize and bind an antigen.[21] In diagnostics the antigen/analyte (the target specimen to be quantitated) is diluted in a biological matrix which can be saliva, urine, plasma, serum or blood. The influence of biological sample properties on the measurement is named matrix effect of an assay.[261] These effects are responsible for erroneous diagnostics of certain diseases, with false positive and negative results, leading to unnecessary treatment or mistreatment of certain conditions. Understanding the biological matrix interference and finding strategies to overcome it is therefore a

paramount in diagnostic industry, especially for Point-of-Care (POC) diagnostic tests where minimal sample treatment is required.[262,263]

The main protein biomarkers currently used in diagnostics, are prostate specific antigen (PSA) for prostate cancer diagnostics, cardiac markers (troponin I and T, BMP, C reactive protein) for cardiovascular accident risk assessment, and cytokine biomarkers for sepsis and other inflammatory diseases, all measured from blood samples. Blood is a highly complex matrix with cellular components ranging in size between 2 μm (platelets) to 20 μm (leukocytes) and a very heterogeneous liquid fraction, plasma, constituted by water (92%), proteins (8%) and other substances in traceable amounts.[237] Important plasma proteins include serum albumin, immunoglobulins (antibodies), blood clothing factors (e.g. fibrinogen) and lipoproteins.

Blood components can interfere in IA, as they change the physical properties of the medium where the analyte is dissolved, such as viscosity, pH or salt concentration. Small changes in blood properties can change the binding efficiency of the antigen/analyte to the bioanalytical antibodies when compared to the same reaction in a different medium.[235,237] Also some proteins, such as hormones and antibodies, and anticoagulants can bind the analyte decreasing its available concentration in solution. For example steroids can bind to sex hormone binding globulin[264] and prevalent autoantibodies to tyroid hormones in non-tyroid autoimmune conditions have been reported.[265] Some other blood compounds, such as heterophilic antibodies (antibodies produced against poorly defined antigens presenting low affinity and weak binding)[266] interfer with the assay by binding to the immobilised bioanalytical antibody or the label antibody in two site sandwich IAs. When the heterophilic antibody, bond to the CapAb, binds to the label antibody, the assay yields false positives. On the contrary, if the heterophilic antibody, bond to the CapAb, does not allow the analyte and the label antibody to bind, it will promote false negative results.[262,263] Interfering antibodies are called heterophilic when they are multispecific and the host individual has not been treated with animal immunoglobulins.[267] Human anti-animal antibodies (HAAA) are generated when the immune system is in contact with animal antibodies. These antibodies show high affinity and compete with the test antigen by cross-reacting with the bionalytical antibodies of the same species.[268] Other plasma proteins such as albumin, lysozyme, fibrogen and paraprotein can interfere with bioanalytical reagents in IAs. [269]

Studies of antibody interference (heterophilic and human anti-animal antibodies) in IAs indicate low interference prevalence from 0.03 to 6%.[270,271] However, a study by *Boscato et al.* (1986) showed that analyte antibody binding substances were detected in 40% of studied samples (688 samples) causing 15% interference in assays.[272]

Techniques for minimizing antibody interferences in IAs include gel chromatography, immunoextraction, precipitation, centrifugation, filtration and heat-treatment. These sample pre-treatment techniques aim to remove the assay interfering antibody/substances.[237,273,274] Other simple techniques rely on the addition of blocking reagents to the sample or directly to the assay as sample diluents.[272,273,275] Sample dilution is another approach for minimizing interferences and it has been reported to be effective even in sensitive systems.[276–278] However, matrix dilutions also implies analyte dilution, therefore compromising assay sensitivity and simplicity.

Recently, quantitative diagnostics have been translated to POC miniaturized platforms, which aim for sensitive, rapid and cost effective diagnostics. Microfluidic IAs platforms are the most common attempt for quantitative POC IAs due to their large surface-area-to-volume ratio (SAV) allowing fast and sensitive IAs.

In POC diagnostics, sample preparation needs to be minimized to speed up the test and eliminate extra cost. Whole blood and urine are the most common sample types,[234] yet, microfluidics research has focused its attention on the improvement of the analytical reaction, with sample pre-treatment still being performed off chip. d*eMello et al.* (2003) reviewed several microfluidic device structures that could possibly integrate sample processing treatment with bioanalytical purposes, like the micro-filter with pillars 3 μm wide and 50 μm surrounding reaction chambers allowing 500 pL sample volumes, for separation of interfering substances from the analyte;[279] and a lateral percolation filter, where the sample penetrates a filter bed and particulates with dimensions larger than the minimum filter features (1.5 mm) were successfully restricted.[280] Another approach is the H-filter where two different laminar flow fluids (carrier stream and diluent stream) are brought together in a central channel and filtration occurs due to the different diffusion coefficients of molecules.[281] Other microfluidic adaptations of liquid/liquid extraction and solid phase extraction have been fully reviewed.[282]

Although laboratories have to deal with biological sample interference, the nature of this interference is still not currently clear. This lack of knowledge extends to

microfluidic IAs, since they are a relatively new approach to diagnostics. Previous studies of PSA sandwich assay in the MCF platform have shown it is possible to manage human serum and whole blood matrix interference in MCF platform through sample dilution or by extending sample incubation times. This relates the matrix interference effect with the viscosity increment of the medium where antibody-antigen binding reaction occurs.[152,153]

This study aims at extending the knowledge and understanding of matrix interference effect in microfluidic IA, by presenting sample interference effects and strategies to overcome it, in three different systems: mouse IgG/anti-IgG direct assay, PSA sandwich assay and IL-1β cytokine sandwich assay in FEP-Teflon microcapillaries. In our approach by changing the capillary diameter, the antibody immobilised density and the sample incubation time is possible to minimize or even overcome the biological samples matrix effect in IA. This will eliminate the need of sample preparation for POC diagnostics. The experiments in this study were performed in the MCF platform (Figure 7:1A), which consists in flat fluoropolymer film with 10 parallel microcapillaries embedded on it. Since the nature of the matrix effect is not clear, it was assumed the biological matrix effect was caused by one factor, named the interfering factor (Figure 7:1B).

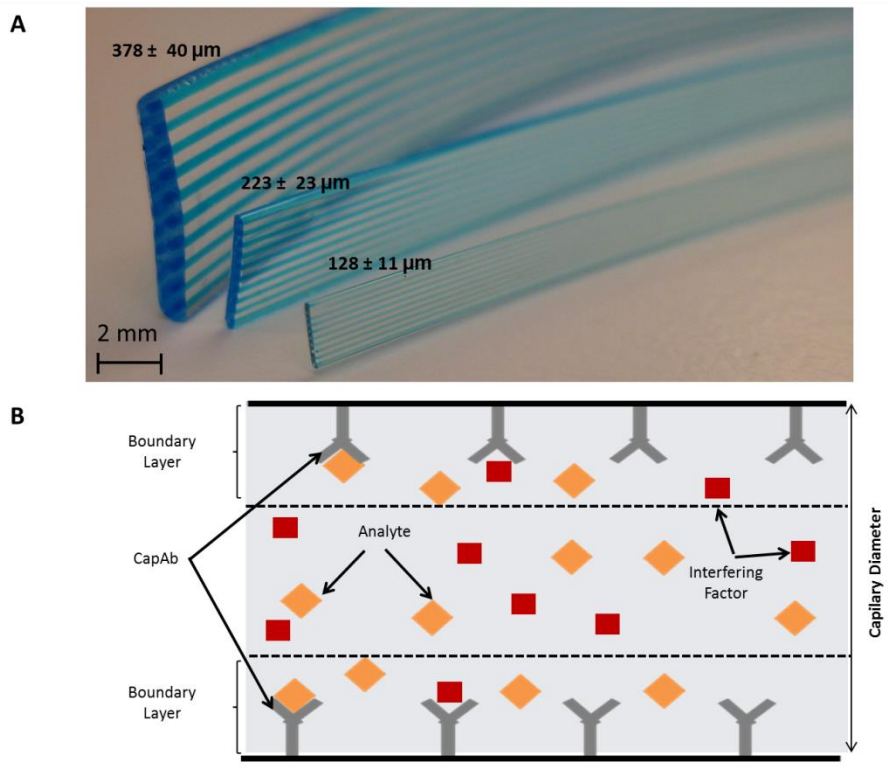

Figure 7:1 – Biological matrix effect in microcapillaries.
A Three different MCFs with mean 378, 223, 128 µm bore diameter were used for solid phase IAs. The capillaries are filled with a food dye for clarity. **B** Components of a solid phase immunoassay in a capillary. The interfering factor is substance from the biological matrix which interferes in the assay in an unknown way.

7.2. Materials an Methods

7.2.1. Materials & Reagents

Mouse IgG (whole antibody) was purchased from Life Technologies (Paisley UK), rabbit anti-IgG (whole molecule) conjugated with peroxidase and SIGMAFAST^{TM} OPD (o-Phenylenediamine dihydrochloride) tablets were supplied from Sigma-Aldrich (Dorset, UK). The BCA Protein Assay Reagent (bicinchoninic acid) was purchase from Thermo Scientific (Lutterworth, UK). The IL-1β recombinant protein, Anti-Human IL-1β biotin and Anti-Human IL-1β purified were supplied from eBiosciences (Hatfield, UK). High sensitivity streptavidin-HRP was supplied by Thermo Scientific (Lutterworth, UK). Human kallikrein 3/ Prostate Specific Antigen (PSA) ELISA kit was purchased from R&D Systems (Minneapolis, USA). The kit contained a monoclonal

mouse Human Kallikrein 3/PSA antibody (CapAb), a Human Kallikrein 3/PSA polyclonal biotinylated antibody (DetAb) and recombinant Human Kallikrein 3/PSA (standard).

Phosphate buffered solution (PBS) and Bovine Serum Albumin (BSA) were sourced from Sigma Aldrich (Dorset, UK). PBS pH 7.4, 10mM was used as the main experimental buffer. The blocking solutions consisted in 3% w/v protease-free BSA diluted in PBS buffer and a Super Blocking solution purchased by Thermo scientific (Lutterworth, UK). For washings, PBS with 0.05% v/v of Tween-20 (Sigma-Aldrich, Dorset, UK) was used. A female human serum was supplied from BBI solutions (Cardiff, UK), aliquot and storage at -20ºC. The human blood was collected into a 5 ml vial with citrate phosphate dextrose (CPD) as anti-coagulant, supplied by healthy volunteers at Loughborough University.

The MCFs were fabricated from fluorinated ethylene propylene co-polymer (FEP-Teflon) by melt-extrusion process by Lamina Dielectrics Ltd. (Billinghurst, West Sussex, UK), presenting 10 parallel microcapillaries. Different MCFs were used in this study with mean hidraulic diameter of 128±11 μm, 223±23 μm, 378± 40 μm.

7.2.2. Sample matrix viscosity effect on kinetics of antibody-antigen binding

Eight MCF strips with 223±23 μm bore diameter were loaded with 40 μg/ml of IL-1β CapAb and incubated for 2h at room temperature. This solution was replaced by the super blocking solution, incubated for an additional 2h at room temperature. The MCF strips were washed with 1 ml of PBS-Tween, the washing buffer and trimmed into 3 cm length test strips. The test strips were introduced into the Multiple Syringe Aspirator (MSA), a fluid handling device that allows simultaneous aspiration of solutions into eight different MCF strips, presented elsewhere.[152]

Three different solutions of BSA with concentrations of 5, 10 and 25 w/v % were used as sample diluents for viscosity increment. Four solutions of 1 ng/ml and 0.1 ng/ml of IL-1β recombinant protein were prepared using as sample diluent PBS buffer, 5, 10 and 25 % of BSA in PBS. These solutions were aspirated into the coated and blocked MCF strips connected to the MSA and left to incubate for variable incubation times of 0, 2, 5, 10, 15 and 30 minutes. For each sample incubation time negative controls, 0 ng/ml of

IL-1β, with the different diluents used were performed simultaneously with the positive controls. After a washing step, a monoclonal anti-IL-1β biotinylated DetAb was added to the MCF test strips and incubated for 10 min followed by another washing step. A solution of 4 µg/ml of high sensitivity streptavidin horseradish peroxidase (HRP) was aspirated into the capillaries and incubated for 10 min followed by an intensive washing step. A 4 mg/ml solution of OPD enzymatic substrate replaced the washing buffer and was incubated for 5 min.

7.2.3. Viscosity measurements

A U-tube viscometer, size B (nominal constant = 0.01cSt/s), supplied from Technico, was used to measure kinematic viscosity (cSt or 1 $mm^2.s^{-1}$) of PBS, BSA (5, 10 and 25%) and serum dilution solutions. The solutions were filled into a tube in a water bath with temperature control set at 20ºC. The time (seconds) for the liquid to move from distance X to Y in the U-tube was measured 3 times for each sample.

The density of each sample was determined by weighing the sample liquid into a vial and determining the volume of the vial by weighing distilled water. Since the density of the water is $1g/cm^3$, it was assumed its weight was proportional to its volume. Each measurement was performed 3 times in a temperature controlled room. The dynamic viscosity (μ) in mPa.s ($=0.001Kg.m^{-1}.s^{-1}$) or c.p. (centipoise) was obtained by multiplying the kinematic viscosity (v) of the sample in cSt ($=1E^{-6}.m^2/s$) by the sample density in kg/dm^3.

7.2.4. Capillary diameter effect on kinetics of antibody-antigen binding in biological matrices

Several transversal sections of three FEP-Teflon MCFs with different bore diameter were trimmed and a long focal distant point microscope was used for imaging. ImageJ software was used to measure the diameter of the 10 capillaries from the microphotographs.

A solution of 200 µg/ml of mouse IgG was filled into three different diameter (128, 223 and 378 µm) MCF strips with 35 cm each. A negative control strip was filled with PBS

buffer. The solutions were incubated for 30 minutes at room temperature and washed with 1 ml of PBS-Tween. A solution of 0.6 µg/ml of mouse anti-IgG peroxidase conjugated, prepared in PBS buffer, was added to the MCF strip and 4 cm strips were trimmed and washed with PBS-Tween after 1, 2, 4,6,8 and 10 minutes of incubation anti-IgG. A 1 mg/ml solution of OPD substrate was added to the strips and digital images taken with a flatbed scanner after 5, 10, 15 and 20 minutes of enzymatic substrate incubation. The procedure was repeated for 0.6 µg/ml mouse anti-IgG peroxidase conjugated solutions prepared in non diluted human serum.

7.2.5. Mass determination of mouse IgG adsorbed by solution depletion technique in variable size MCF

Three MCF strips with 20 cm length and 223 ± 23 µm were filled with 200 µg/ml of mouse IgG solution and incubated for 2 hours at room temperature. The solution was then collected inside the capillaries for protein quantitation.

A 1:2 serial dilution solutions of mouse IgG from 0 to 400 µg/ml were prepared for protein quantitation in a calibration curve. Triplicates of 25 µl of each collected solution were placed in a microwell plate and 200 µl of BCA working reagent (1 reagent B: 50 reagent A) was added to each sample well and mixed for 5 sec with a multiple micropipette. Simultaneously 25 µl of IgG solution was placed in a microwell and mixed with 200 µl of BCA working reagent (1:50). The microwell plate was covered with parafilm and placed at 37 ºC for 3 hours. IgG standards were prepared in triplicates.

After 3 h incubation of IgG standards and samples with BCA working reagent, the microtriter plate was left for a few minutes at room temperature to cool down. The end point absorbance measurements were made at 562 nm in each well with the microplate reader (Epoch, BIOTEK).

The concentration of IgG adsorbed (µg/ml) was obtained by equation (7:1) and the conversation for adsorbed concentration to adsorbed density (ng/cm2) was made through equation (7:2).

$$[\text{Ads IgG}] = [\text{Inicial IgG solution}] - [\text{Remain IgG solution}] \quad (7:1)$$

$$\frac{SA}{V} = \frac{2\,\pi\,rl}{\pi\,r^2 l} = \frac{4}{D} \quad (7:2)$$

Where SA is the surface area, V is the volume and D is the diameter of the capillary.

The quantitation of IgG adsorbed with 200 µg/ml IgG solution was performed, using the same method for 80 cm long strips of 128± 11 µm diameter and for 8 cm length strips of 378± 40µm MCF diameter.

7.2.6. Overcoming biological sample matrix in MCF platform – three antibody-antigen systems

In order to understand the effect of antibody surface coverage and sample incubation time (related to diffusion distance) in overcoming the biological matrix effect in MCF IA, three different assays (mouse IgG/anti-mouse IgG, PSA and IL-1β assay) were studied in 223 µm diameter bore MCF. In the three systems two sets of experiments were performed, one that relates the immobilise antibody surface coverage for shorter and long sample incubation times with the biological matrix effect and another set of experiments, directed for sandwich assays full response curves.

Surface coverage studies and sample incubation time

For the mouse IgG/anti-mouse IgG system study of the effect of surface coverage in the biological matrix interference, eleven MCF strips, with 223 µm diameter and 8 cm length, were filled with eleven different solutions of mouse IgG: 0, 0.1, 1, 4, 8, 12, 16, 25, 50, 100, 200 µg/ml. These solutions were incubated for 30 minutes at room temperature, followed by a wash step. The MCF strips were trimmed into 3 cm strips and were placed in the Multiple Syringe Aspirator (MSA). A solution of 0.6 µg/ml of anti-IgG peroxidase conjugated, prepared in PBS buffer, replaced the wash buffer and was incubated for 10 minutes, followed by another washing step. A solution of 1 mg/ml of OPD enzymatic substrate was aspirated into the MCF strips and the MSA was placed on the flatbed scanner. Digital images were taken for 5, 10, 15, 20, 25 and 30 minutes of

enzymatic substrate incubation time. The same procedure was repeated for anti-IgG solutions prepared in 100% human serum.

For the PSA sandwich assay system study of the effect of surface coverage in the biological matrix interference, eight MCF strips, with 223 μm diameter and 8 cm length, were filled with eight different solutions of PSA CapAb and incubated for 2 hours at room temperature. The strips were then filled with 3% BSA solution which was also incubated inside the capillaries for 2 hours at room temperature, followed by a washing step. The MCF strips were trimmed into 3 cm test strips and placed in the MSA, for simultaneous fill of eight MCF test strips. A solution of 3.75 ng/ml of PSA standard was prepared in PBS buffer, aspirated into the MCF strips and incubated for 30 minutes, followed by a wash step. A solution of 1 μg/ml of biotinylated detection antibody (DetAb) replaced the wash buffer and was incubated for 5 minutes, replaced by a solution of 1 μg/ml of enzyme incubated for 5 minutes. An intensive washing step was performed and a solution of 4 mg/ml of OPD filled the MCF test strips. The MSA was placed on the flatbed scanner and digital images were taken in 1, 3, 5, 10, 15, 20, 25, 30 minutes of enzymatic substrate incubation. The procedure was repeated for PSA standards prepared in 100% human serum.

For the IL-1β sandwich assay system study of the effect of surface coverage in the biological matrix interference, eight MCF strips, with 223 μm diameter and 16 cm length, were filled with eight different solutions of IL-1β CapAb: 0, 5, 10, 20, 40, 80, 100 and 200 μg/ml. Solutions were incubated for 2 hours at room temperature. The strips were then filled with super block solution also incubated for 2 hours at room temperature. The MCF strips were trimmed into 3 cm test strips and eight of them, with eight different concentration of CapAb, were placed in the MSA. A solution of 0.125 ng/ml of IL-1β recombinant protein was prepared in buffer and incubated for 5 minutes, followed by a washing step. A solution of 10 μg/ml of biotinylated DetAb was incubated for 10 minutes followed by a washing step. A 4 μg/ml solution of enzyme was added to the test strips and incubated for 10 minutes followed by an intensive washing step. A solution of 4 mg/ml of OPD enzymatic substrate was added to the strips and the MSA was placed on the flatbed scanner. Digital images were taken at 2, 5, 10, 15, 20, 25 and 30 minutes of OPD incubation. The procedure was repeated for 0.125 ng/ml of IL-1β in 100% human serum and for 0.125 ng/ml of IL-1β incubated for 30 minutes (instead of 5minutes) in buffer and 100% human serum.

Full response curves

For the PSA (prostate specific antigen) sandwich assay two MCF strips with 223 ± 23 μm diameter and 30 cm length were filled with 10 μg/ml of PSA CapAb and incubated for 2 hours at room temperature. This solution was replaced by 3%BSA solution which was incubated for 2 hours at room temperature followed by a washing step with PBS-Tween. The MCF was trimmed into 3 cm test strips which were incorporated into the MSA for simultaneous aspiration of eight MCF test strips. PSA 1:2 serial dilutions in the range of 0 to 60 ng/ml were prepared in buffer and 100% human serum. Eight PSA serial dilutions in buffer were aspirated into eight MCF test strips with the MSA and incubated for 15 minutes. This solution was replaced by 2 μg/ml of PSA biotinylated DetAb (detection antibody) which was incubated for 10 minutes, followed by 4 μg/ml of high sensitivity HRP incubated for 10 minutes. The eight strips were washed with approximately 300 μl of PBS-Tween and a solution of 4mg/ml of OPD was added and incubated for 3 minutes while a digital image was taken by a flatbed scanner.

For the IL-1β full response curve assays five MCF strips with 223 ± 23 μm diameter and 30 cm length were filled with 40 μg/ml of IL-1β CapAb and incubated for 2 hours at room temperature. The strips were then filled with super blocking solution and incubated for 2 hours at room temperature. After a washing step the strips were trimmed into 3cm MCF test strips. Each eight MCF strips were incorporated into the multiple syringe aspirator (MSA) for simultaneous aspiration. Eight 1:2 serial dilutions of IL-1β in the range of 0 to 1 ng/ml were prepared in buffer, 50 and 100% of human serum. The serial dilutions in buffer were simultaneous aspirated into 8 previously coated and blocked MCF strips and incubated for 5 minutes. After a washing step 10 μg/ml of biotinylated anti-IL-1β DetAb was added to the MCF strips and incubated for 10 minutes followed by a washing step. A 4 μg/ml solution of high sensitivity streptavidin HRP enzyme replaced the washing buffer and was incubated for 10 minutes. An intensive washing step was performed in the MCF strips and 4 mg/ml of OPD solution was added and incubated for 2 minutes, while a digital image was taken by a flatbed scanner.

The same procedure was followed for IL-1β recombinant protein serial dilutions made in 50 and 100 % human serum. Two other IL-1β sandwich assays were performed with

30 minutes sample incubation with IL-1β serial dilutions made in buffer and 100% human serum.

In order to compared serum and whole blood sample interference 0, 0.03, 0.125 and 0.5 ng/ml solutions of IL-1β were prepared and assayed in buffer, 50 and 100% whole blood. The sandwich assays were performed with 5 and 30 minutes of sample incubation.

7.2.7. Image analysis of MCF IA strips

RGB digital images were split into 3 separated channels images by *Image J* software (NIH, Maryland, USA). The blue channel images were used to calculate absorbance values, based on the grey scale peak height of each individual capillary of FEP-Teflon MCF as described previously.[127,152] Therefore, absorbance signal is calculated for each capillary, according to equation (7:3).

$$\text{Abs} = -Log_{10}(\frac{\text{I}}{I_0}) \tag{7:3}$$

Where I is the transmitted light and corresponds to I_0 minus peak height, and I_0 is the maximum grey scale value, corresponding to the initial emitted light. The absorbance values presented averages of absorbance from 10 capillaries one MCF stip.

7.2.8. Kinetic model antibody-antigen kinetic

The antibody-antigen kinetic results presented in this study were fitted to a theoretical IA mathematical model that aims describing the role of transport of analyte in a microchannel (convection and diffusion), the kinetics of binding between the analyte and the capture antibodies, and the surface density of the CapAb on the assay. Equation (7:4) can be solved analytically for a constant analyte concentration and was used to estimate the rates of association and dissociation of antibody binding in the MCF system.[204]

$$\Phi = \frac{K_{on}\,\Phi_{max} C}{K_{on}\,C + K_{off}}(1 - \ e^{-(K_{on}\,C + K_{off})t}) \tag{7:4}$$

Where Φ is the surface density at the time *t*, C is the analyte concentration K_{on} the association rate and K_{off} the dissociation rate. And Φ_{max} is the maximum surface coverage, which in this study was taken as the maximum absorbance signal obtained.

7.3. Results and Discussion

7.3.1. Sample matrix viscosity effect on kinetics of antibody-antigen binding

Biological samples present complex matrices that interfere with bioanalytical reagents in IAs in multiple ways depending on the matrix, on the bioanalytical reagents and solid phase platform for the immunoassay.

Previous MCF assays[152,153] and real time antibody-antigen binding studies with optical sensors, e.g. the IAsys system,[235] related biological matrix interferences with viscosity increment of medium. On a previous study, PSA sandwich assays overcame sample matrix effect by sample dilution and by extending sample incubation times, and both strategies can be explained if viscosity is the biological matrix interfering factor.

Solution viscosity can interfere in the diffusion coefficient of a molecule according to Einstein and Stokes equation of spherical particles diffusion through a liquid with low Reynolds number (equation (7:5)):

$$D = \frac{K_B T}{6\pi r \eta} \qquad (7:5)$$

Where *D* is the diffusion coefficient, K_B is the Boltzmann's constant; *T* is the absolute temperature, *r* the radius of a spherical particle and η the dynamic viscosity. Therefore, the higher the viscosity of the medium, the lower the diffusion coefficient of a molecule and consequently the longer the diffusion time, accordingly to the Einstein relation (equation (7:6)):

$$t = \sqrt{2Dx} \qquad (7:6)$$

Where *t* is the diffusion time, *D* the diffusion coefficient of a molecule and *x* the average distance of diffusion. Considering only the effect of viscosity in a solid phase IA capillary, assays with higher viscosity biological solutions would need longer

incubation times to reach the same equilibrium than an assay performed in buffer (lower viscosity solution). This theoretical consideration is confirmed by the results shown in Figure 7:2.

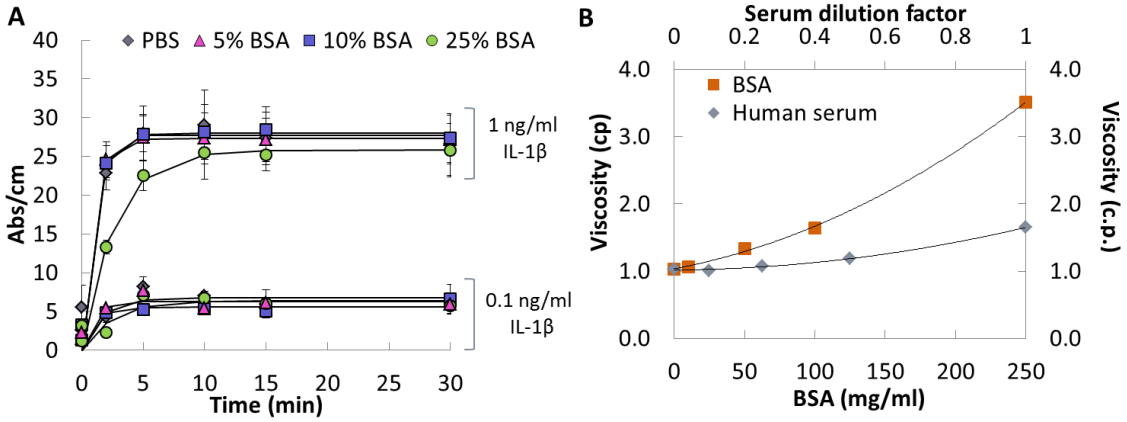

Figure 7:2 – Effect of sample matrix viscosity in antibody-antigen kinetics in an IL-1β sandwich assay, using 223 µm diameter bore MCF.
A Antigen (IL-1β 0.1 and 1 ng/ml) kinetics with sample matrix with different viscosities: PBS, 50, 100 and 250 mg/ml BSA. **B** Viscosity of BSA solutions with different concentrations and viscosity of human serum different dilutions.

Different concentrations of BSA present increasing dynamic viscosity, being PBS solution correspondent to 1.027 c.p., 50 mg/ml of BSA to 1.33 c.p., 100 mg/ml to 1.64 c.p. and 250 mg/ml correspondent to 3.51 c.p., as seen in Figure 7:2B. Figure 7:2A, indicates that kinetics of IL-1β recombinant binding is significantly affected by 250 mg/ml solution of BSA as antigen diluent for antigen concentration of 1 ng/ml. With this diluent the reaction takes longer to reach equilibrium than with other diluents tested. However the equilibrium is not different from the equilibrium of the antigen involved with the other diluents solution. Therefore, it appears that the kinetic delay is due to viscosity increase in the matrix (kinetic constants obtained from fitting equation (7:4), Figure 7:2A are in Table 7:1).

Table 7:1 - Kinetic constants of IL-1β binding for 1 ng/ml of IL-1β shown if Figure 7:2A.

	PBS	**50 mg/ml BSA**	**100 mg/ml BSA**	**250 mg/ml BSA**
$K_{on}\,(M.s^{-1})$	2.36×10^{15}	3.07×10^{11}	2.70×10^{11}	9.56×10^{10}
$K_{off}\,(s^{-1})$	1.11×10^{-1}	1.75×10^{-3}	1.09×10^{-3}	8.88×10^{-4}
$K_A\,(M)$	2.13×10^{14}	1.76×10^{14}	2.48×10^{14}	1.08×10^{14}

This delay in equilibrium was not observed for lower antigen concentrations (Table 7:2), IL-1β 0.1 ng/ml, probably because with small amounts of antigens only the antigens on the boundary layer are bond to the immobilised antibodies, so their association constant (Ka) is not dependent on diffusion from the bulk, being the same independently of the viscosity of the medium.

Table 7:2 - Kinetic constants of IL-1β binding for 0.1 ng/ml of IL-1β shown in Figure 7:2A.

	PBS	**50 mg/ml BSA**	**100 mg/ml BSA**	**250 mg/ml BSA**
$K_{on}\ (M.s^{-1})$	1.79×10^{11}	2.86×10^{11}	2.30×10^{11}	1.08×10^{11}
$K_{off}\ (s^{-1})$	3.81×10^{-4}	1.91×10^{-3}	3.37×10^{-3}	5.57×10^{-4}
$K_A\ (M)$	4.70×10^{14}	1.49×10^{14}	6.83×10^{13}	1.93×10^{14}

Results showed viscosity only interferes in antigen binding kinetics above a certain threshold, which is 3.5 c.p. correspondent to 250 mg/ml of BSA solution. Human serum viscosity is equivalent to 100 mg/ml of BSA viscosity, and this BSA concentration did not cause kinetics delay, as seen in Figure 7:2A, therefore the interference noticed with human serum biological sample matrix does not seem to be related to viscosity, but to other factors.

Whole blood viscosity varies from 3.36 to 5.46 cp[241], however whole blood IL-1β sandwich assay in the MCF platform presents similar matrix interference as human serum, being slightly different from buffer for 5 min sample incubation time, but similar to buffer for 30 min sample incubation time (Figure 7:3A and B).

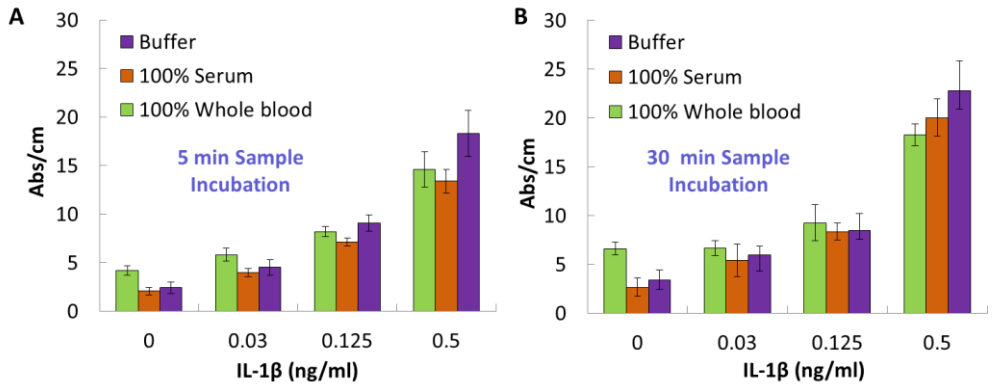

Figure 7:3 – Effect of human serum and whole blood matrices interference in IL-1β assay in the MCF platform in 223 ± 23 µm capillaries.
A IL-1β assay with buffer and 100% human serum and whole blood for 5 minutes sample incubation. **B** IL-1β assay with buffer and 100% human serum and whole blood for 30 minutes sample incubation.

IL-1β sandwich assay showed similar interference in buffer and whole blood samples, which means at least with two different blood samples tested, blood viscosity did not interfere with the assay. The same was found in PSA sandwich assays performed previously.[152] This means that red blood cells appear not to interfere with the IL-1β sandwich assay, which makes this MCF platform assay ideal for POC diagnostics, since there is no need for solid phase separation in whole blood samples.

Data in Figure 7:3 and Figure 7:4 also suggested longer sample incubation times seem to minimise biological matrix interference of human serum, whole blood and higher BSA concentration solutions in IL-1β sandwich assay. This suggests two possible explanations about how the interfering factor affects MCF IA: it can play by changing the rate of diffusion of the antigen towards the immobilised antibody layer or it can bind to the immobilised antibody with lower affinity compared to the antigen. The last explanation means with time the interfering factor (e.g protein, auto-antibody, heterophilic antibody, etc) is displaced giving place to the antigen, explaining why longer incubation times solve biological matrix effect problems in MCF IA.

7.3.2. Capillary diameter effect on kinetics of antibody-antigen binding in biological matrices

As diffusion appeared to affect matrix interference in MCF assays and the extended incubation times are not ideal for POC testing, the following set of experiments aimed at understanding the effect of diffusion distance in MCF assays in matrix interference and incubation time simultaneously. The study of antibody kinetics in MCF with different capillary diameters in buffer and in human serum was performed using mouse IgG and conjugated anti-IgG peroxidase and results shown in Figure 7:4.

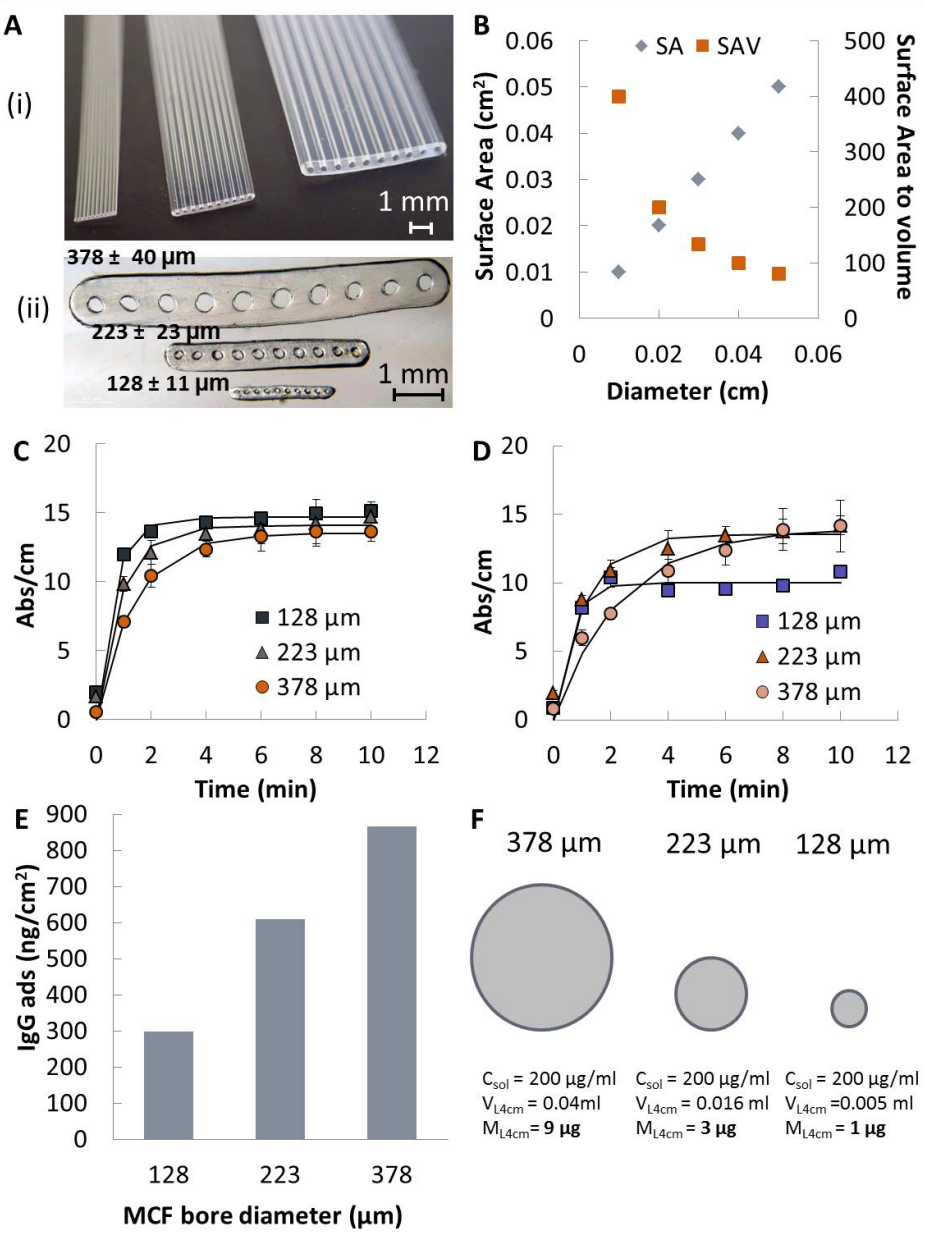

Figure 7:4 – Relationship between human serum matrix effect and capillary diameter in MCF assays.
A (i) Photograph of 3 different MCFs with of 128±11 µm, 223±23 µm, 378± 40 µm mean diameter bore. (ii) Microscope photograph of a cross section from the MCFs with 128, 223, 378 µm diameter bore. **B** The effect of diameter size on total surface area (SA) and on surface-area-to-volume ratio (SAV). **C** IgG-anti-IgG binding kinetics on different diameter MCFs in buffer matrix. **D** IgG-anti-IgG binding kinetics in different diameter MCFs in non diluted human serum matrix. **E** Antibody adsorbed density onto different MCFs bore diameter. **F** Diagram relating capillary size with antibody surface coverage for a MCF test strip of 4 cm length.

Changing the capillary diameter of MCF platform affects the total surface area (SA) available for antibody adsorption, in the sample volume (V), related to the amount of antibody or antigen loaded into the system and, consequently the surface-area-to-

volume ratio (SAV), which is related to the overall reaction throughput and speed. Total SA increases linearly with diameter, whilst SAV decreases linearly with the reciprocal of the diameter (Figure 7:4B). Microfluidic IA systems often only consider SAV as the main geometrical parameter. However, to the best of our knowledge no studies have explored a balance between the SA and V, and therefore an optimum SAV for microfluidic IA performance.

A decrease in capillary diameter from 223 to 128 μm resulted in 2 min faster antibody-antigen equilibrium, while an increase in capillary diameter from 223 to 378 μm postponed the equilibrium 2 min. MCF assays are therefore diffusion limited (Figure 7:4C and Table 7:3). Changing the diameter of the capillary in MCF assays seems to have a similar effect on antibody binding kinetics as changing the viscosity of the matrix in which the antibody/antigen is involved. This can be explained by equations (7:5) and (7:6), where diffusion coefficient is inversely related to viscosity and affects the diffusion time the same way as the mean displacement of the molecule. Consequently, if the interfering factor in biologic human serum matrix was only related to diffusion, performing the assay in smaller capillaries should minimise the interfering factor effect in MCF assays.

Table 7:3 - Kinetic constants of anti-IgG binding in buffer in different capillary diameter MCF.

	100 μm MCF	**200 μm MCF**	**400 μm MCF**
K_{on} ($M.s^{-1}$)	6.39×10^{6}	4.24×10^{6}	2.65×10^{6}
K_{off} (s^{-1})	1.42×10^{-3}	1.71×10^{-3}	1.55×10^{-3}
K_A(M)	4.49×10^{9}	2.48×10^{9}	1.7E x 10^{9}

When a mouse IgG-Anti-IgGAnti-IgG assay was performed in human serum and smaller diameter capillaries (128 μm) the assay was made quicker, compared to the assays in larger capillary diameters, but the equilibrium reached was different (Figure 7:4D and Table 7:4) which did not occur when the assay was performed in buffer (Figure 7:4C). The assay performed in human serum in the MCF platform with capillary diameters 223 and 378 μm reached the same equilibrium, although the assay performed in 378 μm took approximately 4 minutes more to reach the equilibrium, which seems to indicate a cumulative effect of diffusion and the interfering factor from the biological sample matrix. Although in MCF human serum assay interference is not related to

diffusion, this process seems to emphasise the biological matrix interference in MCF assays, which indicates an optimum capillary diameter, where both the role of diffusion and interference are minimised. With smallest capillary diameter tested the effect of the interfering factor is irreversible, presenting lower equilibrium constants, when compared with assays performed in larger capillaries (Table 7:4).

Table 7:4 - Kinetic constants of anti-IgG binding in human serum in different capillary diameter MCF.

	100 µm MCF	**200 µm MCF**	**400 µm MCF**
$K_{on}\,(M.s^{-1})$	5.38×10^{6}	3.35×10^{6}	9.62×10^{7}
$K_{off}\,(s^{-1})$	8.52×10^{-3}	1.91×10^{-3}	4.13×10^{-2}
$K_{A}\,(M)$	6.31×10^{8}	1.75×10^{9}	2.33×10^{9}

One of the causes for the lower equilibrium constant in assays performed in smaller capillaries with human serum matrix, could be related to the adsorption equilibrium of the immobilised antibody onto FEP-Teflon surfaces which will depend on the geometry of the surface. Due to a smaller sample volume loaded, smaller diameter capillaries will present a lower amount of antibody to be adsorbed, compared to larger diameter capillaries (Figure 7:4F). This is shown in Figure 7:4E where the amount of antibody adsorbed determined by solution depletion technique was approximately half on the 128 µm diameter MCF compared to the amount adsorbed on the 223 µm MCF. The 378 µm diameter MCF also presented a significantly higher adsorbed amount when compared to the 223 µm MCF (867.8 ng/cm2 and 609.5 ng/cm2, respectively). This amount is less than the double, which can indicate that there is an antibody adsorption saturation threshold for to FEP-Teflon surfaces, related to the overall SAV of FEP-Teflon surfaces (Figure 7:4E).

7.3.3. Overcoming biological sample matrix in MCF platform – three antibody-antigen systems

The fact, that smaller capillaries present lower immobilised antibody density could be the cause of different equilibrium constants for the same assay performed in different capillary diameter MCF with human serum as biological matrix. This hypothesis is

confirmed with studies of different surface coverage assay effect in equilibrium, using only 223 µm diameter MCF, in buffer and in undiluted human serum (Figure 7:5).

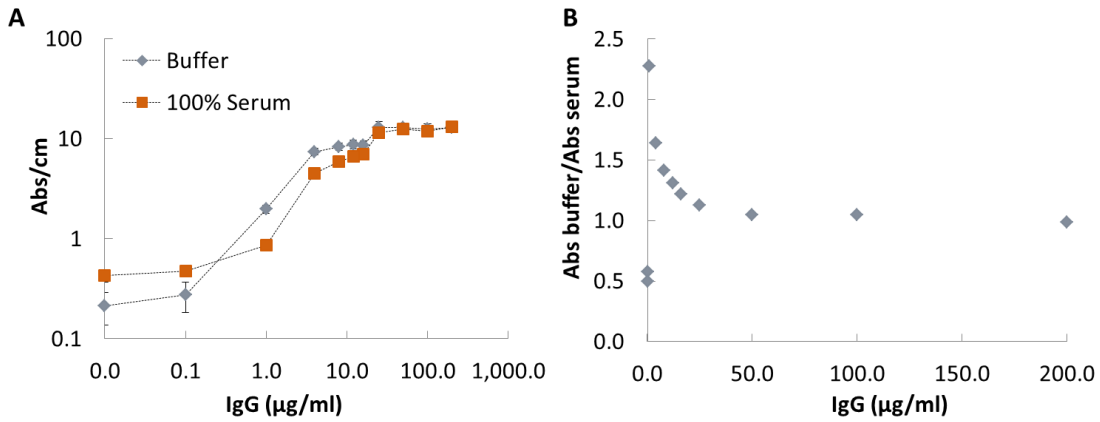

Figure 7:5 - Surface coverage effect on human serum matrix interference on mouse IgG and Anti-IgG binding in 223 µm capillary assays.
A Relation between surface coverage and absorbance signal of anti-IgG in buffer and 100% human serum. **B** Relation between the ratio of Absorbance in buffer and serum and the surface coverage.

The surface coverage effect on matrix interference in IgG-anti-IgG binding studies, made in equilibrium, have shown that the higher the surface coverage the lower the matrix interference of human serum for IgG and anti-IgG system. This relation is very clear in Figure 7:5B where the ratio of absorbance in buffer and serum tends to 1 at higher concentration of mouse IgG (immobilised antibody) used. A concentration of 50 µg/ml of mouse IgG seems to be the minimum concentration of immobilised antibody solution for minimum matrix interfere effect on the assay. Increasing the density of immobilised antibody layer increased the probability of the antigen binding to the immobilised layer. The avidity constant, proportional to the ratio between bond and free antigen (Scatchard model, equation (7:7)) is closer to the affinity constant of individual antibody antigen binding in solution, especially because in mouse IgG and anti-IgG systems immobilised antibody orientation is not an issue, since anti-IgG binds to every part of mouse IgG.

$$\frac{\mathrm{B}}{\mathrm{F}} = k_a.(\mathrm{Ab_t} - \mathrm{B}) \qquad (7:7)$$

Where *B* is bond antigen, *F* is the free antigen in solution, k_a is the association equilibrium constant and Ab_t is the total concentration of antibody-binding sites.

Since there is an excess of total antibody binding sites the effect of the interfering factor from the sample matrix is not evident. If we consider the interfering factor binds to the immobilised antibody with lower affinity than the antigen, higher surface coverages minimise sample matrix interference, even for non equilibrium conditions. Therefore, in addition to long incubation times, immobilised antibody density is a key parameter to minimise sample matrix interference in MCF assays.

Although, mouse IgG-anti-IgG system is commonly used to simulate sandwich assays, they are not sandwich assays since they lack the antigen. For this reason, the study was repeated for PSA sandwich assay in the MCF platform (Figure 7:6). The PSA assay uses a monoclonal CapAb and a polyclonal DetAb and these studies were performed in 223 µm diameter MCF.

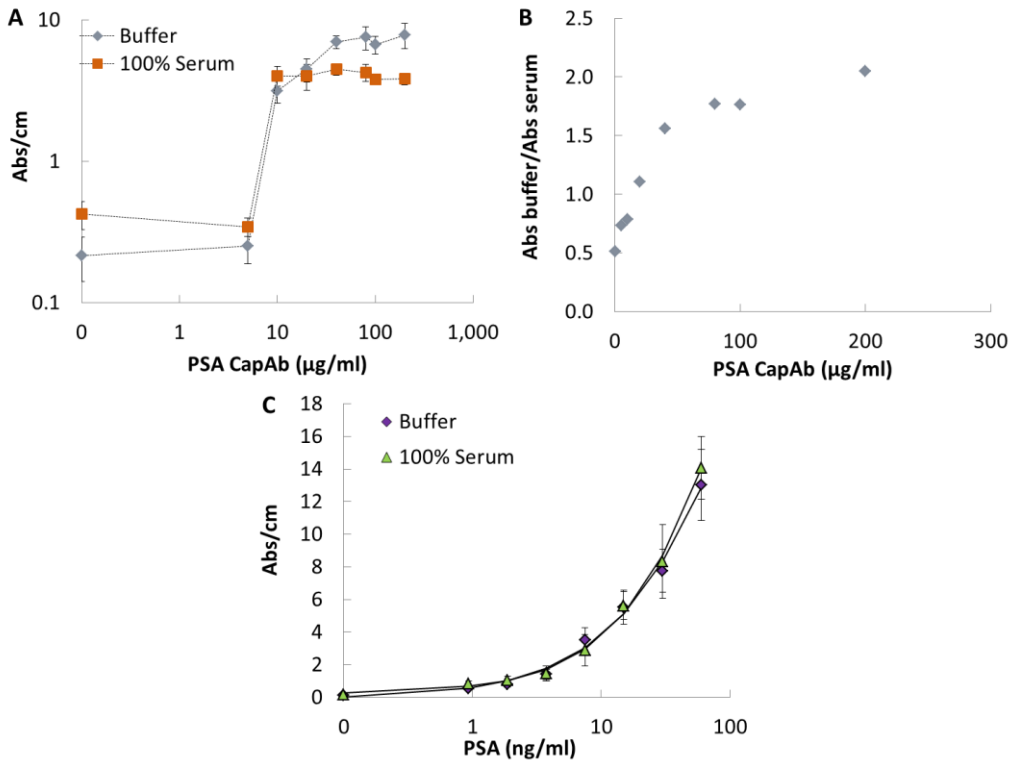

Figure 7:6 - Surface coverage effect on human serum matrix interference of PSA sandwich assay in 223 µm capillary assays.
A Relation between surface coverage and absorbance signal of PSA in buffer and 100% human serum (3.75 ng/ml PSA). **B** Relation between the ratio of absorbance in buffer and serum and the surface coverage (3.75 ng/ml PSA). **C** PSA full response curve in buffer and 100% serum, with 10 µg/ml of CaptAb, 2 µg/ml of DetAb, 4 µg/ml of enzyme and 4 mg/ml of OPD enzymatic substrate.

The relation between sample matrix interference and surface coverage presents an opposite behaviour in the PSA sandwich assay when compared to the IgG-anti-IgG

system. In the PSA sandwich assay higher surface coverages emphasise human serum matrix interference (Figure 7:6A and B), being favourable to the minimum of sample matrix interference the CapAb concentrations between 10 to 20 μg/ml of CapAb. Two full PSA response curves performed with 10 μg/ml of CapAb and 15 minutes sample incubation time in PBS buffer and human serum overlap along the all PSA range of 0.9 to 60 ng/ml presenting similar LLoD (Figure 7:6C and Table 7:5), which validates the previous conclusions. Previous PSA optimization studies demonstrated that the polyclonal DetAb binds directly to the monoclonal CapAb in the absence of antigen and that an increment in CapAb would increase the assay background noise. This might be the cause for different matrix interfering behaviour. As well as the different binding affinity of PSA antibodies. and the importance of immobilised antibody orientation and stability for monoclonal antibodies binding capacity.

Table 7:5 – PSA sandwich assay sensitivity considerations in buffer and in human serum with 15 minutes sample incubation.

	Lower limit of Detection (LLoD) ng/ml	**Precision with 60 ng/ml PSA**	**R2 (with 4PL model)**
Assay in buffer	0.978	16%	0.9966
Assay in 100% human serum	0.532	13%	0.9984

Since the nature of bioanalytical antibodies seem to affect the matrix effect MCF assays, surface coverage studies in buffer and in human serum were performed in IL-1β sandwich assays, where the CapAb and the DetAb are monoclonals. Results are shown in Figure 7:7.

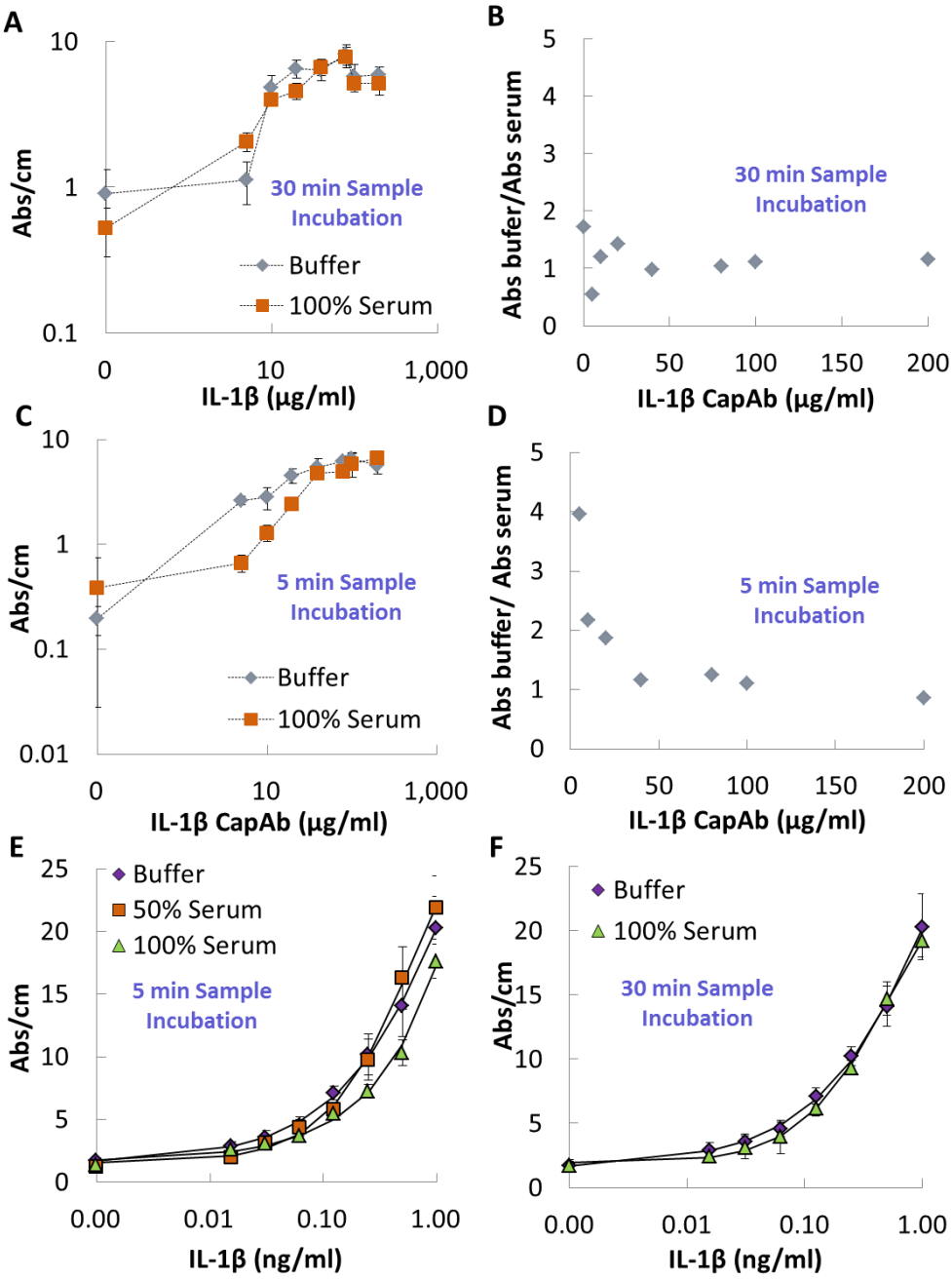

Figure 7:7 - Surface coverage effect on human serum matrix interference of IL-1β sandwich assay in 200 µm capillary assays.

A Relation between surface coverage and absorbance signal of IL-1β in buffer and 100% human serum (0.125 ng/ml IL-1β and 30 minutes sample incubation time). **B** Relation between the ratio of absorbance in buffer and serum and the surface coverage (0.125 ng/ml IL-1β and 30 minutes sample incubation time). **C** Relation between surface coverage and absorbance signal of IL-1β in buffer and 100% human serum (0.125 ng/ml IL-1β and 5 minutes sample incubation time). **D** Relation between the ratio of absorbance in buffer and serum and the surface coverage (0.125 ng/ml IL-1β and 5 minutes sample incubation time). **E** IL-1β full response curve in buffer, 50% serum and 100% serum, with 40 µg/ml of CaptAb and 5 minutes sample incubation. **F** IL-1β full response curve in buffer, 50% serum and 100% serum, with 40 µg/ml of CaptAb and 30 minutes sample incubation.

The matrix effect interference on IL-1β sandwich assays in MCF platform was also minimised by the increment of immobilised CapAb density, as the monoclonal DetAb does not seem to bind to the CapAb, therefore an increment in CapAb concentration does not correspond to a background increment. In equilibrium conditions (30 minutes sample incubation) a concentration range of 40 to 80 μg/ml of CapAb was sufficient to eliminate the human serum matrix interference (Figure 7:7A and B). For non-equilibrium (5 minutes sample incubation) a concentration range of 80 to 200 μg/ml of CapAb can eliminate the matrix interference effect. Two full IL-1β response curves, in buffer and in serum, performed with 40 μg/ml of CapAb and 5 minutes sample incubation time, show an interference effect of undiluted human serum, translated in absorbance signal differences in MCF assays (Figure 7:7E). However, absorbance values were similar when the sample incubation time was 30 min (Figure 7:7F), which is coherent with results shown in Figure 7:7A, B, C and D.

A routine strategy for reducing sample matrix interference with shorter incubation times is diluting the sample. This is the most common approach for dealing with biological matrix interference in diagnostics and it often works, depending on the sample dilution factor.[236,239] Figure 7:7E shows an overlap of full IL-1β response curves in buffer and in 50% human serum. Similar conclusions have been reported for PSA sandwich assays in MCF platform in human serum and whole blood samples with colorimetric and fluorescent detection.[152,153] However, diluting the sample matrix also means diluting the antigen concentration which compromised sensitivity. Since MCF assays are being developed for quantitative POC diagnostic applications, managing the sample matrix interference without any sample treatment is preferred over the dilution procedure. However, Table 7:6shows that the lower limit of detection (LLoD) for IL-1β sandwich assay is 3 times lower in 50% human serum matrix than in 100% human serum, which implies that sensitivity would not be affected by sample dilution in MCF sandwich assays.

Table 7:6 – IL-1β sandwich assay sensitivity considerations in buffer and in human serum, Figure 7:7.

	Lower limit of Detection (LLoD) ng/ml	**Precision with 0.125 ng/ml IL-1β**	**R2 (with 4PL model)**
5 min sample incubation, in buffer	0.021	9%	0.9992
5 min sample incubation, in 100% human serum	0.014	6%	0.9989
30 min sample incubation, in buffer	0.084	20%	0.9929
30 min sample incubation, in 100% human serum	0.051	10%	0.9965
5 min sample incubation, in 50% human serum	0.006	19%	0.9991

The data presented above showed no need for sample preparation in the MCF platform since in certain reactions conditions the antibody-antigen binding can overcome the biological matrix interference.

Although initial studies suggested viscosity as the main interfering factor, the studies presented in this chapter showed equilibrium conditions defined by immobilised antibody surface coverage were actually the main factor in managing matrix effect. Some studies have already suggest this, also mentioning the importance of immobilisation technique, saying that covalently bond antibodies or streptavidin orientated outperform compared to passive adsorbed antibodies.[283] In those studies antibody passive adsorption was also feasible for biological matrix effect interference as long as surface coverage conditions are the appropriate ones. In addition, extended incubation times seem to favour the minimum sample matrix interference for the optimal surface coverage conditions. These observations led to matrix components interference as the main matrix interfering factor. This has been reported by *Sauer et al.* (2012) where Dy-547 anti-fibrogen, anti-lysosyme and anti-IgGa were added to a IL-6 and PCFT sandwich assay and were detected in specific monoclonal CapAb spots, which means that fibrogen, lysozyme and IgG bond non-specifically to monoclonal antibodies.[236]

7.3.4. General methodology for overcoming biological sample matrix in MCF platform

All in all the biological matrix interference can be managed in MCF assays with an appropriate capillary diameter (which is around 200 µm), surface coverage (which depends on bioanalytical antibody system that is being used) and sample incubation time (which also depends on the kinetic equilibrium between bioanalytical antibodies) and sample antigen (Figure 7:8A).

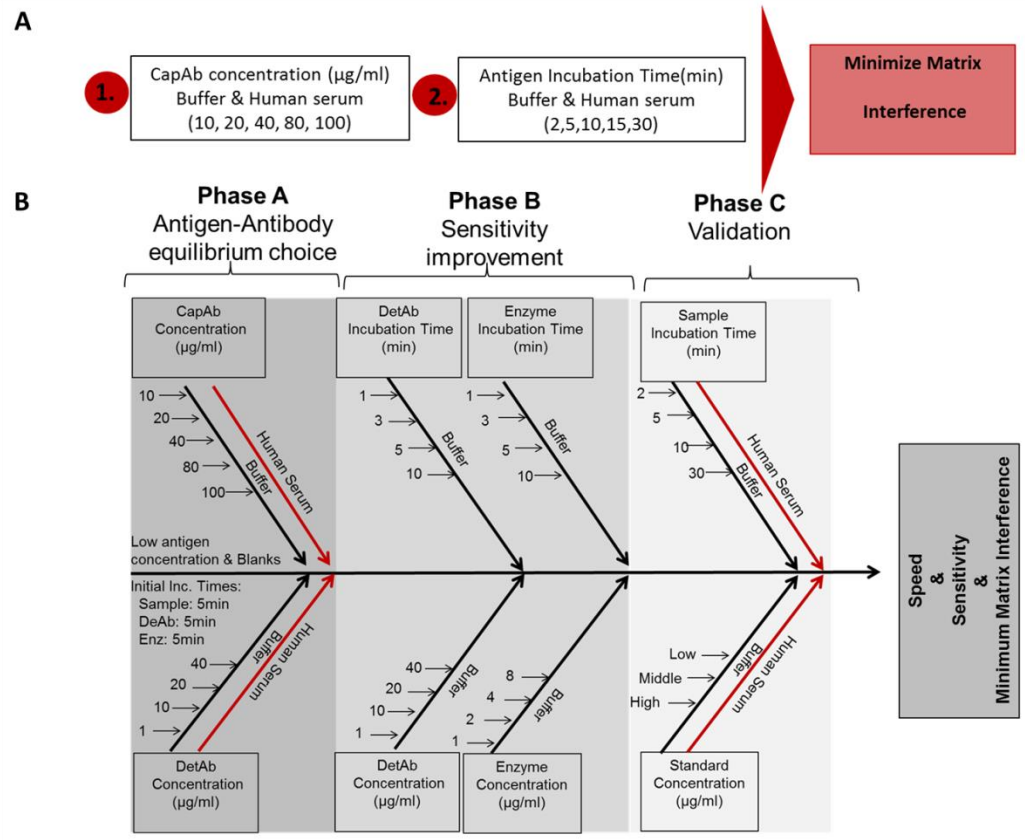

Figure 7:8 – Methodology diagrams for minimizing biological matrix interference in MCF sandwich assays.
A Diagram showing the main variables (CapAb concentration and Antigen incubation time) for minimizing matrix interference in MCF assays. **B** Diagram indicating the methodology for assay development and optimization for fast, sensitive and minimum matrix interference IAs in the MCF platform.

Finding the minimum biological matrix interference in MCF assays is important, however for POC diagnostics procedures, besides the minimum sample matrix interference, the assays also need to be rapid and sensitive. Developing fast, sensitive

and with no sample preparation assays in the MCF platform is possible through an appropriate methodology (Figure 7:8B). Rapid assays are important in POC diagnostics; therefore the incubation time of reagents should be the first limitation, also because limiting time first, allows the choice of fast and sensitive assays simultaneously. 5 minutes of reagent incubation time is therefore suggested to start the optimisation procedure in MCF IA platform. The first phase of MCF assay development is the choice of appropriate antibody-antigen equilibrium. In this phase a lower or middle range antigen concentration should be tested with different combinations of CapAb and DetAb, both in buffer and in serum. After choosing the combination for the best sensitivity and the minimum sample matrix, the next phase of assay development is sensitivity improvement. In this phase, the CapAb choice is set and combinations of DetAb concentration and its incubation time should be performed, in order to choose the conditions with best signal-to-noise ratio, therefore being important to perform blanks for every condition. Since the DetAb and its incubation time are established, the enzyme concentration and its incubation time combinations should be tested in order to find the best signal-to-noise ratio. The last phase for MCF development of quantitative assays for POC diagnostic is the validation phase. In this phase several antigen concentrations should be tested in serum and buffer with different sample incubation times. This allows confirmation of assay conditions for several antigen concentrations and adjustment of the sample incubation time for the minimum assay interference, maximum sensitivity and speed, as long sample incubation times seem to decrease sensitivity in the MCF platform, due to background increment (Table 7:5 and Table 7:6).

7.4. Conclusion

Human samples matrix interference was eliminated in three different IA systems (IgG-anti-IgG, PSA and IL-1β assays) in the novel MCF IA platform. This was achieved through the appropriated choice of CapAb surface coverage and sample incubation time, without any impact on assay sensitivity.

The studies show that higher antibody coverages (above 40 μg/ml of CapAb solution) minimises matrix interference in two of the assays studied, however this conclusion does not apply to the PSA assay, as this antibody system uses a polyclonal DetAb that

binds to the CapAb. Long sample incubation times seem to minimise matrix effect in the three assay system studied.

Sample viscosity changes the antibody-antigen kinetics, as reported in previous studies, however, only above a certain threshold equivalent to whole blood samples. This shows that viscosity is not the only interfering factor in IA, since human serum, which presents lower viscosity than whole blood, also interferes with MCF sandwich assays.

IL-1β assays showed similar values in whole blood and serum samples, which indicates that red blood cells do not interfere with assays performed in FEP-Teflon microcapillaries.

The MCF platform is able to perform sensitive assays without any sample preparation, which brings the platform closer to POC diagnostic applications and also to commercialisation.

8. Particle label detection in FEP-Teflon microfluidic capillaries

8.1. Abstract

In this chapter the use of carbon and gold nanoparticles as immunoassay (IA) labels in a novel microfluidic platform, the Microcapillary Film (MCF), is presented. Biotinylated anti-IL-1β antibody was quantitated in the dynamic range of 10 to 40 μg/ml using carbon nanoparticles conjugated with neutravidin. However, due to low sensitivity of the system using a flatbed scanner imaging no sandwich assay was performed. Prostate specific antigen (PSA) was quantitated using silver enhanced gold nanoparticles in the dynamic range of 10 to 100 μg/ml also using a flatbed scanner for optical detection. Particle detection is important for cost effective one step point of care (POC) diagnostics and extensively used in nitrocellulose lateral flow tests. Due to their low surface area compared to lateral flow membranes, particles are not often used as labels for microfluidic systems, however their use combined with low cost readout systems could bring microfluidic diagnostics closer to the ideal of POC diagnostics.

Keywords: Carbon nanoparticles, gold nanoparticles, silver enhancement, point-of-care, microfluidic, capillary geometry.

8.2. Introduction

Point-of-Care (POC) diagnostics demand simple and rapid test, preferably using a drop of blood, collected from a finger prick, or other type of biological samples (e.g. urine) ideally in one step IAs.[2,234] Nevertheless, some clinical conditions demand sensitive quantitation of certain biomarkers, such as cardiovascular diseases, with a troponin (TnI) clinical threshold of 40 pg/ml,[17]or sepsis, with cytokines TNF-α, IL-6 and IL-10 clinical thresholds below 70 pg/ml, [16] therefore ideally POC diagnostics should not only be simple and rapid tests, but also sensitive tests, capable of detecting a broader number of conditions. Heterogeneous IAs, where the free analyte is separated from the bond forming the antibody-antigen complex, are the most sensitive bioanalytical tool used in

clinical diagnostics. However when translated to POC diagnostics their sensitivity can be compromised by the need to perform rapidly, using small sample volumes of complex biological matrices with low cost signal detectors.[2]

In most heterogeneous sandwich assays the antibody-antigen complex is quantified through label detection. The label conjugated to a DetAb generates a signal proportional to the antigen. The nature of signal depends on the label and will determine the readout system. These two aspects work together setting upthe sensitivity of the assay.

The first labels used in IAs were radioactive isotopes, such as iodine 125,[28] however due to concerns about radioactivity exposure, disposal of radioactive waste and instability of radiolabels reagents other labels were developed.[39] Enzymes,[284] fluorophores,[50] chemiluminophores,[285] microparticles,[286] quantum dots,[287] have been extensively applied to signal generation in IA techniques. Enzymes are the most widely used label due to their flexibility, since different enzymes can generate color, fluorescent or luminescent products from a transparent substrate, and their amplification feature, since a single enzyme can convert up to 10^7 molecules of substrate per minute.[28] However, enzymes are not suitable for one step IAs, which can have a big impact in POC tests simplicity.

Lateral flow (LF) IAs is a well established technology for one step IAs. The pregnancy hormone (hCG), malaria and HIV LF tests are widely commercialized. Nevertheless, this technology lacks the sensitivity necessary to diagnose certain conditions, such as sepsis or cardiovascular diseases, as previously mentioned. Microfluidic tests are trying to fill up this gap creating simple tests with the necessary sensitivity for a broader diagnosis at POC settings, therefore using rapid and simple tests with low cost detection modes.

LF uses a label directly conjugated to the DetAb and so no amplification is performed. The sample is placed in a sample pad, moving through capillary action, mixes with the label antibody in the conjugated pad, and continue to flow through the test zone.[193] The density of label particles in the test zone generates a signal proportional to the analyte concentration. LF technology uses porous membranes, such as nitrocellulose, which present a very high surface area even in a very small test zone (1mm width). Translating one step IAs into microfluidic platforms which do not present such a high surface area, in the detection zone, can be challenging in order to keep the necessary test sensitivity.

Therefore, in order to use particles as labels in microfluidic systems, the readout system used has to be sophisticated or amplification methods have to be applied. In order to achieve higher sensitivities and multiplex capability, microfluidic systems often use fluorophores as labels, which cannot be considered particles, however to detect signal from these fluorescent labels it is necessary to use complex and expensive equipment, such as fluorescent microscopes, flow cytometers and fluorescent scanners. [50,58]

There are few examples of microfluidic IAs systems which used particles as labels and low cost readout systems. *Yet C. et al (2009)* reported a protein A sandwich assay where the capture antibody (CapAb) was immobilised onto glass slides, surrounded by a PDMS structure, the DetAb was conjugated with platinum nanoparticles which suffer silver enhancement. The signal was detected by a flatbed scanner and the detection limit of the assay was 1 ng/ml.[288] *Lu Y. et al* (2009) reported a human IgG/anti-IgG assay, with IgG immobilised onto polystyrene surface inside PDMS channels, with the DetAb label with gold nanoparticles and also silver enhanced. The signal detection was made through a cell phone camera and the detection limit was approximately 1 ng/ml.[289] PSA was of $5x10^{-4}$pM with a Bio-Barcode using Verigene ID Scanning system.[51] Understanding how particle labels can be detected with low cost readout systems can be transformative to microfluidic IAs bringing them closer to an ideal POC diagnostic test.

This chapter aimed exploring two different particle labels, the carbon nanoparticles and gold nanoparticles, in the Microcapillary Film (MCF) platform (Figure 8:1A), in order to move MCF closer to one step IA. The MCF is constituted by melt-extruded FEP-Teflon with 10 parallel microcapillaries with 200 μm diameter average each. This geometry offers a similar surface area of the microwell, considering a 1 cm long MCF strip, but surface-area-to-volume 370 times larger when compared to a 96 microwell plate.

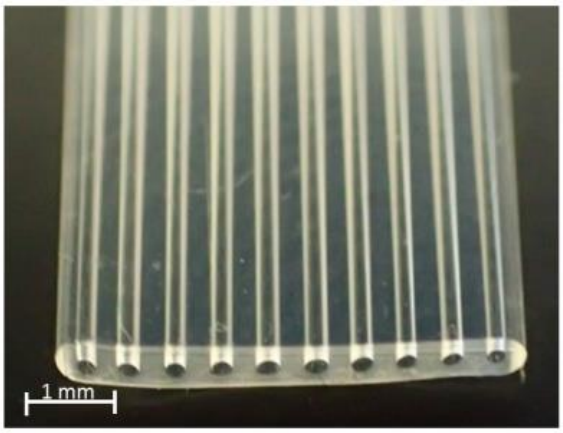

Figure 8:1 – Microcapillary Film (MCF) IA platform.
MCF photograph, showing the transparency of the FEP-Teflon polymer and the 10 parallel capillaries with 200 μm diameter average.

8.3. Materials and Methods

8.3.1. Materials & Reagents

Purified anti-Human IL-1β biotin and anti-Human IL-1β was supplied by e-Biosciences (Hatfield, UK). anti-PSA CapAb and anti-PSA detection antibody (DetAb) conjugated with gold nanoparticles was supplied by Wama Diagnóstica (São Carlos, Brazil). The silver enhancement kit was supplied by Sigma Aldrich (Dorset, UK). The PSA native protein was purchased from Abcam (Cambridge, UK). The Carbon nanoparticles were supplied from Food and Biobased Research, Wageningen University and Research Centre Wageninger. According to the suppliers the particles present irregular shape and an average size of 600 nm.

Phosphate buffered solution (PBS) and Bovine Serum Albumin (BSA) were sourced from Sigma Aldrich (Dorset, UK). PBS pH 7.4, 10mM was used as the main experimental buffer. The blocking solutions consisted in 3% w/v protease-free BSA diluted in PBS buffer. For washings, PBS with 0.05% v/v of Tween-20 (Sigma-Aldrich, Dorset, UK) was used. The FEP-Teflon MicroCapillary Film (MCF) is fabricated from fluorinated ethylene propylene co-polymer by melt-extrusion process by Lamina Dielectrics Ltd. (Billinghurst, West Sussex, UK). FEP-Teflon MCF presents 10 bore parallel capillaries with 223±23 μm diameter.

8.3.2. Neutravidin coated carbon nanoparticles detection

Four solutions of IL-1β biotinylated with 0, 10, 20, 40 and 80 μg/ml and one with 3% of BSA were injected in different capillaries using a 1 ml syringe attached with a needle (i.d. 200 μm) of a 24 cm MCF strip and incubated for 2 hours at room temperature. The biotinylated antibody solution was replaced by 3% BSA solution incubated for 2 hours at room temperature in all the capillaries. The long MCF strip was trimmed in 4 cm lenght strips and several dilutions of neutravidin conjugated carbon nanoparticles solutions (1:1, 1:2, 1:5; 1:7; 1:10 and 1:50) were added to the different 4 cm MCF strips being incubated for 2 hours in an orbital shaker, followed by a washing step with PBS tween. The strips were then imaged with a flated scanner (HP Scanjet G4050) in transmittance mode.

The MCF was cut exposing the surface area coated with the carbon nanoparticles, gold coated for 5 minutes with a Gold Sputter Cater/Carbon evaporator. And placed in a SEM high resolution field emission gun (FEGSEM) for imaging at several magnifications, being the highest 15 000 KW.

8.3.3. Gold nanoparticles detection with silver enhancement.

An MCF strip was filled with 40 μg/ml of anti-PSA CapAb and incubated for 2 hours at room temperature. The solution was replaced by 3% BSA incubated for 2 hours at room temperature. After a washing step the strip was trimmed in 4 cm MCF test strips. Four MCF test strips were filled with 0, 10, 50 and 100 ng/ml of PSA native protein solutions and incubated for 10 min. A solution of 1:50 dilution of anti-PSA DetAb conjugated with gold nanoparticles was incubated for 1 hour in the orbital shaker followed by a washing step. The silver enhancement solution was applied for 10 min at room temperature and the fixing solution for 3 min followed by a distilled water washing step. The strips imaged with the flatbed scanner in transmittance mode.

8.3.4. MCF image analysis

RGB digital images were split into 3 separated channels images by *Image J* software . The green channel images were used to calculate absorbance values, based on the grey scale peak height of each individual capillary of FEP-Teflon MCF as described in previous studies.[127,152] Therefore, absorbance signal was calculated for each capillary, according to equation (8:1).

$$\mathbf{Abs} = -\mathbf{Log}\left(\frac{\mathbf{I}}{\mathbf{I_0}}\right) \quad (8:1)$$

Where I is the transmitted light and corresponds to I_0 minus peak height and I_0 is the maximum grey scale value. The absorbance values presented averages of absorbance from 10 capillaries one MCF stip.

8.4. Results and Discussion

8.4.1. Carbon nanoparticles

The use of particles as labels instead of enzymes can bring microfluidic systems closer to simple one step POC diagnostics, eliminating the time and complexity of multiple steps IAs. However, few studies have been performed in order to detect particles in microfluidic systems with low cost detection modes, essential for POC diagnostic settings.

The use of carbon nanoparticles in LF assays was used in albumin detection from 0.25 μg/ml and kunitz-type for trypsin inhibitor was detected from 2.5 ng/ml in competitive assay format.[290] A study that aimed to enhance the detection limit of lateral flow test through the evaluation and comparison of bioconjugates reported a 10 fold improvement in sensitivity for biotin-streptavidin systems and for dengue detection when compared with silver coated gold nanoparticles.[291] Carbon nanoparticles coated with neutravidin were the first carbon particle system to be detected in the MCF platform. The particles were bond directly to immobilised biotinylated antibodies and a dynamic range between 10 and 40 μg/ml of biotin-antibody was observed with flatbed scanner digital images in transmittance mode, followed by grey scale analysis (Figure

8:2A and Figure 8:2B). In the grey scale image (Figure 8:2B) is possible to observe the difference on the refractive index of MCF capillary walls due to particles attachment.

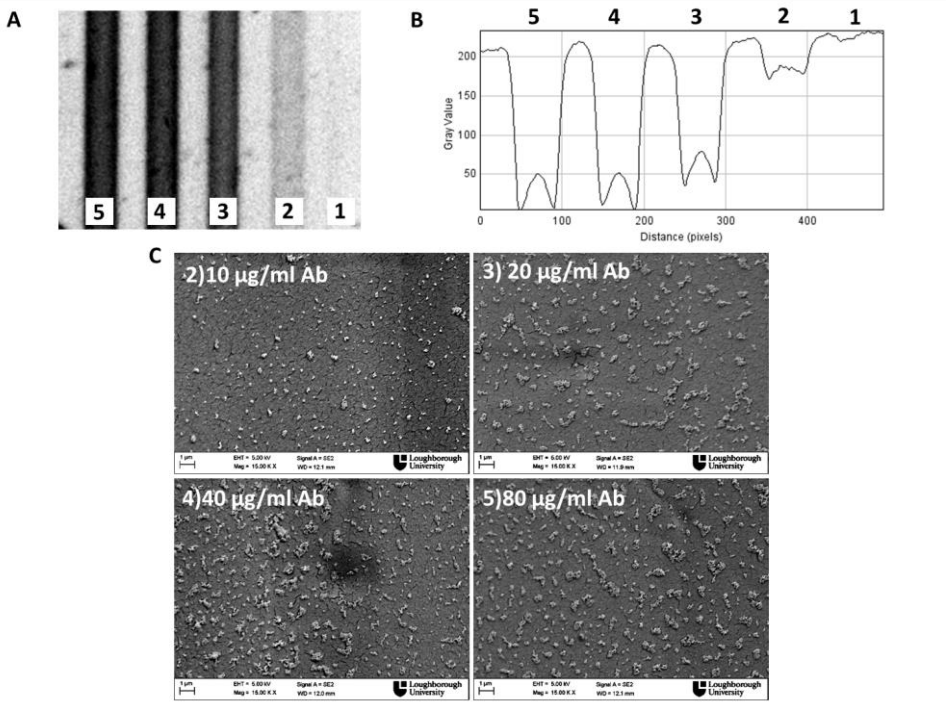

Figure 8:2 – Biotinylated antibody MCF adsorbed detection with carbon nanoparticles neutravidin coated (1:10 dilution).
A MCF flatbed scanner green channel digital image in transmittance mode, showing microcapillaries coated with 80, 40, 20, 10 and 0 µg/ml of biotinylated antibody, 1 to 5 respectively. **B** Correspondenting grey scale showing the concentrations of 80, 40, 20, 10 and 0 µg/ml of biotinylated antibody, 1 to 5 respectively. **C** Scanning Electon Microscope (SEM) pictures with 10, 20, 40 and 80 µg/ml of biotinylated antibody.

The SEM images are coherent with the flatbed scanner images showing an increment in the density of carbon nanoparticles from 10 µg/ml and saturation after from 40 to 80 µg/ml. This showed that it is possible to detect carbon nanoparticles using a flatbed scanner as a readout system. However, optimization should be performed in order to achieve better sensitivity and apply this label to sandwich IAs. Optimization started with screening the concentration of carbon nanoparticle. The results are shown in Figure 8:3.

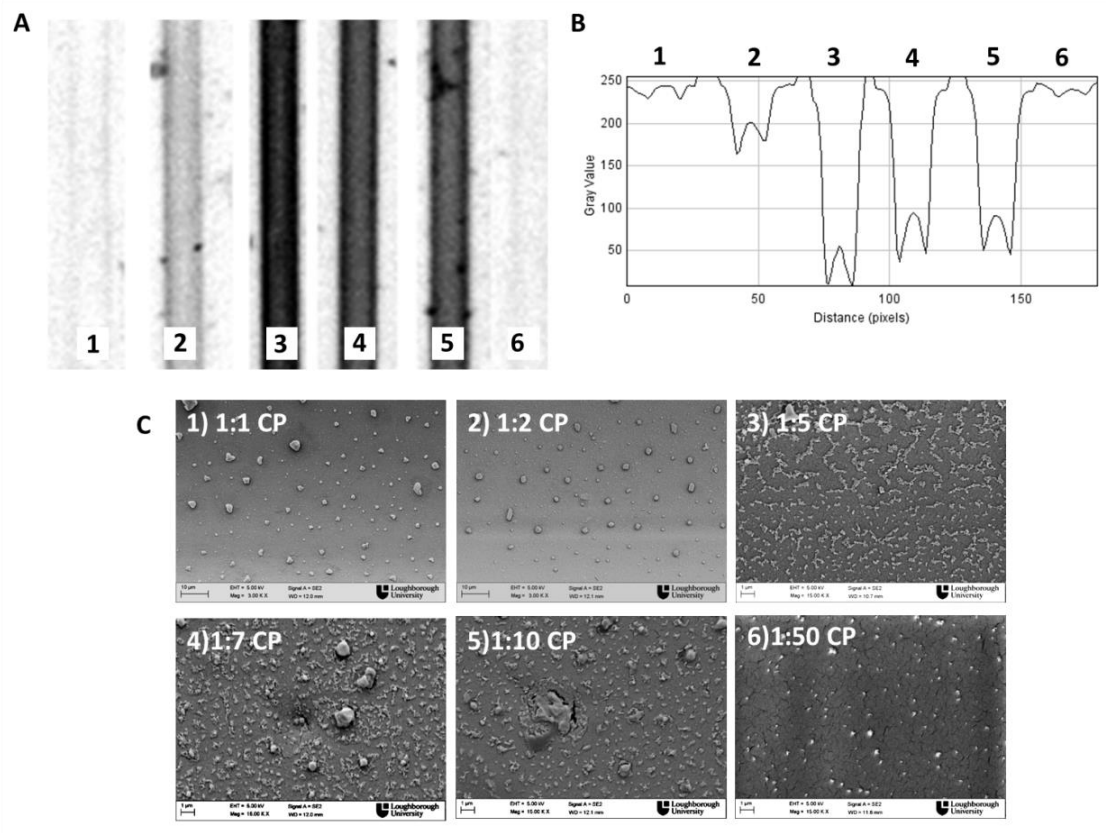

Figure 8:3– Carbon nanoparticles neutravidin coated detection of 40 µg/ml of biotin-antibody in the MCF.
A Flatbed scanner digital image of microcapillaries with 40 µg/ml of biotin-antibody and several dilutions of carbon nanoparticles 1, 2, 3, 4, 5, 6 which corresponds to 1:1, 1:2, 1:5, 1:7, 1:10,1:50 respectively. **B** Correspondent grey scale image with previously mentioned dilutions of carbon nanoparticles and 40 µg/ml of biotin-antibody. **C** Correspondent Scanning Electron Microscope (SEM) pictures with several dilutions of carbon nanoparticles.

Figure 8:3 shows that higher concentrations of carbon nanoparticles are not beneficial for molecular detection in the MCF since flatbed scanner images with 40 µg/ml of biotinylated antibody did not show any signal with non diluted or even 1:2 diluted carbon nanoparticles. In the SEM images of these capillaries (Figure 8:3C) is possible to see crystals with an average perimeter size of 3 µm, considering the carbon particles are irregular in shape and present an average size of 600 nm (according to the manufacturer), therefore in certain conditions the carbon nanoparticles agglomerate, becoming larger and easier to remove during the washing steps. Carbon nanoparticles dilutions above 1:50 are not recommended as well, since there is not enough surface density of particles to be detected with the flatbed scanner, although they are visible in the SEM images (Figure 8:3C).

Optimizing the carbon particles concentration would not be enough to perform sensitive IA in the MCF, since the higher surface density achieved is far from full surface coverage and the total surface area available is not large enough to promote a good naked eye signal. Thus, no attempt of performing a full sandwich assay in MCF with carbon nanoparticles was made. Probably changing the direction of the light towards the capillaries using an LED system and a portable camera could improve the signal intensity.

8.4.2. Gold nanoparticules label with silver enhancement

The other particle system used in the MCF platform was the silver enhanced gold nanoparticles. With this system the prostate specific antigen (PSA) sandwich assay was performed and results shown in Figure 8:4. PSA is a prostate cancer biomarker with a clinical threshold of 4 ng/ml.

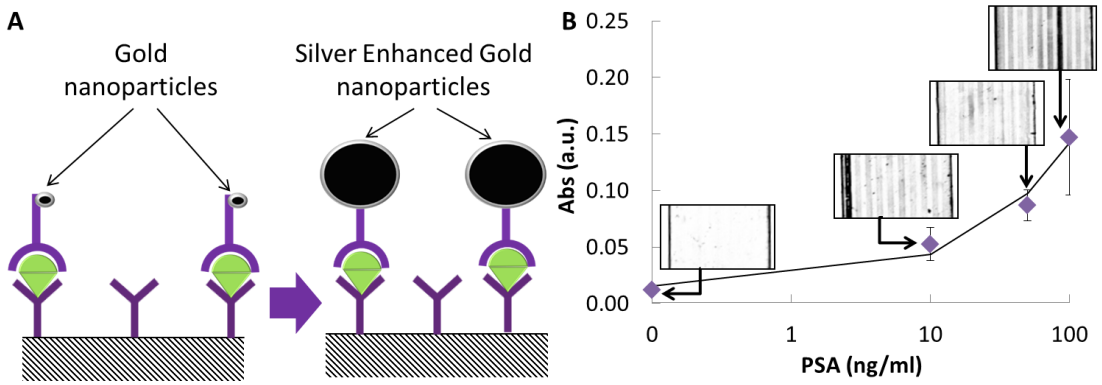

Figure 8:4 – Gold nanoparticles MCF IAs with silver enhancement.
A Sandwich assay diagram with gold nanoparticles silver enhancement step. **B** PSA response curve with gold nanoparticles silver enhanced.

The results show a significant difference between 0 ng/ml of PSA and the lowest concentration of PSA tested 10 ng/ml. This indicates possible improvement in the sensitivity of the assay with optimization. A 4PL (4 parameter logistic) model fitted the data with a cross correlation of 0.999. However, the variability between capillaries of the same MCF test strip is 34% in the highest PSA concentration, which shows that the concentration of gold nanoparticles might not be optimized yielding poor uniformity for higher PSA concentrations.

To the best of our knowledge is the first time a cancer biomarker is quantified using gold nanoparticles silver enhanced in a microfluidic platform. Although, the silver enhancement involves a multistep assay, particle labels are flexible, cost effective and will, therefore, contribute to increase the flexibility of microfluidic POC systems.

8.5. Conclusion

Although the smaller surface area of capillaries when compared to LF test membranes, the PSA was quantified in the MCF with gold nanoparticles silver enhanced, presenting a dynamic range of 10 to 100 ng/ml of PSA. Carbon nanoparticles enable the quantitation of biotinylated antibody in the range of 10 to 40 μg/ml. The assays used a low cost flatbed scanner for signal detection.

Particle detection is possible in the MCF, which opens possibility for development of rapid one step microfluidic IA with low cost detection modes, however from this study concludes that one step particle detection in MCF requires major improvements to yield similar sensitivity to multistep IA.

9. Conclusions and Future Perspectives

Sensitive quantitation of protein biomarkers can provide early detection of many non-communicable diseases, such as cancer and cardiovascular conditions. These are the main causes of deaths worldwide. Therefore, their early detection can increase the life expectancy and quality of general population.

Microfluidic diagnostics aim sensitive protein quantitation due to the high throughput owed to IA miniaturization and precise fluid control. However, these technological advancements are still not enough for POC applications due to high cost of microfluidic devices manufacturing process.

This PhD project aimed developing and optimising novel microfluidic IA platform, the Microcapillary Film (MCF) for POC settings, whose manufacture process is cost-effective and can easily be mass produced. This platform could fill the gap of sensitive protein quantitation at POC currently existing in diagnostic market.

The MCF is produced by melt-extrusion of a fluoropolymer, FEP-Teflon. It consists in a transparent flat film with 10 parallel embedded capillaries with an average internal diameter of 200 μm.

Sensitive quantitation of protein biomarkers is usually performed with sandwich IA. This assay format implies a certain amount of antibody immobilised to a solid surface. The immobilised antibody amount and activity is extremely important for IA performance. Therefore, the first specific objective of this thesis was to study antibody adsorption onto FEP-Teflon capillaries. From this study it was concluded that is possible to irreversibly adsorb antibodies to FEP-Teflon. It was also found that antibodies form a monolayer with maximum coverage of approximately 400 ng/cm^2, which can be related to a theoretical monolayer with antibodies in vertical orientation. However, surface coverages between 200 and 300 ng/cm^2 provide the highest signal in sandwich assays, probably due to antibody steric hindrance in higher density surfaces. The monolayer was formed after 10 minutes due to small capillary diameter. FEP-Teflon presents the best antibody adsorption properties when compared to LLPED which adsorbs 50% less and glass which adsorbs 90% more suggesting multilayer formation, not desirable for IA.

Signal amplification is other important variable for IA sensitivity, especially if the detection method is made off a cost effective, portable and power-free readout system, fundamental features for POC diagnostics. Enzymes are powerful signal amplifiers, however to work at their full potential they need the optimal substrate concentrations and absence of inhibitors. By studying the OPD conversion by HRP enzyme it was found that increasing the OPD concentration from 1.0 to 4.0 mg/ml and OPD/H_2O_2 molar ratio from 1:3 to 1:1 the value rate of enzymatic conversion was increased by 4-fold, which is very beneficial for microfluidic devices that contain short diffusion distances. PSA and IL-1β assay increased sensitivity and/or speed by one or two orders of magnitude when applying the new conditions for OPD conversion by HRP.

Understanding the effect of flow in assay speed and sensitivity is important for device automation, which is extremely important for POC diagnostics. The effect of flow on antibody-antigen bonding showed that a flow rate below 10 µl/min is required for high sensitivity assays. For high analyte systems a flow rate of 10 µl/min can be used, yet extended incubation times are required to avoid any impact on assay sensitivity.

POC diagnostics require minimal sample preparation; however is well know the effect of biological matrices in IA. Therefore, a systematic study of viscosity effect, immobilised antibody coverage and sample incubation time was performed in the MCF platform. It was found that although viscosity delays the antibody-antigen equilibrium above a certain threshold, human serum presents a viscosity value inferior to that threshold, and still affects the assay. Consequently, viscosity is not the fundamental parameter affecting assay performance in biological samples. Other important founding was the evidence that human serum and human whole blood cause the same degree of interference in MCF IA. The main conclusion from matrix effects studies on MCF relies on the fact that manipulating the immobilised antibody surface coverage and sample incubation time the biological matrix interference can be minimised or even eliminated. However, the conditions vary according to the antibody system that is being used. For example, while IL-1β assay requires high antibody surface coverage (above 200 ng/cm^2), the PSA assay requires lower surface coverage (between 50 and 100 ng/cm^2) due to its polyclonal detection antibody that binds to the immobilised antibody in higher extent whenever the last is in higher concentrations. Long sample incubation times minimise sample matrix effects in any of the systems. The MCF platform offers a wide range of conditions that allow minimising or eliminating the biological matrix effect.

These conclusions allowed the fully optimisation of a PSA sandwich assay in whole blood using the Lab-in-a-briefcase. PSA ELISA detection using the lab-in-a-briefcase components was performed in 15 minutes in biological samples with a LLoD of <0.9 ng/ml PSA and 3 to 10% intra-assay variability. This means PSA MCF ELISA was 20x faster than the standard MTP ELISA (laboratory standard method), whilst maintaining similar assay performance in respect to precision and LLoD. The Lab-in-a-briefcase presented a simple and efficient MSA used to simultaneously fill 8 pre-coated MCF test strips or 80 capillaries using an array of 1 ml disposable plastic syringes and a flatbed scanner as readout system. The components of this portable lab allowed the use of conventional ELISA and commercialized assay chemistry on the field, outside the laboratory setting.

Readout systems are a paramount in the conversion of microfluidic devices in POC diagnostic, since it has to be sensitive enough to quantify low analytes concentrations, as well as power-free, low-cost and portable. In order to increase the portability and energy autonomy of the Lab-in-a-briefcase, the flatbed scanner was replaced by a smartphone on an assembled set up named MCFphone. The MCFphone was able to detect and quantify PSA within the dynamic range of 0.9 to 60 ng/ml PSA in 13 minutes using colorimetric detection, and within 0.08 ng/ml to 60 ng/ml of PSA, using fluorescence detection from whole blood samples. Considering the PSA clinical range of 4 ng/ml, for prostate biopsy, the MCFphone can provide reliable measurements for prostate cancer screening and detection in remote areas outside laboratory facilities.

An attempt to speed up the assay by using particle labels instead of enzymes was made, however it was clear that the particle density achieved was not high enough for macroscopic detection desired at POC settings. Therefore, the PSA assay presented a higher LLoD with a dynamic range between 10 to 100 ng/ml of PSA, using gold nanoparticles silver enhanced and flatbed scanner. Carbon nanoparticles enabled the quantitation of biotinylated antibody in the range of 10 to 40 μg/ml with a flatbed scanner, and SEM microphotographs confirmed the increasing of particles density in the capillary surface within this range.

Although, the initial aims were achieved during this PhD project many other suggestions can be presented and discussed, especially concerning the commercialisation of MCF diagnostic tests.

In order to commercialise MCF tests is necessary to perform an up-scale process of the MCF coating method, which implies coating up to 30 meters of MCF film at once. For this purpose, a connector between the MCF and a pump must be built. This connector must be able to completely seal, allowing the uniform filling of the microcapillaries. The coating chemistry should also be general to a series of assay tests, which is possible by replacing passive antibody adsorption by streptavidin coatings, which then can be used with any type of biotinylated CapAb.

For the MCF to become a commercial product, stability studies of immobilised antibodies for minimum 6 months must be performed, which implies conservatives addition and drying procedures with minimal loss of antibody activity.

Fluid automation is another major step towards commercialisation of MCF test strips. Two different approaches can be developed towards automation: passive flow or autonomous pressure driven. To apply the passive flow approach, the inner surface of the capillaries needs to be changed so that capillaries become hydrophilic. The autonomous pressure driven can be achieved using micro pumps systems.

MCF assays still present a number of steps that make it difficult to automate. Reducing the number of steps without compromising sensitivity would be important for successful commercialisation. This could be achieved through elimination of the enzymes as signal amplifiers and introduction of higher amount of active immobilised antibody.

10. Cumulative reference listing

(1) Mao, X.; Huang, T. J. Microfluidic Diagnostics for the Developing World. *Lab Chip* **2012**, *12* (8), 1412–1416.

(2) Gubala, V.; Harris, L. F.; Ricco, A. J.; Tan, M. X.; Williams, D. E. Point of Care Diagnostics: Status and Future. *Anal. Chem.* **2012**, *84* (2), 487–515.

(3) Price, C. P. Point of Care Testing. *BMJ* **2001**, *322* (7297), 1285–1288.

(4) World Health Organization. The top 10 causes of death - Fact sheet http://www.who.int/mediacentre/factsheets/fs310/en/index2.html (accessed May 6, 2015).

(5) World Health Organization. Non-communicable diseases - Fact Sheets http://www.who.int/mediacentre/factsheets/fs355/en/ (accessed May 6, 2015).

(6) Peeling, R. W.; Mabey, D. Point-of-Care Tests for Diagnosing Infections in the Developing World. *Clin. Microbiol. Infect.* **2010**, *16* (8), 1062–1069.

(7) Chin, C. D.; Linder, V.; Sia, S. K. Commercialization of Microfluidic Point-of-Care Diagnostic Devices. *Lab Chip* **2012**, 2118–2134.

(8) Gervais, L.; de Rooij, N.; Delamarche, E. Microfluidic Chips for Point-of-Care Immunodiagnostics. *Adv. Mater.* **2011**, *23* (24), H151–H176.

(9) McDonnell, B.; Hearty, S.; Leonard, P.; O'Kennedy, R. Cardiac Biomarkers and the Case for Point-of-Care Testing. *Clin. Biochem.* **2009**, *42* (7-8), 549–561.

(10) Jaffe, A. S.; Babuin, L.; Apple, F. S. Biomarkers in Acute Cardiac Disease: The Present and the Future. *J. Am. Coll. Cardiol.* **2006**, *48* (1), 1–11.

(11) Quinn, D. A.; Fogel, R. B.; Smith, C. D.; Laposata, M.; Taylor Thompson, B.; Johnson, S. M.; Waltman, A. C.; Hales, C. A. D-Dimers in the Diagnosis of Pulmonary Embolism. *Am. J. Respir. Crit. Care Med.* **1999**, *159* (5 Pt 1), 1445–1449.

(12) Crawford, E. D.; DeAntoni, E. P.; Etzioni, R.; Schaefer, V. C.; Olson, R. M.; Ross, C. A. Serum Prostate-Specific Antigen and Digital Rectal Examination for Early Detection of Prostate Cancer in a National Community-Based Program. The Prostate Cancer Education Council. *Urology* **1996**, *47* (6), 863–869.

(13) Einhorn, N.; Sjövall, K.; Knapp, R. C.; Hall, P.; Scully, R. E.; Bast, R. C.; Zurawski, V. R. Prospective Evaluation of Serum CA 125 Levels for Early Detection of Ovarian Cancer. *Obstet. Gynecol.* **1992**, *80* (1), 14–18.

(14) Brenner, D. E.; Normolle, D. P. Biomarkers for Cancer Risk, Early Detection, and Prognosis: The Validation Conundrum. *Cancer Epidemiol. Biomarkers Prev.* **2007**, *16* (10), 1918–1920.

(15) Weigel, M. T.; Dowsett, M. Current and Emerging Biomarkers in Breast Cancer: Prognosis and Prediction. *Endocr. Relat. Cancer* **2010**, *17* (4), R245–R262.

(16) Bozza, F. A.; Salluh, J. I.; Japiassu, A. M.; Soares, M.; Assis, E. F.; Gomes, R. N.; Bozza, M. T.; Castro-Faria-Neto, H. C.; Bozza, P. T. Cytokine Profiles as Markers of Disease Severity in Sepsis: A Multiplex Analysis. *Crit. Care* **2007**, *11* (2), R49.

(17) Mahajan, V. S.; Jarolim, P. How to Interpret Elevated Cardiac Troponin Levels. *Circulation* **2011**, *124* (21), 2350–2354.

(18) Carlsson, S.; Assel, M.; Sjoberg, D.; Ulmert, D.; Hugosson, J.; Lilja, H.; Vickers, A. Influence of Blood Prostate Specific Antigen Levels at Age 60 on Benefits and Harms of Prostate Cancer Screening: Population Based Cohort Study. *BMJ* **2014**, *348*, g2296.

(19) Yalow, R. *The Immunoassay Handbook*; Elsevier, 2013.

(20) Ekins, R.; Edwards, P. On the Meaning of "Sensitivity". *Clin. Chem.* **1997**, *43* (10), 1824–1831.

(21) Deshpande, S. S. *Enzyme Immunoassays: From Concept to Product Development*; Springer Science & Business Media, 1996.

(22) Kumagai, I. Antigen – Antibody Binding. *Life Sci.* **2001**.

(23) Davies, D. R.; Padlan, E. a; Sheriff, S. Antibody-Antigen Complexes. *Annu. Rev. Biochem.* **1990**, *59*, 439–473.

(24) Eric Arnoys. Chemistry and Biochemistry http://www.calvin.edu/academic/chemistry/faculty/arnoys/arnoys-chem324-IgG.html (accessed Apr 14, 2015).

(25) Liddell, E. Antibodies. In *The Immunoassay Handbook*; Wild, D., Ed.; Elsevier Ltd.: Oxford, 2005; pp 144–163.

(26) Hennion, M. C.; Barcelo, D. Strengths and Limitations of Immunoassays for Effective and Efficient Use for Pesticide Analysis in Water Samples: A Review. In *Analytica Chimica Acta*; 1998; Vol. 362, pp 3–34.

(27) Krska, R.; Becalski, A.; Braekevelt, E.; Koerner, T.; Cao, X.-L.; Dabeka, R.; Godefroy, S.; Lau, B.; Moisey, J.; Rawn, D. F. K.; et al. Challenges and Trends in the Determination of Selected Chemical Contaminants and Allergens in Food. *Anal. Bioanal. Chem.* **2012**, *402* (1), 139–162.

(28) Suresh, M. R. Cancer Markers. In *The Immunoassay Handbook*; Wild, D., Ed.; Elsevier Ltd.: Oxford, 2005; pp 664–694.

(29) Christopoulos, E. P. D. ; T. K. *Immunoassay*; San Diego ; London : Academic Press, 1996.

(30) Findlay, J. W.; Smith, W. C.; Lee, J. W.; Nordblom, G. D.; Das, I.; DeSilva, B. S.; Khan, M. N.; Bowsher, R. R. Validation of Immunoassays for Bioanalysis: A Pharmaceutical Industry Perspective. *J. Pharm. Biomed. Anal.* **2000**, *21* (6), 1249–1273.

(31) Ederveen, J. *Practical Approach to Biological Assay Validation*; Hoofddorp, 2010.

(32) Cox, K. L.; Devanarayan, V.; Kriauciunas, A.; Manetta, J.; Montrose, C.; Sittampalam, S. Immunoassay Methods. Eli Lilly & Company and the National Center for Advancing Translational Sciences December 24, 2014.

(33) Davies, C. Introduction to Immunoassay Principles. In *The Immunoassay Handbook*; Wild, D., Ed.; Elsevier Ltd.: Oxford, 2005; pp 34–38.

(34) Stenberg, M.; Nygren, H. Kinetics of Antigen-Antibody Reactions at Solid-Liquid Interfaces. *J. Immunol. Methods* **1988**, *113* (1), 3–15.

(35) Lacharme, F.; Vandevyver, C.; Gijs, M. a. M. Magnetic Beads Retention Device for Sandwich Immunoassay: Comparison of off-Chip and on-Chip Antibody Incubation. *Microfluid. Nanofluidics* **2009**, *7* (4), 479–487.

(36) Law, B. *Immunoassay : A Practical Guide*; London : Taylor & Francis, 1996.

(37) Schall, R. F.; Tenoso, H. J. Alternatives to Radioimmunoassay: Labels and Methods. *Clin. Chem.* **1981**, *27* (7), 1157–1164.

(38) Durkin, M. M.; Connolly, P. A.; Wheat, L. J. Comparison of Radioimmunoassay and Enzyme-Linked Immunoassay Methods for Detection of Histoplasma Capsulatum Var. Capsulatum Antigen. *J. Clin. Microbiol.* **1997**, *35* (9), 2252–2255.

(39) Weeks, I.; Kricka, L. J. The Immunoassay Handbook. In *The Immunoassay Handbook*; Elsevier, 2013; pp 267–285.

(40) Benner, S. A. Enzyme Kinetics and Molecular Evolution. *Chem. Rev.* **1989**, *89* (4), 789–806.

(41) Berg, J. M.; Tymoczko, J. L.; Stryer, L. Enzymes Can Be Inhibited by Specific Molecules. W H Freeman 2002.

(42) Strelow, J.; Dewe, W.; Iversen, P. W.; Brooks, H. B.; Radding, J. A.; McGee, J.; Weidner, J. Mechanism of Action Assays for Enzymes. Eli Lilly & Company and the National Center for Advancing Translational Sciences October 1, 2012.

(43) Longuet, C.; Yamada, A.; Chen, Y.; Baigl, D.; Fattaccioli, J. Spatially-Controlled Protein Crystallization in Microfluidic Chambers. *J. Cryst. Growth* **2014**, *386*, 179–182.

(44) An, D.; Kim, K.; Kim, J. Microfluidic System Based High Throughput Drug Screening System for Curcumin/TRAIL Combinational Chemotherapy in Human Prostate Cancer PC3 Cells. *Biomol. Ther. (Seoul).* **2014**, *22* (4), 355–362.

(45) Araz, M. K.; Tentori, A. M.; Herr, A. E. Microfluidic Multiplexing in Bioanalyses. *J. Lab. Autom.* **2013**, *18* (5), 350–366.

(46) Werner, M.; Palankar, R.; Arm, L.; Hovius, R.; Vogel, H. Microfluidic Single-Cell Analysis with Affinity Beads. *Small* **2015**, *11* (22), 2607–2613.

(47) Elvira, K. S.; Casadevall i Solvas, X.; Wootton, R. C. R.; deMello, A. J. The Past, Present and Potential for Microfluidic Reactor Technology in Chemical Synthesis. *Nat. Chem.* **2013**, *5* (11), 905–915.

(48) Whitesides, G. M. The Origins and the Future of Microfluidics. *Nature* **2006**, *442* (7101), 368–373.

(49) Kemp, M.; Donovan, J.; Higham, H.; Hooper, J. Biochemical Markers of Myocardial Injury. *Br. J. Anaesth.* **2004**, *93* (1), 63–73.

(50) Cesaro-Tadic, S.; Dernick, G.; Juncker, D.; Buurman, G.; Kropshofer, H.; Michel, B.; Fattinger, C.; Delamarche, E. High-Sensitivity Miniaturized Immunoassays for Tumor Necrosis Factor Alpha Using Microfluidic Systems. *Lab Chip* **2004**, *4* (6), 563–569.

(51) Goluch, E. D.; Nam, J.-M.; Georganopoulou, D. G.; Chiesl, T. N.; Shaikh, K. A.; Ryu, K. S.; Barron, A. E.; Mirkin, C. A.; Liu, C. A Bio-Barcode Assay for on-Chip Attomolar-Sensitivity Protein Detection. *Lab Chip* **2006**, *6* (10), 1293–1299.

(52) Torabi, F.; Mobini Far, H. R.; Danielsson, B.; Khayyami, M. Development of a Plasma Panel Test for Detection of Human Myocardial Proteins by Capillary Immunoassay. *Biosens. Bioelectron.* **2007**, *22* (7), 1218–1223.

(53) Herrmann, M.; Veres, T.; Tabrizian, M. Quantification of Low-Picomolar Concentrations of TNF-Alpha in Serum Using the Dual-Network Microfluidic ELISA Platform. *Anal. Chem.* **2008**, *80* (13), 5160–5167.

(54) Sista, R. S.; Eckhardt, A. E.; Srinivasan, V.; Pollack, M. G.; Palanki, S.; Pamula, V. K. Heterogeneous Immunoassays Using Magnetic Beads on a Digital Microfluidic Platform. *Lab Chip* **2008**, *8* (12), 2188–2196.

(55) Bruls, D. M.; Evers, T. H.; Kahlman, J. A. H.; van Lankvelt, P. J. W.; Ovsyanko, M.; Pelssers, E. G. M.; Schleipen, J. J. H. B.; de Theije, F. K.; Verschuren, C. A.; van der Wijk, T.; et al. Rapid Integrated Biosensor for Multiplexed

Immunoassays Based on Actuated Magnetic Nanoparticles. *Lab Chip* **2009**, *9* (24), 3504–3510.

(56) Gervais, L.; Delamarche, E. Toward One-Step Point-of-Care Immunodiagnostics Using Capillary-Driven Microfluidics and PDMS Substrates. *Lab Chip* **2009**, *9* (23), 3330–3337.

(57) Wang, X.; Zhao, M.; Nolte, D. D.; Ratliff, T. L. Prostate Specific Antigen Detection in Patient Sera by Fluorescence-Free BioCD Protein Array. *Biosens. Bioelectron.* **2011**, *26* (5), 1871–1875.

(58) Ikami, M.; Kawakami, A.; Kakuta, M.; Okamoto, Y.; Kaji, N.; Tokeshi, M.; Baba, Y. Immuno-Pillar Chip: A New Platform for Rapid and Easy-to-Use Immunoassay. *Lab Chip* **2010**, *10* (24), 3335–3340.

(59) Thompson, J. A.; Du, X.; Grogan, J. M.; Schrlau, M. G.; Bau, H. H. Polymeric Microbead Arrays for Microfluidic Applications. *J. Micromechanics Microengineering* **2010**, *20* (11), 115017.

(60) Wang, C.; Wu, J.; Zong, C.; Ju, H.; Yan, F. Highly Sensitive Rapid Chemiluminescent Immunoassay Using the DNAzyme Label for Signal Amplification. *Analyst* **2011**, *136* (20), 4295–4300.

(61) Tang, J.; Tang, D.; Niessner, R.; Chen, G.; Knopp, D. Magneto-Controlled Graphene Immunosensing Platform for Simultaneous Multiplexed Electrochemical Immunoassay Using Distinguishable Signal Tags. *Anal. Chem.* **2011**, *83* (13), 5407–5414.

(62) Browne, A. W.; Ramasamy, L.; Cripe, T. P.; Ahn, C. H. A Lab-on-a-Chip for Rapid Blood Separation and Quantification of Hematocrit and Serum Analytes. *Lab Chip* **2011**, *11* (14), 2440–2446.

(63) Luchansky, M. S.; Washburn, A. L.; McClellan, M. S.; Bailey, R. C. Sensitive on-Chip Detection of a Protein Biomarker in Human Serum and Plasma over an Extended Dynamic Range Using Silicon Photonic Microring Resonators and Sub-Micron Beads. *Lab Chip* **2011**, *11* (12), 2042–2044.

(64) Triroj, N.; Jaroenapibal, P.; Shi, H.; Yeh, J. I.; Beresford, R. Microfluidic Chip-Based Nanoelectrode Array as Miniaturized Biochemical Sensing Platform for Prostate-Specific Antigen Detection. *Biosens. Bioelectron.* **2011**, *26* (6), 2927–2933.

(65) Wang, S.; Ge, L.; Song, X.; Yu, J.; Ge, S.; Huang, J.; Zeng, F. Paper-Based Chemiluminescence ELISA: Lab-on-Paper Based on Chitosan Modified Paper Device and Wax-Screen-Printing. *Biosens. Bioelectron.* **2012**, *31* (1), 212–218.

(66) Kai, J.; Puntambekar, A.; Santiago, N.; Lee, S. H.; Sehy, D. W.; Moore, V.; Han, J.; Ahn, C. H. A Novel Microfluidic Microplate as the next Generation Assay Platform for Enzyme Linked Immunoassays (ELISA). *Lab Chip* **2012**, *12* (21), 4257–4262.

(67) Sasso, L. A.; Johnston, I. H.; Zheng, M.; Gupte, R. K.; Ündar, A.; Zahn, J. D. Automated Microfluidic Processing Platform for Multiplexed Magnetic Bead Immunoassays. *Microfluid. Nanofluidics* **2012**, *13* (4), 603–612.

(68) Yu, X.; Xia, H.-S.; Sun, Z.-D.; Lin, Y.; Wang, K.; Yu, J.; Tang, H.; Pang, D.-W.; Zhang, Z.-L. On-Chip Dual Detection of Cancer Biomarkers Directly in Serum Based on Self-Assembled Magnetic Bead Patterns and Quantum Dots. *Biosens. Bioelectron.* **2013**, *41*, 129–136.

(69) Hu, W.; Lu, Z.; Liu, Y.; Chen, T.; Zhou, X.; Li, C. M. A Portable Flow-through Fluorescent Immunoassay Lab-on-a-Chip Device Using ZnO Nanorod-Decorated Glass Capillaries. *Lab Chip* **2013**, *13* (9), 1797–1802.

(70) Adel Ahmed, H.; Azzazy, H. M. E. Power-Free Chip Enzyme Immunoassay for Detection of Prostate Specific Antigen (PSA) in Serum. *Biosens. Bioelectron.* **2013**, *49*, 478–484.

(71) Tajudin, A. A.; Petersson, K.; Lenshof, A.; Swärd-Nilsson, A.-M.; Aberg, L.; Marko-Varga, G.; Malm, J.; Lilja, H.; Laurell, T. Integrated Acoustic Immunoaffinity-Capture (IAI) Platform for Detection of PSA from Whole Blood Samples. *Lab Chip* **2013**, *13* (9), 1790–1796.

(72) Yan, J.; Yan, M.; Ge, L.; Ge, S.; Yu, J. An Origami Electrochemiluminescence Immunosensor Based on Gold/graphene for Specific, Sensitive Point-of-Care Testing of Carcinoembryonic Antigen. *Sensors Actuators B Chem.* **2014**, *193*, 247–254.

(73) Mohammed, M. I.; Desmulliez, M. P. Y. Autonomous Capillary Microfluidic System with Embedded Optics for Improved Troponin I Cardiac Biomarker Detection. *Biosens. Bioelectron.* **2014**, *61*, 478–484.

(74) Garcia-Cordero, J. L.; Maerkl, S. J. A 1024-Sample Serum Analyzer Chip for Cancer Diagnostics. *Lab Chip* **2014**, *14* (15), 2642–2650.

(75) Schonhorn, J. E.; Fernandes, S. C.; Rajaratnam, A.; Deraney, R. N.; Rolland, J. P.; Mace, C. R. A Device Architecture for Three-Dimensional, Patterned Paper Immunoassays. *Lab Chip* **2014**, *14* (24), 4653–4658.

(76) Volpetti, F.; Garcia-Cordero, J.; Maerkl, S. J. A Microfluidic Platform for High-Throughput Multiplexed Protein Quantitation. *PLoS One* **2015**, *10* (2), e0117744.

(77) Vashist, S. K.; Marion Schneider, E.; Zengerle, R.; von Stetten, F.; Luong, J. H. T. Graphene-Based Rapid and Highly-Sensitive Immunoassay for C-Reactive Protein Using a Smartphone-Based Colorimetric Reader. *Biosens. Bioelectron.* **2015**, *66*, 169–176.

(78) Lee, W. S.; Sunkara, V.; Han, J.-R.; Park, Y.-S.; Cho, Y.-K. Electrospun TiO2 Nanofiber Integrated Lab-on-a-Disc for Ultrasensitive Protein Detection from Whole Blood. *Lab Chip* **2015**, *15* (2), 478–485.

(79) Vashist, S. K.; Schneider, E. M.; Luong, J. H. T. Surface Plasmon Resonance-Based Immunoassay for Human C-Reactive Protein. *Analyst* **2015**, *140*, 4445–4452.

(80) Vermeer, A. W. P.; Bremer, M. G. E. G.; Norde, W. Structural Changes of IgG Induced by Heat Treatment and by Adsorption onto a Hydrophobic Teflon Surface Studied by Circular Dichroism Spectroscopy. *Biochim. Biophys. Acta - Gen. Subj.* **1998**, *1425* (1), 1–12.

(81) Feldman, R. G.; Hamel, M. E.; Breukels, M. A.; Concepcion, N. F.; Anthony, B. F. Solid-Phase Antigen Density and Avidity of Antibodies Detected in Anti-Group B Streptococcal Type III IgG Enzyme Immunoassays. *J. Immunol. Methods* **1994**, *170* (1), 37–45.

(82) Rusmini, F.; Zhong, Z.; Feijen, J. Protein Immobilization Strategies for Protein Biochips. *Biomacromolecules* **2007**, *8* (6), 1775–1789.

(83) *Lab on a Chip Technology: Fabrication and Microfluidics, Volume 1*; Horizon Scientific Press, 2009; Vol. 3.

(84) Sellborn, A.; Andersson, M.; Hedlund, J.; Andersson, J.; Berglin, M.; Elwing, H. Immune Complement Activation on Polystyrene and Silicon Dioxide Surfaces. Impact of Reversible IgG Adsorption. *Mol. Immunol.* **2005**, *42* (5), 569–574.

(85) Eteshola, E.; Leckband, D. Development and Characterization of an ELISA Assay in PDMS Microfluidic Channels. *Sensors Actuators B Chem.* **2001**, *72* (2), 129–133.

(86) Vashist, S. K.; Dixit, C. K.; MacCraith, B. D.; O'Kennedy, R. Effect of Antibody Immobilization Strategies on the Analytical Performance of a Surface Plasmon Resonance-Based Immunoassay. *Analyst* **2011**, *136* (21), 4431–4436.

(87) Kim, D.; Herr, A. E. Protein Immobilization Techniques for Microfluidic Assays. *Biomicrofluidics* **2013**, *7* (4), 41501.

(88) Glass, N. R.; Tjeung, R.; Chan, P.; Yeo, L. Y.; Friend, J. R. Organosilane Deposition for Microfluidic Applications. *Biomicrofluidics* **2011**, *5* (3), 36501–365017.

(89) Krenková, J.; Foret, F. Immobilized Microfluidic Enzymatic Reactors. *Electrophoresis* **2004**, *25* (21-22), 3550–3563.

(90) Washburn, A. L.; Gunn, L. C.; Bailey, R. C. Label-Free Quantitation of a Cancer Biomarker in Complex Media Using Silicon Photonic Microring Resonators. *Anal. Chem.* **2009**, *81* (22), 9499–9506.

(91) Singh, A. K.; Flounders, A. W.; Volponi, J. V; Ashley, C. S.; Wally, K.; Schoeniger, J. S. Development of Sensors for Direct Detection of Organophosphates. Part I: Immobilization, Characterization and Stabilization of

Acetylcholinesterase and Organophosphate Hydrolase on Silica Supports. *Biosens. Bioelectron.* **1999**, *14* (8-9), 703–713.

(92) Jung, Y.; Lee, J. M.; Jung, H.; Chung, B. H. Self-Directed and Self-Oriented Immobilization of Antibody by Protein G-DNA Conjugate. *Anal. Chem.* **2007**, *79* (17), 6534–6541.

(93) Jung, Y.; Kang, H. J.; Lee, J. M.; Jung, S. O.; Yun, W. S.; Chung, S. J.; Chung, B. H. Controlled Antibody Immobilization onto Immunoanalytical Platforms by Synthetic Peptide. *Anal. Biochem.* **2008**, *374* (1), 99–105.

(94) Kozlov, I. A.; Melnyk, P. C.; Stromsborg, K. E.; Chee, M. S.; Barker, D. L.; Zhao, C. Efficient Strategies for the Conjugation of Oligonucleotides to Antibodies Enabling Highly Sensitive Protein Detection. *Biopolymers* **2004**, *73* (5), 621–630.

(95) Hirlekar Schmid, A.; Stanca, S. E.; Thakur, M. S.; Thampi, K. R.; Raman Suri, C. Site-Directed Antibody Immobilization on Gold Substrate for Surface Plasmon Resonance Sensors. *Sensors Actuators B Chem.* **2006**, *113* (1), 297–303.

(96) Park, J.; Sunkara, V.; Kim, T.-H.; Hwang, H.; Cho, Y.-K. Lab-on-a-Disc for Fully Integrated Multiplex Immunoassays. *Anal. Chem.* **2012**, *84* (5), 2133–2140.

(97) Ressine, A.; Ekström, S.; Marko-Varga, G.; Laurell, T. Macro-/nanoporous Silicon as a Support for High-Performance Protein Microarrays. *Anal. Chem.* **2003**, *75* (24), 6968–6974.

(98) Lee, S.; Kim, S.; Malm, J.; Jeong, O. C.; Lilja, H.; Laurell, T. Improved Porous Silicon Microarray Based Prostate Specific Antigen Immunoassay by Optimized Surface Density of the Capture Antibody. *Anal. Chim. Acta* **2013**, *796*, 108–114.

(99) Yu, X.; Xia, H.-S.; Sun, Z.-D.; Lin, Y.; Wang, K.; Yu, J.; Tang, H.; Pang, D.-W.; Zhang, Z.-L. On-Chip Dual Detection of Cancer Biomarkers Directly in Serum Based on Self-Assembled Magnetic Bead Patterns and Quantum Dots. *Biosens. Bioelectron.* **2013**, *41*, 129–136.

(100) Lim, C. T.; Zhang, Y. Bead-Based Microfluidic Immunoassays: The next Generation. *Biosens. Bioelectron.* **2007**, *22* (7), 1197–1204.

(101) Gorkin, R.; Park, J.; Siegrist, J.; Amasia, M.; Lee, B. S.; Park, J.-M.; Kim, J.; Kim, H.; Madou, M.; Cho, Y.-K. Centrifugal Microfluidics for Biomedical Applications. *Lab Chip* **2010**, *10* (14), 1758–1773.

(102) Mani, V.; Chikkaveeraiah, B. V; Rusling, J. F. Magnetic Particles in Ultrasensitive Biomarker Protein Measurements for Cancer Detection and Monitoring. *Expert Opin. Med. Diagn.* **2011**, *5* (5), 381–391.

(103) Adel Ahmed, H.; Azzazy, H. M. E. Power-Free Chip Enzyme Immunoassay for Detection of Prostate Specific Antigen (PSA) in Serum. *Biosens. Bioelectron.* **2013**, *49*, 478–484.

(104) Hosokawa, K.; Sato, K.; Ichikawa, N.; Maeda, M. Power-Free Poly(dimethylsiloxane) Microfluidic Devices for Gold Nanoparticle-Based DNA Analysis. *Lab Chip* **2004**, *4* (3), 181–185.

(105) Randall, G. C.; Doyle, P. S. Permeation-Driven Flow in Poly(dimethylsiloxane) Microfluidic Devices. *Proc. Natl. Acad. Sci. U. S. A.* **2005**, *102* (31), 10813–10818.

(106) Zimmermann, M.; Schmid, H.; Hunziker, P.; Delamarche, E. Capillary Pumps for Autonomous Capillary Systems. *Lab Chip* **2007**, *7* (1), 119–125.

(107) Yetisen, A. K.; Akram, M. S.; Lowe, C. R. Paper-Based Microfluidic Point-of-Care Diagnostic Devices. *Lab Chip* **2013**, *13* (12), 2210–2251.

(108) Gosling, J. P. Enzyme Immunoassay. In *Immunoassay*; Elsevier, 1996; pp 287–308.

(109) Gao, Z.; Hou, L.; Xu, M.; Tang, D. Enhanced Colorimetric Immunoassay Accompanying with Enzyme Cascade Amplification Strategy for Ultrasensitive Detection of Low-Abundance Protein. *Sci. Rep.* **2014**, *4*, 3966.

(110) Brooks, J. L.; Mirhabibollahi, B.; Kroll, R. G. Increased Sensitivity of an Enzyme-Amplified Colorimetric Immunoassay for Protein A-Bearing Staphylococcus Aureus in Foods. *J. Immunol. Methods* **1991**, *140* (1), 79–84.

(111) Liu, Y.; Zhang, D.; Alocilja, E. C.; Chakrabartty, S. Biomolecules Detection Using a Silver-Enhanced Gold Nanoparticle-Based Biochip. *Nanoscale Res. Lett.* **2010**, *5* (3), 533–538.

(112) Liu, R.; Zhang, Y.; Zhang, S.; Qiu, W.; Gao, Y. Silver Enhancement of Gold Nanoparticles for Biosensing: From Qualitative to Quantitative. *Applied Spectroscopy Reviews*. Taylor & Francis August 12, 2013.

(113) Yeh, C.-H.; Hung, C.-Y.; Chang, T. C.; Lin, H.-P.; Lin, Y.-C. An Immunoassay Using Antibody-Gold Nanoparticle Conjugate, Silver Enhancement and Flatbed Scanner. *Microfluid. Nanofluidics* **2008**, *6* (1), 85–91.

(114) Warsinke, A.; Benkert, A.; Scheller, F. W. Electrochemical Immunoassays. *Fresenius. J. Anal. Chem. 366* (6-7), 622–634.

(115) Becker, H. It's the Economy... *Lab Chip* **2009**, *9* (19), 2759–2762.

(116) Waldbaur, A.; Rapp, H.; Länge, K.; Rapp, B. E. Let There Be Chip—towards Rapid Prototyping of Microfluidic Devices: One-Step Manufacturing Processes. *Anal. Methods* **2011**, *3* (12), 2681.

(117) Hallmark, B.; Gadala-Maria, F.; Mackley, M. R. The Melt Processing of Polymer Microcapillary Film (MCF). *J. Nonnewton. Fluid Mech.* **2005**, *128* (2-3), 83–98.

(118) Hornung, C. H.; Hallmark, B.; Hesketh, R. P.; Mackley, M. R. The Fluid Flow and Heat Transfer Performance of Thermoplastic Microcapillary Films. *J. Micromechanics Microengineering* **2006**, *16* (2), 434–447.

(119) Hallmark, B.; Hornung, C. H.; Broady, D.; Price-Kuehne, C.; Mackley, M. R. The Application of Plastic Microcapillary Films for Fast Transient Micro-Heat Exchange. *Int. J. Heat Mass Transf.* **2008**, *51* (21-22), 5344–5358.

(120) Hornung, C. H.; Hallmark, B.; Baumann, M.; Baxendale, I. R.; Ley, S. V.; Hester, P.; Clayton, P.; Mackley, M. R. Multiple Microcapillary Reactor for Organic Synthesis. *Ind. Eng. Chem. Res.* **2010**, *49* (10), 4576–4582.

(121) Hornung, C. H.; Mackley, M. R. The Measurement and Characterisation of Residence Time Distributions for Laminar Liquid Flow in Plastic Microcapillary Arrays. *Chem. Eng. Sci.* **2009**, *64* (17), 3889–3902.

(122) Hallmark, B.; Darton, N. J.; Han, X.; Palit, S.; Mackley, M. R.; Slater, N. K. H. Observation and Modelling of Capillary Flow Occlusion Resulting from the Capture of Superparamagnetic Nanoparticles in a Magnetic Field. *Chem. Eng. Sci.* **2008**, *63* (15), 3960–3965.

(123) Darton, N. J.; Hallmark, B.; James, T.; Agrawal, P.; Mackley, M. R.; Slater, N. K. H. Magnetic Capture of Superparamagnetic Nanoparticles in a Constant Pressure Microcapillary Flow. *J. Magn. Magn. Mater.* **2009**, *321* (10), 1571–1574.

(124) Darton, N. J.; Hallmark, B.; Han, X.; Palit, S.; Slater, N. K. H.; Mackley, M. R. The in-Flow Capture of Superparamagnetic Nanoparticles for Targeting Therapeutics. *Nanomedicine Nanotechnology, Biol. Med.* **2008**, *4* (1), 19–29.

(125) Hornung, C. H.; Hallmark, B.; Mackley, M. R.; Baxendale, I. R.; Ley, S. V. A Palladium Wall Coated Microcapillary Reactor for Use in Continuous Flow Transfer Hydrogenation. *Adv. Synth. Catal.* **2010**, *352* (10), 1736–1745.

(126) Dorfling, C.; Hornung, C. H.; Hallmark, B.; Beaumont, R. J. J.; Fovargue, H.; Mackley, M. R. The Experimental Response and Modelling of a Solar Heat Collector Fabricated from Plastic Microcapillary Films. *Sol. Energy Mater. Sol. Cells* **2010**, *94* (7), 1207–1221.

(127) Edwards, A. D.; Reis, N. M.; Slater, N. K. H.; Mackley, M. R. A Simple Device for Multiplex ELISA Made from Melt-Extruded Plastic Microcapillary Film. *Lab Chip* **2011**, *11* (24), 4267–4273.

(128) Scheiff, F.; Mendorf, M.; Agar, D.; Reis, N.; Mackley, M. The Separation of Immiscible Liquid Slugs within Plastic Microchannels Using a Metallic Hydrophilic Sidestream. *Lab Chip* **2011**, *11* (6), 1022–1029.

(129) Darton, N. J.; Reis, N. M.; Mackley, M. R.; Slater, N. K. H. Fast Cation-Exchange Separation of Proteins in a Plastic Microcapillary Disc. *J. Chromatogr. A* **2011**, *1218* (10), 1409–1415.

(130) Reis, N. M.; Li Puma, G. A Novel Microfluidic Approach for Extremely Fast and Efficient Photochemical Transformations in Fluoropolymer Microcapillary Films. *Chem. Commun. (Camb).* **2015**, *51* (40), 8414–8417.

(131) Extruded Materials Having Capillary Channels, April 17, 2008.

(132) Hallmark, B.; Mackley, M. R.; Gadala-Maria, F. Hollow Microcapillary Arrays in Thin Plastic Films. *Adv. Eng. Mater.* **2005**, *7* (6), 545–547.

(133) Medina, D. I.; Hallmark, B.; Lord, T. D.; Mackley, M. R. The Development of Voidage and Capillary Size within Extruded Plastic Films. *J. Mater. Sci.* **2008**, *43* (15), 5211–5221.

(134) Hallmark, B.; Parmar, C.; Walker, D.; Hornung, C. H.; Mackley, M. R.; Davidson, J. F. The Experimental Observation and Modelling of Microdroplet Formation within a Plastic Microcapillary Array. *Chem. Eng. Sci.* **2009**, *64* (22), 4758–4764.

(135) Medina, D. I.; Chinesta, F.; Mackley, M. R. Heat Melding of Voided Polyethylene Microstructures. *Polymer (Guildf).* **2009**, *50* (14), 3302–3310.

(136) Immunoassays, Methods for Carrying out Immunoassays, Immunoassay Kits and Method for Manufacturing Immunoassay Kits, September 29, 2011.

(137) Elvira, K. S.; Wootton, R. C. R.; Reis, N. M.; Mackley, M. R.; deMello, A. J. Through-Wall Mass Transport as a Modality for Safe Generation of Singlet Oxygen in Continuous Flows. *ACS Sustain. Chem. Eng.* **2013**, *1* (2), 209–213.

(138) Ricardo Guraieb Chahin. Quantitative Detection of a Cancer Biomarker in Plastic Microcapillary Films, University of Cambridge, 2010.

(139) NG, X. W. *Optimisation of the Microcapillary Film (MCF) Platform for Enzyme Immunosorbent Assays (ELISA)*; 2011.

(140) Diana S. Aga; E. M. Thurman. *Immunochemical Technology for Environmental Applications*; Aga, D. S., Thurman, E. M., Eds.; ACS Symposium Series; American Chemical Society: Washington, DC, 1997; Vol. 657.

(141) Samarajeewa, U.; Wei, C. I.; Huang, T. S.; Marshall, M. R. Application of Immunoassay in the Food Industry. *Crit. Rev. Food Sci. Nutr.* **1991**, *29* (6), 403–434.

(142) Darwish, I. A. Immunoassay Methods and Their Applications in Pharmaceutical Analysis: Basic Methodology and Recent Advances. *Int. J. Biomed. Sci.* **2006**, *2* (3), 217–235.

(143) Chin, C. D.; Linder, V.; Sia, S. K. Lab-on-a-Chip Devices for Global Health: Past Studies and Future Opportunities. *Lab Chip* **2007**, *7* (1), 41–57.

(144) Sandin, S.; Ofverstedt, L.-G.; Wikström, A.-C.; Wrange, O.; Skoglund, U. Structure and Flexibility of Individual Immunoglobulin G Molecules in Solution. *Structure* **2004**, *12* (3), 409–415.

(145) Christopoulos, T.; Diamandis, E. Theory of Immunoassays. In *Immunoassay*; Christopoulos, T., Diamandis, E., Eds.; 1996; pp 25–26.

(146) Mastichiadis, C.; Niotis, A. E.; Petrou, P. S.; Kakabakos, S. E.; Misiakos, K. Capillary-Based Immunoassays, Immunosensors and DNA Sensors – Steps towards Integration and Multi-Analysis. *TrAC Trends Anal. Chem.* **2008**, *27* (9), 771–784.

(147) Novo, P.; Prazeres, D. M. F.; Chu, V.; Conde, J. P. Microspot-Based ELISA in Microfluidics: Chemiluminescence and Colorimetry Detection Using Integrated Thin-Film Hydrogenated Amorphous Silicon Photodiodes. *Lab Chip* **2011**, *11* (23), 4063–4071.

(148) Lin, C.-C.; Wang, J.-H.; Wu, H.-W.; Lee, G.-B. Microfluidic Immunoassays. *J. Assoc. Lab. Autom.* **2010**, *15* (3), 253–274.

(149) Ng, A. H. C.; Uddayasankar, U.; Wheeler, A. R. Immunoassays in Microfluidic Systems. *Anal. Bioanal. Chem.* **2010**, *397* (3), 991–1007.

(150) Nakanishi, K.; Sakiyama, T.; Imamura, K. On the Adsorption of Proteins on Solid Surfaces, a Common but Very Complicated Phenomenon. *J. Biosci. Bioeng.* **2001**, *91* (3), 233–244.

(151) Rabe, M.; Verdes, D.; Seeger, S. Understanding Protein Adsorption Phenomena at Solid Surfaces. *Adv. Colloid Interface Sci.* **2011**, *162* (1-2), 87–106.

(152) Barbosa, A. I.; Castanheira, A. P.; Edwards, A. D.; Reis, N. M. A Lab-in-a-Briefcase for Rapid Prostate Specific Antigen (PSA) Screening from Whole Blood. *Lab Chip* **2014**.

(153) Barbosa, A. I.; Gehlot, P.; Sidapra, K.; Edwards, A. D.; Reis, N. M. Portable Smartphone Quantitation of Prostate Specific Antigen (PSA) in a Fluoropolymer Microfluidic Device. *Biosens. Bioelectron.* **2015**, *70*, 5–14.

(154) Castanheira, A. P.; Barbosa, A. I.; Edwards, A. D.; Reis, N. M. Multiplexed Femtomolar Quantitation of Human Cytokines in a Fluoropolymer Microcapillary Film. *Analyst* **2015**, *140* (16), 5609–5618.

(155) Wright, G. G.; Schomaker, V. Studies on the Denaturation of Antibody. IV. The Influence of pH and Certain Other Factors on the Rate of Inactivation of Staphylococcus Antitoxin in Urea Solutions. *Journal of Biological Chemistry*. American Society for Biochemistry and Molecular Biology August 1, 1948, pp 169–177.

(156) Buijs, J.; Lichtenbelt, J. W. T.; Norde, W.; Lyklema, J. Adsorption of Monoclonal IgGs and Their F(ab′)2 Fragments onto Polymeric Surfaces. *Colloids Surfaces B Biointerfaces* **1995**, *5* (1-2), 11–23.

(157) Vörös, J. The Density and Refractive Index of Adsorbing Protein Layers. *Biophys. J.* **2004**, *87* (1), 553–561.

(158) Wiseman, M. E.; Frank, C. W. Antibody Adsorption and Orientation on Hydrophobic Surfaces. *Langmuir* **2012**, *28* (3), 1765–1774.

(159) Couston, R. G.; Skoda, M. W.; Uddin, S.; van der Walle, C. F. Adsorption Behavior of a Human Monoclonal Antibody at Hydrophilic and Hydrophobic Surfaces. *MAbs 5* (1), 126–139.

(160) Oom, A.; Poggi, M.; Wikström, J.; Sukumar, M. Surface Interactions of Monoclonal Antibodies Characterized by Quartz Crystal Microbalance with Dissipation: Impact of Hydrophobicity and Protein Self-Interactions. *J. Pharm. Sci.* **2012**, *101* (2), 519–529.

(161) Xu, H.; Lu, J. R.; Williams, D. E. Effect of Surface Packing Density of Interfacially Adsorbed Monoclonal Antibody on the Binding of Hormonal Antigen Human Chorionic Gonadotrophin. *J. Phys. Chem. B* **2006**, *110* (4), 1907–1914.

(162) Vermeer, A. Adsorption of IgG onto Hydrophobic Teflon. Differences between the Fab and Fc Domains. *Biochim. Biophys. Acta - Gen. Subj.* **2001**, *1526* (1), 61–69.

(163) Jönsson, U.; Ivarsson, B.; Lundström, I.; Berghem, L. Adsorption Behavior of Fibronectin on Well-Characterized Silica Surfaces. *J. Colloid Interface Sci.* **1982**, *90* (1), 148–163.

(164) Sethuraman, A.; Han, M.; Kane, R. S.; Belfort, G. Effect of Surface Wettability on the Adhesion of Proteins. *Langmuir* **2004**, *20* (18), 7779–7788.

(165) Silverton, E. W.; Navia, M. A.; Davies, D. R. Three-Dimensional Structure of an Intact Human Immunoglobulin. *Proc. Natl. Acad. Sci. U. S. A.* **1977**, *74* (11), 5140–5144.

(166) Zangmeister, R. A. Application of X-Ray Photoelectron Spectroscopic Analysis to Protein Adsorption on Materials Relevant to Biomanufacturing. *J. Pharm. Sci.* **2012**, *101* (4), 1639–1644.

(167) Mark, D.; Haeberle, S.; Roth, G.; von Stetten, F.; Zengerle, R. Microfluidic Lab-on-a-Chip Platforms: Requirements, Characteristics and Applications. *Chem. Soc. Rev.* **2010**, *39* (3), 1153–1182.

(168) Henares, T. G.; Mizutani, F.; Hisamoto, H. Current Development in Microfluidic Immunosensing Chip. *Anal. Chim. Acta* **2008**, *611* (1), 17–30.

(169) Li, T.; Lin, H.; Yu, L.; Xue, M.; Ge, S.; Zhao, Q.; Zhang, J.; Xia, N. Development of an Enzyme-Linked Immunospot Assay for Determination of Rotavirus Infectivity. *J. Virol. Methods* **2014**, *209*, 7–14.

(170) Leahy, B. J.; Christiansen, K. J.; Shellam, G. Standardisation of a Microplate in Situ ELISA (MISE-Test) for the Susceptibility Testing of Herpes Simplex Virus to Acyclovir. *J. Virol. Methods* **1994**, *48* (1), 93–108.

(171) Saadi, H.; Seillier, M.; Sandi, M. J.; Peuget, S.; Kellenberger, C.; Gravis, G.; Dusetti, N. J.; Iovanna, J. L.; Rocchi, P.; Amri, M.; et al. Development of an ELISA Detecting Tumor Protein 53-Induced Nuclear Protein 1 in Serum of Prostate Cancer Patients. *Results Immunol.* **2013**, *3*, 51–56.

(172) Kamath, S. D.; Thomassen, M. R.; Saptarshi, S. R.; Nguyen, H. M. X.; Aasmoe, L.; Bang, B. E.; Lopata, A. L. Molecular and Immunological Approaches in Quantifying the Air-Borne Food Allergen Tropomyosin in Crab Processing Facilities. *Int. J. Hyg. Environ. Health* **2014**, *217* (7), 740–750.

(173) Ngo, T. T.; Lenhoff, H. M. Enzymes as Versatile Labels and Signal Amplifiers for Monitoring Immunochemical Reactions. *Mol. Cell. Biochem.* **1982**, *44* (1), 3–12.

(174) Taton, T. A. Scanometric DNA Array Detection with Nanoparticle Probes. *Science (80-.).* **2000**, *289* (5485), 1757–1760.

(175) Göröcs, Z.; Ozcan, A. Biomedical Imaging and Sensing Using Flatbed Scanners. *Lab Chip* **2014**, *14* (17), 3248–3257.

(176) Erickson, D.; O'Dell, D.; Jiang, L.; Oncescu, V.; Gumus, A.; Lee, S.; Mancuso, M.; Mehta, S. Smartphone Technology Can Be Transformative to the Deployment of Lab-on-Chip Diagnostics. *Lab Chip* **2014**.

(177) Lee, J.; Kwak, Y. H.; Paek, S.-H.; Han, S.; Seo, S. CMOS Image Sensor-Based ELISA Detector Using Lens-Free Shadow Imaging Platform. *Sensors Actuators B Chem.* **2014**, *196*, 511–517.

(178) Irawan, R.; Tjin, S. C. Detection of Fluorescence Generated in Microfluidic Channel Using in-Fiber Grooves and in-Fiber Microchannel Sensors. *Methods Mol. Biol.* **2009**, *503*, 403–422.

(179) Giri, B.; Dutta, D. Improvement in the Sensitivity of Microfluidic ELISA through Field Amplified Stacking of the Enzyme Reaction Product. *Anal. Chim. Acta* **2014**, *810*, 32–38.

(180) Yanagisawa, N.; Dutta, D. Microfluidic Enzyme-Linked Immunosorbent Assay in a Region of Finite Length. *Anal. Chim. Acta* **2014**, *817*, 28–32.

(181) De Angelis, G.; Rittenhouse, H. G.; Mikolajczyk, S. D.; Blair Shamel, L.; Semjonow, A. Twenty Years of PSA: From Prostate Antigen to Tumor Marker. *Rev. Urol.* **2007**, *9* (3), 113–123.

(182) Institute, N. C. Prostate-Specific Antigen (PSA) Test http://www.cancer.gov/cancertopics/factsheet/detection/PSA (accessed May 5, 2015).

(183) Stenken, J. A.; Poschenrieder, A. J. Bioanalytical Chemistry of Cytokines-A Review. *Anal. Chim. Acta* **2015**, *853*, 95–115.

(184) Bozza, F. A.; Salluh, J. I.; Japiassu, A. M.; Soares, M.; Assis, E. F.; Gomes, R. N.; Bozza, M. T.; Castro-Faria-Neto, H. C.; Bozza, P. T. Cytokine Profiles as Markers of Disease Severity in Sepsis: A Multiplex Analysis. *Crit. Care* **2007**, *11* (2), R49.

(185) Sauer, U.; Domnanich, P.; Preininger, C. Protein Chip for the Parallel Quantification of High and Low Abundant Biomarkers for Sepsis. *Anal. Biochem.* **2011**, *419* (1), 46–52.

(186) Quinn, J.; Gratalo, D.; Haden, K.; Moon, J. Accurate Multiplex Cytokine Assay Developed with VeraCode Technology. *White Pap. DNA Anal. illumina Inc.* **2010**.

(187) FitzGerald, S. P.; McConnell, R. I.; Huxley, A. Simultaneous Analysis of Circulating Human Cytokines Using a High-Sensitivity Cytokine Biochip Array. *J. Proteome Res.* **2008**, *7* (1), 450–455.

(188) Nice, J. A.; Wright, H. A Model of Peroxidase Activity with Inhibition by Hydrogen Peroxide. *Enzyme Microb. Technol.* **1997**, *0229* (97), 302–310.

(189) Sivakumar, a.; Srinivasaraghavan, T.; Swaminathan, T.; Baradarajan, A. Extended Monod Kinetics for Substrate Inhibited Systems. *Bioprocess Eng.* **1994**, *11* (5), 185–188.

(190) Sharma, R. Enzyme Inhibition : Mechanisms and Scope. In *Enzyme Inhibition and Bioapplications*; InTech, 2012; pp 3–36.

(191) Brena, B.; González-Pombo, P.; Batista-Viera, F. Immobilization of Enzymes: A Literature Survey. *Methods Mol. Biol.* **2013**, *1051*, 15–31.

(192) *Immobilization of Enzymes and Cells*; Guisan, J. M., Ed.; Methods in Biotechnology™; Humana Press: Totowa, NJ, 2006; Vol. 22.

(193) *Lateral Flow Immunoassay*; Wong, R., Tse, H., Eds.; Humana Press: Totowa, NJ, 2009.

(194) Lee, S.; Oncescu, V.; Mancuso, M.; Mehta, S.; Erickson, D. A Smartphone Platform for the Quantification of Vitamin D Levels. *Lab Chip* **2014**, *14* (8), 1437–1442.

(195) Posthuma-Trumpie, G. A.; Korf, J.; van Amerongen, A. Development of a Competitive Lateral Flow Immunoassay for Progesterone: Influence of Coating

Conjugates and Buffer Components. *Anal. Bioanal. Chem.* **2008**, *392* (6), 1215–1223.

(196) Fu, E.; Liang, T.; Houghtaling, J.; Ramachandran, S.; Ramsey, S. A.; Lutz, B.; Yager, P. Enhanced Sensitivity of Lateral Flow Tests Using a Two-Dimensional Paper Network Format. *Anal. Chem.* **2011**, *83* (20), 7941–7946.

(197) Karim, O.; Rao, A.; Emberton, M.; Cochrane, D.; Partridge, M.; Edwards, P.; Walker, I.; Davidson, I. Point-of-Care PSA Testing: An Evaluation of PSAwatch. *Prostate Cancer Prostatic Dis.* **2007**, *10* (3), 270–273.

(198) Fernández-Sánchez, C.; McNeil, C. J.; Rawson, K.; Nilsson, O.; Leung, H. Y.; Gnanapragasam, V. One-Step Immunostrip Test for the Simultaneous Detection of Free and Total Prostate Specific Antigen in Serum. *J. Immunol. Methods* **2005**, *307* (1-2), 1–12.

(199) Xiang, T.; Jiang, Z.; Zheng, J.; Lo, C.; Tsou, H.; Ren, G.; Zhang, J.; Huang, A.; Lai, G. A Novel Double Antibody Sandwich-Lateral Flow Immunoassay for the Rapid and Simple Detection of Hepatitis C Virus. *Int. J. Mol. Med.* **2012**, *30* (5), 1041–1047.

(200) *Rapid Lateral Flow Test Strips: Considerations for Product Development*; Bedford, 2013.

(201) Rivas, L.; Medina-Sánchez, M.; de la Escosura-Muñiz, A.; Merkoçi, A. Improving Sensitivity of Gold Nanoparticle-Based Lateral Flow Assays by Using Wax-Printed Pillars as Delay Barriers of Microfluidics. *Lab Chip* **2014**, *14* (22), 4406–4414.

(202) Parolo, C.; Medina-Sánchez, M.; de la Escosura-Muñiz, A.; Merkoçi, A. Simple Paper Architecture Modifications Lead to Enhanced Sensitivity in Nanoparticle Based Lateral Flow Immunoassays. *Lab Chip* **2013**, *13* (3), 386–390.

(203) Hu, G.; Gao, Y.; Li, D. Modeling Micropatterned Antigen-Antibody Binding Kinetics in a Microfluidic Chip. *Biosens. Bioelectron.* **2007**, *22* (7), 1403–1409.

(204) Zimmermann, M.; Delamarche, E.; Wolf, M.; Hunziker, P. Modeling and Optimization of High-Sensitivity, Low-Volume Microfluidic-Based Surface Immunoassays. *Biomed. Microdevices* **2005**, *7* (2), 99–110.

(205) Hitzbleck, M.; Delamarche, E. Reagents in Microfluidics: An "in" and "out" Challenge. *Chem. Soc. Rev.* **2013**, *42* (21), 8494–8516.

(206) Yang, J.; Zeng, H.; Xue, S.; Chen, F.; Nakajima, H.; Uchiyama, K. Quantitative-Nanoliter Immunoassay in Capillary Immune Microreactor Adopted Inkjet Technology. *Anal. Methods* **2014**, *6* (9), 2832.

(207) Cole, L. A. "Background" Human Chorionic Gonadotropin in Healthy, Nonpregnant Women. *Clin. Chem.* **2005**, *51* (10), 1765–1766.

(208) Ridker, P. M. Clinical Application of C-Reactive Protein for Cardiovascular Disease Detection and Prevention. *Circulation* **2003**, *107* (3), 363–369.

(209) Sauer, U.; Domnanich, P.; Preininger, C. Protein Chip for the Parallel Quantification of High and Low Abundant Biomarkers for Sepsis. *Anal. Biochem.* **2011**, *419* (1), 46–52.

(210) Parsa, H.; Chin, C. D.; Mongkolwisetwara, P.; Lee, B. W.; Wang, J. J.; Sia, S. K. Effect of Volume- and Time-Based Constraints on Capture of Analytes in Microfluidic Heterogeneous Immunoassays. *Lab Chip* **2008**, *8* (12), 2062–2070.

(211) Stewart, M. E.; Yao, J.; Maria, J.; Gray, S. K.; Rogers, J. A.; Nuzzo, R. G. Multispectral Thin Film Biosensing and Quantitative Imaging Using 3D Plasmonic Crystals. *Anal. Chem.* **2009**, *81* (15), 5980–5989.

(212) Welschof, M.; Terness, P.; Kipriyanov, S. M.; Stanescu, D.; Breitling, F.; Dörsam, H.; Dübel, S.; Little, M.; Opelz, G. The Antigen-Binding Domain of a Human IgG-Anti-F(ab')2 Autoantibody. *Proc. Natl. Acad. Sci. U. S. A.* **1997**, *94* (5), 1902–1907.

(213) Gervais, L.; Hitzbleck, M.; Delamarche, E. Capillary-Driven Multiparametric Microfluidic Chips for One-Step Immunoassays. *Biosens. Bioelectron.* **2011**, *27* (1), 64–70.

(214) Ferlay, J.; Shin, H.; Bray, F.; Forman, D.; Mathers, C.; Parkin, D. *GLOBOCAN 2008, Cancer Incidence and Mortality Worldwide: IARC CancerBase No. 10. Lyon, France: International Agency for Research on Cancer*; 2010.

(215) Brawer, M. K.; Beatie, J.; Wener, M. H.; Vessella, R. L.; Preston, S. D.; Lange, P. H. Screening for Prostatic Carcinoma with Prostate Specific Antigen: Results of the Second Year. *J. Urol.* **1993**, *150* (1), 106–109.

(216) Schmid, H.-P.; Riesen, W.; Prikler, L. Update on Screening for Prostate Cancer with Prostate-Specific Antigen. *Crit. Rev. Oncol. Hematol.* **2004**, *50* (1), 71–78.

(217) Ulmert, D.; Cronin, A. M.; Björk, T.; O'Brien, M. F.; Scardino, P. T.; Eastham, J. A.; Becker, C.; Berglund, G.; Vickers, A. J.; Lilja, H. Prostate-Specific Antigen at or before Age 50 as a Predictor of Advanced Prostate Cancer Diagnosed up to 25 Years Later: A Case-Control Study. *BMC Med.* **2008**, *6* (1), 6.

(218) Parsons, J. K.; Partin, A. W.; Trock, B.; Bruzek, D. J.; Cheli, C.; Sokoll, L. J. Complexed Prostate-Specific Antigen for the Diagnosis of Biochemical Recurrence after Radical Prostatectomy. *BJU Int.* **2007**, *99* (4), 758–761.

(219) Stephenson, A. J.; Kattan, M. W.; Eastham, J. A.; Dotan, Z. A.; Bianco, F. J.; Lilja, H.; Scardino, P. T. Defining Biochemical Recurrence of Prostate Cancer after Radical Prostatectomy: A Proposal for a Standardized Definition. *J. Clin. Oncol.* **2006**, *24* (24), 3973–3978.

(220) Albertsen, P. C.; Handley, J. A.; Penson, D. F.; Fine, J. Validation of Increasing Prostate Specific Antigen as a Predictor of Prostate Cancer Death after Treatment of Localized Prostate Cancer with Surgery or Radiation. *J. Urol.* **2004**, *171* (6), 2221–2225.

(221) Buyyounouski, M. K.; Pickles, T.; Kestin, L. L.; Allison, R.; Williams, S. G. Validating the Interval to Biochemical Failure for the Identification of Potentially Lethal Prostate Cancer. *J. Clin. Oncol.* **2012**, *30* (15), 1857–1863.

(222) Fritz H. Schröder, Jonas Hugosson, Gunnar Aus, A. V. Prostate-Cancer Mortality at 11 Years of Follow-Up. *N. Engl. J. Med.* **2012**, *vol. 366*, 981–990.

(223) Vickers, A. J.; Ulmert, D.; Sjoberg, D. D.; Bennette, C. J.; Bjork, T.; Gerdtsson, A.; Manjer, J.; Nilsson, P. M.; Dahlin, A.; Bjartell, A.; et al. Strategy for Detection of Prostate Cancer Based on Relation between Prostate Specific Antigen at Age 40-55 and Long Term Risk of Metastasis: Case-Control Study. *Bmj* **2013**, *346* (apr15 5), 1–11.

(224) Pelaez-Lorenzo, C.; Diez-Masa, J. C.; Vasallo, I.; de Frutos, M. Development of an Optimized ELISA and a Sample Preparation Method for the Detection of Beta-Lactoglobulin Traces in Baby Foods. *J. Agric. Food Chem.* **2010**, *58* (3), 1664–1671.

(225) Voss, J. D.; Schectman, J. M. Prostate Cancer Screening Practices and Beliefs. *J. Gen. Intern. Med.* **2001**, *16* (12), 831–837.

(226) Wallner, L.; Frencher, S.; Hsu, J.-W.; Loo, R.; Huang, J.; Nichol, M.; Jacobsen, S. Prostate Cancer Screening Trends in a Large, Integrated Health Care System. *Perm. J.* **2012**, *16* (3), 4–9.

(227) Ahmed, M. Prostate Cancer Diagnosis in a Resource-Poor Setting: The Changing Role of Digital Rectal Examination. *Trop. Doct.* **2011**, *41* (3), 141–143.

(228) Oh, S. W.; Kim, Y. M.; Kim, H. J.; Kim, S. J.; Cho, J.-S.; Choi, E. Y. Point-of-Care Fluorescence Immunoassay for Prostate Specific Antigen. *Clin. Chim. Acta* **2009**, *406* (1-2), 18–22.

(229) Posthuma-Trumpie, G. a; Korf, J.; van Amerongen, A. Lateral Flow (immuno)assay: Its Strengths, Weaknesses, Opportunities and Threats. A Literature Survey. *Anal. Bioanal. Chem.* **2009**, *393* (2), 569–582.

(230) Nie, S.; Henley, W. H.; Miller, S. E.; Zhang, H.; Mayer, K. M.; Dennis, P. J.; Oblath, E. A.; Alarie, J. P.; Wu, Y.; Oppenheim, F. G.; et al. An Automated Integrated Platform for Rapid and Sensitive Multiplexed Protein Profiling Using Human Saliva Samples. *Lab Chip* **2014**, *14* (6), 1087–1098.

(231) DuPont. DuPont FEP Information Bulletin www2.dupont.com/Teflon_Industrial/en_US/assets/downloads/h55007.pdf (accessed Jun 22, 2010).

(232) Kusnezow, W.; Syagailo, Y. V; Rüffer, S.; Baudenstiel, N.; Gauer, C.; Hoheisel, J. D.; Wild, D.; Goychuk, I. Optimal Design of Microarray Immunoassays to Compensate for Kinetic Limitations: Theory and Experiment. *Mol. Cell. Proteomics* **2006**, *5* (9), 1681–1696.

(233) Tekin, H. C.; Gijs, M. A. M. Ultrasensitive Protein Detection: A Case for Microfluidic Magnetic Bead-Based Assays. *Lab Chip* **2013**, *13* (24), 4711–4739.

(234) Von Lode, P. Point-of-Care Immunotesting: Approaching the Analytical Performance of Central Laboratory Methods. *Clin. Biochem.* **2005**, *38* (7), 591–606.

(235) Morgan, C. L.; Newman, D. J.; M. Burrin, J.; Price, C. P. The Matrix Effects on Kinetic Rate Constants of Antibody–antigen Interactions Reflect Solvent Viscosity. *J. Immunol. Methods* **1998**, *217* (1-2), 51–60.

(236) Sauer, U.; Pultar, J.; Preininger, C. Critical Role of the Sample Matrix in a Point-of-Care Protein Chip for Sepsis. *J. Immunol. Methods* **2012**, *378* (1-2), 44–50.

(237) Chiu, M. L.; Lawi, W.; Snyder, S. T.; Wong, P. K.; Liao, J. C.; Gau, V. Matrix Effects—A Challenge Toward Automation of Molecular Analysis. *J. Assoc. Lab. Autom.* **2010**, *15* (3), 233–242.

(238) Hoadley, M. E.; Hopkins, S. J. Overcoming Matrix Matching Problems in Multiplex Cytokine Assays. *J. Immunol. Methods* **2013**, *396* (1-2), 157–162.

(239) Taylor, T. P.; Janech, M. G.; Slate, E. H.; Lewis, E. C.; Arthur, J. M.; Oates, J. C. Overcoming the Effects of Matrix Interference in the Measurement of Urine Protein Analytes. *Biomark. Insights* **2012**, *7*, 1–8.

(240) Bélanger, A.; van Halbeek, H.; Graves, H. C.; Grandbois, K.; Stamey, T. A.; Huang, L.; Poppe, I.; Labrie, F. Molecular Mass and Carbohydrate Structure of Prostate Specific Antigen: Studies for Establishment of an International PSA Standard. *Prostate* **1995**, *27* (4), 187–197.

(241) Rosenson, R. S.; McCormick, A.; Uretz, E. F. Distribution of Blood Viscosity Values and Biochemical Correlates in Healthy Adults. *Clin. Chem.* **1996**, *42* (8 Pt 1), 1189–1195.

(242) Caplan, A.; Kratz, A. Prostate-Specific Antigen and the Early Diagnosis of Prostate Cancer. *Pathol. Patterns Rev.* **2002**, *117* (1), 104–108.

(243) Catalona, W. J.; Hudson, M. A.; Scardino, P. T.; Richie, J. P.; Ahmann, F. R.; Flanigan, R. C.; DeKernion, J. B.; Ratliff, T. L.; Kavoussi, L. R.; Dalkin, B. L.; et al. Selection of Optimal Prostate Specific Antigen Cutoffs for Early Detection of Prostate Cancer: Receiver Operating Characteristic Curves. *J. Urol.* **1994**, *152* (6 I), 2037–2042.

(244) Zhu, H.; Roehl, K. A.; Antenor, J. A. V; Catalona, W. J. Biopsy of Men with PSA Level of 2.6 to 4.0 ng/mL Associated with Favorable Pathologic Features

and PSA Progression Rate: A Preliminary Analysis. *Urology* **2005**, *66* (3), 547–551.

(245) Grandke, J.; Resch-Genger, U.; Bremser, W.; Garbe, L.-A.; Schneider, R. J. Quality Assurance in Immunoassay Performance-Temperature Effects. *Anal. Methods* **2012**, *4* (4), 901.

(246) Imagawa, M.; Yoshitake, S.; Hashida, S.; Ishikawa, E. Effect Of Temperature on the Sensitivity of Sandwich Enzyme Immunoassay with Fab'-Horseradish Peroxidase Conjugate. *Anal. Lett.* **1982**, *15* (18), 1467–1477.

(247) Altintas, Z.; Fakanya, W. M.; Tothill, I. E. Cardiovascular Disease Detection Using Bio-Sensing Techniques. *Talanta* **2014**, *128*, 177–186.

(248) Coelho, F. R.; Martins, J. O. Diagnostic Methods in Sepsis: The Need of Speed. *Rev. Assoc. Med. Bras.* **2012**, *58* (4), 498–504.

(249) Zhang, B.; Cai, F. F.; Zhong, X. Y. An Overview of Biomarkers for the Ovarian Cancer Diagnosis. *Eur. J. Obstet. Gynecol. Reprod. Biol.* **2011**, *158* (2), 119–123.

(250) Loeb, S.; Catalona, W. J. Prostate-Specific Antigen in Clinical Practice. *Cancer Lett.* **2007**, *249* (1), 30–39.

(251) Zhu, H.; Isikman, S. O.; Mudanyali, O.; Greenbaum, A.; Ozcan, A. Optical Imaging Techniques for Point-of-Care Diagnostics. *Lab Chip* **2013**, *13* (1), 51–67.

(252) Pierce, M. C.; Weigum, S. E.; Jaslove, J. M.; Richards-Kortum, R.; Tkaczyk, T. S. Optical Systems for Point-of-Care Diagnostic Instrumentation: Analysis of Imaging Performance and Cost. *Ann. Biomed. Eng.* **2014**, *42* (1), 231–240.

(253) Myers, F. B.; Lee, L. P. Innovations in Optical Microfluidic Technologies for Point-of-Care Diagnostics. *Lab Chip* **2008**, *8* (12), 2015–2031.

(254) Park, T. S.; Li, W.; McCracken, K. E.; Yoon, J.-Y. Smartphone Quantifies Salmonella from Paper Microfluidics. *Lab Chip* **2013**, *13* (24), 4832–4840.

(255) Shen, L.; Hagen, J. a; Papautsky, I. Point-of-Care Colorimetric Detection with a Smartphone. *Lab Chip* **2012**, *12* (21), 4240–4243.

(256) Oncescu, V.; O'Dell, D.; Erickson, D. Smartphone Based Health Accessory for Colorimetric Detection of Biomarkers in Sweat and Saliva. *Lab Chip* **2013**, *13* (16), 3232–3238.

(257) Coskun, A. F.; Nagi, R.; Sadeghi, K.; Phillips, S.; Ozcan, A. Albumin Testing in Urine Using a Smart-Phone. *Lab Chip* **2013**, *13* (21), 4231–4238.

(258) Lee, L.; Nordman, E.; Johnson, M.; Oldham, M. A Low-Cost, High-Performance System for Fluorescence Lateral Flow Assays. *Biosensors* **2013**, *3* (4), 360–373.

(259) Rajendran, V. K.; Bakthavathsalam, P.; Jaffar Ali, B. M. Smartphone Based Bacterial Detection Using Biofunctionalized Fluorescent Nanoparticles. *Microchim. Acta* **2014**, *181*, 1815–1821.

(260) Darain, F.; Yager, P.; Gan, K. L.; Tjin, S. C. On-Chip Detection of Myoglobin Based on Fluorescence. *Biosens. Bioelectron.* **2009**, *24* (6), 1744–1750.

(261) Miller, W. G.; Myers, G. L.; Rej, R. Why Commutability Matters. *Clin. Chem.* **2006**, *52* (4), 553–554.

(262) Tate, J.; Ward, G. Interferences in Immunoassay. *Clin. Biochem. Rev.* **2004**, *25* (2), 105–120.

(263) Johan Schiettecatte, E. A. and J. S. *Advances in Immunoassay Technology*; Chiu, N., Ed.; InTech, 2012.

(264) Slaats, E. H.; Kennedy, J. C.; Kruijswijk, H. Interference of Sex-Hormone Binding Globulin in the "Coat-A-Count" Testosterone No-Extraction Radioimmunoassay. *Clin. Chem.* **1987**, *33* (2 Pt 1), 300–302.

(265) Després, N.; Grant, A. M. Antibody Interference in Thyroid Assays: A Potential for Clinical Misinformation. *Clin. Chem.* **1998**, *44* (3), 440–454.

(266) Levinson, S. S.; Miller, J. J. Towards a Better Understanding of Heterophile (and the Like) Antibody Interference with Modern Immunoassays. *Clin. Chim. Acta.* **2002**, *325* (1-2), 1–15.

(267) Kaplan, I. V.; Levinson, S. S. When Is a Heterophile Antibody Not a Heterophile Antibody? When It Is an Antibody against a Specific Immunogen. *Clin. Chem.* **1999**, *45* (5), 616–618.

(268) Selby, C. Interference in Immunoassay. *Ann. Clin. Biochem.* **1999**, *36 (Pt 6)*, 704–721.

(269) Weber, T. H.; Käpyaho, K. I.; Tanner, P. Endogenous Interference in Immunoassays in Clinical Chemistry. A Review. *Scand. J. Clin. Lab. Invest. Suppl.* **1990**, *201*, 77–82.

(270) Bjerner, J.; Nustad, K.; Norum, L. F.; Olsen, K. H.; Bormer, O. P. Immunometric Assay Interference: Incidence and Prevention. *Clin. Chem.* **2002**, *48* (4), 613–621.

(271) Ward, G.; McKinnon, L.; Badrick, T.; Hickman, P. E. Heterophilic Antibodies Remain a Problem for the Immunoassay Laboratory. *Am. J. Clin. Pathol.* **1997**, *108* (4), 417–421.

(272) Boscato, L. M.; Stuart, M. C. Incidence and Specificity of Interference in Two-Site Immunoassays. *Clin. Chem.* **1986**, *32* (8), 1491–1495.

(273) Kricka, L. J. Human Anti-Animal Antibody Interferences in Immunological Assays. *Clin. Chem.* **1999**, *45* (7), 942–956.

(274) Ismail, A. A. A. A Radical Approach Is Needed to Eliminate Interference from Endogenous Antibodies in Immunoassays. *Clin. Chem.* **2005**, *51* (1), 25–26.

(275) Martins, T. B.; Pasi, B. M.; Litwin, C. M.; Hill, H. R. Heterophile Antibody Interference in a Multiplexed Fluorescent Microsphere Immunoassay for Quantitation of Cytokines in Human Serum. *Clin. Diagn. Lab. Immunol.* **2004**, *11* (2), 325–329.

(276) Dams, R.; Huestis, M. A.; Lambert, W. E.; Murphy, C. M. Matrix Effect in Bio-Analysis of Illicit Drugs with LC-MS/MS: Influence of Ionization Type, Sample Preparation, and Biofluid. *J. Am. Soc. Mass Spectrom.* **2003**, *14* (11), 1290–1294.

(277) Wei, F.; Wang, J.; Liao, W.; Zimmermann, B. G.; Wong, D. T.; Ho, C.-M. Electrochemical Detection of Low-Copy Number Salivary RNA Based on Specific Signal Amplification with a Hairpin Probe. *Nucleic Acids Res.* **2008**, *36* (11), e65.

(278) Gau, V.; Wong, D. Oral Fluid Nanosensor Test (OFNASET) with Advanced Electrochemical-Based Molecular Analysis Platform. *Ann. N. Y. Acad. Sci.* **2007**, *1098*, 401–410.

(279) Andersson, H.; Ahmadian, A.; Wijngaart, W. van der; Nilsson, P.; Enoksson, P.; Uhlen, M.; Stemme, G. Micromachined Flow-through Filter-Chamber for Solid Phase DNA Analysis. **2000**, 473–476.

(280) He, B.; Tan, L.; Regnier, F. Microfabricated Filters for Microfluidic Analytical Systems. *Anal. Chem.* **1999**, *71* (7), 1464–1468.

(281) Tokeshi, M.; Minagawa, T.; Kitamori, T. Integration of a Microextraction System on a Glass Chip: Ion-Pair Solvent Extraction of Fe(II) with 4,7-Diphenyl-1,10-Phenanthrolinedisulfonic Acid and Tri- N -Octylmethylammonium Chloride. *Anal. Chem.* **2000**, *72* (7), 1711–1714.

(282) De Mello, A. J.; Beard, N. Focus. Dealing with ?real? Samples: Sample Pre-Treatment in Microfluidic Systems. *Lab Chip* **2003**, *3* (1), 11N.

(283) Wu, F. B.; He, Y. F.; Han, S. Q. Matrix Interference in Serum Total Thyroxin (T4) Time-Resolved Fluorescence Immunoassay (TRFIA) and Its Elimination with the Use of Streptavidin-Biotin Separation Technique. *Clin. Chim. Acta.* **2001**, *308* (1-2), 117–126.

(284) Gan, S. D.; Patel, K. R. Enzyme Immunoassay and Enzyme-Linked Immunosorbent Assay. *J. Invest. Dermatol.* **2013**, *133* (9), e12.

(285) Wang, L.; Yang, C.; Tan, W. Dual-Luminophore-Doped Silica Nanoparticles for Multiplexed Signaling. *Nano Lett.* **2005**, *5* (1), 37–43.

(286) Okano, K.; Takahashi, S.; Yasuda, K.; Tokinaga, D.; Imai, K.; Koga, M. Using Microparticle Labeling and Counting for Attomole-Level Detection in Heterogeneous Immunoassay. *Anal. Biochem.* **1992**, *202* (1), 120–125.

(287) Sun, H.; Wang, M.; Wang, J.; Tian, M.; Wang, H.; Sun, Z.; Huang, P. Development of Magnetic Separation and Quantum Dots Labeled Immunoassay for the Detection of Mercury in Biological Samples. *J. Trace Elem. Med. Biol.* **2015**, *30*, 37–42.

(288) Yeh, C. H.; Wang, I. L.; Lin, H. P.; Chang, T. C.; Lin, Y. C. A Novel Immunoassay Using Platinum Nanoparticles, Silver Enhancement and a Flatbed Scanner. *Procedia Chem.* **2009**, *1* (1), 256–260.

(289) Lu, Y.; Shi, W.; Qin, J.; Lin, B. Low Cost, Portable Detection of Gold Nanoparticle-Labeled Microfluidic Immunoassay with Camera Cell Phone. *Electrophoresis* **2009**, *30* (4), 579–582.

(290) Van Amerongen, A.; Wichers, J. H.; Berendsen, L. B.; Timmermans, A. J.; Keizer, G. D.; van Doorn, A. W.; Bantjes, A.; van Gelder, W. M. Colloidal Carbon Particles as a New Label for Rapid Immunochemical Test Methods: Quantitative Computer Image Analysis of Results. *J. Biotechnol.* **1993**, *30* (2), 185–195.

(291) Linares, E. M.; Kubota, L. T.; Michaelis, J.; Thalhammer, S. Enhancement of the Detection Limit for Lateral Flow Immunoassays: Evaluation and Comparison of Bioconjugates. *J. Immunol. Methods* **2012**, *375* (1-2), 264–270.